

eman ta zabal zazu



Universidad
del País Vasco

Euskal Herriko
Unibertsitatea

Universidad del País Vasco

Departamento de Ingeniería Química y del Medio Ambiente

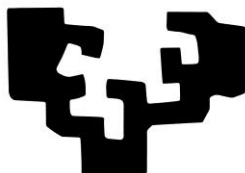
PdD Thesis

**POTENTIAL USE OF IONIC LIQUIDS IN
TRIBOLOGY**

Francesco Pagano

Bilbao, 2017

eman ta zabal zazu



Universidad
del País Vasco

Euskal Herriko
Unibertsitatea

Universidad del País Vasco

Departamento de Ingeniería Química y del Medio Ambiente

Programa de Doctorado en:

Ingeniería de Materiales Avanzados

Tesis Doctoral

**POTENTIAL USE OF IONIC LIQUIDS IN
TRIBOLOGY**

Presentada por: Francesco Pagano

Dirigida por: Prof. Ángel Valea Pérez

Dra. Raquel Bayón González

*Ai miei genitori,
per essersi sacrificati
tanto durante la loro
vita senza mai chiedere
niente in cambio.*

Acknowledgements

This thesis was the result of my work in the MINILUBES project; a project that changed radically my life taking me to Bilbao, where I had to start a new and rewarding life. For this reason, I would like to thank all the people that helped me during these years to complete my thesis, not only with their professional help but also with their friendship and love.

First of all I would like to thank my mentors, in the UPV and in IK4-TEKNIKER. Prof. Angel Valea for supporting me and for being always available when I needed his help.

Dr. Raquel Bayon Gonzalez, who was also my supervisor in IK4-TEKNIKER, for helping me since the beginning of my professional path in the company.

Many thanks to Dr. Amaya Igartua, for her great contribution to the development of my thesis. She has always been following the different sides of my research proposing new experiments.

I have the impression that the quality of the work that I have realized with the ionic liquids has improved significantly after meeting Prof. Ichiro Minami. For this reason I want to thank him and I hope that there will be more opportunity to work together.

Thanks to the entire MINILUBES group, from Dr. Doerr, who organized such a good project, to all the colleagues and friends that participated. Thanks to Lucia, Adina, Parvin, Catarina, Maria, Markus, etc.

I would like to thank Francesca, who boarded on this adventure together with me and since then has always been by my side, even after the end of our common project.

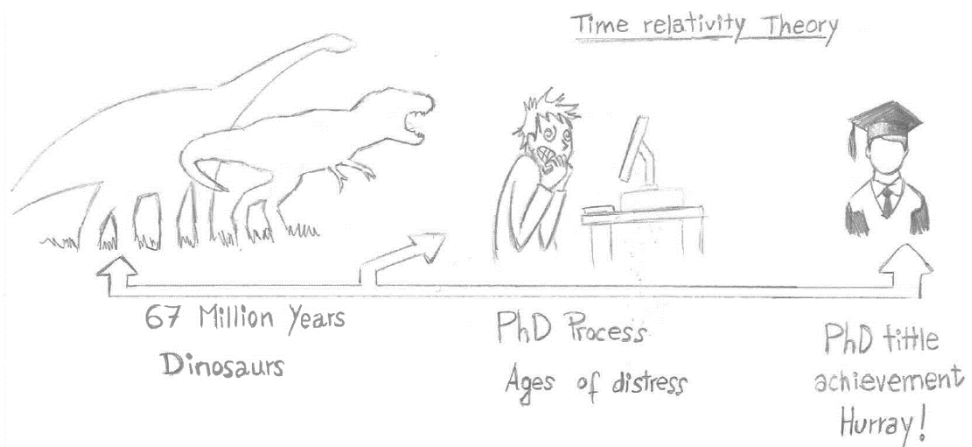
A big thank to my first good friends in the Basque Country, Marcello and Camille. They took care of me when I arrived and helped me to feel home.

Many thanks to my colleagues of IK4-TEKNIKER for standing my company for so long. Thanks to Ainara for pushing me more than anyone for finishing my PhD (this

include staying over the working time on Friday afternoon); Virginia for feeding me with delicious chocolates, cakes and whatever (I should start a diet after the thesis); Cristina for her patience during these last months; Bihotz because, if she wouldn't be here, I would arrive half of the times late at work (the other half she would be late without me); Olatz for not being pissed off with me even if I tease her with cultural issues (actually she gets angry); Lucia, "mi cariño" since time of the master.

Finally, the most important thanks, to all the people that made me love Bilbao and that I hope to continue to have close to me.

Most of work realized was financially supported by MINILUBES (FP7 Marie Curie Initial Training Network, under contract PITNGA-2008-216011, www.minilubes.net) by the European Commission and complemented with the Basque Programme EMAITEK. Parts of the work presented were also funded by the Austrian COMET program (project XTribology, no. 849109) and carried out in cooperation with the "Excellence Centre of Tribology" (AC2T research GmbH).



Abstract

Ionic liquids are a special class of fluids with ionic structure that give the possibility to design ions with specific tailor-made characteristics. Just by changing the combination cation-anion, it is possible to obtain a huge variety of compounds. For this reason in the last 25 years, since it was possible to synthesize more stable structures, a lot of efforts have been dedicated to the design and characterization of new ionic liquids for their potential in a wide variety of applications.

The objective of this doctoral thesis was the analysis of different categories of ionic liquids and to evaluate their potentiality in tribology, both as neat lubricants and as additives for other base oils.

The dissertation is divided in seven chapters. The first one gives a basic overview on tribology and the ionic liquids. The second chapter describes all the materials that were used and the instruments that were necessary for carrying out this work. The following four chapters present the experimental work that was realized and the conclusions that were drawn.

Chapter 3 describes the tribological performance of 4 pyridinium ionic liquids that were expressly synthesized. The choice of these ionic liquids was based on the fact that this kind of cations were still not studied from a tribological point of view and that they could present favorable properties. In addition, two of the ionic liquids studied had monocationic structure while the other two had the dicationic analogue. The chapter reports the results of the tribological tests of the neat lubricants and of the mixtures of glycerol and ionic liquids.

Chapter 4 shows the results obtained with 11 dicationic ionic liquid which had two cationic parts linked through a polyethylene glycol chain. According to the literature, dicationic ionic liquids are attractive because they show higher melting point, wider liquid range and better thermal stability. In addition to this, the presence of double ionic group should be beneficial for creating bonds with the anion and to

keep the alkyl chain close to the surface. The cationic moieties were based on imidazolium and pyrrolidinium groups. The anions used were chloride, bis(trifluoromethane sulfonyl)imide, methylsulfonate and butylsulfonate. In this chapter, the tribological and thermal properties of the ionic liquids were examined as neat lubricants. In addition, the most promising ionic liquids were tested as additives in polypropylene glycol monobutyl ether base oil. After the tribotests, the surfaces were analyzed by SEM and XPS and it was possible to determine the nature of the tribolayer created during the tribotests with the lubricant that was considered the best.

Dicationic ionic liquids are quite interesting but they are somehow more complicated to be synthesized and could be synthesized only in small amount in laboratory. For this reason, for the study reported in chapter 5 the ionic liquids studied were butyl-trimethyl-phosphonium dimethylphosphate and tetrabutyl-phosphonium diethylphosphorodithionate. These ionic liquids were chosen because of their ability to form metal-phosphate tribolayer. The experiments in this case verified the tribological properties of the ionic liquids, as neat lubricants and as additives, and determined by XPS the composition of the tribolayer generated. The thermal degradation and the corrosiveness of the ionic liquids was also studied.

Because of their low volatility, ionic liquids are very suitable for working in vacuum conditions. For this reason, chapter 6 presents an investigation of the tribological properties of some ionic liquids in vacuum and atmospheric conditions. The ionic liquids selected in this case were a group of alkylphosphonium alkylsilylalkylsulphonate. The experiments were carried out with Si_3N_4 balls against steel and titanium surfaces. During the vacuum tribotests, the gasses released from the ionic liquid were detected with a mass spectrometer in order to have an idea of the lubricant's decomposition. The surfaces were also analyzed by SEM in order to understand if there was a protective tribolayer in the wear scar.

Finally, the chapter 7 is a summary of the conclusions that could be drawn from all the experiments realized so far.

Abbreviations

AISI	American Iron and Steel Institute
ASTM	American Society for Testing and Materials
ATR	Attenuated total reflection
BASIL	Biphasic Acid Scavenging utilising Ionic Liquids
BF ₄	Tetra fluoroborate
BMIM	Butylmethylimidazolium
Bu ₃ MeP	Tributylmethylphosphonium
Bu ₄ P	Tetrabutylmethylphosphonium
CSLM	Confocal Scanning Laser Microscopes
DILS	Dicationic ionic liquids
EIS	Electrochemical impedance spectroscopy
EHL	Elestohydrodynamic lubrication
ESI-TOF	Electrospray ionization-Time of flight mass spectrometry
EtTPhos	Diethylphosphorodithioate
FAP	Trifluorotris(pentafluoroethyl) phosphate
FeF ₂	Metal fluoride
F _f	Friction force
F _N	Normal force
FTIR	Fourier Transfer Infra-Red spectroscopy
HRC	Hardness Rockwell scale
HRMS-ESI	High Resolution Mass Spectroscopy – Electrospray Ionization
IL	Ionic liquid
MAC	Multiply alkylated ciclopentane
MePhos	Dimethylphosphate
MTM	Mini Traction Machine
NMR	Nuclear Magnetic Resonance

NTf ₂	Bis(trifluoromethanesulfonyl)imide
NTP	Normal Temperature Pressure
OECD	Organization for Economic Cooperation and Development
OCP	Open circuit potential
PEG	Polyethylene glycol
PFPE	Perfluoropolyethers
PF ₆	Hexafluorophosphate
REACH Chemicals	Registration, Evaluation, Authorisation and Restriction of Chemicals
RTIL	Room Temperature Ionic Liquid
SEM	Scanning electron microscopy
SRV	Schwing-Reib-Verschleiss
TCP	Tricresyl phosphate
TFSA	Bis(trifluoromethanesulfonyl)imide
TOF-SIMS	Time-of-Flight Secondary Ion Mass Spectrometry
UHV	Ultra-high vacuum
VI	Viscosity index
VTF	Vogel-Tamman-Fulcher
WSD	Wear scar diameter
W _v	Wear volume
w/w	weight/weight %
XPS	X-ray photoelectron spectroscopy
ZDDP	Zinc dialkyl dithiophosphate
η	Dynamic viscosity
μ	Coefficient of friction
ν	Kinematic viscosity

Index

1 INTRODUCTION.....	3
1.1 Tribology.....	3
1.1.1 History of tribology.....	4
1.1.2 Fundamental concepts of tribology.....	8
1.1.3 Lubrication and lubricants.....	12
1.2 Ionic liquids.....	22
1.2.1 Introduction to ionic liquids.....	22
1.2.2 History of ionic liquids.....	25
1.2.3 Physico-chemical properties of ionic liquids.....	32
1.2.4 Ionic liquids in tribology.....	39
2 MATERIALS AND EQUIPMENT.....	51
2.1 Materials used.....	51
2.1.1 Lubricants.....	51
2.2 Tribological systems studied.....	61
2.3 Equipment.....	62
2.3.1 Tribometers.....	62
2.3.2 Thermal analysis.....	68
2.3.3 Surface analysis.....	69
2.3.4 Other instruments.....	77
3 COMPARISON OF MONOCATIONIC AND DICATIONIC PYRIDINIUM BASED IONIC LIQUIDS ...	81
3.1 Introduction.....	81
3.2 Experimental details.....	82
3.2.1 Materials.....	82
3.2.2 Thermal analysis.....	85
3.2.3 Tribological Experiments.....	86
3.3 Results and discussion.....	87
3.3.1 Thermal properties.....	87
3.3.2 Solubility.....	88
3.3.3 Tribological performance.....	89

3.4 Conclusions	98
-----------------------	----

4 DICATIONIC IONIC LIQUIDS.....101

4.1 Introduction	101
4.2 Experimental details	103
4.2.1 Materials	103
4.2.2 Thermal analyses	107
4.2.3 Tribological experiments	108
4.2.4 Surface analysis	109
4.2.5 Corrosion experiments	110
4.3 Results and discussion	110
4.3.1 Thermal properties	110
4.3.2 Tribological performance	112
4.3.3 Surface analysis	119
4.3.4 Corrosiveness	122
4.4 Conclusions	125

5 PHOSPHONIUM BASED IONIC LIQUIDS AS ANTI-WEAR ADDITIVES IN SYNTHETIC BASE OIL131

5.1 Introduction	131
5.2 Experimental	134
5.2.1 Materials	134
5.2.2 Thermal analysis	134
5.2.3 Viscosity and density	136
5.2.4 Tribological experiments	136
5.2.5 Surface analysis	137
5.2.6 Thermal degradation and corrosion	138
5.2.7 Tribocorrosion test	139
5.3 Results and discussion	140
5.3.1 Thermal properties	140
5.3.2 Viscosity and density	142
5.3.3 Tribological performance	143
5.3.4 Surface analysis	148
5.3.5 Thermal degradation and corrosion analysis	150
5.3.6 Tribocorrosion analysis	154
5.4 Conclusions	156

6 TRIBOREACTIVITY IN VACUUM OF HALOGEN-FREE IONIC LIQUIDS	161
6.1 Introduction	161
6.2 Experimental	165
6.2.1 Materials	165
6.2.2 Tribological experiments	167
6.2.3 Surface analysis	170
6.3 Results and Discussion	171
6.3.1 Tribological performance	171
6.3.2 Surface analysis	184
6.4 Conclusions	187
7 CONCLUSIONS	192
BIBLIOGRAPHY	196
ARTICLES PUBLISHED	210

Chapter 1

1 Introduction

1.1 TRIBOLOGY

Tribology is a multidisciplinary field that studies, at various scales, the interaction of bodies in contact in relative motion. It is based on principles taken from physics, chemistry, material science, mechanical engineering and chemical engineering. The major topics studied are friction, wear and lubrication but there can be many other aspects that should be considered as for example contact mechanics, nanotribology, biotribology, tribocorrosion, etc. It is an interdisciplinary science that goes from fundamental research, as nanotechnology and surface science, to industrial application.

The purpose of tribology is to understand and to control the phenomena that take place when two bodies are sliding one against the other. Depending on the application, the objective can be to reduce friction, to have a stable friction coefficient, to reduce the wear, to wear a surface in order to obtain a specific roughness, heat dissipation, particles removal, etc.

Recently Holmberg et al. have started to calculate the global energy consumption due to friction losses in different fields as for example in the passenger cars [1], in trucks and buses [2] and in paper machines [3]. And the results obtained are astonishing. By taking advantage of new technology for friction reduction, there would be, in a long term period, an annual global saving of 576,000 million euro and 960 million tonnes of CO₂ for the passenger cars, 105,000 million euro and 200 million tonnes of CO₂ for the trucks and buses, 4,200 million euro and 22.7 million tonnes for the paper machines. The picture that came out from these studies is that it is necessary to develop and apply new tribological solutions to the industry, not just for economical reasons, also for reducing the environmental impact of our lifestyle.

1.1.1 History of tribology

Tribology is a word that was used for the first time in the 1966 to describe the science and technology of interacting surfaces in relative motion and associated practices [4]. It was written in what is today known as the Peter Jost Report [5], a document where, for the first time, was demonstrated the importance of a complete and thorough study of the phenomena that take place when two surfaces are sliding one against the other. This report was commissioned to H. Peter Jost by the British Minister of State for Science in order to investigate the reason beyond the great number of failures in the industry due to the inadequate lubrication. The commission formed came up with a clear vision of the economic value of tribology to the industry, estimating that the total economic loss due to inadequate solutions was of 515,000,000 £ [4].

Nowadays the modern tribology is a complex and multidisciplinary subject that involve mainly physic, chemistry and material science but its history started long before the 1966.

- The first documented example of adopted tribological solution was found on a painting in the tomb of Djehutihotep at Dayr Al Barsha, and belongs to the Egiptian period around the 1900 BC (Figure 1. 1). The picture represents a

statue 7 meters high being transported by 172 workers and with a man pouring a liquid under the sled in order to reduce the friction.

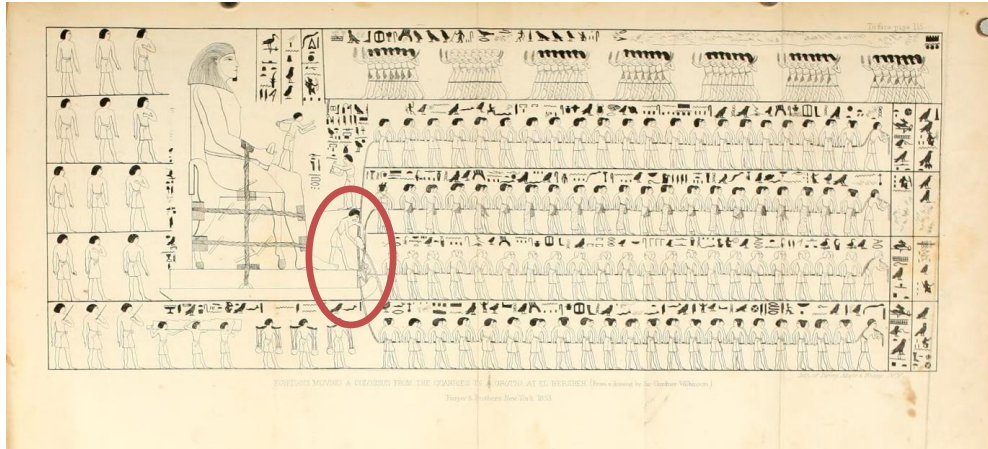


Figure 1. 1 -Reproduction of the painting found in the tomb of Djehutihotep. It belongs to the Egyptian period and depicts a man who is facilitating the transport of a statue by pouring a lubricant.

- The first very important tribological mechanism invented by the man was the wheel. There is still discussion about the culture that first used a wheel but it is sure that during the second half of the fourth millennium BCE there were wheeled vehicles in Mesopotamia, in Caucasus and in Central Europe.
- Many important scientists have tried to explain the friction forces with laws and theories. Leonardo Da Vinci understood since the 15th century the importance of the friction force for the working machines and explained two important friction concepts that will be used centuries later as the first and the second laws of tribology:
 1. The dimension of the surfaces in contact has not influence on the friction force.
 2. If the weight of the body is doubled, also the friction force is doubled.
- Unfortunately these two laws were almost unknown for more than two centuries, until the 1699, when Guillame Amontons published them for the

first time, together with a third one: Kinetic friction is independent of the sliding velocity [6]. These laws were verified in 1781 by Charles-Augustin de Coulomb for dry contact.

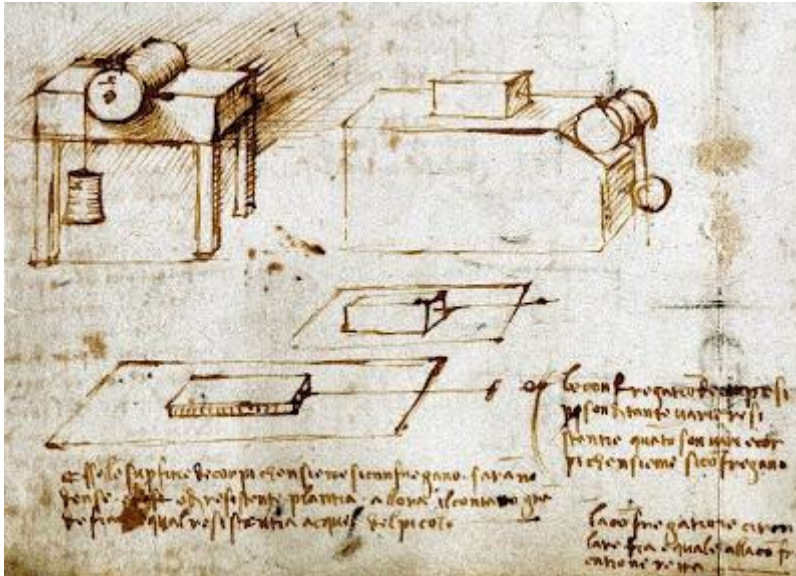


Figure 1. 2 – A plan made by Leonardo Da Vinci that illustrate some friction experiments realized. This sketch is included in the Codex Arundel.

- It was the industrial revolution that led to new interest and new developments in the field of tribology, mainly for two reasons. From one side demanding working conditions required new solutions for the mechanical failures and from the other side the technological advancement made possible the use of components of higher quality.
- Although Leonardo Da Vinci, Galileo Galilei and many other scientists had represented and described examples of ball bearings in the past, it was in the 1794 that Philip Vaughan patented it for the first time [7].
- In the same period there were also great advancements in the development of lubricants. First of all because there was the substitution of vegetable and

animal oils with mineral oils and also because of the formulation of new theories in fluid mechanics and viscous flow properties.

- Between the end of the 19th century and the beginning of the 20th century Tower, Reynolds and Sommerfeld formulated interesting theories related with the hydrodynamic lubrication, which are still the bases of many modern studies.
- At the beginning of the 20th century Richard Stribeck published his famous papers *Kugellager für beliebige Belastungen* [8] and *Die wesentlichen Eigenschaften der Gleit- und Rollenlager* [9] setting the bases for the principles of the elastohydrodynamic lubrication.
- During the First World War the machines had been working in more exigent conditions in terms of temperature, speed and load causing high tribological stress on the components and failures. For this reason, at the beginning of the 1920s, when the industry started to move on again, a big effort was dedicated to the development of new lubricants that could be able to withstand more extreme conditions. In 1923 Frans Fischer and Hans Tropsch developed a process for converting a mixture of carbon monoxide and hydrogen into liquid hydrocarbons. This process allowed the production of synthetic lubricants with a high purity level and sulfur free.
- Between the 1930s and 1940s there was also an important increase of attention to the development of lubricant additives. The zinc dialkyldithiophosphate (ZDDP) was patented in the 1941 and up to now is the most used anti-wear additive in the market.
- As told before, in the 1966 that Peter H. Jost presented a report to the British Parliament, explaining the importance to start to teach tribology in the university.

While in the initial period the focus of the tribologist was especially toward the increase of energetic efficiency and extension of the machineries lifetime, nowadays the tribology has become an essential support for many advanced

technological applications (biomedical systems, nanotechnology, renewable energy systems, etc.).

1.1.2 Fundamental concepts of tribology

As a simplification, the tribological system can be thought as if it is composed by four elements: a contacting surface, an opposing contacting pair, an interface between the two and the environment [10]. All the phenomena described in the following parts of this dissertation are generated by the interaction of these four elements.

1.1.2.1 Friction

Friction is the resistance force that the surface of a solid body experiences against the surface of another body or a fluid when they are in relative motion.

When two surfaces in contact have a relative motion, the kinetic energy of the bodies diminishes because of the friction force and the initial energy is converted in thermal energy. Obviously, higher friction force goes with higher energy conversion.

The friction force is influenced by the nature of the rubbing surfaces but cannot be extrapolated considering just the materials in contact. It is function of the whole system, hence it is necessary to consider also the morphology of the surfaces, the temperature, the load applied, the relative velocity, humidity, etc.

Knowing the normal force applied F_N to the bodies in contact, the friction force F_f can be put in relation with coefficient of friction μ through the equation (1.1)

$$\mu = \frac{F_f}{F_N} \quad (1.1)$$

The coefficient of friction is a dimensionless parameter that has to be measured empirically.

In function of the state of the bodies in relative motion, it is possible to distinguish between many different types of friction:

Dry friction: is referred to the force between the surfaces in contact of two solids in relative motion.

Dealing with the dry friction, it is possible to distinguish between two different types of friction forces: static friction and kinetic friction. The difference between them is that static friction is the force necessary to start a relative motion between the bodies when they are not moving, kinetic friction instead is the force necessary to keep in movement two bodies in relative motion. Usually static friction is superior to kinetic friction.

Lubricated friction: takes place when two solid surfaces are separated by a fluid. The function of the lubricant in this kind of system is to prevent the direct contact between the solid surfaces and thus to smoothen the contact conditions. In a lubricated contact, normal load, relative velocity of the bodies and viscosity of the lubricant have a great influence on the friction coefficient and can determine four different lubrication regimes: boundary, mixed, elasto-hydrodynamic and hydrodynamic.

Fluid friction: describes the internal resistance of the fluids and is also known as viscosity.

It can be calculated as relation between the shear stress and shear rate. When the viscosity is constant as we increase the shear rate the fluid is called Newtonian. There are many fluids that can be considered as quasi Newtonian, as for example the water, but most of the oils cannot be treated as Newtonians. There are other kinds of classification of the fluids in function of the viscosity dependence with parameters as shear rate, time of shearing, etc. (pseudoplastic, dilatant, shear time dependent, thixotropic, etc.).

In addition to the three described before, there are many other types of friction as for example drag friction, internal friction, rolling resistance, radiation friction but they will not be explained since they are specific of systems that are very dissimilar from the systems described in the experimental part of this dissertation.

1.1.2.2 Wear

Wear is a mechanical process that takes place when two solid surfaces are rubbing one against the other. It consists in a superficial damage that leads to the material loss.

In tribology, there are many different wear mechanisms that have been identified.

Adhesive wear: It is a common phenomenon on metallic surfaces and takes place when the surfaces in contact, under relatively high compressive load, build up localized strong adhesive unions. The mechanism was described by Archard and it is the base for its wear law. The main concept is that when two smooth surfaces come in contact, the interaction is limited to their asperities. In an initial moment, the asperities are plastically deformed and afterwards they are welded together because of the localized high pressure. Eventually, due to the sliding, the welded parts are broken producing a material transfer from a surface to the other or completely removed as wear debris. The visible effect of this wear mechanism is the presence of cavities on one of the surfaces and material accumulation on the other. This process is described by the Archard wear law:

$$W = \frac{kF_N S}{H} \quad (1.2)$$

Where W is the total volume of wear debris, k is a dimensionless constant, F_N is the normal load, S is the sliding distance and H is the hardness of the softest material in contact.

In case of lubricated contact this law is not enough for describing the phenomenon because the lubricant is interposed between the asperities and reduce the real area in contact. In addition, the presence of additives could also change the chemical composition of the surfaces in contact.

Abrasive wear: this process occurs when one of the surfaces has higher hardness than the other. In this case, the hardest surface produces grooves on the softest one. In order to reduce the probability of abrasive wear, the surfaces in contact should

have similar hardness but this is not enough to be sure that there will not be abrasion. Indeed it is possible that the problem is generated by hard wear particles present between the two rubbing surfaces. Sometimes they can be impurities but in other cases they could also be hardened particles previously detached from the surfaces in contact. This case of abrasion due to wear debris is called third body abrasive wear.

The Archard wear law (1.2) is valid also in the case of abrasive wear.

Surface fatigue: this is a mechanical damage that can be observed when the surface suffers cyclic loading. Because of the cyclic mechanical stress there is the appearance of micro-cracks that slowly grows and can develop in material detachment. Fatigue wear comes out when the applied load or the shear stress is higher than the fatigue strength of the material. The initiation of the micro-cracks is superficial but they propagate in the subsurface and after many cycles this can lead to delamination or cracking. In rolling bearing, the fatigue wear initially appears with micro-pitting on the surface and can eventually lead to spalling, a damage of hundreds of microns.

Fretting: it could seem as a special type of fatigue wear but, in this case, the relative movement of the two bodies is very small. The main cause of failure for fretting is material loss. When a surface suffers fretting, the area around the contact presents oxide particles. When these particles are removed, new oxide layers are generated. If this continues for a long period, the joint of the mechanisms loose in precision and this can lead to the failure.

Corrosive wear or tribocorrosion: this is due to the combined effect of chemical, electrochemical and mechanical factors. It can influence the tribological behaviour of the surfaces generating both wear and corrosion. When a metallic surface is exposed to aggressive environment, as for example acids, chemicals or electrolytes, it can form a soft corrosion layer. If the system is also mechanically stressed by rubbing, this layer can be easily removed and a new exposed surface appears. The damage that the system could suffer in case of tribocorrosion can be much worse

than the single contributions given by wear and corrosion, as can be seen in Figure 1.3 [11].

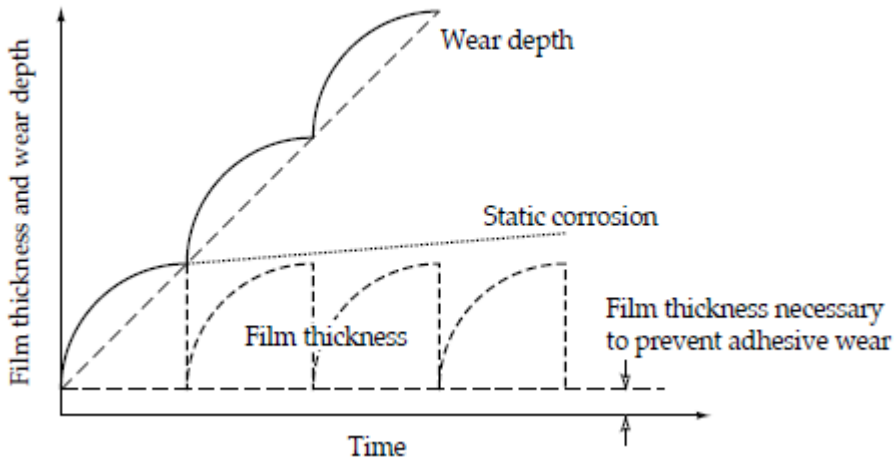


Figure 1.3 Model of corrosive wear by repeated removal of passivating films [11,12].

Erosive wear: erosive wear occurs when a prolonged flow of small particles or liquid droplets impact against a surface. There are many parameters that influence the effect of erosion as the impingement angle, number of particles per area, particles velocity, particles dimension and morphology. In function of the parameters involved in the erosive process and the characteristic of the surface, the result of the damage can be very different. There could be signs of abrasion, fatigue, plastic deformation, brittle fracture. In some case it was observed also melting or atomic erosion [13].

1.1.3 Lubrication and lubricants

The main objective of a lubricant is the reduction of friction and wear of two rubbing surfaces but there are also other secondary functions that are desired and necessary for getting a good performance of the systems, as for example cooling, cleaning, sealing, corrosion protection, load balancing. In order to be able to realize their function, modern lubricants are made of a complex mixture of different compounds (base oil and additives). It is not easy to realize the right formulation of a lubricant

for two reasons. First of all because it is necessary to test and study the compatibility of the different elements that compose the lubricant. It is quite common to find bases or additives that are able to improve some properties but when they are mixed with other compounds, their effect is not the same anymore. The second reason is the great variety and complexity of the working conditions. The ideal lubricant that could work properly in any condition does not exist and it is impossible to formulate. Each lubricant has to be designed for a specific set of conditions and by changing just one of the working parameters it is possible that the performance will drop drastically.

1.1.3.1 Lubrication conditions

Although there are a large number of parameters involved in a tribocontact, the lubrication conditions can be expressed in function of the film thickness that is created when two surfaces are sliding one against the other in presence of a lubricant. In 1902 Richard Stribeck proposed a theory that put in relationship the friction coefficient with the sliding speed, the fluid viscosity and the normal load [8]. He showed that by creating a graph with the friction coefficient on the y-axis and viscosity times velocity divided by load in the x-axis, it was possible to identify four regions as in Figure 1. 4.

In the first region on the left, corresponding to **boundary lubrication**, the film thickness is small in comparison with the roughness of the surface. In this condition the lubricant is not able to separate completely the surfaces and there is the possibility to have dry contact between the asperities. The function of the lubricant in this case is the formation of a molecular layer which has to reduce the shear strength and wear. In common lubricants, the protective tribolayer is formed thanks to specific additives that can interact with the surface in order to promote chemical reactions, adsorption or chemisorption. Tribological parameters as contact pressure and local temperature are extremely important for the activation of these reactions.

The second region corresponds to the **mixed lubrication**. And can be considered as a combination of boundary and fluid lubrication. In this situation, part of the load is sustained by hydrodynamic or elasto-hydrodynamic lubrication (EHL) mechanism but there are still a few points of contact between the asperities, hence the formation of boundary layers using anti-wear additives is required. Mixed lubrication is typical in machines during the start and stop operations.

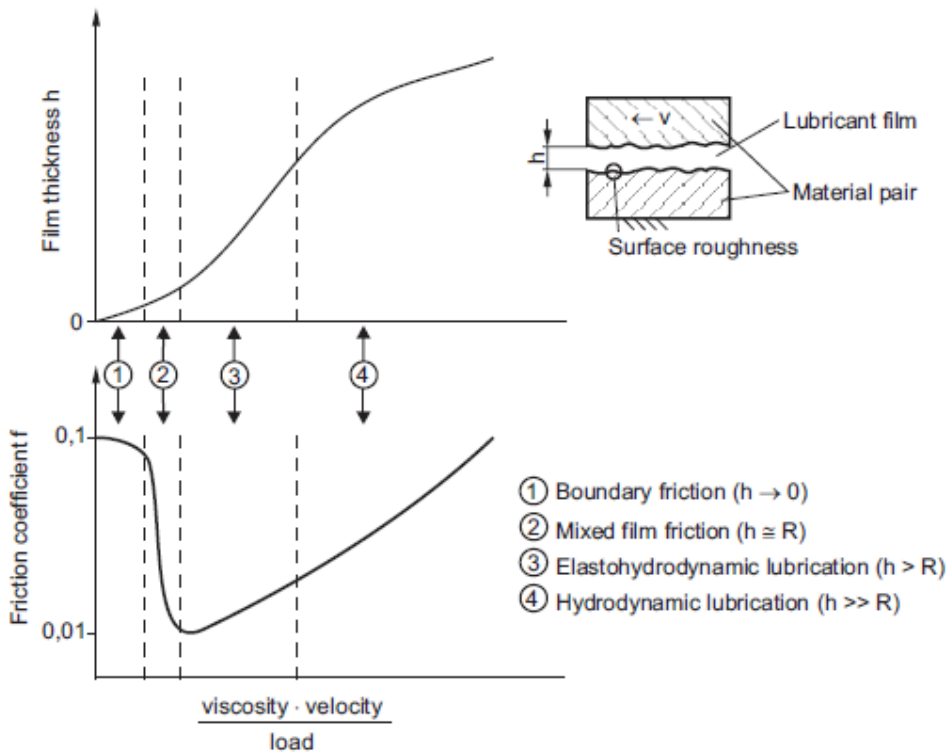


Figure 1. 4 - Stribeck graph according to H. Czichos and K.-H. Habig [14,15].

Elasto-hydrodynamic lubrication occurs when the fluid film formed between the surfaces sliding is thick enough to avoid the direct contact but the pressure on the surfaces is still high enough to cause elastic deformation. Figure 1. 5 shows schematically the effect of EHL on the surfaces.

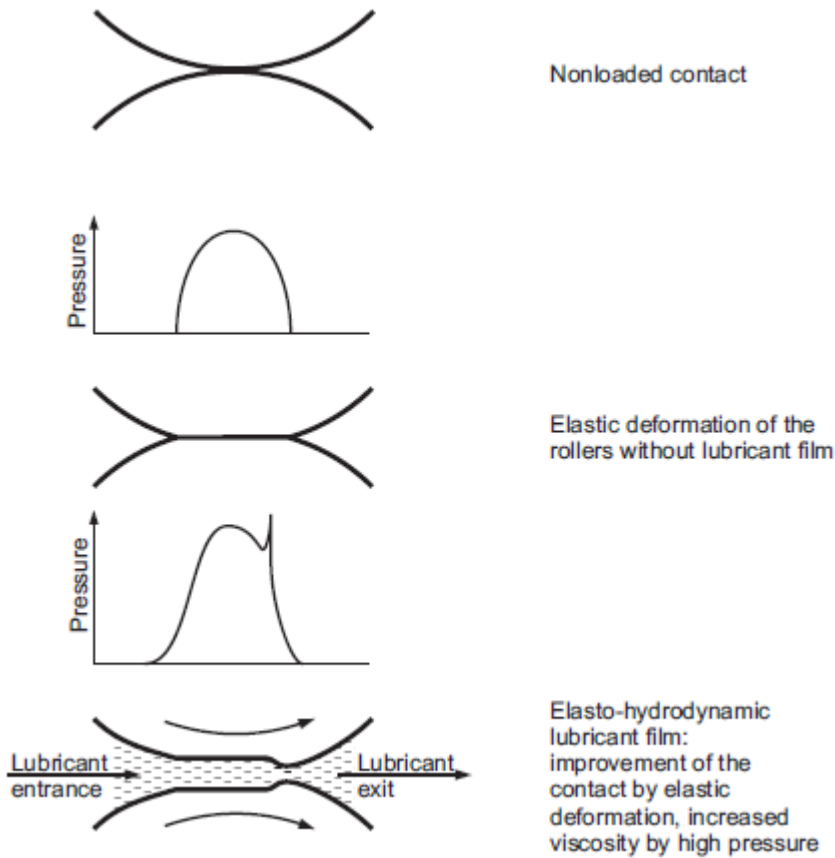


Figure 1. 5 – Effect of EHL on the sliding surfaces. Even though there is not a direct contact of the surfaces, the pressure exercised by the fluid is enough to generate elastic deformation on the rollers [10].

The last region in Figure 1. 4 corresponds to **hydrodynamic lubrication**. In conditions of moderate load, sufficiently high viscosity and sufficiently high sliding velocity it is possible to get a thick lubrication film that provides low friction and theoretically zero wear. The hydrodynamic film in this case is formed because of the pressure developed by the fluid on the sliding surfaces. The pressure has to be sufficient to sustain the weight of the upper body. The theoretical bases of the hydrodynamic lubrication were formulated by Reynolds in 1886 [15].

Figure 1. 6 shows a simplified representation of the film formation and pressure distribution in the case of a rolling element.

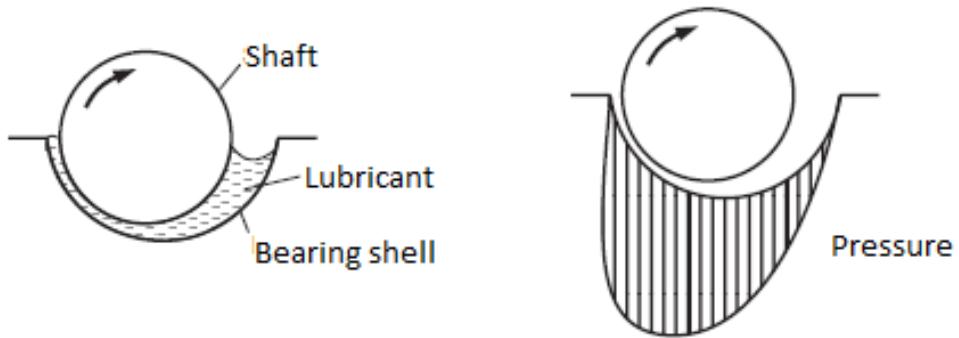


Figure 1. 6 - Formation of a hydrodynamic liquid lubricant film and development of pressure in the hydrodynamic film in a rolling element [10].

From what said before, it is evident that the relation between the lubricant film thickness and the roughness of the surfaces has a major importance for the identification of the lubrication conditions. This relationship can be expressed with the parameter λ .

$$\lambda = \frac{\text{minimum film thickness}}{\sqrt{R_{a1}^2 + R_{a2}^2}} \quad (1.3)$$

Where R_{ai}^2 is the mean roughness of the sliding surface. The hydrodynamic lubrication regime starts from values of $\lambda > 3$.

1.1.3.2 Lubricants

There are many different types of lubricants but when we are talking about their general state, it is possible to divide them in 3 groups:

- Oils (liquid lubricants)
- Greases
- Solid lubricants

Oils

The oils are classified in function of their three main base stock sources:

- Mineral oils
- Synthetic oils
- Vegetable oils

Mineral oils are, by far, the most commonly used lubricants in the industry because of their good combination of performance and price. They are derivatives of the petroleum, obtained by fractional distillation. After the separation in function of their volatility, they get a refining process in order to remove waxes (which could be solid at relatively high temperature), aromatic hydrocarbons (which could diminish the viscosity index), compounds containing sulphur and nitrogen (which could cause corrosion or worsen the tribological properties). The result obtained after refining is a complex mixture of hydrocarbons. It is impossible to get a pure product. The real objective is just to obtain a product with specific characteristics.

Synthetic oils were developed at the beginning of the 20th century as a substitute for mineral oil but due to the higher cost, their use have been essentially limited to specific applications where the mineral oils cannot guarantee a good performance. Synthetic oils can be preferred in conditions of high temperature, as for example in gas turbine engines or in vacuum applications, where very low vapour pressure is needed. The advantage in this case is that by synthesis is possible to select and control accurately the compounds present in the oil. The category of the synthetic oils includes a big variety of compounds. The most common are polyalphaolefins, esters, cyclo-aliphatics and polyglycols but for some very specific applications it is possible to have more complex structure. For space application for example, where the volatility is a major issue, the most important liquid lubricants are perfluoropolyethers (PFPE) and multiply alkylated cyclopentane (MAC).

Mineral oils are poorly biodegradable and contain hazardous contaminants for the environment and for the human health. Even though there are strict regulations about

the treatment and disposal of used mineral oils, large part of them ends up in the environment contaminating the water and the soil. In addition, mineral oils are found in food as result of contamination and from various intentional uses in food production [16]. Vegetable oils are considered the “green” alternative to the use of mineral oils. Most of them are made of triacylglycerides (even called triglycerides) which are glycerol molecules with three fatty acid chains attached at the hydroxyl group via ester linkage [17]. Some examples of vegetable oil are: castor oil, palm oil and rape-seed oil. They are used where there is the risk that the oil could contaminate a product that has to be in contact with humans, as for example food or pharmaceutical products. Even though they demonstrate very high lubricity and excellent viscosity index (VI), they have not sufficient oxidative stability [17].

Greases

They are not very different from oils. They are obtained by the dispersion of a thickening agent in a liquid lubricant. Greases are not solid but it is also difficult to classify them as liquid, for this reason they have been named non-fluid oils [18]. In a grease the oil molecules are trapped in minute pockets formed by soap fibers.

Greases are mainly used in mechanism where a liquid oil would spill out or where there is not a need of frequent lubrication.

According to Lansdown [19], the main advantages of grease lubricants are:

- They have less problems in the running in phase
- They perform efficiently under squeeze film conditions (when the film thickness decrease with time)
- They are good at sealing
- They give surplus lubricant without a special design
- Greases help to avoid contamination of clean products
- They unable the use of solid additives.

The main disadvantages, instead, in comparison with liquids lubricants are:

- The heat transfer is quite low
- They have lower speed limit because of their higher viscosity
- They suffer more of oxidation

Solid lubricants

Solid lubricants are used especially when the working conditions are very severe (high temperature, vacuum, corrosive environment) and liquid lubricants or greases are not able to control friction and wear [20,21]. Sometimes it is also possible to combine solid lubricants with liquid lubricants or greases in order to get a synergistic effect on the tribological performance.

There are many kinds of solid lubricants and the working mechanism can change a lot from one to the other. Anyway there is a big group of materials, with a lamellar or layered crystal structure, that have similar behavior. In this case, the atoms that are positioned on the same plane are strongly bonded while the connection that they have with the atoms that belongs to other layers is not so strong. In these conditions, when the shear stress is produced due to the friction forces, these layers get aligned parallel to the sliding direction and they can slide one on the other providing low friction. In addition, strong interatomic bonding and packing in each layer is thought to help reduce wear damage [22].

The solid lubricants with a layered crystal structure are graphite, hexagonal boron nitride, boric acid, and the transition-metal dichalcogenides MX_2 (where M is molybdenum, tungsten, or niobium, and X is sulfur, selenium, or tellurium) [22].

Certain classes of material that work properly at high temperature are composed of oxides, fluorides and sulfates. At high temperature they became softer and thus can facilitate the shearing [23,24].

Self-lubricating composites are prepared through the dispersion of a lubricating solid in a polymeric, metallic or ceramic matrix. In this way there is a core that is made of

a resistant, tough and hard material and some scattered regions made of lubricant that have the function to lower the friction coefficient [25,26].

Some polymers, as the polytetrafluoroethylene, have long molecular chains with high chemical inertness and low surface energy, which make them insensitive to chemical bonding, thus lowering the friction coefficient.

Finally, there is a class of metal that are characterized by being soft. They provide low friction forces thanks to their low shear strength, rapid recovery and recrystallization. Some of the metals that enter in this category are Sn, Pb, Pt, Au, Ag [27,28]

Solid lubricants can be applied to a tribological surface in a variety of forms: sprinkled, rubbed, burnished [29,30], sprayed, bonded to a surface using adhesives and epoxy resins [31], mixed with oils and greases [25,26]. However, in most modern applications, thin films of solid lubricants are preferred over powders or bonded forms. They are typically deposited on surfaces by advanced vacuum deposition processes (e.g., sputtering, ion plating, and ion-beam-assisted deposition) to achieve strong bonding, dense microstructure, uniform thickness, and long wear life [22].

1.1.3.3 Additives for lubricants

There is large number of additives that are normally added to the lubricants in order to improve their performance: antioxidants, corrosion inhibitors, detergents, pour point depressants, viscosity index improvers, dispersants, foam inhibitors, friction modifiers and antiwear agents. The last two types of additives are especially important for the tribological behavior of the lubricant.

Antiwear additives for boundary and mixed lubrication work in two different ways. Either they promote a reaction with the metallic surface or they are physically adsorbed into it.

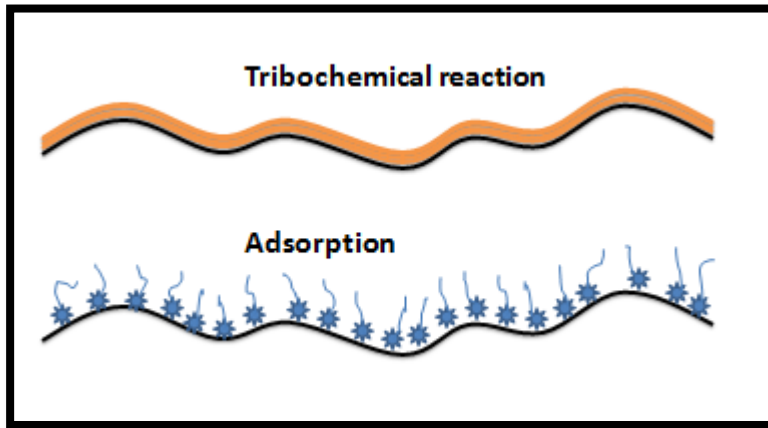


Figure 1. 7 - Antiwear additive's activation mechanism: tribochemical reaction and surface adsorption.

The most common antiwear additive for engine oils, the zinc dialkyl dithiophosphate, known also with the acronyms ZDDP, belongs to the group that are adsorbed on the surface in order to form a tribolayer. This compound was patented as lubricant additive in the US at the beginning of the 1940s [32-36], but initially it was considered mainly as an antioxidant and anticorrosion agent. Nowadays it is accepted the idea that, because of the high temperature and high pressure met during the tribocontact, the ZDDPs breakdown and generate reaction products that form an antiwear sacrificial film which improves the wear characteristics of the metal [37,38].

In particular, it has been observed that the film has a layered structure which contains both phosphates and thiophosphates, where polyphosphate with shorter chain are located in the bulk while longer chain polyphosphate were found on the surface. In this matrix zinc cations act as the primary glass network modifiers [38-41]. Even if the formation process of the film has not been completely understood, the mechanism postulated is that the ZDDPs are partially adsorbed into the metallic surface and then transformed by triboreaction into a polyphosphate. Anyway it should be highlighted that the special conditions generated during the tribocontact is

absolutely necessary for the formation of the protective tribolayer and that the nature of the tribofilm is greatly influenced by the working parameters, the duration of the contact and on the nature and microstructure of the metals in contact [42,44].

Even though the performance of ZDDPs is excellent, they are harmful to the environment. They are toxic for humans and aquatic wildlife and the presence of zinc and phosphates clogs the catalytic converters compromising their ability to reduce toxic pollutants in exhaust gas.

For these reasons, the governments of the most developed countries have been limiting the maximum level of ZDDP in the motor oil over the past 40 years and there is the urgent need to find a valid substitute for the future.

Another common additive used for high temperature operations is the tricresyl phosphate, (TCP) which is commonly used in turbine engines [45].

Studies realized on TCPs suggest that the antiwear protection afforded is the result of the formation of a reaction film on the rubbing surfaces of the metals. Generally, these reaction films are composed of a number of metal phosphates or phosphides.

1.2 IONIC LIQUIDS

1.2.1 Introduction to ionic liquids

“Ionic liquid” is simply the name that was attributed to salts when they are found in liquid state. Sometimes this term has been restricted only to the salts that are liquid below an arbitrary temperature (for example 100 °C) but from a chemical point of view it is difficult to found a reason to distinguish between salts with high melting point and low melting point. What could be determinant instead for the differentiation of the salts in liquid state at relatively low temperature are the practical applications that could be found.

The conventional temperature of fusion for a salt is normally considerably high (for example in the case of the sodium chloride is 803 °C) and this precludes their use in

many applications. On the contrary, with a compound that shows low melting point it is possible to obtain all the benefits that come out from having ionic bonds between the moieties but at a relatively low temperature, often even at room temperature.

In order to decrease the melting temperature, the ionic liquids are constituted by a low symmetry organic cations. In this way, due to the asymmetric and delocalized charge, the lattice energy is lower and the anion-cation interaction minimized.

In tribology, initially alkyimidazolium cations were the most commonly studied because it could be easily found. After the first period, also alkylammonium, alkyrrolidinium and alkylphosphonium were investigated thoroughly. Figure 1. 8 shows their structures.

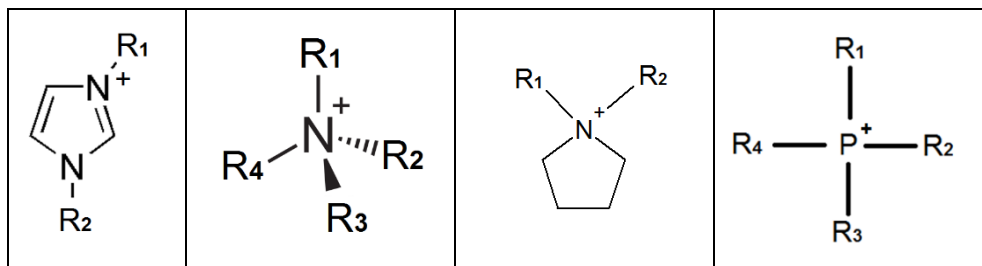


Figure 1. 8 - Cations normally used for ionic liquids synthesis: a) imidazolium, b) ammonium, c) pyrrolidinium, d) phosphonium.

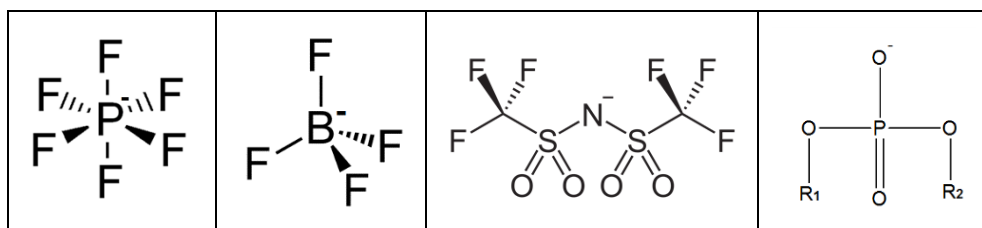


Figure 1. 9 – Anions normally used in the synthesis of ionic liquids: a) hexafluorophosphate, b) tetrafluoroborate, c) bis(trifluoromethylsulfonyl)imide and d) dialkylphosphate.

For the anion, initially many efforts were spent in the characterization of hexafluorophosphate and tetrafluoroborate but because of problems related with hydrolysis and corrosion the investigations were focused more toward structures as bis(trifluoromethylsulfonyl)imide and alkylphosphates (Figure 1. 9).

A common statement about the ionic liquids is that they have many outstanding properties:

- Negligible vapor pressure
- Broad liquid range
- High thermal stability
- Controlled miscibility
- Large electrochemical window
- Non flammability
- Low toxicity.

Even though this is partially true, it can be considered a sweeping statement that can lead to confusion. Although some of these characteristics that are undeniable for the ionic liquids, such as high conductivity and low vapor pressure, for other characteristics it is more difficult to generalize. They depend on the ionic chemical structure and on the cation/anion interaction.

Even if it is difficult, if not impossible, to find all the good properties mentioned in a single ionic liquid, it is feasible to design specific structure, through substitution of the anion or of the cation, and to obtain compounds with tailor-designed properties as to assure the application requirements. For example, it has been demonstrated that changes in the anion can influence the chemical behaviour and the stability of the ionic liquids: bis(methanesulfonyl)amide and the bis(trifluoromethanesulfonyl)-imide anions give high hydrogen bonding, fluorination and conductivity [46,47] while the ionic liquids with carboranes and ortoborates are inert, low coordinating and non fluorinated [48,49]. Moreover, the use of different cations can have effect on the physical properties, as viscosity, melting point and density [50-53].

Just to give an idea of the high number of ionic liquids that can be produced, it has been estimated that it is possible to synthesize at least one million of simple ionic

liquids and that considering binary and ternary mixtures there are approximately 10^{18} accessible room temperature ionic liquids [54].

1.2.2 History of ionic liquids

Concerning the history of ionic liquids, it is worth mentioning that the first ionic liquid found in literature was a “red oil” obtained during a Friedel-Crafts reactions using benzene, chloromethane and AlCl_3 [55,56]. This happened during the second half of the 19th century but it was only in the following century that analyzing this compound by NMR it was discovered that this red fluid has a tetrachloroaluminate anion and an alkylated aromatic ring cation, which means that it was an ionic liquid [57].

Again in the 19th century, precisely in the 1888, S. Gabriel and J. Weiner [58] discovered the ethanollammonium nitrate ionic liquid which had a melting point of 52-55 °C.

These first examples of ionic liquids were created just by chance but did not generated great interest in the scientific community.

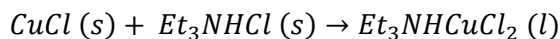
As first example in the history of voluntarily synthesized ionic liquid we should mention the Ethylammonium nitrate ($[\text{C}_2\text{H}_5\text{NH}_3][\text{NO}_3]$), which was created in the 1914 by Paul Walden [59], a Latvian scientist who was leader of the Chemical Laboratories of the Accademy of Science in Saint Petersburg. The ionic liquid synthesized was a RTIL (Room Temperature Ionic Liquid) with a melting point of 12 °C. The ethylammonium nitrate was obtained through a process of neutralization of ethylamine with concentrated nitric acid. Unfortunately this ionic liquid didn't attract the attention of the scientific community because of its explosive nature.

In the 1934 Charles Graenacher patented an organic salt (N-ethylpyridinium chloride) that could have been used as solvent for cellulose but since the melting point was of 118 °C it had little practical value [60].

A few years after the end of the Second World War, in 1948, Hurley and Weir at Rice University patented an invention that “relates to the electrodeposition of aluminium on a suitable cathode from an electrolyte comprising a fused or liquid mixture of a suitable aluminium salt with an N-alkyl pyridinium halide” [61,62]. The problem in this case was that the system based on AlCl_3 and 1-ethylpyridinium bromide was chemically complicated and difficult to investigate. It took 27 years to overcome this problem.

1961 was an important year for the IL history, not because of new scientific discoveries but thanks to Bloom, who coined the term “ionic liquid” during a lecture at the Faraday Society on the “Structure and properties of ionic melts” [63].

In the sixties the interest for the ionic liquids grew and for the first time groups of researchers focused mainly on this issue were created. In 1963 John Yoke at the Oregon State University, with his group of researchers, has synthesized the triethylammonium dichlorocuprate that at 25 °C appeared as a light green “oil” [64]. This ionic liquid was obtained from a mixture of copper chloride and alkylammonium chlorides.



In the same year Lowell King, at the U.S. Air Force Academy, has started a research project in order to find a good substitute for the molten salts used as electrolytes in thermal batteries. Since the main difficulty was due to the high temperature of the electrolyte (in the range between 375 and 550 °C), which was giving worries both for the battery itself and for the other devices in close proximity, his self-evident choice was to orient the study toward the ionic liquids. Since then the U.S. Air Force Academy has always had a group of researcher working in this field [50].

In 1973 Bockris dedicated a whole chapter of his book on electrochemistry to a particular kind of molten salts based on tetraalkylammonium cation that can guarantee stability at low temperature and can have a broad liquid range [65]. It was

a sign of appreciation of the potential of the ionic liquids from a scientist that was not directly involved in this field.

In 1975 a group headed by Osteryoung found out that a mixture of aluminum chloride and 1-butylpyridinium chloride have a liquid state at low temperature for a concentration of aluminium chloride between 60 and 67%. This result was particularly important because this system could be considered as an extension of the study conducted by Hurley in 1948 with the difference that this mixture had a much easier chemical formulation compared with the previous one. The application of this ionic liquid has been patented by the United States Air Force as battery electrolyte [66]. The main problem for the system of ionic liquids that has been elaborated was that it had a narrow compositional range as can be seen in Figure 1. 10.

In 1984 Magnuson thought to use ionic liquids as reaction media for enzymatic catalysis. The aim of the research was to figure out the influence of the ethylammonium nitrate $[\text{C}_2\text{H}_5\text{NH}_3][\text{NO}_3]$ on the activity and stability of the enzyme alkaline phosphatase. The result was that the enzyme was less active in aqueous solution of ionic liquid than in water [67].

All the results reported until now are about ionic liquid that were unstable, prone to hydrolysis and for this reason difficult to handle but in the 1990 Zaworotko, who has taken a sabbatical leave at the Air Force Academy, decided to focus his work on the synthesis and characterization of salts with dialkylimidazolium cations with water-stable anions [50]. In the 1992 Wilkes and Zaworotko reported the results of this study: 1-ethyl-3-methylimidazolium cation with hexafluorophosphate (PF_6) or tetrafluoroborate (BF_4) as anion has been the first ionic liquid stable in presence of air and water. Due to the importance of this new achievement the researchers decided to classify the air/water stable ionic liquids in a new category, the second generation ionic liquids [68].

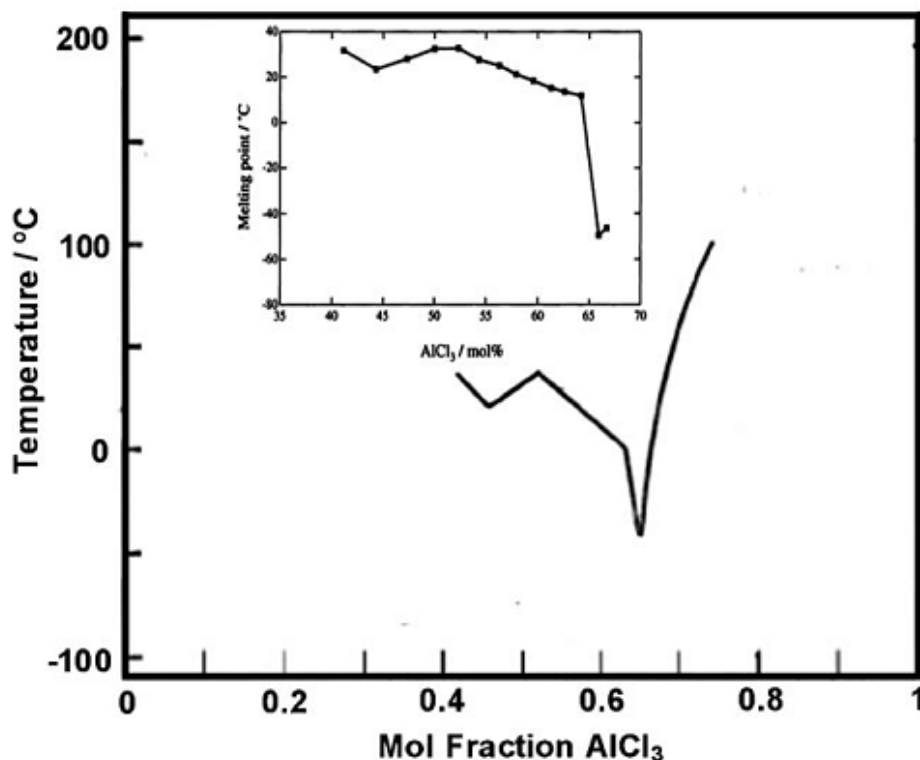


Figure 1.10 – Two partial phase diagrams for [C₄Py]Cl–AlCl₃ [66].

The 20th of April 1999 a consortium of 16 industrial members gave birth to the QUILL (Queen's University Ionic Liquid Laboratories) Research Centre in Belfast. In this research center have worked and still work many of the most brilliant scientists that study ionic liquid as John S. Wilkes, Doug MacFarlane, etc.

Another important event in the history of the ILs has been the workshop organized by the NATO in Crete in 2000. The title was “Green Industrial Applications of Ionic Liquids” and there were 65 scientists coming from all around the world. During the meeting a round table was held in order to outline the strategy for the development of ILs for industrial applications [69]. Among the other points, it was established that:

- in order to encourage development of applications it was necessary to have a good number of compounds well characterized and free of intellectual property
- it was necessary to have data about toxicity, biodegradability, bio-accumulation, safety, health and environment impact
- a website had to be created with the database of the physical and thermodynamic properties and it had to be accessible to everybody
- it was essential to encourage international collaboration, also including different areas of expertise.

Another important issue that was discussed during the meeting was the concept, introduced by Davis Jr., of task-specific ionic liquids. It was the beginning of the third generation of ionic liquids.

Since this thesis is centered on tribology it could be opportune to talk about the research of Liu et al. In 2001 they started to investigate imidazolium tetrafluoroborate ionic liquids as lubricants for various tribo pairs. In all the cases, ionic liquids showed significant friction reduction. It was the first tribological investigation about ILs and since then number of published articles in scientific journals in field of tribology is constantly increasing [20].

In 2002 BASF announce the first commercial process using ionic liquids with the name of BASIL (Biphasic Acid Scavenging utilising Ionic Liquids). This process is used in industrial scale to remove acid by product. The method used before 2002 was based on the use of tertiary amines that had as final product of the reaction solid salts floating as suspension. Unlike the laboratory process, were a suspension is not difficult to remove, in an industrial scale these solid particles were source of problems. By replacing the triethylamine with the 1-methylimidazole the salt produced in the reaction was a 1-methylimidazolium chloride, an ionic liquid with melting point of 75°C and then easier to handle.

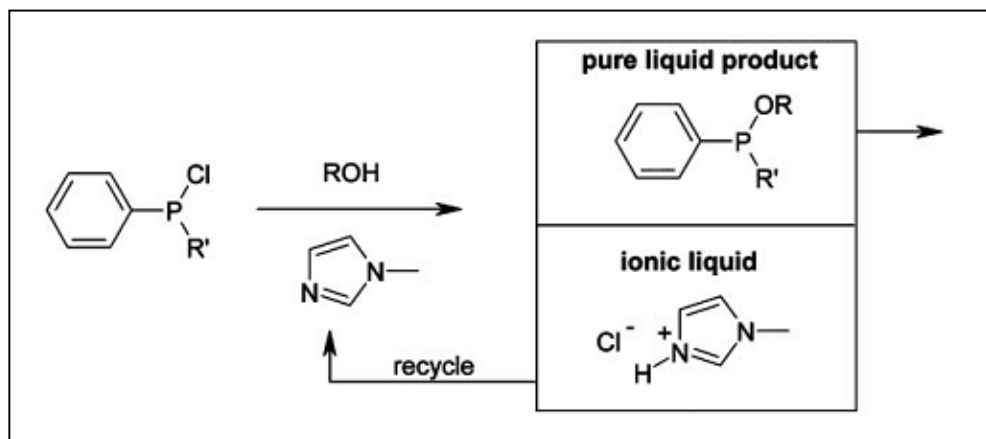


Figure 1. 11 – Schematic representation of the BASIL process [69].

The BASIL process improved the space-time yield¹ from $8 \text{ Kg} \cdot \text{m}^{-3}\text{h}^{-1}$ to $690,000 \text{ Kg} \cdot \text{m}^{-3}\text{h}^{-1}$ [69] Figure 1. 11.

In 2006, when it was almost universally believed that ionic liquids had not evaporation, Earle et al. demonstrated that at high temperature and low pressure it was possible to distil ionic liquids and that they could be separated by fractional distillation [70]. This finding at first generated a perplexity in the community of the researchers that were working with ionic liquids because they had always asserted that due to their negligible volatility they could have been included in the list of the green materials. But in the same year and from one of the author that had collaborated with Earle it was clearly explained that even if in extreme conditions there is evaporation, in ambient conditions the volatility is negligible and for this reason it can be assured that they cannot produce atmospheric pollution, especially in comparison with other liquid solvents [71].

¹ The space time yield σ_p represents the mass of a product P formed per volume of the reactor and time. $\sigma_p = \frac{m_p}{vt}$

Since the year 2000 the number of publications related with ionic liquids have continued to grow, not just in tribology but in many fields, as can be seen in Figure 1. 12.

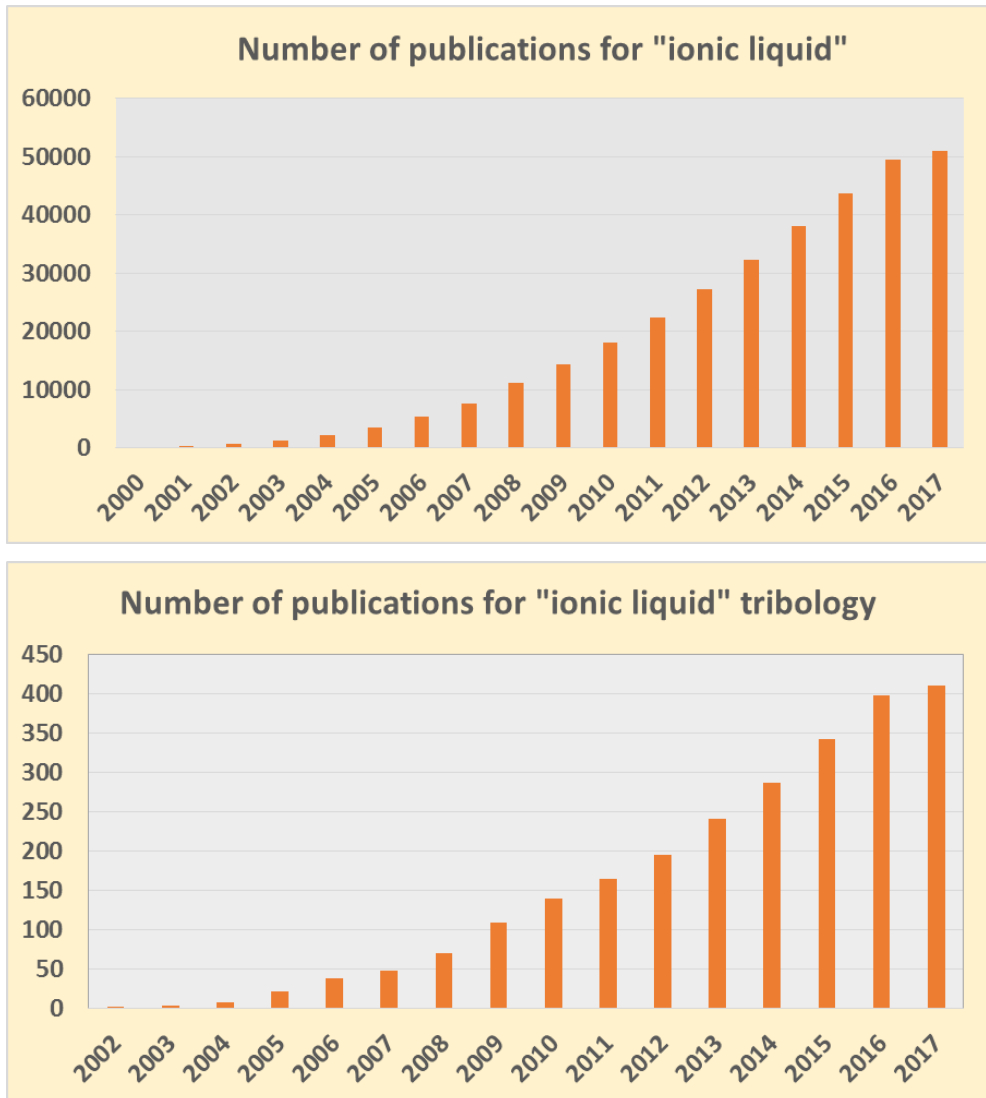


Figure 1. 12 – Number of publications found on Scopus with the terms “ionic liquids” and “ionic liquid” + tribology. The results correspond to the global number in the year indicated.

1.2.3 Physico-chemical properties of ionic liquids

It has already been said that the growing interest generated by the ionic liquids is due to the peculiar characteristics that they show. This chapter will consider just a few of them, those who have a closer link with tribology.

1.2.3.1 *Melting point, thermal stability and liquid range*

In the definition of the ionic liquids there are two important properties that are mentioned. The first one is the ionic nature of the bond between cation and anion, and the second is the state of the compound, that has to be liquid (possibly with melting point inferior to 100 °C). It is obvious therefore that many studies have been carried out in order to establish criteria for the formulation of salts with low melting point. The main difference that can be found between normal molten salts and ionic liquids is that the seconds have usually “ugly” molecules. This means that they are composed by an organic ion with large asymmetric chains. In this way the irregular shape prevents the ions from packing together neatly and lowers their lattice energy. In the 2010 Dean et al. have listed the parameters that can influence the melting point of the molten salts [72]. The parameters that play a role on the melting temperature are:

- The size of the anion: bigger anions have lower melting point;
- The conformational flexibility: higher flexibility of the chain lead to lower melting point;
- Packing efficiency: a better packing corresponds to a higher melting point;
- Symmetry of the cation: cations with higher symmetry show superior melting point;
- Length and conformation of the organic chain;
- The addition of functional groups: the presence of functional groups decreases the melting point;
- Charge delocalization: the bigger is the distance between ions the lower is the lattice energy and as consequence the lower is the melting point.

The impurities content has also a really important effect on the transition temperature but it is not easy to fix correlation even because in most of the works the contamination content is not mentioned.

An important phenomenon that can be often noticed with the ionic liquids is the supercooling. Ngo et al. have observed through Differential Scanning Calorimetry (DSC) that the freezing point is, in many cases, significantly lower than the melting point. In Figure 1. 13 is shown the result of the analysis on iso-propylmethyl imidazolium hexafluorophosphate salt that demonstrate this phenomenon [73]. According to this study the imidazolium salts have lower melting point while the halides display greater supercooling. These effects can be explained with the tendency of the ionic liquids to create metastable glass phases.

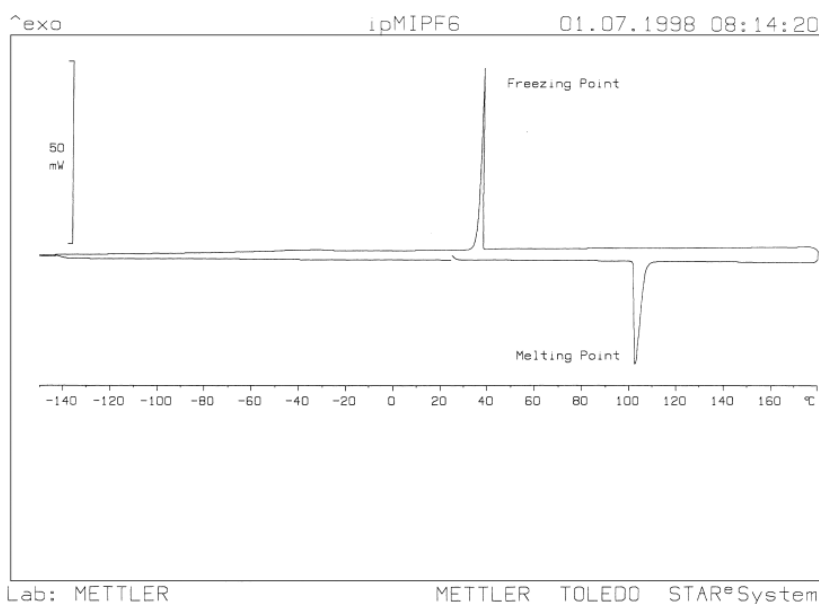


Figure 1. 13 – Difference between the melting point and the freezing point of iso-propylmethyl imidazolium PF6 ionic liquid [73].

The thermal stability corresponds to the onset temperature of the liquid, which means the limit temperature after which there is degradation. The liquid range instead is given by the difference between the boiling point and the melting point. Because of

their low vapor pressure, in the case of the ILs the decomposition comes before the evaporation, so that in this case the liquid range is calculated between the degradation and the melting point. For the water at ambient conditions, the liquid range goes from 0° C to 100° C while the ionic liquids have a melting point lower than 100 °C and in some cases their degradation point is over 400 °C, which means a difference of temperature 3 times bigger than what we have for the water. Hence it is easy to understand why they have attracted the attention of the researchers and of the industry as transfer heat fluids and as solvents.

Anyway, it should be noticed that the majority of the data collected about the thermal degradation of the ionic liquids refer to thermogravimetric analysis (TGA) tests performed with fast scan (10-20 °C/min) under dry nitrogen. In an article published in the 2004, Komulsky et al. state that these conditions do not correspond to the actual ones that we find in real applications and for this reason have less validity [74].

Komulsky demonstrated that the heating rate can have a relevant importance in determining the onset point. As it can be seen in Figure 1. 14, using a lower scan rate the degradation starts at lower temperature. Obviously it is impossible to deny the importance of the scan rate in this kind of tests, and it could be useful to have more data of test performed in different conditions; but it is reasonable to think that if the majority of the tests have been performed in similar conditions there is still the possibility to have a reliable comparison of results.

It has also been reported that the nature of the material in contact with the ionic liquid can have influence on the thermal stability. For instance, if the test is performed in a crucible of aluminum, the resistance to the thermal stress is reduced in comparison to the test with aluminum oxide.

1.2.3.2 Density

Generally the density of the ionic liquids is bigger than the density of the water and varies in the range between 1 and 1.6 g/cm³ [75], even if it is possible to find ionic

liquids out of this range. Among the parameters that can have influence on the density it is worth mentioning the length of the organic chain of the ions. For similar ionic liquids the density decreases with the increase in the weight of the organic ions [73].

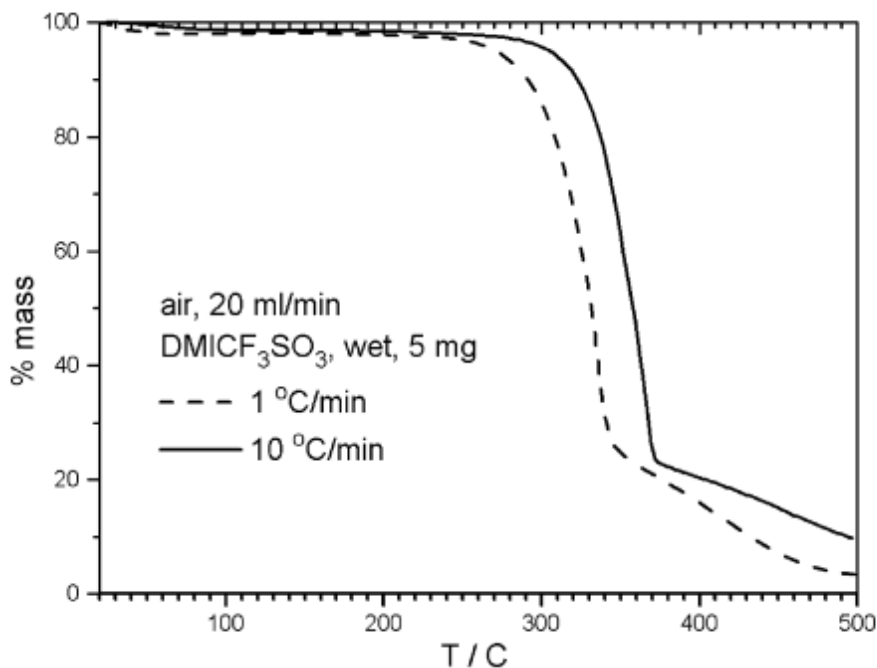


Figure 1. 14 - Effect of the scan rate on the same ionic liquid. [74].

There are also many studies that have analyzed the influence of temperature on the density of the ionic liquids and the result is that exists an almost linear decrease of density with the increase of temperature. The typical value of thermal expansion coefficient is around $5 \cdot 10^{-4} K^{-1}$. This value is the double of the coefficient of thermal expansion for the water and three times lower than what can be found for the common organic solvents [75].

The density is probably the physical property of the ionic liquids that is less affected by the impurities. Jacquemin et al. have measured the density for 6 hydrophobic and

hydrophilic ionic liquids in dry and saturated conditions and as result they have found that the difference is negligible (1-2%) [76].

1.2.3.3 Viscosity

The term viscosity indicates the resistance to flow for a fluid and can be expressed as dynamic viscosity (Pa·s or Poise) or cinematic viscosity (cm²/s or Stokes). The relation between the two dimensional units is that cinematic viscosity correspond to the dynamic viscosity divided by the density ($v = \eta/\rho$; where η is the dynamic viscosity, ρ the density and v is the cinematic viscosity).

The viscosity is a key parameter for a lot of practical applications where a fluid medium is required since it plays an important role in stirring, mixing and pumping operations. For some applications it could be required a low viscosity while in other applications it is more suitable a fluid with high viscosity. In the case of solvents for example it is necessary to have a fluid with low resistance to flow, instead for tribological applications the viscosity should be much higher.

Thanks to their great variety and thanks to the possibility to create tailored-made ionic liquids it is possible to cover a wide range of viscosity in function of the properties required. Till now the viscosities found for the room temperature ionic liquids vary from 10 cP to 10⁵ cP.

There are many factors that have influence on the viscosity of the ionic liquids; among these, one of the most important is the temperature even if it is not so easy to fix correlations between these two parameters since it has been demonstrated by many authors that often the ILs don't follow Arrhenius equation [77].

Okoturo and Noot have evaluated the behavior of 23 ionic liquids with different structures and have found out that there is a relation between the cation's symmetry and the plot viscosity-temperature:

- ionic liquids containing less symmetrical cations and without functional groups in the alkyl chain have a viscosity temperature plot that is described by the Arrhenius model:

$$\ln \eta = \ln \eta_{\infty} + E_{\eta}/RT$$

Where E_{η} is the activation energy for viscous flow and η_{∞} is the viscosity at infinite temperature

- ionic liquids with small, symmetrical cations and low molar mass have a behavior described by the VTF (Vogel–Tammann–Fulcher) model:

$$\eta = (A_{\eta}\sqrt{T}) \exp[-k_{\eta}/(T - T_0)]$$

Where T_0 is glass transition temperature, k_{η} is a constant and the product $k_{\eta} R$ has been identified with the Arrhenius activation energy and A_{η} is another constant

- ionic liquids that have cations with low symmetry, with functional groups and high molar mass cannot be described through Arrhenius or Vogel-Tamman-Fulcher (VTF) model.

The data present in literature about the viscosity show a low reproducibility of the results with the same ionic liquid. Obviously the variability can be caused by different procedures or different machines but there is also another factor that is responsible: the impurities.

1.2.3.4 Environmental impact

Starting from the 1 June 2007, the European Community has established new restrictive norms for the use of chemical substances through the REACH (**R**egistration, **E**valuation, **A**uthorisation and **R**estriction of **C**hemical substances) and it has become impossible to use in large scale any new compound, including the ionic liquids, without a deep analysis of its toxicity and biodegradability.

Due to their low volatility, the ionic liquids have always been known as fluids with a low impact on the pollution of the air, but in the last years the concern about other environmental issues has grown; in particular, considering the fact that the ILs have a non volatile nature and could be easily soluble in water, it is particularly important to determine what is the impact on the aquatic ecosystem.

The normative says that the kind of tests that have to be performed depends on the total amount of material that should be produced. It means that, while for a small production the cost of this study is reasonable, in the case of an industrial production the expense can be of the order of hundred thousand euro. This is the reason that has led many universities and research centres to focus their work on the determination of a correlation between the chemical structure and the potential environmental hazard.

Stefan Stolte et al. analyzed a great number of compounds in order to understand the influence of the structure and of the physico-chemical properties on the toxicity and the biodegradability of the ionic liquids [78].

The toxicity tests carried out were *Daphnia magna*, *Selenastrum capricornutum*, *vibrio fischeri*, Cytotoxicity and Acetylcholinesterase. In these types of tests a small amount of ionic liquids is introduced in an environment in which some microorganisms are present. The objective is to check, after a fixed period of time, if the population has been affected by the presence of the substance examined.

They found out that the toxicity of the ionic liquids depends mainly on the cation and in particular an increase of the alkyl chain causes an increase of toxicity. The same influence has been observed by Couling et al. who formulated an interesting theory to justify this behaviour: "Many ILs are similar to cationic surfactants, which are known to induce polar narcosis due to their ability to be incorporated into biological membranes. Therefore, longer alkyl chains may be incorporated into the polar headgroups of the phospholipid bilayer, which are the major structural

components of membranes. Narcosis then results because membrane-bound proteins are disrupted by the toxicant” [79].

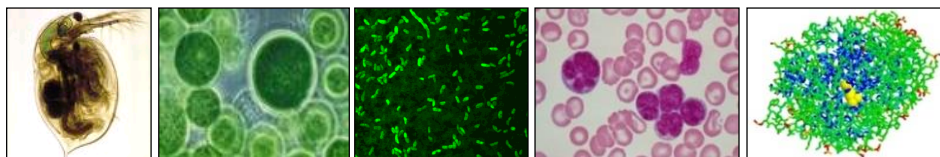


Figure 1.15 - Toxicity tests: *Daphnia magna*, *Selenastrum capricornutum*, *Vibrio fischeri*, Cytotoxicity and Acetylcholinesterase

In the same paper it has also been emphasized that imidazolium and pyridinium compounds are more toxic than common solvents as acetone methanole and acetonitrile, while ionic liquids with quaternary ammonium and short alkyl chain and ILs containing choline can be environmental friendly.

The biodegradability is usually evaluated with some standardized tests classified as OECD 301 D (Closed bottle), OECD 301 F (Manometric respirometry), OECD 301 B (CO₂ evolution). In this case what is important to observe is the quantity of oxygen needed to degrade the compound in a determined period of time.

Observing the results of the studies carried out till now on the biodegradability of the ionic liquids it is difficult to draw strict conclusions about the influence of the structure; however there are some functional groups that are known to be more biodegradables than others. “The studies indicated that biodegradation increased when a compound contained a functionality that might undergo enzymatic hydrolysis, or a functional group like a hydroxyl, an aldehyde, a carboxylate group, an unsubstituted linear alkyl chains or phenyl rings” [80].

1.2.4 Ionic liquids in tribology

As already mentioned, the first experiment of ILs in tribology was reported in 2001 with the work of Liu et al. [81]. In that research, imidazolium tetrafluoroborate was tested as IL-based lubricant for various tribo-pairs and, in all experiments, the use of the IL showed significant friction reduction. Since that time, the interest of scientists

in tribological properties of ILs has considerably increased [82,83], especially for boundary conditions. This is because, even if they can work properly also in other lubrication conditions, their more important tribological properties is the ability to easily generate a protective tribolayer between the rubbing surfaces

As a general conclusion, from what was observed by most of the researchers, both anion and cation play a fundamental role for the tribological performance of the lubricant. The high reactivity of the anion joint with the adsorption ability of the cation are able to create effective tribofilms on the metallic surfaces.

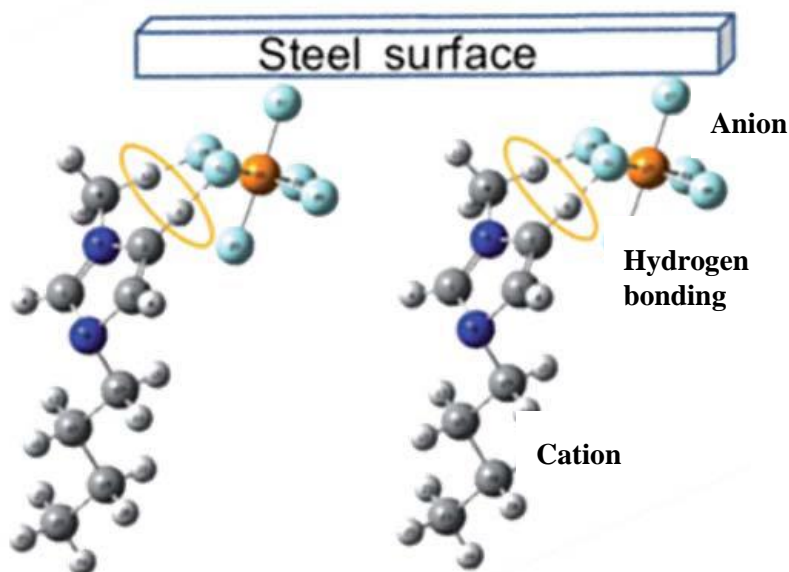


Figure 1. 16 - Interaction of the ionic liquid with the metallic surface [84].

In 2009 Minami wrote a quite complete review of the tribological investigations carried out on the ionic liquids [85]. From the data collected in the review, it is possible to see that for the first period the tribological studies were considering almost exclusively imidazolium structures. The choice of this cationic group was mainly due to the fact that the synthetic reaction necessary for introducing functional groups in the imidazole ring were already known but there were also other reasons. The thermal stability of the imidazolium cations was attractive for tribological

applications and the imidazolium group was considered quite versatile for designing molecules with specific properties.

The correlation between the imidazolium alkyl chain length and the friction coefficient was studied using ionic liquids containing NTf_2 anion. It was demonstrated that the increase of the alkyl chain leads to the reduction of friction forces. This phenomenon could be attributed to the increase of the viscosity and to the fact that, in a Bowden-Tabor model, a longer chain is beneficial for preventing direct contact between the surfaces [85-88].

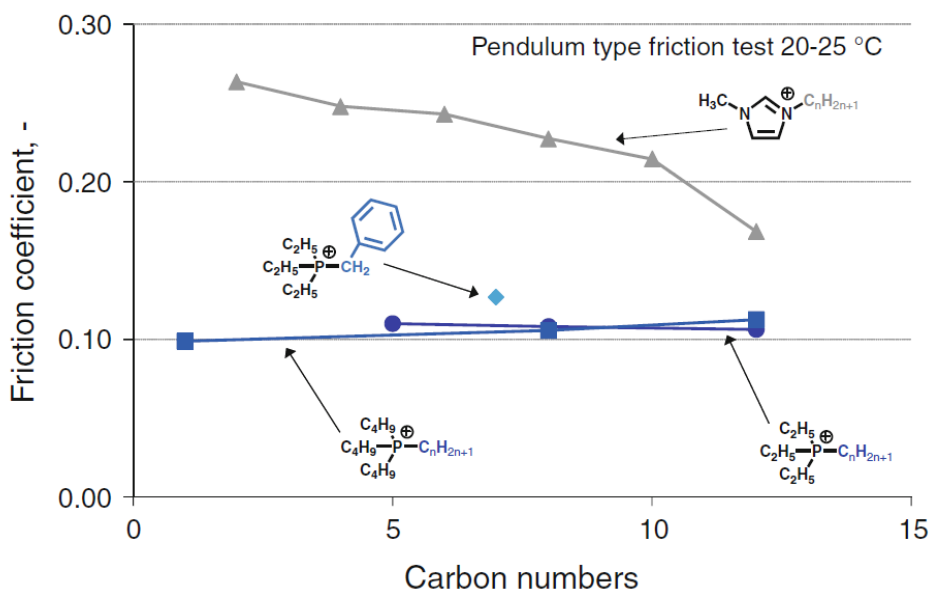


Figure 1. 17 - Structure–friction relationship for NTf_2 salts. Influence of the cationic alkyl chain on the tribological performance [87].

In Figure 1. 17 it is possible to see the variation of the friction coefficient with different structures depending on the length of the cationic alkyl chain. All the experiments were realized with ionic liquids based on NTf_2 anion.

More recently, the investigations have dedicated many attention to the alkyphosphonium moieties because they should have better thermal stability than

the imidazolium ones and they should be soluble in many oils [89,90]. The Oak Ridge National Laboratory, in collaboration with other institutes, studied many different types of phosphonium based ILs in order to understand the effects of the cation alkyl chain and the interaction cation-anion on the performance of the ionic liquids oils [91,92]. As result, it was found that the cationic alkyl chain length can be a key parameter for the solubility in nonpolar hydrocarbon oils. The longer the chain, the better the solubility (six carbons being the critical minimum). Another important parameter found was the symmetry of the cation. Symmetric phosphonium cation presented higher viscosity, thermal stability and density because of closer packing. From the tribological point of view, the combination with the anion is a very important. The anion that performed better with phosphonium cations was organophosphate. After this there was carboxylate and finally the worst result was obtained with sulfonate.

Also Minami et al. analysed many phosphonium ILs trying to understand their behaviour and to figure out the tribo-chemical reactions that take place on the surface [90]. First of all, they realized that the coefficient of friction is not very much influenced by the alkyl chain length. In Figure 1. 17 it is possible to see the difference observed between the imidazolium cations and the phosphonium ones. The addition of a benzyl group was not beneficial to the friction coefficient of the lubricant since the friction increased. The X-ray photoelectron spectroscopy (XPS) of the surfaces allowed the creation of a model of tribofilms that can be found using phosphonium and imidazolium cations with phosphate, thiophosphate and NTf_2 anions. For imidazolium cation with NTf_2 anion a tribolayer made of metal fluoride was found. The same kind of tribolayer, was observed also with tributylmethylphosphonium bis(trifluoromethylsulfonyl)amide ($\text{Bu}_3\text{MeP-TFSA}$) when it was working in high load conditions. With lower load instead, $\text{Bu}_3\text{MeP-TFSA}$ generated on the rubbed surface a tribolayer with the presence of metal fluoride, metal phosphate and organic fluoride. With the phosphate and thiophosphate ionic liquids, that have a structure similar to that one of conventional antiwear additives (ZDDP), the protective

tribolayer is made of iron phosphate. Small traces of sulphide were found on the surface lubricated with thiophosphate IL. Considering the fact that the performance of thiophosphate was better than the performance of NTf_2 it can be considered that the phosphate tribolayer is more effective than the fluoride one.

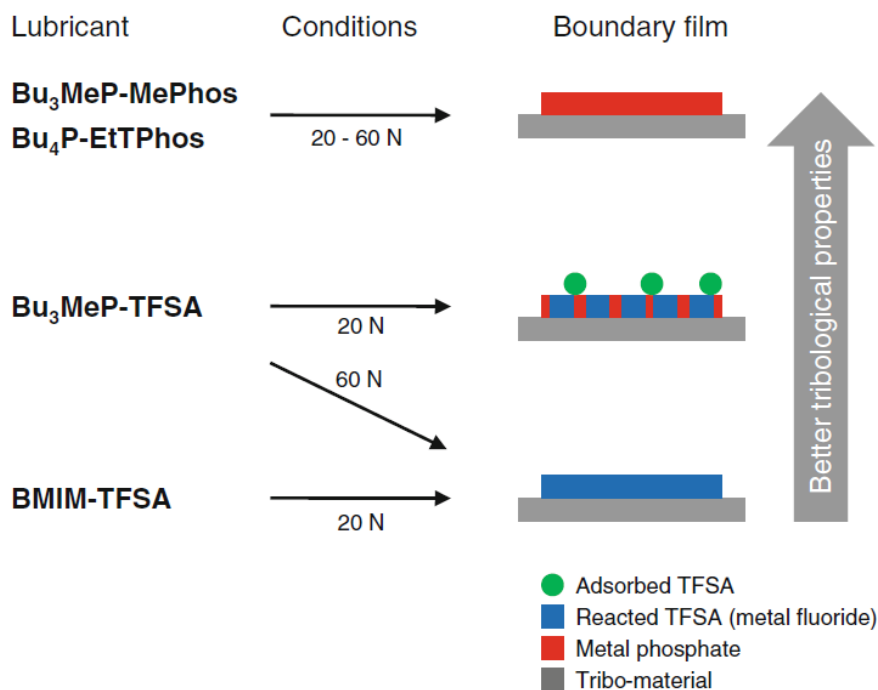


Figure 1. 18 - Proposed model of boundary film derived from phosphonium [90]. In the graph BMIM is butylmethylimidazolium, Bu₃MeP is tributylmethylphosphonium, BU₄P is tetrabutylphosphonium, TFSA is bis(trifluoromethylsulfonyl)amide, MePhos is dimethylphosphate and EtTPhos is diethylphosphorodithioate.

It is evident then that the structure of the anion is extremely important for defining the tribological performance of the ionic liquids because it is determinant for the formation of a protective tribolayer [87].

The synthesis of the ionic liquids is not easy and inexpensive, especially if you want to limit the presence of contaminants and water. For this reason, at the beginning many studies experiments were realized on tetrafluoroborate and hexafluorophosphate, that “were easily available as reagents at a reasonable cost”

[85]. In 2002 Liu et al. published the results of their tests with 3 alkyimidazolium tetrafluoroborate ionic liquids and two other fluorine containing lubricants for space applications. The tests were carried out in air and in vacuum with steel/steel contact and showed that the ionic liquids can have friction coefficient and wear lower than the other tested lubricants. XPS analysis on the worn area detected a layer formed of metal fluoride, most probably FeF_2 and B_2O_3 which should be responsible of the friction and wear reduction.

Jimenez, under the guidance of Bermudez, studied the lubrication of aluminium steel contact using alkyl imidazolium BF_4 and PF_6 [93-96]. They saw that these fluorine containing anions can have good tribological performance but they can cause tribocorrosion when they are used as neat lubricants. Using them as additives could improve their performance since the risk of corrosion would be much lower; anyway the type of base lubricant should be considered carefully. While the ionic liquids tested were not miscible in ester base oils, they showed good miscibility and tribological performance with mineral oils (sometimes they behave better as additives than as neat lubricants). The effectiveness of the IL performance when it is used as additive, depends on many factors (chain length, anion composition, miscibility with the base oil, atmospheric moisture, etc.) and cannot be extrapolated simply by the behaviour as neat lubricant [95]. Finally, analyzing the worn surfaces after the tests, they found out that the wear debris generated were made of aluminium fluoride while in the wear scar aluminium oxide was mainly present. Also, using BF_4 it was possible to detect boron oxide and iron fluoride, while with PF_6 a tribolayer containing aluminium and phosphorous was found on the steel ball [93].

Most of the studies realized with ionic liquids describe tests with metals, since it is known that the anion can easily react with the rubbed surfaces. Nonetheless, there are also studies that demonstrated good lubricity of the ionic liquids with ceramic materials. Phillips and Zabinski investigated the effect of two alkyimidazolium ionic liquids (with BF_4 and PF_6 anion) diluted in water for a ceramic/ceramic contact [97]. Water is already a good lubricant for ceramics. It is known that with Si_3N_4 an

hydrated silicon oxide layer is generated, which make the surface finely polished and gives friction coefficients typical of hydrodynamic lubrication. Anyway, before getting such a low friction, the surfaces undergo a running-in period with high friction. The experiments showed that using 2% w/w of ionic liquid in water incredibly reduces the running-in, from 8000-9000 cycles to less than 400 cycles. The mechanism proposed is based on the existence of an electric double layer made of molecules with opposite charges. The Si_3N_4 surface has a negative charge, which means that it should be able to attract the cations close to the surface. This kind of model had already been formulated for water systems [98,99] but it is likely that it can work even more efficiently with an ionic film.

The film thickness provided by BF_4 and PF_6 ionic liquids with imidazolium cation on a ceramic surface was thoroughly investigated by Arora and Cann [100]. By using an MTM (Mini Traction Machine) tribometer and a ball on disc optical device they could study the performance of the ionic liquids with different slide/roll ratio and the film thickness variation, depending on the sliding velocity and on the sliding duration. The experiments showed again the formation of an electrical double layer film formation

Despite their friction and wear reduction, BF_4 and PF_6 anions suffer hydrolysis in imidazolium-based ionic liquids [101] and this lead to formation of hydrogen fluoride, therefore problems with corrosion. Better properties in terms of corrosion, but also from a tribological point of view, were observed with hydrolytically stable and hydrophobic structures as (trifluoromethylsulfonyl)imide bis((trifluoromethane)sulfonyl)imide (NTf_2) and trifluoro-tris(pentafluoroethyl) phosphate (FAP) [90,93,102,104].

Hernandez et al. studied the behaviour of some ILs with bis((trifluoromethane)sulfonyl)imide as anion [102] and found out that the thickness of the tribolayer created can change according to the testing conditions. It was found out that, for higher loads and longer tests, the surfaces developed a thicker tribolayer.

For the same anion, Kamimura et al. tried to explain the mechanism that was leading to the formation of the protective film [87]. They analyzed the rubbed surfaces by XPS and Time-of-Flight Secondary Ion Mass Spectrometry (TOF-SIMS) and found the presence of organic fluoride, iron fluoride and iron sulphate, coming from the anion. An interesting point was that there was a difference in the boundary film structure between the area in the middle of the wear scar and the area in the border. Organic fluoride was observed mainly on the border of the worn area while the internal part was composed mainly by iron fluoride and sulphate. The difference in this case can be due to the harsh conditions met in the centre of the wear scar, where the contact pressure is superior. The process suggested by the results was of adsorption of the anionic moiety, followed by a tribochemical reaction.

Quite excellent properties were demonstrated also for FAP anion. It's high hydrolytic stability and hydrophobicity make it a better choice than BF_4 and PF_6 . It is also known that the thermo-oxidative stability of the ionic liquids increases with their hydrophobicity [105].

Minami et al. tested many cations in combination with FAP anion [104]. All the FAP ionic pairs tested showed coefficient of friction around 0.1 or lower. It was shown as the length of the cationic alkyl chain can influence the friction and wear with this kind of lubricants. Longer chains protect better the rubbed surface and reduce friction. Analyzing the surfaces lubricated with the ionic liquids, they arrived to propose the structure of the protective tribolayer generated. Organic fluoride and metal fluoride are present on the surface but only metal fluoride in the subsurface. Small traces of phosphorous containing substances were found on the surface by TOF-SIMS, which should confirm the decomposition of the anion. In addition to provide the mechanism of tribolayer generation, this study provided a comparison between the two ionic liquids with FAP anion and two analogues with NTf_2 . The results showed that the tribological performance of FAP is quite better than the performance shown with NTf_2 .

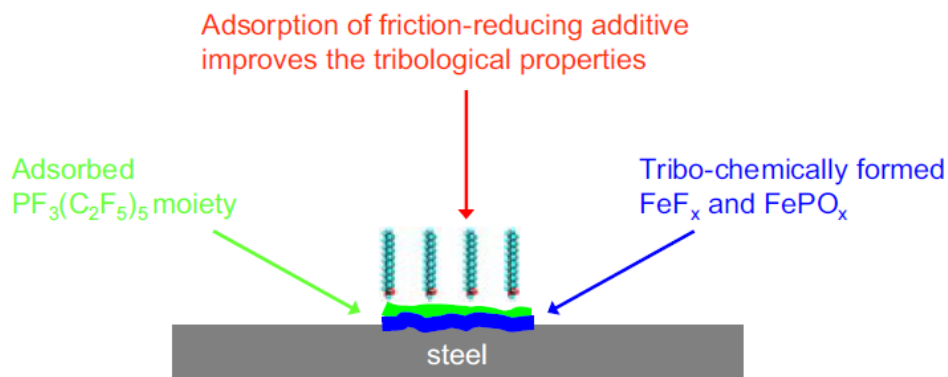


Figure 1. 19 - A proposed model of boundary film for lubrication with ionic liquids containing FAP anion [104].

Although many ionic liquids containing fluorine have shown excellent tribological performance, nowadays, the trend is to avoid the use of ionic liquids that contain halogen elements. Indeed, even though the reactivity of the halogens can provide a rapid tribolayer formation it could have the drawback of promoting corrosion.

An alternative to the use of fluorine containing anion could be the use of phosphorus containing ionic liquids.

Zhang et al. investigated three phosphate based ionic liquids with steel/steel sliding pairs [106] and found out that these ionic liquids did not cause corrosion. The ionic liquids had alkylimidazolium cation and a correlation was found between the cationic chain length and the tribological performance. As observed also in other cases, longer alkyl chains help in reducing the coefficient of friction. Analyzing the composition of the tribolayer, it was possible to observe the presence of and iron (III) phosphate that should provide good performance under boundary lubrication.

Ionic liquid with dimethylphosphate anion was also studied as additives for allylimidazole tributylborane and ethylimidazole tributylborane [107]. These base fluids were chosen because they have properties similar to that of the ionic liquids in terms of viscosity and melting point. Even though on their own they have not

shown good tribological properties [108], they could be still be valid base for ionic liquids, since they are capable of dissolving salts [109]. Totolin et al. confirmed that, although allylimidazole tributylborane and ethylimidazole tributylborane could react with the metallic surface and generate an oxide layer, the coefficient of friction and the wear were still too high for a lubricant. Instead, with the addition of a small percentage of phosphonium phosphate ionic liquid, the performance improved considerably, giving low friction and irrelevant wear. The XPS analysis showed that the ionic liquid formed an iron phosphate tribolayer. In the same study, also NTf_2 was used as additive. Its performance was good but not as much as for the phosphonium phosphate IL. The tribolayered generated was made of organic and inorganic fluoride, together with sulphates. Anyway, even if NTf_2 was able to reduce friction and wear, it was possible to observe a few spots of pitting corrosion due to the fluorine containing anion.

Although many advances have been made in the study of the ionic liquids, there are still many problems that should be solved and many aspects that need to be investigated. The main objective of this thesis was to widen the knowledge acquired up to now about the properties of the ionic liquids by studying new structures and by using new methods.

Chapter 2

2 Materials and Equipment

In this chapter, there is a description of the materials and equipment used for carrying out the tests. There is a description of the different kind of ionic liquids that were used, the base oils used for realizing the mixtures with the ionic liquids as additives and the specimens used for the experiments. There is also a description of the different instruments employed for realizing the characterization of the fluids, the tribological experiments and the analysis of the specimens and surfaces after the tests. The testing conditions are also detailed in the chapter.

2.1 MATERIALS USED

2.1.1 Lubricants

Different kind of ionic liquids have been studied in neat form and as additives. Here there is a description of the ionic liquids and of the base oils used.

2.1.1.1 *Ionic liquids*

The work realized is divided in 4 chapters and in each of them, the ionic liquids studied presented different characteristics. All the structures of the ionic liquids with their codifications are listed in Table 2. 1.

Pyridinium based ionic liquids: four ionic liquids were used for the research work described in the Chapter 3 (**IL1-IL4**). All the ionic liquids were synthesized in the University of Vigo within the framework of the Marie Curie Initial Training Network MINILUBES with Grant Agreement n° 216011-2. Two of them were new dicationic ionic liquids incorporating polyethylene glycol chains linking two N-alkylpyridinium moieties through ring position 2. Alkylsulfate and bis(trifluoromethanesulfonyl)imide (NTf₂) were selected as anions. The other two ionic liquids were the monocationic analogues, methylpyridinium methylsulfate [C₁Py]⁺ [C₁OSO₃]⁻ and methylpyridinium bis(trifluoromethanesulfonyl)imide [C₁Py]⁺ [NTf₂]⁻. The synthetic procedures are described in a published article [110]. The analysis of the chemicals obtained was realized by ¹H, ¹³C and ¹⁹F Nuclear Magnetic Resonance (NMR), Fourier Transfer Infra-Red spectroscopy (FTIR) and High Resolution Mass Spectroscopy – Electrospray Ionization (HRMS-ESI). The characterization of the fluids was carried out by the University of Vigo with the collaboration of IK4-TEKNIKER. The chemical characterization of the compounds is not part of this dissertation but it can be found in the PhD thesis of Maria Mahrova [111].

Dicationic ionic liquids: Also the ILs used for this study were synthesized, in the context of the Marie Curie Initial Training Network MINILUBES, by the Martin Luther University Halle-Wittenberg in Germany and by the University of Vigo in Spain. The basic concept of the dicationic IL made use of two different types of cationic groups, N-methylimidazolium and N-methylpyrrolidinium, which are connected by tetraethylene glycol (**IL5** to **IL10**), hexaethylene glycol (**IL11** to **IL13**) and oligoethylene glycol (**IL14** and **IL15**). For the synthesis of **IL14** and **IL15**, polyethylene glycol PEG1500 was used, which gave an average polymerization degree of 22 and 20, respectively. As illustrated in Table 2. 1, **IL11** to **IL15**, the cationic groups have been attached to the linking chain through additional triazole groups. The cations obtained have been paired with chloride, bis(trifluoromethanesulfonyl)imide, methylsulfonate and butylsulfonate anions. In

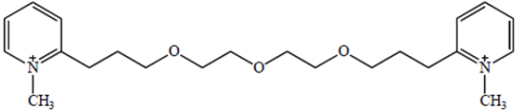
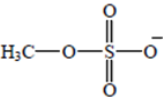
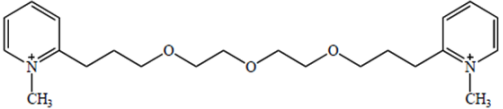
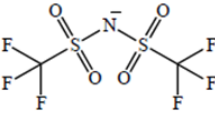
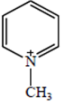
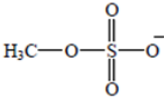
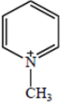
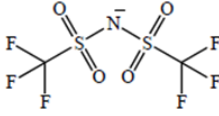
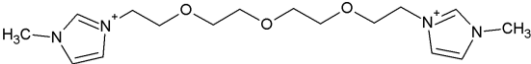
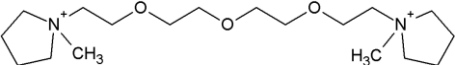
addition, one IL was formulated as a 9:1 stoichiometric mixture of tetraethylene glycol N-methylimidazolium NTf₂ and tetraethylene glycol N-methylimidazolium methanesulfonate to give **MIX**.

Phosphonium ionic liquids: For the study reported in Chapter 5, two ionic liquids were provided by Nippon Chemical Industrial (Tokyo, Japan). Both ILs are composed of phosphonium cations with alkyl side chains up to C₄ length, which according to Yu *et al.* could satisfactorily improve the miscibility of the compound in the oil [89]. The anions are dimethylphosphate in case of **IL16** and diethylphosphorodithionate for **IL17**.

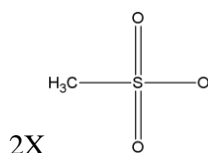
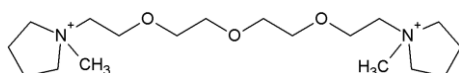
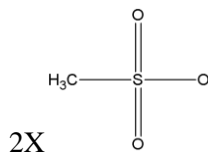
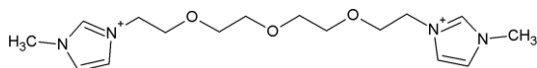
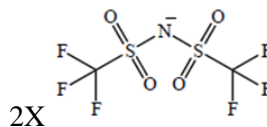
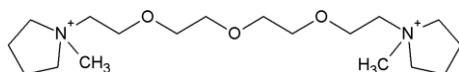
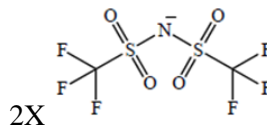
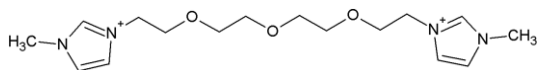
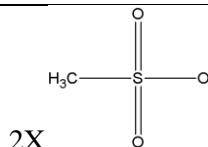
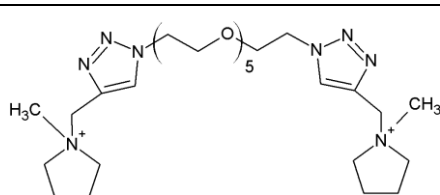
Alkylphosphonium trialkylsilyl sulphonates: In Chapter 6, five alkylphosphonium ionic liquids were analyzed under vacuum conditions in order to evaluate their tribological behaviour and to understand the process occurring during the tribocontact (**IL18-IL22**). The cationic moiety was chosen because of its supposed good thermo-oxidative stability and ability to generate metal-phosphate boundary film. In addition, their structure is similar to the structure of common friction modifiers and the long alkyl groups should increase their hydrophobicity and help hydrocarbon-mimicking behaviour [112]. The anion, which was formed by trialkylsilyl group, was designed considering that sulfonate helps the adsorption of the IL into the metallic surface, hence facilitate the formation of a boundary film, the structure of the trialkylsilyl group, with quaternary carbons should give better rheological properties and the hydrocarbon present on the silicon atom should increase the oleophilic and hydrophobic tendency [112].

The codification of the different ionic liquids is based on their structure and it is shown in Table 2. 1. On the left, there is the representation of the cation, in the centre the anion and below the structures it is indicated the corresponding IL codification.

Table 2. 1 - Structure and codification of the ionic liquids used. In the codification Py=Pyridinium, Im=Imidazolium, Pyrr=Pyrrolidinium, Tr=Triazole

Cation	Anion
	 2X
IL1 - [C ₁ PyC ₂ H ₄ (CH ₂ OCH ₂) ₃ C ₂ H ₄ PyC ₁] ⁺ [C ₁ SO ₄] ⁻ ₂	
	 2X
IL2 - [C ₁ PyC ₂ H ₄ (CH ₂ OCH ₂) ₃ C ₂ H ₄ PyC ₁] ⁺ [NTf ₂] ⁻ ₂	
	
IL3 - [C ₁ Py] ⁺ [C ₁ SO ₄] ⁻	
	
IL4 - [C ₁ Py] ⁺ [NTf ₂] ⁻	
	2X Cl ⁻
IL5 - [C ₁ ImCH ₂ (CH ₂ OCH ₂) ₃ CH ₂ ImC ₁] ⁺ [Cl] ⁻ ₂	
	2X Cl ⁻
IL6 - [C ₁ Pyrr CH ₂ (CH ₂ OCH ₂) ₃ CH ₂ PyrrC ₁] ⁺ [Cl] ⁻ ₂	

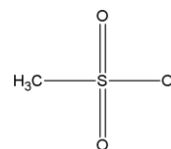
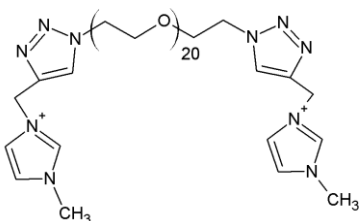
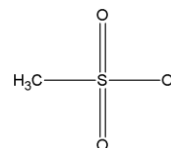
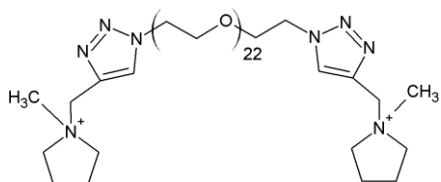
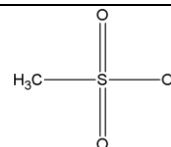
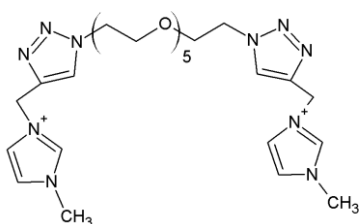
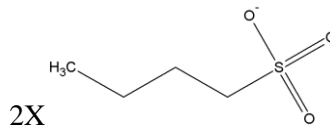
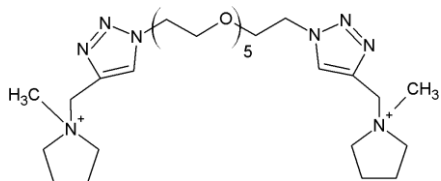
Follow from Table 2. 1

Cation**Anion****MIX IL7 + IL9 (90%-10%)**

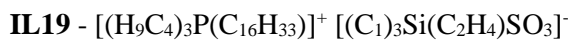
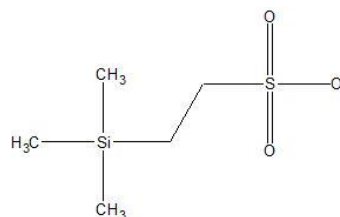
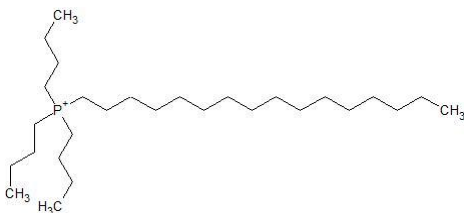
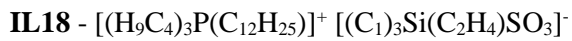
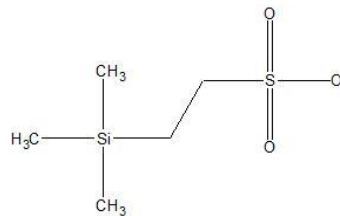
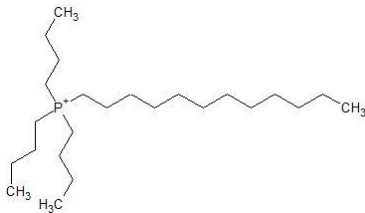
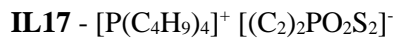
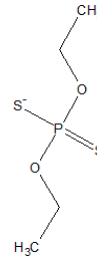
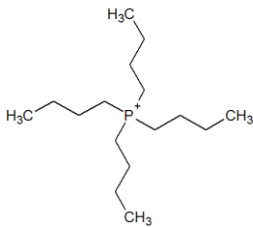
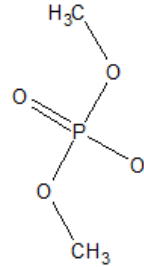
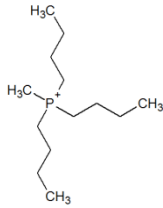
Follow from Table 2. 1

Cation

Anion



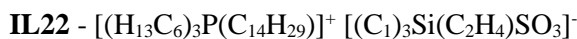
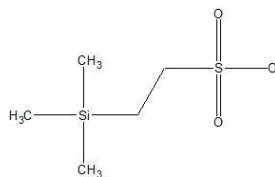
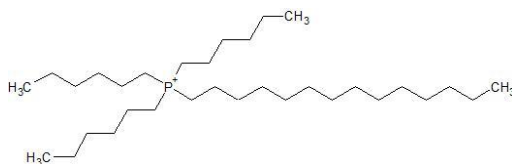
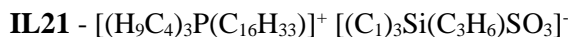
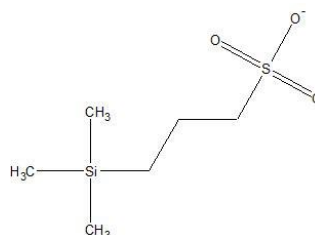
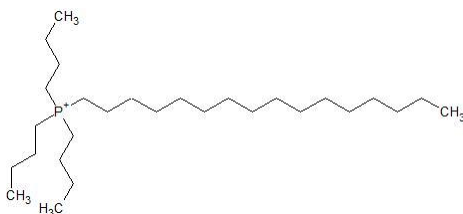
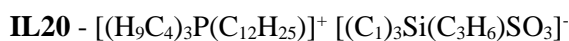
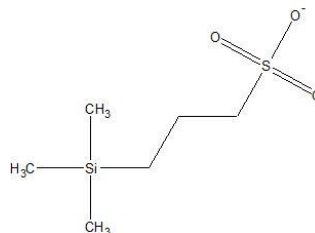
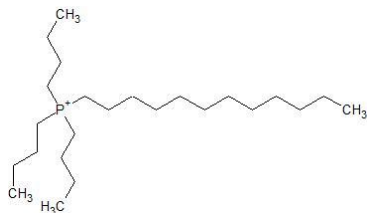
Follow from Table 2. 1

Cation**Anion**

Follow from Table 2. 1

Cation

Anion



2.1.1.2 Base oils and mixtures

Two different base lubricants were selected for the realization of the mixtures with ILs used in the experiments described in this dissertation. All the concentrations of mixtures considered have been calculated as weight/weight % (w/w).

For the analysis of the tribological properties of the pyridinium based ionic liquids as additives, in the Chapter 3, the base lubricant was glycerol with purity $\geq 95\%$. Glycerol was chosen because it was considered a convenient polar lubricant, which

could have helped in getting an acceptable solvency of the ionic liquids. Part of the experiments described in Chapter 3 was carried out with mixtures of ionic liquid and glycerol. The mixtures used were 0.25 w/w%, 0.50 w/w% and 1 w/w% of ionic liquid concentrations in glycerol.

For the study reported in Chapter 4 and Chapter 5, the base lubricant used was a synthetic polypropylenglycol monobutylether with CAS number 9003-13-8 and commercial name Synalox™ 100-30B (The Dow Chemical Company, West Virginia, USA). It is a colorless liquid with a mild odour. It features high viscosity index, low pour point, clean burn properties, low foam characteristics and low surface tension. It is insoluble in water and exhibits miscibility in a wide range of hydrocarbon solvents and oils. SYNALOX™ 100-30B is designed with special characteristics in order to be an excellent choice as a base-stock of industrial lubricants for paper and plastic calendar lubricants. Good heat transfer characteristics allow it to be used as heating oil for calendar bowls. The high load bearing properties make it suitable for use as a gear lubricant base-stock, particularly in formulating worm gear lubricants. It can also be used as compressor fluid when working with non-oxidizing gases such as ethylene, neon, helium, and argon. Other applications include diverse uses such as a plasticizer, a chemical intermediate and a component of greases and mold release agents.

It offers the advantage of being biodegradable in neat products. In high temperature applications where decomposition can occur, SYNALOX™ 100-30B typically do not leave black carbon or sticky residues. The decomposition products are volatile or are solubilized into the base-stock. Oxidation stability can be improved by the inclusion of antioxidants. The physic-chemical characteristics of this lubricant are reported in the Table 2. 2

Table 2. 2 - Properties of the base lubricant SYNALOX™ 100-30B

Property	Synalox 100-30B	Test method
Molecular weight	950	
Viscosity @ 40°C cSt	45	ASTM D445
Viscosity @ 100°C cSt	9	ASTM D445
ISO Viscosity grade	46	ISO 3448
Viscosity Index	186	ASTM D2270
Flash Point °C	213	ASTM D93
Pour Point °C	-41	ASTM D97

In the chapter 4, SYNALOX™ 100-30B was used as base oil for a binary mixture with 1% w/w of the most promising ionic liquid.

In Chapter 5, instead SYNALOX™ 100-30B was used as base oil to obtain binary mixtures of 0.25%, 0.50%, 1.00%, 2.00%, 5.00% w/w selected ILs concentrations. All the mixtures described were realized using an analytical balance RADWAG XA 210/X. The homogeneity of the solutions was guaranteed by using a probe sonicator HD2070 (BANDELIN Electronics, Berlin, Germany). The sonication was realized in three steps: Two minutes of sonication with 50% of the maximum energy allowed in a pulse mode 3, two minutes of pause in order to decrease the temperature of the fluid and two minutes more of sonication with 50% of the maximum energy allowed in pulse mode 3. Complete dispersion was obtained for all the mixtures and tribotests were carried out immediately after sonication. The emulsion showed a good stability for more than 12 hours that is much longer than the time needed for the tribotests, thus, the results obtained can be considered valid.

In Chapter 6, the ionic liquids were compared with a perfluoropolyether lubricant (PFPE) commonly used for vacuum and space applications. The lubricant was provided by Brugarolas and its properties are listed in Table 2. 3.

Table 2. 3 – Properties of PFPE 107/500 according to the data provided by the supplier.

PFPE 107/500		
Fluid type		Branched PFPE
Kinematic viscosity:	@ 20 °C [mm ² /s]	1600
	@ 40°C [mm ² /s]	448
	@ 50°C [mm ² /s]	270
	@ 100°C [mm ² /s]	43
Viscosity index (VI)		148
ISO Viscosity Grade		460
Density @ 20°C [g/cm ³]		1.92
Flash point [°C]		Does not have
Freezing point [°C]		-30
Vapour pressure	@ 20°C [torr]	6 x 10 ⁻⁹
	@ 200°C [torr]	3 x 10 ⁻⁴

2.2 TRIBOLOGICAL SYSTEMS STUDIED

All the studies realized in atmospheric conditions (Chapter 3, Chapter 4 and Chapter 5) were realized with steel/steel contact using balls and discs purchased from Optimol Instruments Prüftechnik (Optimol Instruments Prüftechnik GmbH, Munich, Germany). The quality of the material was certified to be in conformity with international standards. The maximum contact pressure was 1GPa, calculated as suggested by the Hertzian contact theory in the case of a sphere on a flat surface. The testing parameters used correspond to lubrication in boundary regime. Boundary

lubrication was selected because it was considered that ionic liquids can be particularly helpful in these conditions, since they have the ability work as antiwear additives and to react with the surfaces in order to create a protective tribofilm. The balls were made of steel AISI 52100 with a diameter of 10 mm, roughness of 0.012 mm and hardness HRC 63 ± 2 . Discs were also made of steel AISI 52100 with a diameter of 24 mm, thickness of 7.9 mm and roughness of 0.56 μm . Discs and balls were cleaned before and after the experiments by immersion in ultrasonic baths with petroleum ether and acetone (5 min in each solvent).

The experiment shown in Chapter 6 were realized under ultra-high vacuum conditions and the tribopairs used were a silicone nitride ball with a diameter of 3 mm and flat specimen made of steel 440C and titanium grade 5.

2.3 EQUIPMENT

In this dissertation, the main objective was the study of the tribological properties of the ionic liquids. For this reason many techniques and many devices were used.

2.3.1 Tribometers

Four different models of tribometer were used during the tests. Two of them were standard commercially available tribometers, one of them was designed in IK4-TEKNIKER and can perform tests in vacuum conditions and the forth tribometer was used was carrying out a tribocorrosion test.

2.3.1.1 CETR UMT-3

For the tests described in Chapter 3, the experiments were carried out with the CETR UMT-3 (Bruker AXS Inc, Madison, USA). This tribometer is extremely versatile, can accommodate both upper and lower samples of practically any shape and can operate in various test modes (pin on disc, ball on disc, ball on one, two or three balls, pin on V-block, block on ring, disc on disc, flat on flat and screw in nut).

The upper specimen is connected to a vertical linear motion system that has a travel length of 150 mm. A precision spindle rotating at speeds from 0.001-rpm up to 5,000-rpm moves the lower specimen in rotatory motion or, through an additional component in reciprocating motion. Ultra-accurate strain-gauge sensors perform simultaneous measurements of normal load and torque. A normal-load sensor provides feedback to the vertical motion controller, actively adjusting the sample position to ensure a constant load during testing. The tester has fully automated PC-based motor-control and data-acquisition. The tests can be performed controlling the temperature and the humidity of the system [113].

The configuration used for the experiments in Chapter 3 was ball on flat with linear reciprocating movement. The load is applied vertically downward through the ball specimen, against the horizontally mounted flat specimen.

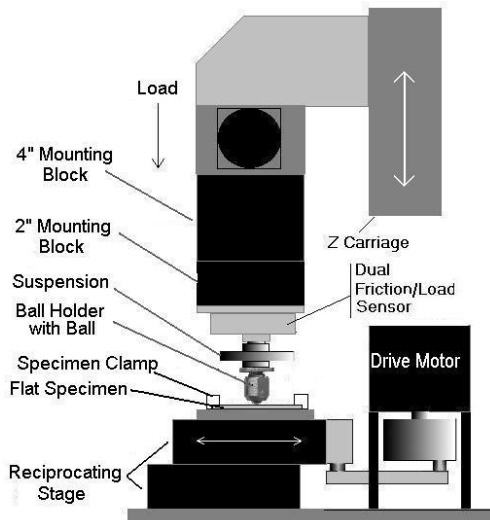


Figure 2. 1 - Schematic representation of the UMT CETR tribometer [113].

2.3.1.2 SRV Optimol

The tribometer used for the studies described in the Chapter 4 and Chapter 5 was an SRV Optimol tribometer (Optimol Instruments Pruftechnik, Germany). SRV is an abbreviation for Schwingung Reibung Verschleiß which is German for reciprocating friction and wear and is a term generally used for the tribometers that operates in linear reciprocating motion.

This is a very robust machine that is able to work in very severe conditions and at the same time to give high repeatability in the tests.

Figure 2. 2 shows the tribometer and a schematic representation of the testing system.

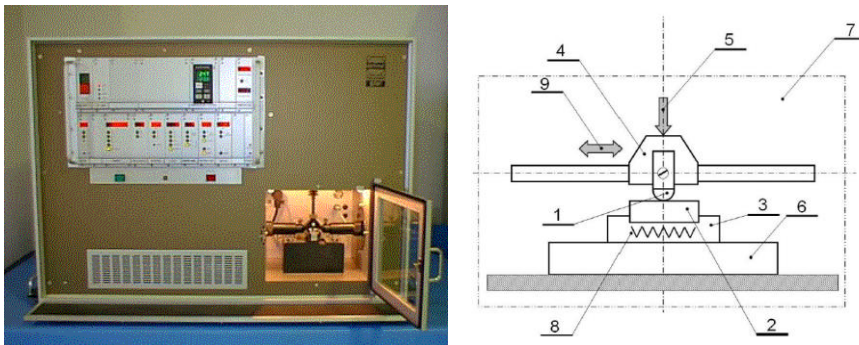


Figure 2. 2 - Optimol SRV on the left and schematic representation on the right: 1) ball; 2) disc; 3) disc holder; 4) ball holder; 5) loading mechanism; 6) piezo sensor; 7) testing cell; 8) heating system; 9) reciprocating sliding mechanism [114].

The testing unit has a stationary base where flat specimen with the shape of 24 mm discs can be mounted. Below the base, there is a force sensor that measures the friction force during the tests. On the upper part is mounted another specimen holder that could have different shape in function of the testing configuration chosen (ball, pin, cylinder). In the experiments realized, the configuration ball on flat was chosen, with a 10 mm diameter ball. The test bench can operate with normal load in the range between 1 N and 2000 N and with temperature ranging from -35 °C (using liquid nitrogen) till 900 °C. It is also possible to introduce nitrogen in the testing chamber

in order to realize tests in inert atmosphere. The stroke can be adjusted between 50 μm (for fretting tests) and 4 mm.

2.3.1.3 CATRI © UHV

The experimental system CATRI © UHV with reciprocating ball-on-flat configuration was used for characterization of the ionic liquids in the Chapter 6. This is a tribometer designed in IK4-TEKNIKER for studying solid or liquid lubricating systems simulating atmospheric, vacuum, high vacuum or ultra-high vacuum conditions [115]. It is possible to realize experiments in the range of temperature between $-55\text{ }^{\circ}\text{C}$ and $350\text{ }^{\circ}\text{C}$ with loads in the range between 0,1-20 N, speeds in the range of 0.02-10 mm/s and maximal displacement of the pin of 20 mm. The tribometer uses a force sensor that was developed and patented in IK4-TEKNIKER [116].

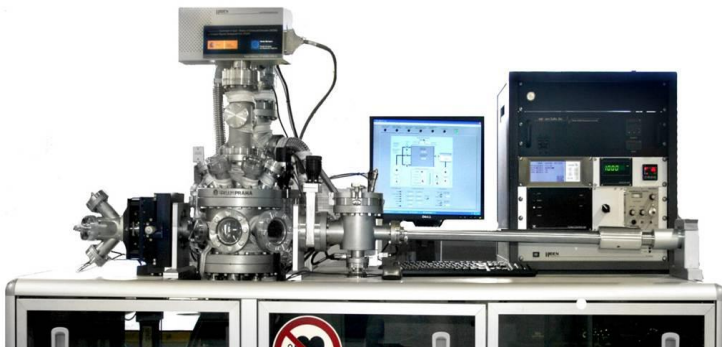


Figure 2. 3 – Tribometer CATRI © UHV at IK4-TEKNIKER.

The bench test is equipped with a quadrupole mass-spectrometer and a dynamic gas expansion system for measuring minute gas emission rates. In addition, the reciprocating friction cell was specially designed to avoid undesired gas emission from its components. MSGE-MS allows identification of gas species emitted during friction using behavioural analysis of the mass-spectrometric data [117].

Table 2. 4 - Testing parameters used for the tribological tests in the different case study presented

Test parameters	Chapter 3	Chapter 4	Chapter 5	Chapter 6
Tribometer used	CETR UMT-3	SRV Optimol	SRV Optimol	CATRI © UHV
Normal load [N]	10	300	300	10
Velocity [mm/s]	50	100	100	3
Stroke [mm]	5	1	1	3
Frequency [Hz]	5	50	50	0.5
Temperature [°C]	100	50, 100, 150	100	Room temperature
Duration [s]	2000			
Ball Material	AISI 52100	AISI 52100	AISI 52100	Si ₃ N ₄
Ball diameter [mm]	10	10	10	3
Disc material	AISI 52100	AISI 52100	AISI 52100	AISI 440C – Ti6Al4V
Base lubricant/Reference	Glycerol	Synalox	Synalox	PFPE
Concentrations [%]	0; 0.25; 0.5; 1; 100	0; 1; 100	0; 0.25; 0.5; 1; 2; 5; 100	0; 100

2.3.1.4 *MicroTest MT/10/SCM and Autolab-Metrohm PGSTAT30 potentiostat*

Tribocorrosion tests were carried out with a unidirectional MicroTest MT/10/SCM tribometer. This system is composed by a rotative plate and an arm with a torque sensor installed on it. The disc is mounted on the rotative place, inside an electrochemical cell where the electrochemical parameters are monitored. The ball instead is installed on the arm. The electrochemical response of the system was monitored by using an Autolab-Metrohm PGSTAT30 potentiostat.



Figure 2. 4 MicroTest MT/10/SCM tribometer with the electrodes installed for the tribocorrosion test.

2.3.1.5 *Testing conditions*

A summary of the testing conditions used in the different case studies presented in this dissertation are presented in Table 2. 4.

2.3.1.6 *Friction coefficient*

Friction force and load were automatically recorded by the tribometers during the tests. With the tribometers used for performing tests in reciprocating motion, the

coefficient of friction can still be calculated with the Amonton's first law (equation 1.1) but it is necessary to use an algorithm for analyzing the results since the friction force is positive in the first part of the cycle and negative in the other part. In addition, it should be considered that the speed is not constant but it varies from zero to a maximum and then decrease again to zero every half sinusoidal cycle. The CETR UMT-3 and SRV Optimol tribometers use algorithms that are implemented in the software for data acquisition. The elaboration of the data acquired with the CATRI © UHV was done with a MATLAB® script specifically elaborated.

2.3.2 Thermal analysis

For a lubricant, it is extremely important to have an opportune range of liquid stability. For this reason, the thermal properties of the lubricant studied were analyzed by means of differential scanning calorimetry (DSC) and thermogravimetric analysis (TGA).

2.3.2.1 Differential Scanning Calorimetry (DSC)

DSC is a thermoanalytical technique that measure the heat required to raise the temperature of a sample. The instrument heats contemporary the sample and a reference with the same heating rate. A software calculates the difference of power that is needed and in this way it gives a measure of the heat capacity of the materials. DSC analysis was realized in order to check melting point and phase transition of the fluids studied. It was performed at 10 °C/min heating rate under dry nitrogen atmosphere using a Mettler-Toledo 822-E (Mettler-Toledo, Greifensee, Zurich, Switzerland) and a Mettler-Toledo DSC 1, STAR^e System (Mettler-Toledo, Greifensee, Zurich, Switzerland). Stainless steel medium pressure crucibles (ME-29990, Mettler-Toledo) were filled with ionic liquid and hermetically sealed.

2.3.2.2 *Thermogravimetric analysis (TGA)*

TGA is a thermoanalytic technique that measures the weight changes in function of the temperature. The samples are introduced in a crucible weighted constantly during the whole test. The temperature can be increased (usually linearly) or kept constant for a certain time. The weight loss or increase gives information about phenomena as decomposition, vaporization, sublimation, absorption, desorption, etc.

Thermogravimetric analyses were carried out using a SDT Q600 (TA Instruments, USA) and a TGA/SDTA 851E (Mettler Toledo, Greifensee, Zurich, Switzerland). The investigated temperature range spanned from ambient temperature up to minimum 500 °C (in some cases up to 600 °C) with linearly increasing heating rate of 10 °C/min. The experiments were performed under inert atmosphere, applying a constant flow of nitrogen. The crucibles used for these experiments were made of alumina or platinum and they were filled with a maximum of 15 mg of IL.

2.3.3 **Surface analysis**

Surface analysis is essential in any tribological study for understanding the mechanisms and the processes that have taken place in the tribosystem. Thanks to the different techniques used, it was possible to have a qualitative and quantitative evaluation of the performance and also to formulate hypothesis about the reaction mechanisms that are generated during the tests between the sliding surfaces and the lubricants.

2.3.3.1 *Optical microscopy*

The optical microscope uses a system of lenses and visible light to amplify the image of the surfaces examined. It is the oldest and among the easiest to use microscopes. The image reflected by the sample can be captured with a normal CCD (Charge-coupled device) camera in order to visualize directly on the computer a digital image of the surface.

Wear volume

In the Chapter 3 and Chapter 4, the wear volume of the balls was calculated by measuring the wear scar diameter (WSD) with an optical microscope.

In the Chapter 4 the wear volume of the balls was calculated according to the procedure described in the standards ASTM D6425–05 [118] and DIN 51834-2:2010-11 [119]:

“Place the cleaned test ball on a suitable holder, and using a microscope, measure to the nearest 0.01 mm the scar width in the direction of sliding (d_1) and again at 90° to the direction of sliding (d_2). The mean wear scar diameter (WSD or D_k) is the average of these two measurements ($\text{WSD} = (d_1 + d_2) / 2$) (Figure 2. 5). If the wear scar diameter is smaller than 1.1 times the Hertzian contact diameter, the profile of the wear scar in the center should be measured in order to calculate the wear volume, (W_v). If the wear scar diameter is greater than 1.1 times the Hertzian contact diameter, the wear scar diameter should only be reported. The wear volume, W_v (mm^3), should be used”.

W_v is the loss of volume from the ball after a test.

The Hertzian contact diameter “ a ” was calculated with the formulas reported from Stachowiak for the contact between a sphere and a flat surface [120]:

$$a = \left(\frac{3WR'}{E'} \right)^{1/3} \quad (2.1)$$

Where W is the load expressed in Newton, R' is the reduced radius of curvature and E' is the reduced young's modulus.

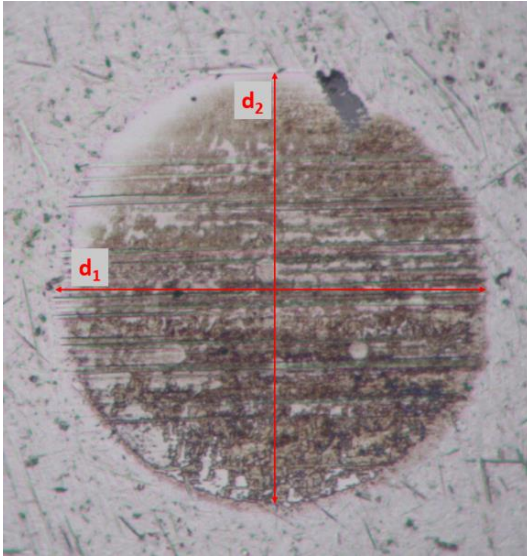


Figure 2. 5 – Determination of the wear scar diameter (WSD)

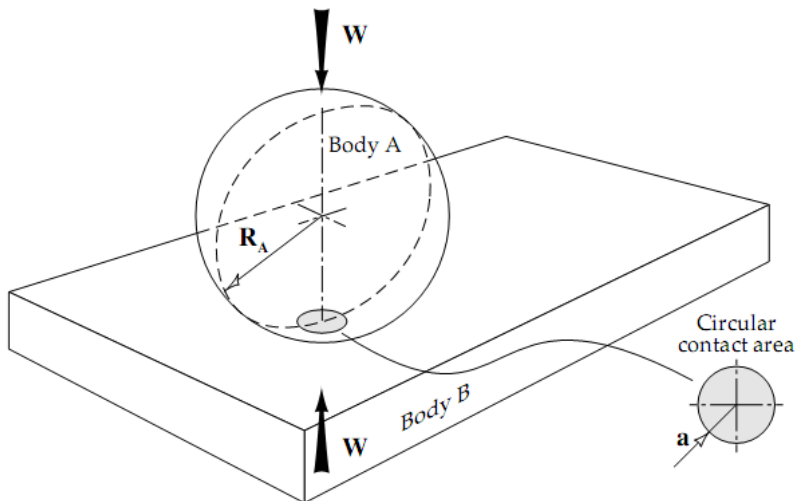


Figure 2. 6 - Contact between a sphere and a flat surface (1)

In the case of ball and disc of the same material R' and E' can be calculated with the following equations:

$$\frac{1}{R'} = \frac{1}{R_{Ax}} + \frac{1}{R_{Bx}} + \frac{1}{R_{Ay}} + \frac{1}{R_{By}} = \frac{2}{R_A} + \frac{2}{\infty} = \frac{2}{R_A} \quad (2.2)$$

R_{Ax} and R_{Ay} are the radius of the ball R_A , R_{Bx} and R_{By} are the radius of the second body that in this case is a plane.

$$\frac{1}{E'} = \frac{1}{2} \left[\frac{1 - \nu_A^2}{E_A} + \frac{1 - \nu_B^2}{E_B} \right] = \frac{1 - \nu_A^2}{E_A} \quad (2.3)$$

E and ν are the Young's modulus and Poisson's ratios of the materials in contact.

Finally, considering the WSD, the wear volume is calculated by geometrical analysis with the formula:

$$V = \pi h^2 * \left[\frac{WSD}{2} - \frac{h}{3} \right] \quad (2.4)$$

And h is given by the Pythagorean Theorem:

$$h = R - \sqrt{R^2 - \left(\frac{WSD}{2} \right)^2} \quad (2.6)$$

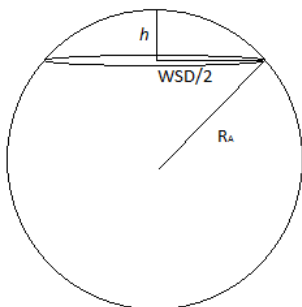


Figure 2. 7 - Schematic drawing of a ball with a missing "cap", corresponding to a wear scar. [121]

Also the load carrying capacity has been reported as geometric contact pressure P_{geom} at test end according to the following equation:

$$P_{geom} = \frac{4W}{\pi WSD^2} \quad (2.5)$$

where: W = normal force (test load), P_{geom} = geometric contact pressure, and
 WSD = mean wear scar diameter

2.3.3.2 Confocal microscopy

It is an optical imaging technique that enables the reconstruction of 3D images through the optical sectioning of the surface. In comparison with conventional optical microscope, which capture the all the light reflected by the analyzed object, the confocal microscope can detect only a specific emitted light passing through a pinhole, which means that it has a very limited depth of focus. By moving the specimen in the vertical axis it is possible to analyse different planes, thus having a complete 3D representation of the surface.

Balls and discs used in the tribological experiments described in Chapter 4 and Chapter 5 were analyzed by a white light confocal microscope (NanoFocus AG, Oberhausen, Germany). The measuring system consists of a white light source and a CCD camera mounted behind a Nipkow disc. Here, the reflected light from the surface reaches a maximum intensity detected by the CCD when the investigated spot on the surface is in focus. This point is pictured. The xy-scan was provided by means of the Nipkow disc and the z-scan is performed by a piezo actuator [122].

The wear volume was calculated from the $\mu\text{surf}^{\text{®}}$ data by the use of a MATLAB[®] based program developed at AC²T research GmbH. For the balls, an ideal spherical surface is defined as “reference surface”. In order to obtain this reference surface, the approximate non-worn region of the ball is selected interactively as shown in Figure 2. 8Figure 2. 8 - Wear scar analysis: a) Confocal white light microscope, b) Wear scar region on ball,(black shaded region) and the reference surface is fitted to

this region. In the second step, the worn region is selected interactively (white shaded region). Finally, the program calculates the wear volume from the difference between the reference surface and the measured surface in the white shaded region. With this software, it is even possible to determine the wear volume (W_v) of small wear scars. For the discs, an ideal plane is defined as reference surface. Again, the non-worn part of the surface is selected interactively and the wear volume is calculated as difference between reference and measured surface [122].

The wear volume was calculated using MATLAB based software by processing the 3D topographical data obtained from the confocal microscope.

The wear track generated with the tribotests described in Chapter 3 and Chapter 6 were analyzed with a ME600 Eclipse Microscope from Nikon Instruments Inc. (Tokyo, Japan) which use the PL μ software. In comparison with Confocal Scanning Laser Microscopes (CSLM), in this system the pinhole that should correspond to the confocal aperture is substituted by a structured pattern consisting of a set of parallel slits. The photodetector that should measure the light intensity passing through the confocal aperture was replaced instead by a CCD. In this way, it is possible to get the confocal information in all the line instead than collecting the information point by point. The data collected with the confocal microscope were then analyzed with a MATLAB script which analyze the points acquired and, by selecting a planar section as basic plane, is able to calculate the volume of the scanned surface that is under the basic plane, and over the basic plane. The difference between these values can be considered as the total wear volume.

2.3.3.3 Field Emission - Scanning Electron Microscope / Energy Dispersive Spectroscopy (FE-SEM/EDS)

A scanning electron microscope is an instrument that reproduces images of a sample by scanning it with a focused beam of electrons. The electrons are emitted by an electron gun, that interacts with atoms in the sample and produce signals that contain

information about the sample's surface topography and composition. SEM has a magnification power of 300,000X while optical microscopes are limited by the light wavelength to a maximum magnification of about 1000X.

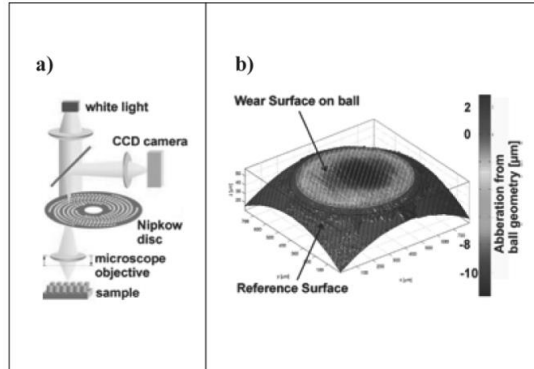


Figure 2. 8 - Wear scar analysis: a) Confocal white light microscope, b) Wear scar region on ball [122].

After the tribological tests, the wear scar produced were analyzed by FE-SEM with embedded EDS using a FE-SEM Gemini ULTRA plus (Zeiss, Germany) in order to have a clearer analysis of the surface morphology and eventually of the tribofilm composition.



Figure 2. 9 – FE-SEM Gemini ULTRA plus

2.3.3.4 X-ray photoelectron spectroscopy (XPS)

XPS is an advanced analytical technique for studying the elemental composition, chemical and electronic state of the elements present on the surface of the samples.

An X-rays source emits a beam toward the surface that should be analyzed. An electron energy analyzer is located close to the sample and measures the kinetic energy and the number of electrons that have been released from the most superficial layers of atoms (up to 10 nm)

In Chapter 4, Chapter 5 and Chapter 6, XPS analyses were performed on the discs used for the tribological experiments in order to understand triboreaction that had taken place during the tribocontact and the eventual formation of tribolayers on the rubbed metallic surfaces.

The equipment used was a Thermo Fisher Scientific Theta Probe (East Grinstead, United Kingdom) with a monochromatic Al K α X-ray source ($h\nu = 1486.6$ eV). The base pressure during the measurements was consistent at 3×10^{-7} Pa. The discs for XPS analysis were thoroughly cleaned directly after the tribological experiments by immersion in petroleum ether and toluene, 2-propanol, respectively, applying an ultrasonic bath for 15 minutes at room temperature for each step.



Figure 2. 10 - XPS Thermo Fisher Scientific Theta Probe (East Grinstead, United Kingdom) at AC2T research GmbH.

For the studies in Chapter 4 and Chapter 5, spots inside and outside of the worn area of the discs were defined and analyzed with a spot diameter of 100 μm at a 200 eV pass energy for the survey spectra. Detail spectra were recorded at a pass energy of 50 eV. For the imaging XPS experiments, the whole wear scar and the adjacent surrounding area was scanned with a spot and step size of 100 μm . All elements detected by the survey analyses, were recorded in the imaging XPS experiments as snap shots with a 15 eV wide binding energy window and a resulting pass energy of 150.5 eV.

For the study described in Chapter 6, the samples were analyzed after cleaning by Ar^+ etching for 20 seconds with 3 kV, 1 μA and an area of 3 x 3 mm^2 (approximately 0.5 nm of the surface were removed). As spot resolution, 300 μm were defined for the Ti-6Al-4V samples and 100 μm for the 440C steel samples.

The elemental composition of the surface was determined by survey scans with 200 eV pass energy. The chemical binding states of the respective elements were investigated in detail with a pass energy of 50 eV.

Three different points of the specimens' surface were examined:

- REF: surface outside of the wear track
- MI: surface in the middle of the wear track
- TP: the turning point at the extremity of the wear track

The spectra were processed with the Avantage Data System software (East Grinstead, UK), using Gaussian-Lorentzian peak fitting.

2.3.4 Other instruments

2.3.4.1 Infrared spectrometer (IR)

In Chapter 5, an analysis of the thermal degradation of the ionic liquids was realized using the Thermo Scientific Nicolet™ iS™10 FT-IR spectrometer. It has an Attenuated Total Reflectance (ATR) module.

2.3.4.2 *Sonicators*

A sonicator works introducing high power ultrasound into a liquid, thus generating alternating high-pressure (compression) and low-pressure (rarefaction) cycles into the fluid. The frequency applied influence the frequency of the compression-depression cycles. The intensity of sonication is proportional to the power used and inversely proportional to the surface area of the sonotrode.

Probe-type ultrasonic homogenizers were used for the homogenization of the mixtures of base lubricant and base oil. Bandelin SONOPULS HD 2070 and Sonics Vibra Cell VCX 500.

For cleaning the samples after the test, a sonicator bath was used.

Sonication was performed for 30 s applying 21 % of the maximum vibration amplitude with a maximum output power of 500 W and with pulses of 2 second duration in 2 second intervals. The blends of base oil and ILs were visually checked.

2.3.4.3 *Viscosimeter*

In Chapter 4, viscosity and density of the ILs studied have been calculated as function of the temperature using a Stabinger viscometer SVM3000 (Anton Paar, Graz, Austria). The range of temperatures studied spans from 20 °C up to 100 °C with 20 °C interval. The viscosity index was also determined using this device according to the ASTM D2270-04 standard.

Chapter 3

3 Comparison of monocationic and dicationic Pyridinium based ionic liquids

3.1 INTRODUCTION

Ionic Liquids (ILs) have gained increasing importance both in the scientific and industrial engineering community during last decade. Due to their remarkable and interesting properties, such as negligible vapour pressure, non-flammability, high polarity, and high thermal stability [50], ILs are finding widespread use as engineering fluids or as novel lubricating systems [85,123]. Moreover, the polar nature of ILs is directly connected with good tribological behaviour, since their strong interactions with surfaces lead to the formation of adsorbed films, reducing friction and wear.

Since 2001, the interest of scientists in tribological properties of ILs has considerably increased [82,83]. Jones et al. have shown that the presence of polyether chains can significantly improve tribological behavior of ILs [124]. Jin et al. have examined some polyethylene glycol functionalized ILs as high temperature lubricants, showing how the presence of fluorine in the IL favorably boosts its anti-wear performance [125]. On the other side, dicationic ILs (DILs) have shown good thermal stability

comparing with their monocationic analogues [126]. It has also been shown that the acute toxicity of DILs is in many cases below the levels observed for those monocationic and that the use of head groups connected via polyethylene glycol could be identified as structural elements reducing the toxicity [127]. Hence, the combination of the tribologically favourable properties of polyethylene glycol and DILs may lead to a series of novel and advanced lubricating systems.

Ionic structures containing imidazolium [128,129] or pyrrolidinium [130] cation have been widely studied for lubrication and have shown very promising results. Nevertheless, to our knowledge, no papers were published about using pyridinium DILs as lubricants or lubricant additives. It is known that pyridinium cation can show exceptionally high levels of biodegradation under aerobic conditions and can be classified as “ready biodegradable” [131]. In addition, studies on the acute toxicity of DILs have shown in many cases levels below those observed for monocationic ILs [132].

For all these reasons, these ILs were synthesized in the University of Vigo and the tribological properties of a series of DILs that incorporate polyethylene glycol chains linking two alkylpyridinium moieties were studied in IK4-TEKNIKER. Alkylsulfate $[\text{RSO}_4]^-$ and $[\text{NTf}_2]^-$ were selected as anions taking into account the reduction on wear and friction observed when these anions were used in previous works on monocationic ILs [133,134].

3.2 EXPERIMENTAL DETAILS

3.2.1 Materials

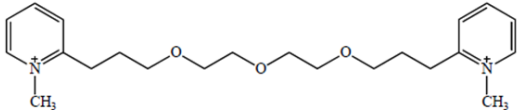
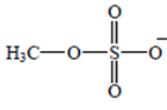
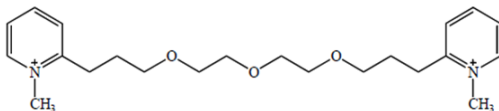
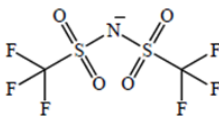
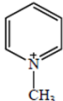
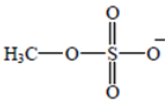
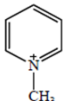
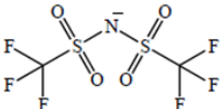
Ionic liquids: Four ionic liquids were used for the experiments. All the ionic liquids were synthesized in the University of Vigo within the framework of the Marie Curie Initial Training Network MINILUBES. Two of them were dicationic ionic liquids synthesized by applying a procedure previously developed [135] and incorporating

polyethylene glycol chains linking two N-alkylpyridinium moieties through rings position 2. Alkylsulfate and bis(trifluoromethanesulfonyl)imide (NTf₂) were selected as anions (**IL1** - [C₁PyC₂H₄(CH₂OCH₂)₃C₂H₄PyC₁]⁺ [C₁SO₄]⁻² and **IL2** - [C₁PyC₂H₄(CH₂OCH₂)₃C₂H₄PyC₁]⁺ [NTf₂]⁻²). The other two ionic liquids were the monocationic analogues, methylpyridinium methylsulfate **IL3** - [C₁Py]⁺ [C₁SO₄]⁻ and methylpyridinium bis(trifluoromethanesulfonyl)imide **IL4** - [C₁Py]⁺ [NTf₂]⁻.

The structures of all synthesized compounds were confirmed by ¹H, ¹³C, ¹⁹F NMR and FTIR spectroscopy as well as high resolution ESI-TOF mass spectrometry. All ILs were dried by heating at (100 to 110 °C) and stirring under high vacuum (2 x 10⁻¹ Pa) during 48 h before using it. Their purity was estimated by ¹H NMR (400 MHz) showing to be no less than 99%. More information about the synthesis and the chemical analysis of these ionic liquids can be found elsewhere [111]. The structure and codification of the ILs can be found in Table 3. 1.

Base oil: Glycerol (or Glycerin, Glycerine), C₃H₈O₃, is a purified chemical compound containing ≥95% of glycerol. Due to the presence of three hydroxyl groups in the molecular structure and resulting good hygroscopic properties, glycerol is often used as a polar model liquid in tribological studies. Glycerol is colorless, odorless, a high viscous liquid that is widely used: in pharmacy; oxygen compressors, where the resistance to oxidation is important; pumps and bearings that are exposed to gasoline, benzene and similar fluids [136].

Table 3. 1 – Structure and codification of the Pyridinium ionic liquids used

Cation	Anion
	 2X
1,13-bis(1N-methyl-2-pyridinium)-4,7,10-trioxatridecane methylsulfate	
IL1 - $[\text{C}_1\text{PyC}_2\text{H}_4(\text{CH}_2\text{OCH}_2)_3\text{C}_2\text{H}_4\text{PyC}_1]^+ [\text{C}_1\text{SO}_4]^-_2$	
	 2X
1,13-bis(1N-methyl-2-pyridinium)-4,7,10-trioxatridecane bis(trifluoromethane sulfonyl)imide	
IL2 - $[\text{C}_1\text{PyC}_2\text{H}_4(\text{CH}_2\text{OCH}_2)_3\text{C}_2\text{H}_4\text{PyC}_1]^+ [\text{NTf}_2]^-_2$	
	
N-Methylpyridinium methylsulfate	
IL3 - $[\text{C}_1\text{Py}]^+ [\text{C}_1\text{SO}_4]^-$	
	
N-Methylpyridinium bis(trifluoromethane sulfonyl)imide	
IL4 - $[\text{C}_1\text{Py}]^+ [\text{NTf}_2]^-$	

Lubricant mixtures: 0.25, 0.5 and 1.0 wt % of the ILs in glycerol were prepared using a RADWAG XA 210/X analytical balance. The ideal homogeneity of the mixtures was achieved using a sonicator HD2070 (BANDELIN electronics, Berlin, Germany). The sonication process consisted of 3 steps: two minutes of sonication with 50% of the maximum energy allowed in a pulse mode 3, two minutes of pause in order to decrease the temperature of the fluid and two minutes more of sonication with 50% of the maximum energy allowed in pulse mode 3. Complete dispersion was obtained for all the mixtures and tribotests were carried out immediately after sonication. The emulsion showed a good stability for more than 12 h that is much longer than the time needed for the test. Thus, the results obtained can be considered valid.

3.2.2 Thermal analysis

Differential Scanning Calorimetry (DSC) was used to measure thermal transitions of the ILs in a temperature range from -30 °C to 160 °C. The samples were measured in closed aluminium pans with a small hole in the lid using a Mettler-Toledo DSC, model DSC 1, STAR^e System with automatic sample changer. The sample weight was between 15 and 20 mg and all experiments were performed under a nitrogen flow of 50 mL/min. In order to avoid the effect of the presence of volatiles in ILs, the samples were pre-heated at 120 °C for 20 min inside the furnace of the DSC. The thermal treatment includes: heating the IL from -40 °C to 160 °C with a heating rate of 10 °C/min and final cooling from 160 °C to -40 °C with a cooling rate of -10 °C/min.

The thermal stabilities of the ILs were measured using TGA. 10-15 mg of the samples were measured in open platinum pans using a SDT Q600 (TA Instruments, USA) under nitrogen flow (50 mL/min). The measurements started at room temperature and were completed at 600 °C with a heating rate of 10 °C/min. TGA was utilized to measure several decomposition temperatures (T_{start} , $T_{\text{d,onset}}$ and T_{peak}). The onset temperature (T_{onset}) is the intersection of the baseline weight from the

beginning of the experiment and the tangent of the weight vs temperature curve as decomposition occurs. The start temperature (T_{start}) is the temperature at which the decomposition of the sample begins. The peak temperature (T_{peak}) is the temperature at which the decomposition of sample ends and stays constant.

3.2.3 Tribological Experiments

Tribological experiments were carried out on the CETR UMT3 (Bruker AXS Inc, Madison, USA) universal tribometer. Test parameters and tribopairs are summarized in Table 3. 2

Table 3. 2 - Tribological test parameters and materials tested

Test parameters	
Tribometer used	CETR UMT-3
Normal load [N]	10
Velocity [mm/s]	50
Stroke [mm]	5
Frequency [Hz]	5
Temperature [°C]	100
Duration [s]	2000
Ball Material	AISI 52100
Ball diameter [mm]	10
Disc material	AISI 52100
Base lubricant/Reference	Glycerol
Concentrations [w/w %]	0; 0.25; 0.50; 1.00; 100.00

Load applied was 10 N. Other parameters were: stroke of 5 mm with frequency of 5 Hz and for a total distance of 100 m. The temperature during the tests was of 100 °C. Both balls and discs have been purchased from Optimol Instruments Prüftechnik and the quality of the material was certified to be in conformity with international standards. The maximum contact pressure, calculated as suggested by the Hertzian indentation theory for contact between a sphere and a flat surface [120], was 1 GPa. The testing parameters used correspond to lubrication in boundary regime. The balls were made of steel AISI 52100 with a diameter of 10 mm, roughness of 0.012 μm and hardness HRC 63 ± 2 . Discs were also made of steel AISI 52100 with a diameter of 24 mm, thickness of 7.9 mm and roughness of 0.56 μm .

Discs and ball were cleaned before and after the tribotests by immersion in ultrasonic bath with petroleum ether and acetone for 5 minutes each.

The wear on the balls was measured with the optical microscope as described in 2.3.3.1

The wear on the disc was analyzed by optical microscope and confocal microscope.

3.3 RESULTS AND DISCUSSION

3.3.1 Thermal properties

The thermal stabilities of the prepared ILs were studied using thermogravimetric analysis (TGA). The data corresponding to the thermal stabilities are summarized in Table 3. 3. As it was expected, ILs containing NTf_2 anions exhibited higher thermal stability than those containing alkylsulfate anions, confirming that the anion is the most relevant moiety related to the IL thermal stability. Thus, the dicationic alkylsulfate is stable up to around 127 °C, onsets of decomposition temperatures occurring from 210 °C to 284 °C (8% – 15% of the mass is gone), while NTf_2 dicationic IL did not show significant mass loss up to around 287 °C, onsets of decomposition temperatures occurring from 369 °C to 401 °C (8% – 23% of the mass

is gone). On the other hand, the $T_{d,onset}$ of monocationic **IL3** - $[C_1Py]^+ [C_1SO_4]^-$ was found to be 328 °C and the compound was stable up to 118 °C, while monocationic **IL4** - $[C_1Py]^+ [NTf_2]^-$ exhibited higher thermal stability ($T_{d,onset}$ at 431 °C) and was stable up to 325 °C.

The thermal stability of dicationic ILs was superior to the thermal stability of monocationic ILs. While monocationic **IL3** - $[C_1Py]^+ [C_1SO_4]^-$ presents the $T_{d,onset}$ at 210 °C, the dicationic analogous **IL1** - $[C_1PyC_2H_4(CH_2OCH_2)_3C_2H_4PyC_1]^+ [C_1SO_4]^-_2$ shows the $T_{d,onset}$ at 328 °C; following the same tendency, monocationic **IL4** - $[C_1Py]^+ [NTf_2]^-$ presents the $T_{d,onset}$ at 401 °C, and dicationic **IL2** - $[C_1PyC_2H_4(CH_2OCH_2)_3C_2H_4PyC_1]^+ [NTf_2]^-_2$ shows the $T_{d,onset}$ at 431 °C. Similar $T_{d,onset}$ values around 367-407 °C were found for pyridinium DILs incorporating an alkyl chain joining the two cations through the nitrogens [137].

The thermal behaviour of the prepared ILs was studied using differential scanning calorimetry (DSC). The measurements were conducted in a temperature range from -40 °C to 160 °C under nitrogen atmosphere. In the case of the monocationic, no phase transitions were observed for **IL3** - $[C_1Py]^+ [C_1SO_4]^-$ while **IL4** - $[C_1Py]^+ [NTf_2]^-$ showed a melting temperature (T_m) at 46 °C and a freezing temperature (T_f) at -22 °C (see Table 3. 3).

3.3.2 Solubility

The synthesized dicationic ILs were tested for their solubility behaviour in polar and non-polar solvents. Dicationic IL derived from alkylsulfate anions exhibited good solubility in high polar solvents such as dimethyl sulfoxide, acetonitrile, methanol and water. All of them were non-soluble in non-polar solvents such as hexane, diethyl ether, dichloromethane and ethyl acetate. Dicationic ILs derived from NTf_2 anion exhibited slightly different solubility properties. They were soluble in ethyl acetate, dimethyl sulfoxide, acetonitrile and methanol; partial soluble in dichloromethane and water, and non-soluble in hexane and diethyl ether.

Table 3. 3 Thermal properties of synthesized pyridinium ILs, where T_m , melting temperature ($^{\circ}\text{C}$); T_f , freezing temperature ($^{\circ}\text{C}$); T_{start} , the start of decomposition temperature (100), $T_{d,onset}$ ($^{\circ}\text{C}$), the onset of decomposition temperature (100).

IL	T_{start}	$T_{d,onset}^a$	$T_{m,onset}$	T_f
$[\text{C}_1\text{Py}(\text{CH}_2\text{OCH}_2)_3\text{C}_1\text{Py}][\text{C}_1\text{SO}_4]_2$	118	328 (19)		
$[\text{C}_1\text{Py}(\text{CH}_2\text{OCH}_2)_3\text{C}_1\text{Py}][\text{NTf}_2]_2$	325	431 (23)	46	-22
$[\text{C}_1\text{Py}][\text{C}_1\text{SO}_4]$	117	210 (15)		
$[\text{C}_1\text{Py}][\text{NTf}_2]$	284	401 (15)		

^aweight loss indicated in % between brackets

3.3.3 Tribological performance

In order to investigate the potential use of the new synthesized ILs as lubricants, the tribological properties of dicationic ILs **IL1** - $[\text{C}_1\text{PyC}_2\text{H}_4(\text{CH}_2\text{OCH}_2)_3\text{C}_2\text{H}_4\text{PyC}_1]^+ [\text{C}_1\text{SO}_4]_2^-$ and **IL2** - $[\text{C}_1\text{PyC}_2\text{H}_4(\text{CH}_2\text{OCH}_2)_3\text{C}_2\text{H}_4\text{PyC}_1]^+ [\text{NTf}_2]_2^-$, as well as the monocationic ILs **IL3** - $[\text{C}_1\text{Py}]^+ [\text{C}_1\text{SO}_4]^-$ and **IL4** - $[\text{C}_1\text{Py}]^+ [\text{NTf}_2]^-$, were studied.

Neat Ionic Liquids. The coefficients of friction (COF) and WSD measured on the balls are represented in Figure 3. 1 for the tests performed with the reference lubricant (glycerol) and with the neat ILs. Almost all tested ILs, except **IL3** - $[\text{C}_1\text{Py}]^+ [\text{C}_1\text{SO}_4]^-$, gave lower friction than glycerol. The average COF registered during the tests with **IL1** - $[\text{C}_1\text{PyC}_2\text{H}_4(\text{CH}_2\text{OCH}_2)_3\text{C}_2\text{H}_4\text{PyC}_1]^+ [\text{C}_1\text{SO}_4]_2^-$ was extremely low (0.036), less than one third of what was found with glycerol. Unfortunately this good result in terms of friction did not correspond to a good result in terms of wear. The WSD measured on the balls used for the tests with methylsulfates ILs **IL1** - $[\text{C}_1\text{PyC}_2\text{H}_4(\text{CH}_2\text{OCH}_2)_3\text{C}_2\text{H}_4\text{PyC}_1]^+ [\text{C}_1\text{SO}_4]_2^-$ and **IL3**

$-\text{[C}_1\text{Py]}^+ \text{[C}_1\text{SO}_4\text{]}^-$, was much higher than the WSD measured on the balls used with the other ILs. More interesting performance was achieved in the case of DILs containing $[\text{NTf}_2]$ anion (**IL2** - $[\text{C}_1\text{PyC}_2\text{H}_4(\text{CH}_2\text{OCH}_2)_3\text{C}_2\text{H}_4\text{PyC}_1]^+ [\text{NTf}_2]^-_2$ and **IL4** - $[\text{C}_1\text{Py}]^+ [\text{NTf}_2]^-$, that showed good improvement of COF with a wear on the ball comparable with the reference lubricant.

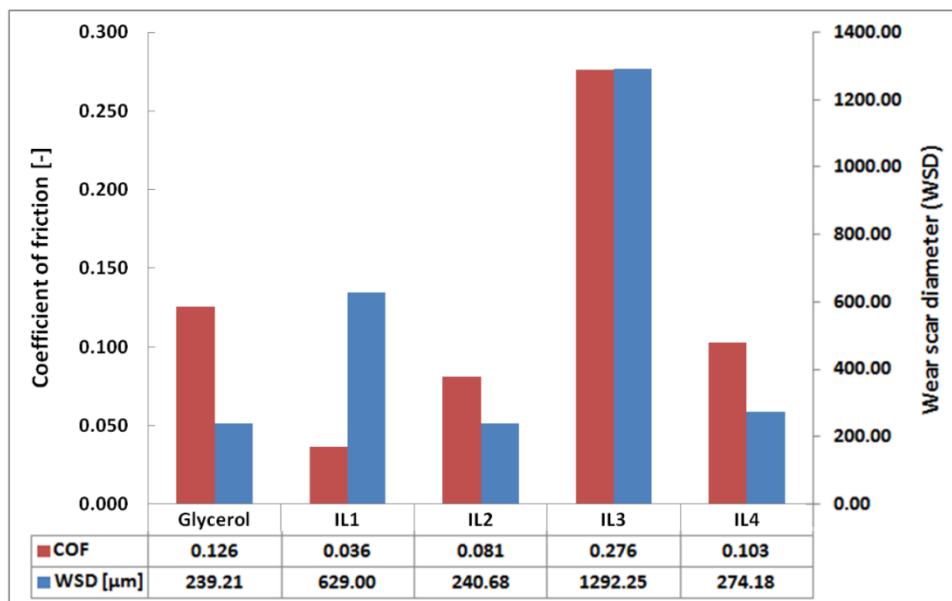


Figure 3. 1 - Comparison of COF and WSD of the balls for neat ILs and glycerol.

Figure 3. 2 shows the images of the wear scar of the steel balls lubricated with glycerol and neat ILs taken by optical microscope. Figure 3. 2a it shows the worn scar obtained when using neat glycerol. Despite the small dimension of the WSD, it is possible to notice that the rubbed surface presents numerous spots and deep grooves that could be the result of adhesion and abrasion phenomena. This phenomenon is typical when the formed oxide film is so thin that it does not prevent the surfaces from direct contact [120]. Different wear mechanism can be detected on the surfaces lubricated by ILs. In the case of **IL2** - $[\text{C}_1\text{PyC}_2\text{H}_4(\text{CH}_2\text{OCH}_2)_3\text{C}_2\text{H}_4\text{PyC}_1]^+ [\text{NTf}_2]^-_2$ and **IL4** - $[\text{C}_1\text{Py}]^+ [\text{NTf}_2]^-$

(Figure 3. 2c and Figure 3. 2d), the wear scar exhibited by the balls after the tests is in the same order of magnitude than that obtained with neat glycerol but the surface is smoother; it means that the lubricant was able to generate a protective tribolayer through reaction of the surfaces in contact. However, the ILs **IL1** - $[\text{C}_1\text{PyC}_2\text{H}_4(\text{CH}_2\text{OCH}_2)_3\text{C}_2\text{H}_4\text{PyC}_1]^+ [\text{C}_1\text{SO}_4]^-_2$ and **IL3** - $[\text{C}_1\text{Py}]^+ [\text{C}_1\text{SO}_4]^-$ (Figure 3. 2d and Figure 3. 2e) show signs that could be due to tribocorrosion process. The process itself is not so different from that one seen for the $[\text{NTf}_2]$ structures (**IL2** - $[\text{C}_1\text{PyC}_2\text{H}_4(\text{CH}_2\text{OCH}_2)_3\text{C}_2\text{H}_4\text{PyC}_1]^+ [\text{NTf}_2]^-_2$ and **IL4** - $[\text{C}_1\text{Py}]^+ [\text{NTf}_2]^-$), but in these cases the oxidized layers generated are not strong enough to resist to the mechanical stress experimented during the tribotest. It should be noticed that the magnification used in Figure 3. 2a, Figure 3. 2c and Figure 3. 2e is the half of the magnification used in Figure 3. 2b and Figure 3. 2d.

Figure 3. 3 shows the tracks left on the discs after the tribotests. The discs were only worn after lubrication with glycerol. Only results with **IL2** - $[\text{C}_1\text{PyC}_2\text{H}_4(\text{CH}_2\text{OCH}_2)_3\text{C}_2\text{H}_4\text{PyC}_1]^+ [\text{NTf}_2]^-_2$ and **IL4** - $[\text{C}_1\text{Py}]^+ [\text{NTf}_2]^-$ are shown because they were considered the most noteworthy tests. It is evident how the test performed with glycerol left evident and deep grooves on the surface of the disc, while with neat ILs the scar is almost undetectable and the marks left during the polishing procedure are still perfectly visible. On the disc lubricated with **IL4** - $[\text{C}_1\text{Py}]^+ [\text{NTf}_2]^-$, it is visible a soft mark due to the tribologically induced oxidation, generated during the tribocontact. Figure 3. 4 shows a comparison of the tracks detected by SEM on the discs lubricated with glycerol and **IL4** - $[\text{C}_1\text{Py}]^+ [\text{NTf}_2]^-$. Also in this case it is possible to notice that the lubrication with glycerol left deep grooves and there are signs of third body inclusions. Lubricating with IL, instead, the surface was properly protected.

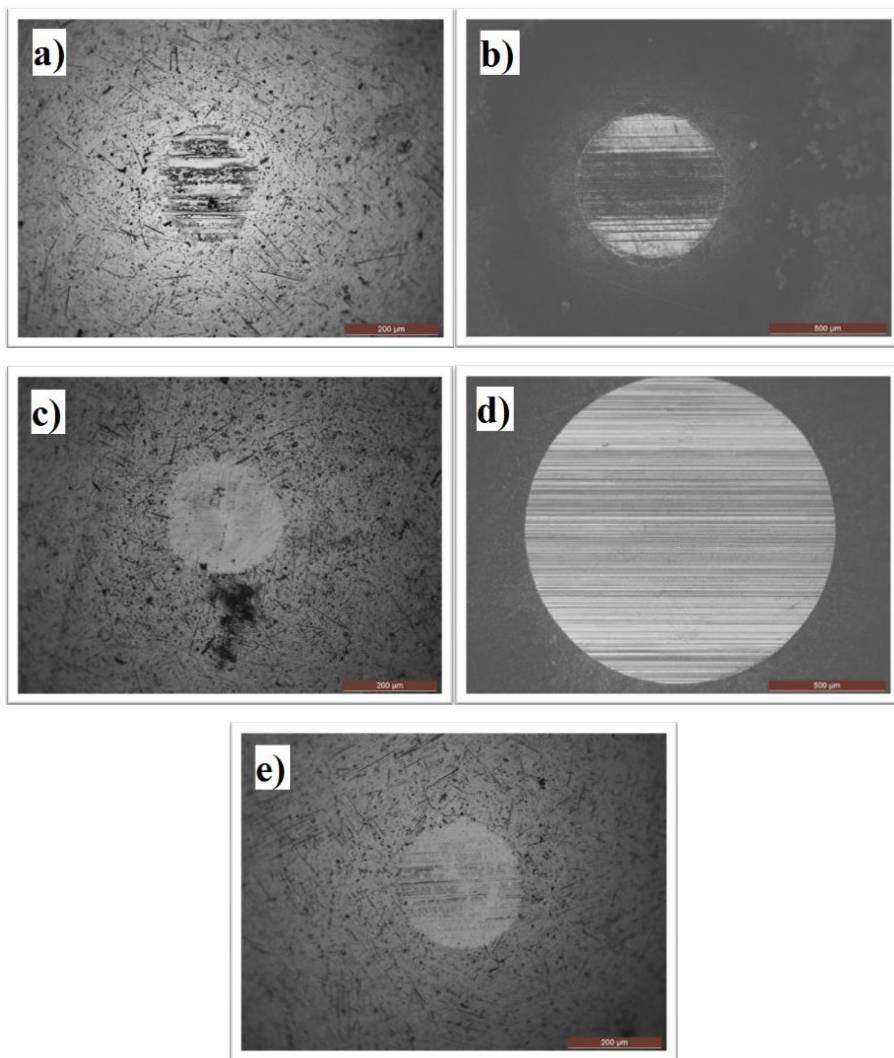


Figure 3. 2 - Wear scar on the steel AISI 52100 ball after lubrication with: (a) neat glycerol (magnification 100X); (b) **IL1** - $[C_1PyC_2H_4(CH_2OCH_2)_3C_2H_4PyC_1]^+ [C_1SO_4]^-_2$ (magnification 50X); (c) **IL2** - $[C_1PyC_2H_4(CH_2OCH_2)_3C_2H_4PyC_1]^+ [NTf_2]^-_2$ (magnification 100X); (d) **IL3** - $[C_1Py]^+ [C_1SO_4]^-$ (magnification 50X); (e) **IL4** - $[C_1Py]^+ [NTf_2]^-$ (magnification 100X).

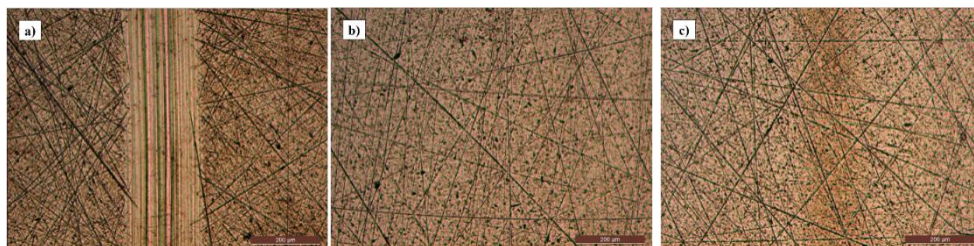


Figure 3.3 - Wear scar on the test specimens. Discs lubricated with: a) glycerol, b) **IL2** - $[C_1PyC_2H_4(CH_2OCH_2)_3C_2H_4PyC_1]^+ [NTf_2]^-_2$, c) **IL4** - $[C_1Py]^+ [NTf_2]^-$.

The main consideration that can be drawn from the analysis of these results is that the anion has a particularly relevant influence on the performance of the lubricants. The compounds containing $[C_1SO_4]$ anion showed serious wear, probably due to the decomposition of the anion. Due to the harsh testing conditions, the methylsulfate anion could be hydrolysed giving origin to sulfuric acid. Because of the high hygroscopicity and moisturizing effect of the sample, the ILs absorb some ppm of water from the humidity in the air [85]. On the other hand, the good tribological properties of $[NTf_2]$ anion will be shown again in the next chapter where it was possible to detect by XPS the presence of a tribolayer of inorganic fluoride, which is very likely the responsible of the good performance. Additionally, dicationic **IL1** - $[C_1PyC_2H_4(CH_2OCH_2)_3C_2H_4PyC_1]^+ [C_1SO_4]^-_2$ and **IL2** - $[C_1PyC_2H_4(CH_2OCH_2)_3C_2H_4PyC_1]^+ [NTf_2]^-_2$ have demonstrated better response than the monocationic analogues **IL3** - $[C_1Py]^+ [C_1SO_4]^-$ and **IL4** - $[C_1Py]^+ [NTf_2]^-$, which confirms that dicationic moieties are better than monocationic for tribological application.

Mixture of glycerol with Ionic Liquids. The testing conditions used for the tests with mixtures of ILs and glycerol are the same that were the same that were used for the neat ionic liquids. Figure 3.5 shows the average values of COF blends of ILs and glycerol. In terms of friction, it was observed that, by mixing

ILs containing $[C_1SO_4]$ (**IL1** - $[C_1PyC_2H_4(CH_2OCH_2)_3C_2H_4PyC_1]^+ [C_1SO_4]^-_2$ and **IL3** - $[C_1Py]^+ [C_1SO_4]^-$) with glycerol, the performance of the lubricants did not change significantly. At all tested concentrations, the COF was around 0.120-0.135.

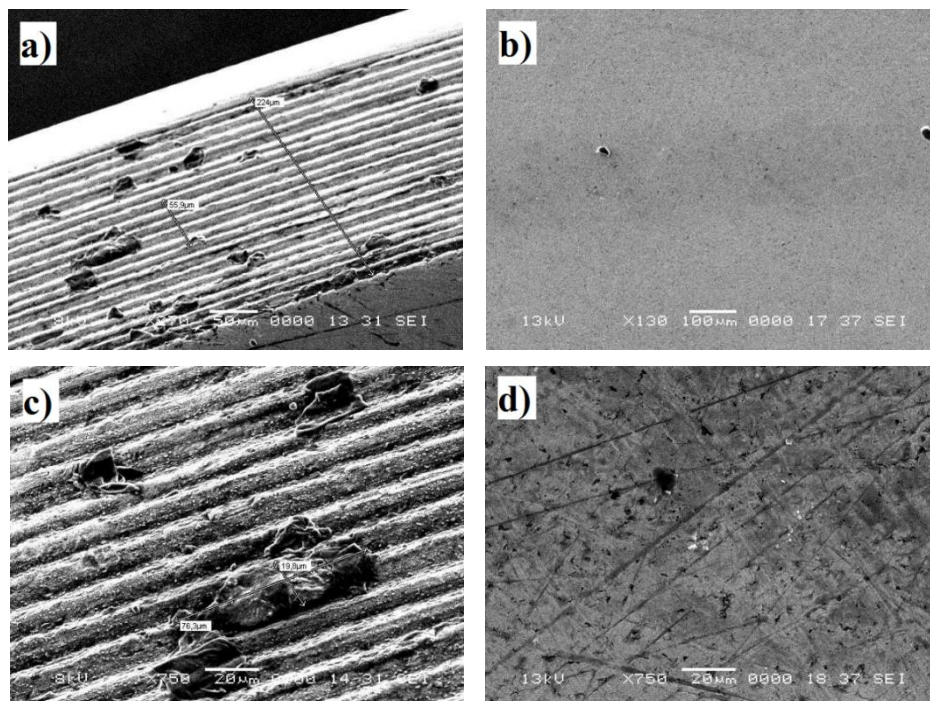


Figure 3. 4 - SEM micrographics with two different magnification of the discs rubbed in the tribotests lubricated with glycerol (a and c) and neat IL **IL4** - $[C_1Py]^+ [NTf_2]^-$ (b and d).

Better effect was obtained in the case of lubricating the surfaces with $[NTf_2]$ ILs **IL2** - $[C_1PyC_2H_4(CH_2OCH_2)_3C_2H_4PyC_1]^+ [NTf_2]^-_2$ and **IL4** - $[C_1Py]^+ [NTf_2]^-$. The mixtures of glycerol and monocationic **IL4** - $[C_1Py]^+ [NTf_2]^-$ showed a decrease of coefficient of friction with an increase of concentration of the IL. Increasing from 0% to 0.5% the concentration of **IL4** - $[C_1Py]^+ [NTf_2]^-$ in the mixture, the performance improvement of the lubricant is almost imperceptible. Nevertheless, at 1.0% it starts to be tangible and the COF goes down to 0.106. Better response was

given in the case of **IL2** - $[C_1PyC_2H_4(CH_2OCH_2)_3C_2H_4PyC_1]^+ [NTf_2]^-_2$, where noticeable reduction of COF (0.099), even with an addition of 0.25% of IL was observed. At 0.5% and 1.0% there is a further diminution of the average COF measured around 0.09, which means that in comparison with neat glycerol it was reduced to the 72%.

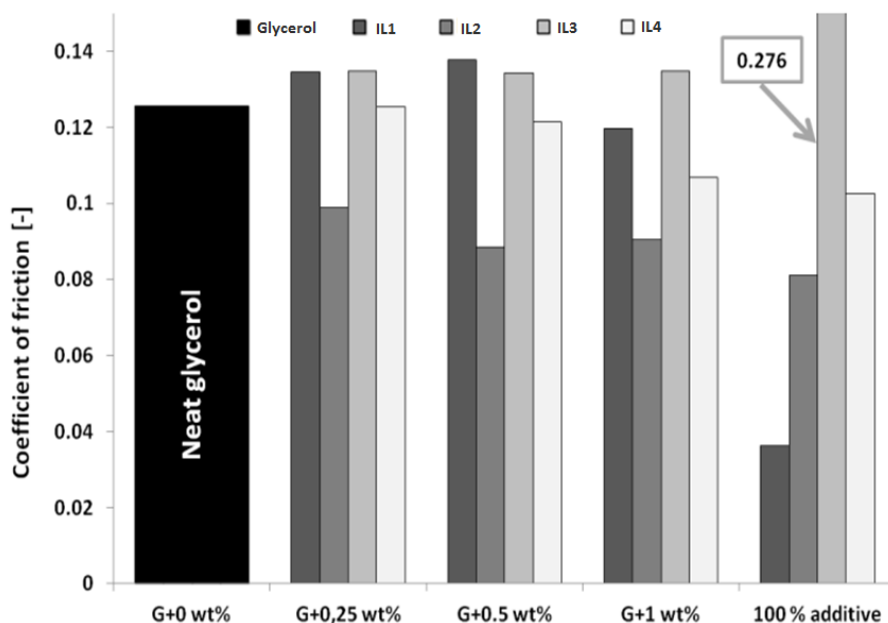


Figure 3. 5 - Representation of the registered average coefficient of friction (COF) with the mixtures of tested lubricants. The friction measured with neat **IL3** - $[C_1Py]^+ [C_1SO_4]^-$ was out of scale and the average COF is indicated in the graph.

Figure 3. 6 represents the wear scars generated during the tests lubricated with mixtures 0.25% w/w of ILs in glycerol. In comparison with the scar shown in Figure 3. 2a (neat glycerol), it can be noticed that the addition of 0.25% of IL was enough to cause a change in the wear mechanism. The wear scar is larger but the grooves seem smoother and the worn surface appears more regular.

This behavior can be explained by the reactivity of the ILs. The common anti-wear and EP additives operate creating a tribochemical reactive layer with high wear resistance. In this case, it seems that the ILs studied are able to create a tribolayer but its resistance to wear is low and they generate in this case a phenomenon called tribocorrosion. Particularly strong tribocorrosion was generated with the monocationic **IL3** – $[C_1Py]^+ [C_1SO_4]^-$, while dicationic **IL1** – $[C_1PyC_2H_4(CH_2OCH_2)_3C_2H_4PyC_1]^+ [C_1SO_4]^-_2$ had the lowest influence, both in terms of friction and wear.

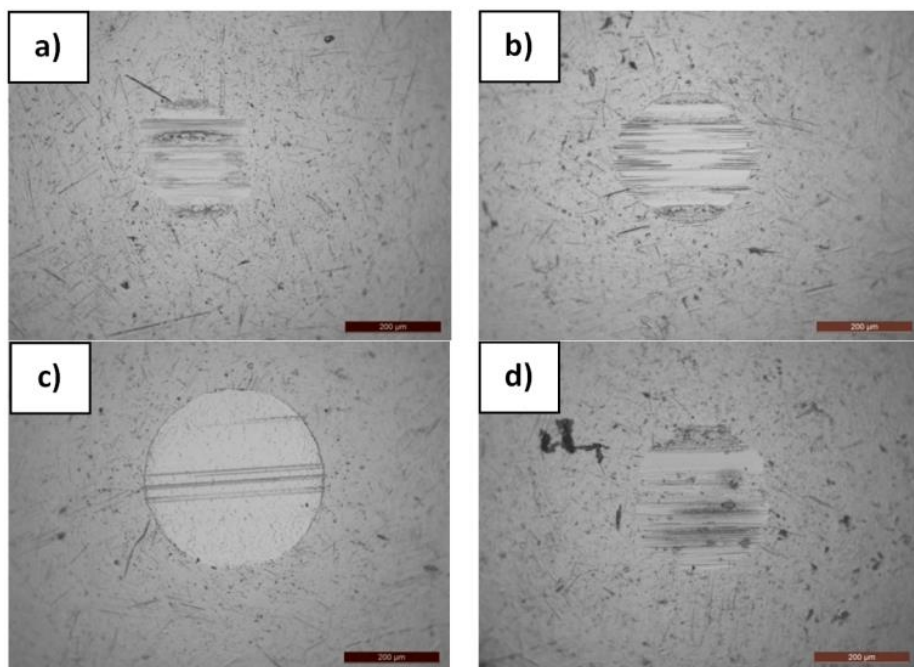


Figure 3. 6 - Wear scar on the 100Cr6 balls after lubrication with mixture of 0.25 wt % of IL in glycerol: (a) 0.25 wt % of **IL1** – $[C_1PyC_2H_4(CH_2OCH_2)_3C_2H_4PyC_1]^+ [C_1SO_4]^-_2$; (b) 0.25 wt% of **IL2** – $[C_1PyC_2H_4(CH_2OCH_2)_3C_2H_4PyC_1]^+ [NTf_2]^-_2$; (c) 0.25 wt % of **IL3** – $[C_1Py]^+ [C_1SO_4]^-$; (d) 0.25 wt % of **IL4** – $[C_1Py]^+ [NTf_2]^-$.

Confocal microscope was used in order to get a tridimensional projection of the worn tracks of the discs and to have a better understanding of the wear

process. Figure 3. 7 confirms what was found by optical microscope: the surface lubricated with neat glycerol presents deep scratches while on the surface lubricated with ILs the scar was too thin to be distinguished. For what concerns the surfaces lubricated with blends of glycerol and ILs, it can be observed Figure 3. 7c) and Figure 3. 7d) that they present larger scars but the grooves are smoother than in Figure 3. 7a).

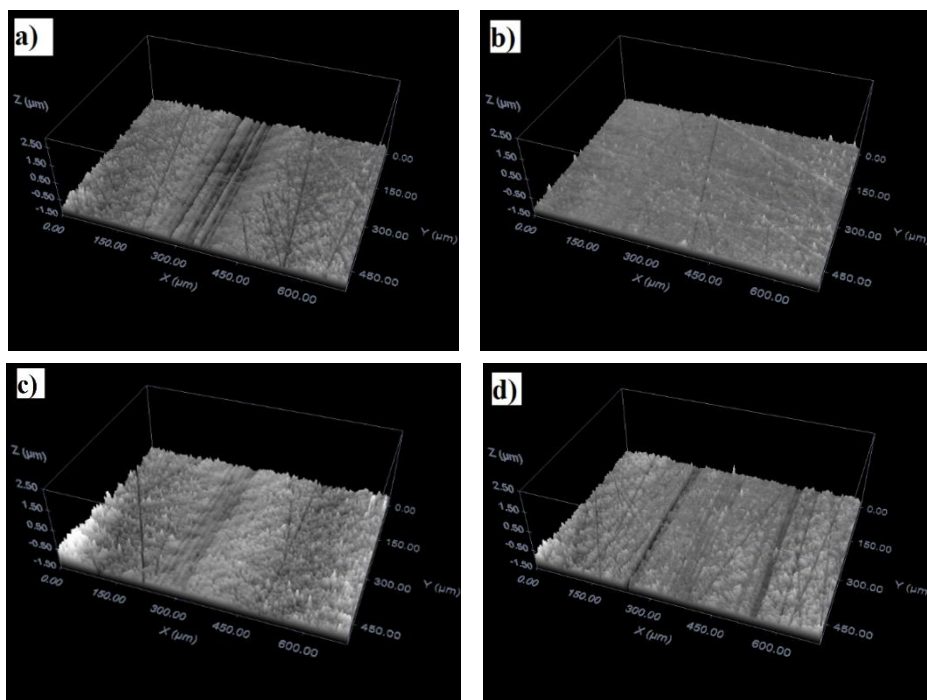


Figure 3. 7 - Representation of the wear scars obtained by confocal microscope on the discs lubricated with: a) glycerol, b) **IL4** - $[C_1Py]^+ [NTf_2]^-$, c) mixture of glycerol and 1% of **IL2** - $[C_1PyC_2H_4(CH_2OCH_2)_3C_2H_4PyC_1]^+ [NTf_2]^-_2$, d) mixture of glycerol and 1% of **IL4** - $[C_1Py]^+ [NTf_2]^-$.

3.4 CONCLUSIONS

Two new dicationic ILs that incorporate polyethylene glycol chains linking two alkyipyridinium moieties through rings position 2, were synthesized, together with the correspondent monocationic ILs.

The thermal analysis of the ILs synthesized showed that dicationic ILs incorporating polyethylene glycol chains linking two N-alkyipyridinium moieties through rings position 2, present higher thermal stability than simple monocationic N-alkyipyridinium ILs.

The matrix of ILs used allowed drawing some important conclusions about the structures that are more interesting for tribological investigation. First of all, it was established that the methylsulfate anion, $[C_1SO_4]$, should be avoided because of the high corrosiveness demonstrated.

Bis(trifluoromethanesulfonyl)imide anion, should be preferred since provides better performance both in terms of friction, wear and thermal stability. Similarly, dicationic structures had better performance than monocationic structures both in terms of friction and wear.

The Ionic liquid with dicationic moiety and NTf_2 anion has demonstrated good properties as neat lubricant. It had low coefficient of friction and a wear comparable with the reference lubricant. Even more interesting could be its use as friction modifier additive since an important change in the coefficient of friction was achieved with a really low concentration of ionic liquid.

Chapter 4

4 Dicationic ionic liquids

4.1 INTRODUCTION

In order to decrease the melting point, ILs are generally constituted from an organic cation with low symmetry and a weakly coordinated anion. This way, lattice energy is lower and the anion-cation interaction is minimized due to the asymmetric and delocalized charge [72].

The reason for the growing interest in IL can be explained by their excellent physical-chemical properties: large electrochemical window [138], controlled miscibility [139], high thermal stability [140], negligible vapour pressure [71,141] and in some cases, environmental harmlessness [142,143]. In addition to these qualities, it is pointed out that it is possible to obtain compounds with tailor-designed properties by tuning the structure through substitution and structural modification of the anion or of the cation.

In 2001, Liu *et al.* started the first tribological investigation with IL. This research group studied imidazolium tetrafluoroborate as IL based lubricant for various tribo-pairs [81] and, in all the experiments, the use of IL showed significant friction reduction. After this first research, many other authors have studied the tribological

behavior of IL and the number of papers published on this issue grows rapidly every year [85,144,145].

Dicationic IL have been investigated for their tribological behaviour and showed good performances. Anderson *et al.* have synthesized and analyzed the physico-chemical properties of 39 dicationic IL [146], finding that the thermal stabilities of the dicationic IL are greater than those of most traditional monocationic IL.

Palacio and Bushan have investigated the nanotribological properties of a group of novel lubricant for magnetic tapes: perfluoropolyethers, a monocationic IL and a dicationic IL [147]. The results of the research have shown that all lubricants involved have improved the nanotribological performance of the material under examination, in particular the dicationic IL 1,1'-(pentane-1,5-diyl)bis(3-hydroxyethyl-1*H*-imidazolium-1-yl) di[bis(trifluoromethanesulfonyl)imide] exhibited superior performance than the monocationic IL 1-butyl-3-methylimidazolium hexafluorophosphate in improving the adhesion and friction properties of the tape surface.

Jin *et al.* have examined some polyethylene glycol functionalized IL as high temperature lubricants [148], showing how the presence of fluorine in the IL favourably boosts its anti-wear performance. A dicationic IL with bis(trifluoromethanesulfonyl)imide as fluorine containing anion and a dication composed of two propylimidazolium moieties linked by tetraethylene glycol could maintain low friction at 300 °C.

The focus of this study will be the systematic evaluation of a group of novel dicationic IL to identify those structures being more suitable for tribological applications both as neat lubricants and as additives for synthetic base oil. The matrix of IL created offers the possibility to investigate on the one hand, the effect of ionic moieties, and on the other hand the general influence of the oligoethylene glycol

chain length on the tribological performance of the IL. Thus, the objectives of this research are the identification of the most performing IL and also the determination of general guidelines for the design of future IL.

4.2 EXPERIMENTAL DETAILS

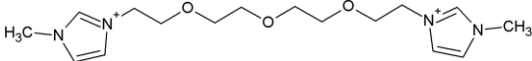
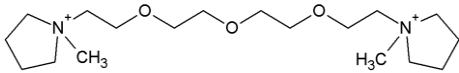
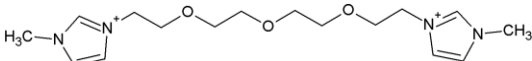
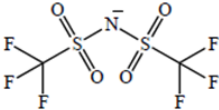
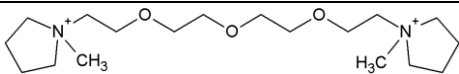
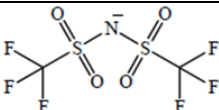
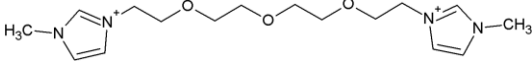
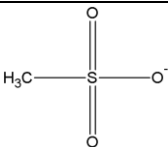
4.2.1 Materials

The ILs used for this work were synthesized, in the context of the Marie Curie Initial Training Network MINILUBES, by the Martin Luther University Halle-Wittenberg in Germany and by the University of Vigo in Spain. They were produced for the first time through a facile synthetic route for the preparation of dicationic poly(ethylene glycol)-containing ionic liquids based on azide/alkyne “click” chemistry. In contrast to the conventionally used quaternization reaction, a microwave assisted azide/alkyne “click” reaction between diazido- ethylene glycols and the corresponding alkyne containing IL-head group resulted in higher yields even with longer polymer chains.

The chemical structures together with the codifications used for these dicationic ILs are shown in Table 4. 1 and in Table 4. 2.

The basic concept of the dicationic IL made use of 2 different types of cationic groups, *N*-methylimidazolium and *N*-methylpyrrolidinium which are connected by tetraethylene glycol (IL5 to IL10), hexaethylene glycol (IL11 to IL13) and oligoethylene glycol (IL14 and IL15). The number of ethylene groups is referred to the molecules used for the synthesis. For the synthesis **IL14** - $[\text{C}_1\text{PyrTrCH}_2(\text{CH}_2\text{OCH}_2)_{22}\text{CH}_2\text{TrPyrC}_1]^+ [\text{C}_1\text{SO}_3]_2^-$ and **IL15** - $[\text{C}_1\text{ImTrCH}_2(\text{CH}_2\text{OCH}_2)_{20}\text{CH}_2\text{TrImC}_1]^+ [\text{C}_1\text{SO}_3]_2^-$, PEG1500 was used, which gave an average polymerization degree of 23 and 21, respectively. As illustrated in Table 4. 2, **IL11** to **IL15**, the cationic groups have been attached to the linking chain through additional triazole groups.

Table 4. 1 - Structure and codification of the ionic liquids synthesized in the Martin Luther University Halle-Wittenberg

Cation	Anion
	2X Cl ⁻
1,11-bis(3N-methyl-1-imidazolium)-3,6,9-trioxaundecane Chloride IL5 - [C ₁ ImCH ₂ (CH ₂ OCH ₂) ₃ CH ₂ ImC ₁] ⁺ [Cl] ⁻ ₂	
	2X Cl ⁻
1,11-bis(1N-methyl-1-pyrrolidinium)-3,6,9-trioxaundecane Chloride IL6 - [C ₁ Pyrr CH ₂ (CH ₂ OCH ₂) ₃ CH ₂ PyrrC ₁] ⁺ [Cl] ⁻ ₂	
	 2X
1,11-bis(3N-methyl-1-imidazolium)-3,6,9-trioxaundecane bis(trifluoromethanesulfonyl)imide IL7 - [C ₁ ImCH ₂ (CH ₂ OCH ₂) ₃ CH ₂ ImC ₁] ⁺ [NTf ₂] ⁻ ₂	
	 2X
1,11-bis(1N-methyl-1-pyrrolidinium)-3,6,9-trioxaundecane bis(trifluoromethanesulfonyl)imide IL8 - [C ₁ Pyrr CH ₂ (CH ₂ OCH ₂) ₃ CH ₂ PyrrC ₁] ⁺ [NTf ₂] ⁻ ₂	
	 2X
1,11-bis(3N-methyl-1-imidazolium)-3,6,9-trioxaundecane methanesulfonate IL9 - [C ₁ ImCH ₂ (CH ₂ OCH ₂) ₃ CH ₂ ImC ₁] ⁺ [C ₁ SO ₃] ⁻ ₂	

Continue from Table 4. 1

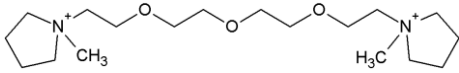
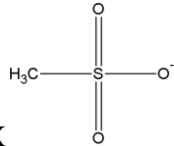
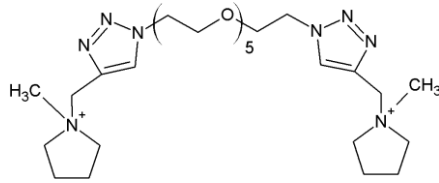
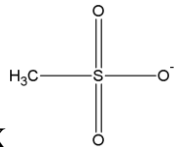
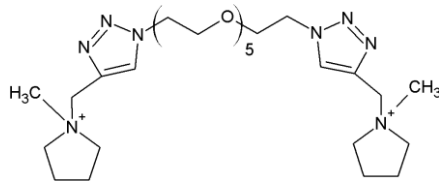
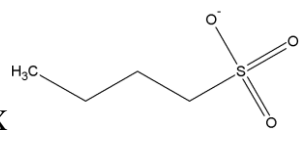
Cation	Anion
	 2X
1,11-bis(1N-methyl-1-pyrrolidinium)-3,6,9-trioxaundecane methylsulfonate IL10 - $[\text{C}_1\text{Pyr}\text{rCH}_2(\text{CH}_2\text{OCH}_2)_3\text{CH}_2\text{Pyr}\text{rC}_1]^+ [\text{C}_1\text{SO}_3]_2^-$	
IL7 + IL9 (90%-10%) MIX	

Table 4. 2 - Structure and codification of the ionic liquids synthesized in the University of Vigo

Cation	Anion
	 2X
1,17-bis[4-(1N-methyl-1-pyrrolidinium)methyl-1,2,3-triazolyl]-3,6,9,12,15-pentaoxaheptadecene methanesulfonate IL11 - $[\text{C}_1\text{Pyr}\text{rTrCH}_2(\text{CH}_2\text{OCH}_2)_5\text{CH}_2\text{TrPyr}\text{rC}_1]^+ [\text{C}_1\text{SO}_3]_2^-$	
	 2X
1,17-bis[4-(1N-methyl-1-pyrrolidinium)methyl-1,2,3-triazolyl]-3,6,9,12,15-pentaoxaheptadecene butanesulfonate IL12 - $[\text{C}_1\text{Pyr}\text{rTrCH}_2(\text{CH}_2\text{OCH}_2)_5\text{CH}_2\text{TrPyr}\text{rC}_1]^+ [\text{C}_4\text{SO}_3]_2^-$	

Continue from Table 4. 2

Cation	Anion
2X	
<p>1,17-bis[4-(3N-methyl-1-imidazolium)methyl-1,2,3-triazolyl]-3,6,9,12,15-pentaoxaheptadecene methanesulfonate</p>	
<p>IL13 - $[\text{C}_1\text{ImTrCH}_2(\text{CH}_2\text{OCH}_2)_5\text{CH}_2\text{TrImC}_1]^+ [\text{C}_1\text{SO}_3]_2^-$</p>	
2X	
<p>Poly(ethyleneoxide)-1,omega-bis[4-(1N-methyl-1-pyrrolidinium)methyl-1,2,3-triazole] methanesulfonate</p>	
<p>IL14 - $[\text{C}_1\text{PyrTrCH}_2(\text{CH}_2\text{OCH}_2)_{22}\text{CH}_2\text{TrPyrC}_1]^+ [\text{C}_1\text{SO}_3]_2^-$</p>	
2X	
<p>Poly(ethyleneoxide)-1,omega-bis[4-(1N-methyl-1-imidazolium)methyl-1,2,3-triazole] methanesulfonate</p>	
<p>IL15 - $[\text{C}_1\text{ImTrCH}_2(\text{CH}_2\text{OCH}_2)_{20}\text{CH}_2\text{TrImC}_1]^+ [\text{C}_1\text{SO}_3]_2^-$</p>	

The cations obtained have been paired with chloride, bis(trifluoromethanesulfonyl)imide, methylsulfonate and butylsulfonate anions. In addition, one IL was formulated as a 9:1 stoichiometric mixture of tetraethylene glycol *N*-methylimidazolium NTf₂ and tetraethylene glycol *N*-methylimidazolium methanesulfonate to give a new lubricant that was named as **MIX**.

A Synalox™ 100-30B polypropylene glycol monobutyl ether (CAS 9003-13-8) provided by The Dow Chemical Company has been used as base oil for binary mixtures with 1 % w/w of selected dicationic ILs. An ultra-sonicator Sonics Vibra Cell VCX 500 (Sonics & Materials Inc., USA) was used for achieving a good distribution of IL in the base oil. The sonication was performed for 30 s with 21 % of the maximum vibration amplitude and with pulses 2 seconds ON and 2 seconds OFF. Methanesulfonate ILs were subject to the treatment twice with an interval of thirty minutes due to the limited solubility and the appearance in the solid state at room temperature.

Thus, the dicationic ILs matrix created offers the opportunity to investigate a) the influence of cation and anion variation, b) the influence of the oligoethylene glycol chain length on the tribological performance of the IL and c) the usefulness of promising dicationic IL as anti-wear additives.

4.2.2 Thermal analyses

In order to study the thermal degradation of the dicationic IL, Thermogravimetric Analysis (TGA) and Differential Scanning Calorimetry (DSC) have been applied. The equipment used for thermal analysis was a SDT Q600 (TA Instruments, USA), capable of performing DSC and TGA simultaneously.

The thermal analyses have been performed in a dynamic mode, with temperature linearly increasing at a rate of 10 °C/min under a constant flow of nitrogen. The TGA and DSC experiments started at ambient temperature and were completed at 500 °C. The pans used for holding the samples were made of platinum.

The onset temperature (T_{onset}) is the intersection of the baseline weight from the beginning of the experiment and the tangent of the weight vs temperature curve as decomposition occurs. The start temperature (T_{start}) is the temperature at which the decomposition of the sample begins.

4.2.3 Tribological experiments

For the evaluation of the tribological performances of the IL, the Schwing-Reib-Verschleiss (SRV) tribometer (Optimol Instruments Prüftechnik, Germany) with reciprocating ball-on-disc configuration, was used. The experiments have been performed following the guidelines of the standard method ASTM D 6425 –11 [118]. According to this procedure, the load applied was 300 N and the experiments lasted 2 hours. Other parameters were: stroke of 1 mm and frequency of 50 Hz. Both balls and discs have been purchased from Optimol Instruments Prüftechnik and the quality of the material was certified to be in conformity with international standards. The balls were made of steel AISI 52100 with a diameter of 10 mm, roughness of 0.012 μm and hardness HRC 63 ± 2 . Discs were also made of steel AISI 52100 with a diameter of 24 mm, thickness of 7.9 mm and roughness of 0.56 μm . Discs and ball were cleaned before the tribotests by immersion in ultrasonic bath with acetone and petroleum ether for 5 minutes each. The maximum contact pressure, calculated as suggested by Stachowiak for contact between a sphere and a flat surface [120], was 3.14 GPa. Experiments have been performed twice at 50, 100 and 150 °C with neat IL. For IL in base oil, tribometrical experiments were carried out at 100 °C.

Average coefficients of friction (COF) were calculated from the data recorded during the tribotests after a running-in period of 500 s.

The ball wear volumes were examined for the neat IL by optical microscope DM 2500 MH (Leica, Germany). And quantified according to the method described in Chapter 2.3.3.1.

For the mixtures of base oil and IL the wear volume was calculated by confocal 3D microscope μ surf (NanoFocus, Germany).

4.2.4 Surface analysis

Scanning Electron Microscopy Energy Dispersive Spectroscopy (SEM-EDS) with an ULTRA FE-SEM (Zeiss, Germany) was used to study the surface topography and tribofilm composition of the ball wear scars.

X-ray Photoelectron Spectroscopy (XPS) has been performed on the disc specimens for the determination of the elemental composition and chemical environment of the elements identified in and outside the wear scar. The equipment used was a Thermo Fisher Scientific Theta Probe (East Grinstead, United Kingdom) with a monochromatic Al K α X-ray source ($h\nu = 1486.6$ eV). The base pressure during the measurements was consistently at 3×10^{-9} mbar. The discs for XPS analysis were thoroughly cleaned directly after the tribological experiments by immersion in toluene in an ultrasonic bath for 15 minutes at room temperature, followed by 2-propanol and petroleum ether for the same duration. Spots in and outside of the worn area of the discs were defined and analyzed with a spot diameter of 100 μ m at a 200 eV pass energy for the survey spectra. Detail spectra were recorded at a pass energy of 50 eV. For the imaging XPS experiments, an area of 1.8×1.5 mm² was scanned with a spot and step size of 100 μ m, resulting in 285 individual measuring spots as shown in Figure 4. 1. All elements detected by the survey analyses, were recorded in the imaging XPS experiments as snap shots with a 15 eV wide binding energy window and a resulting pass energy of 150.5 eV. The collected analytical data were processed with the Advantage Data System software from Thermo Fisher Scientific (East Grinstead, United Kingdom), using Gaussian-Lorentzian peak fitting.

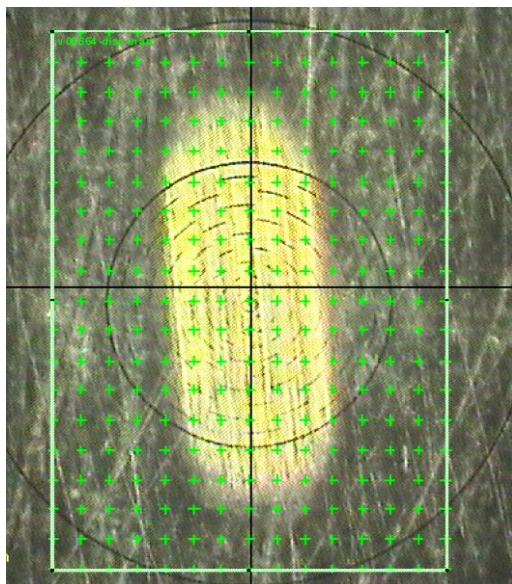


Figure 4.1 – Grid over the disc wear track defining the spots for individual measurements (green crosses).

4.2.5 Corrosion experiments

In order to screen the potential of the dicationic IL for corrosiveness, simple corrosion experiments were performed by application of a drop of each neat IL on the polished surface of an SRV disc. The discs were kept in an oven at 100 °C for one week. The degradation of the steel surface due to the action of the different IL was evaluated by means of optical microscopy.

4.3 RESULTS AND DISCUSSION

4.3.1 Thermal properties

The thermal stabilities of the IL were determined. All IL were found to be stable up to temperatures of at least 150 °C, which was the highest temperature chosen for the tribological measurements (unpublished results).

Table 4. 3 Thermal stability measured by TGA

Ionic liquid	Melting point [°C]	T _{Start} [°C]	T _{Onset} [°C]
IL5	RTIL	212	244
IL6	RTIL	178	245
IL7	RTIL	375	425
IL8	RTIL	295	402
IL9	RTIL	310	350
IL10	RTIL	200	265
MIX	-53	370	428
IL11	RTIL	225	288
IL12	RTIL	210	292
IL13	RTIL	215	290
IL14	42	210	310
IL15	44	245	261

By DSC measurements, it has been possible to determine the melting points of **IL14** - $[\text{C}_1\text{PyrrTrCH}_2(\text{CH}_2\text{OCH}_2)_{22}\text{CH}_2\text{TrPyrrC}_1]^+ [\text{C}_1\text{SO}_3]^-_2$ and **IL15** - $[\text{C}_1\text{ImTrCH}_2(\text{CH}_2\text{OCH}_2)_{20}\text{CH}_2\text{TrImC}_1]^+ [\text{C}_1\text{SO}_3]^-_2$ that were 42 °C and 44 °C, respectively (Figure 4. 2). The other IL occurred in the liquid state at room temperature and no significant phase transitions were detected within the tribological measuring range.

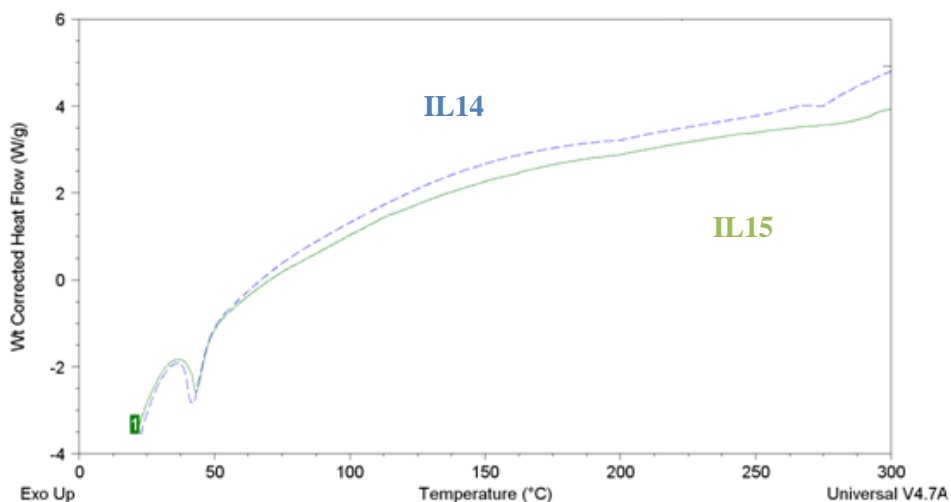


Figure 4. 2 – DSC curves with **IL14** - $[C_1\text{PyrrTrCH}_2(\text{CH}_2\text{OCH}_2)_{22}\text{CH}_2\text{TrPyrrC}_1]^+ [C_1\text{SO}_3]_2^-$ and **IL15** - $[C_1\text{ImTrCH}_2(\text{CH}_2\text{OCH}_2)_{20}\text{CH}_2\text{TrImC}_1]^+ [C_1\text{SO}_3]_2^-$ in the temperature range from 22 °C to 300 °C. Curve at temperatures higher than 300 °C was excluded due to strongly irregular progress caused by ionic liquid degradation.

4.3.2 Tribological performance

4.3.2.1 Performance of neat IL

The main parameters considered for the evaluation of the tribological properties have been COF and W_v . The graphs in Figure 4. 3, Figure 4. 4 and Figure 4. 5 summarize the mean values and the standard deviations in terms of friction and wear at the temperatures 50, 100 and 150 °C, respectively.

The findings of the chloride based IL, **IL5** - $[C_1\text{ImCH}_2(\text{CH}_2\text{OCH}_2)_3\text{CH}_2\text{ImC}_1]^+ [\text{Cl}]_2^-$ and **IL6** - $[C_1\text{PyrrCH}_2(\text{CH}_2\text{OCH}_2)_3\text{CH}_2\text{PyrrC}_1]^+ [\text{Cl}]_2^-$ have not been included. Preliminary experiments at 100 °C revealed that their tribological properties were not adequate for their use as lubricant: COF was not stable during the entire experiments and the specimens suffered from frequent microwelding events causing severe wear. Thus, the tribometrical data obtained with **IL5** -

$[C_1ImCH_2(CH_2OCH_2)_3CH_2ImC_1]^+ [Cl]^-_2$ and **IL6** - $[C_1PyrrCH_2(CH_2OCH_2)_3CH_2PyrrC_1]^+ [Cl]^-_2$ are not shown.

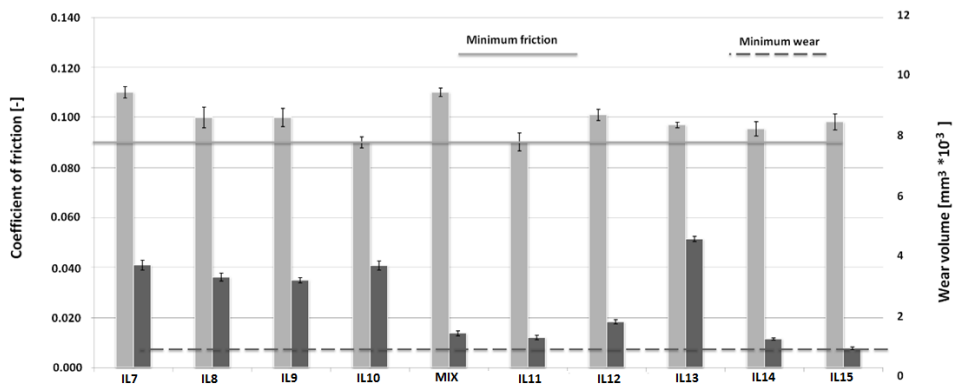


Figure 4. 3 – Ball wear volume and friction of the ionic liquids at 50 °C, light (left) columns indicate COF, dark (right) columns indicate ball wear volume.

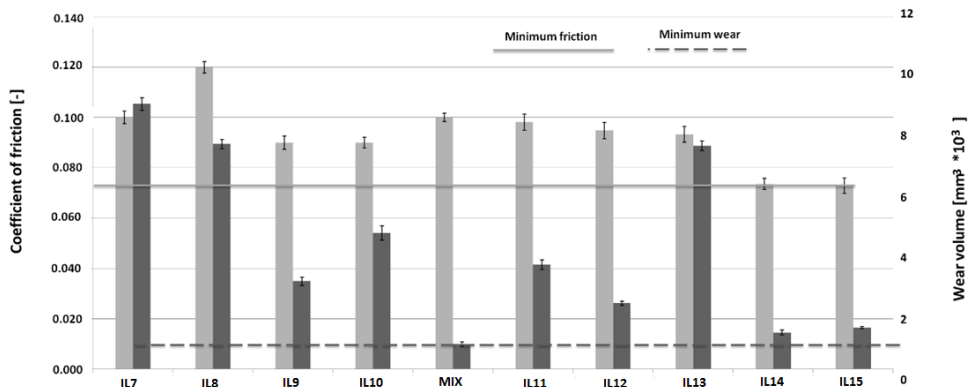


Figure 4. 4 – Ball wear volume and friction of the ionic liquids at 100 °C, light (left) columns indicate COF, dark (right) columns indicate ball wear volume.

An in-depth result interpretation for each temperature shows that all the IL have an average COF between 0.090 and 0.110 at 50 °C (light columns in Figure 4. 3, Figure 4. 4 and Figure 4. 5), which means that they provided low friction in comparison with other formulated lubricants.

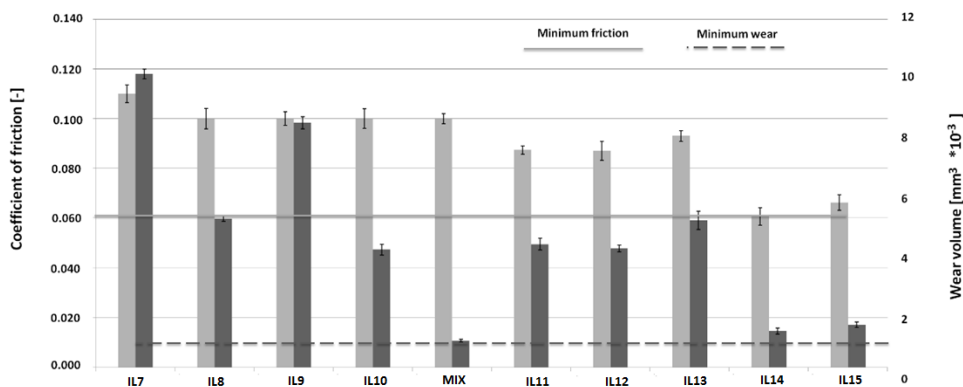


Figure 4. 5 – Ball wear volume and friction of the ionic liquids at 150 °C, light (left) columns indicate COF, dark (right) columns indicate ball wear volume.

The tests described in the standard ASTM D6245-11 [118] were performed under the same conditions and gave coefficient of friction ranging from 0.126 to 0.140 for the engine oils and from 0.111 to 0.119 for the hydraulic oil. Even more interesting results have been obtained at 100 °C and 150 °C. As matter of fact, most of the IL studied have shown a very similar performance at all temperatures but **IL14** - $[\text{C}_1\text{PyrrTrCH}_2(\text{CH}_2\text{OCH}_2)_{22}\text{CH}_2\text{TrPyrrC}_1]^+ [\text{C}_1\text{SO}_3]_2^-$ and **IL15** - $[\text{C}_1\text{ImTrCH}_2(\text{CH}_2\text{OCH}_2)_{20}\text{CH}_2\text{TrImC}_1]^+ [\text{C}_1\text{SO}_3]_2^-$ resulted in a significant decrease of friction with an increase of temperature. At 100 °C, the COF for **IL14** - $[\text{C}_1\text{PyrrTrCH}_2(\text{CH}_2\text{OCH}_2)_{22}\text{CH}_2\text{TrPyrrC}_1]^+ [\text{C}_1\text{SO}_3]_2^-$ and **IL15** - $[\text{C}_1\text{ImTrCH}_2(\text{CH}_2\text{OCH}_2)_{20}\text{CH}_2\text{TrImC}_1]^+ [\text{C}_1\text{SO}_3]_2^-$ was 0.074 and 0.073, respectively, in comparison with a COF range between 0.090 and 0.120 for the other dicationic IL. At 150 °C, COF was further diminished to 0.061 and 0.066, respectively, while the other IL varied from 0.087 to 0.110 being comparable to the ranges found at the lower temperatures. In general, a stable COF was achieved within a short period, less than 500 s, being the evidence for rapid tribofilm formation.

Regarding wear generation during the tests (dark columns in Figure 4. 3, Figure 4. 4 and Figure 4. 5), the wear tracks resulting from the experiments at 50 °C show that

the best result was obtained with **IL15** - $[\text{C}_1\text{ImTrCH}_2(\text{CH}_2\text{OCH}_2)_{20}\text{CH}_2\text{TrImC}_1]^+ [\text{C}_1\text{SO}_3]^-_2$. Also other IL have shown promising anti-wear properties, in particular **MIX**, **IL11** - $[\text{C}_1\text{PyrrTrCH}_2(\text{CH}_2\text{OCH}_2)_5\text{CH}_2\text{TrPyrrC}_1]^+ [\text{C}_1\text{SO}_3]^-_2$, **IL12** - $[\text{C}_1\text{PyrrTrCH}_2(\text{CH}_2\text{OCH}_2)_5\text{CH}_2\text{TrPyrrC}_1]^+ [\text{C}_4\text{SO}_3]^-_2$ and **IL14** - $[\text{C}_1\text{PyrrTrCH}_2(\text{CH}_2\text{OCH}_2)_{22}\text{CH}_2\text{TrPyrrC}_1]^+ [\text{C}_1\text{SO}_3]^-_2$ have given results of wear comparable with the values normally obtained with conventional lubricants commercially available [118].

By increasing the temperature to 100 °C and 150 °C, a different situation can be observed: **IL11** - $[\text{C}_1\text{PyrrTrCH}_2(\text{CH}_2\text{OCH}_2)_5\text{CH}_2\text{TrPyrrC}_1]^+ [\text{C}_1\text{SO}_3]^-_2$ and **IL12** - $[\text{C}_1\text{PyrrTrCH}_2(\text{CH}_2\text{OCH}_2)_5\text{CH}_2\text{TrPyrrC}_1]^+ [\text{C}_4\text{SO}_3]^-_2$ are losing their capability to protect the surface which results in higher wear than at 50 °C. The ionic liquids **IL14** - $[\text{C}_1\text{PyrrTrCH}_2(\text{CH}_2\text{OCH}_2)_{22}\text{CH}_2\text{TrPyrrC}_1]^+ [\text{C}_1\text{SO}_3]^-_2$ and **IL15** - $[\text{C}_1\text{ImTrCH}_2(\text{CH}_2\text{OCH}_2)_{20}\text{CH}_2\text{TrImC}_1]^+ [\text{C}_1\text{SO}_3]^-_2$ maintain their good anti-wear properties at 100 °C and 150 °C. Mathematically, **MIX** has the best performance among the dicationic IL, in fact the wear volume produced on the steel balls during the experiments with **MIX** is relatively constant at all temperatures and is between 8.4 and $11.7 \times 10^{-4} \text{ mm}^3$, corresponding to a wear scar diameter of about 560 μm .

In order to better understand the outstanding lubrication performance of **MIX**, SEM-EDS analysis has been applied to the balls used for the experiments with **MIX**. At 100°C, only small amounts of oxygen and sulfur were detected in the wear scar area. But at 150°C, both oxygen and sulfur were found in considerable quantities (Figure 4. 6). It can be concluded that there is a change in the lubrication mechanism; at elevated temperature it is suggested that a more pronounced tribolayer has been originated due to the reactivity of the steel with the sulfur containing anions.

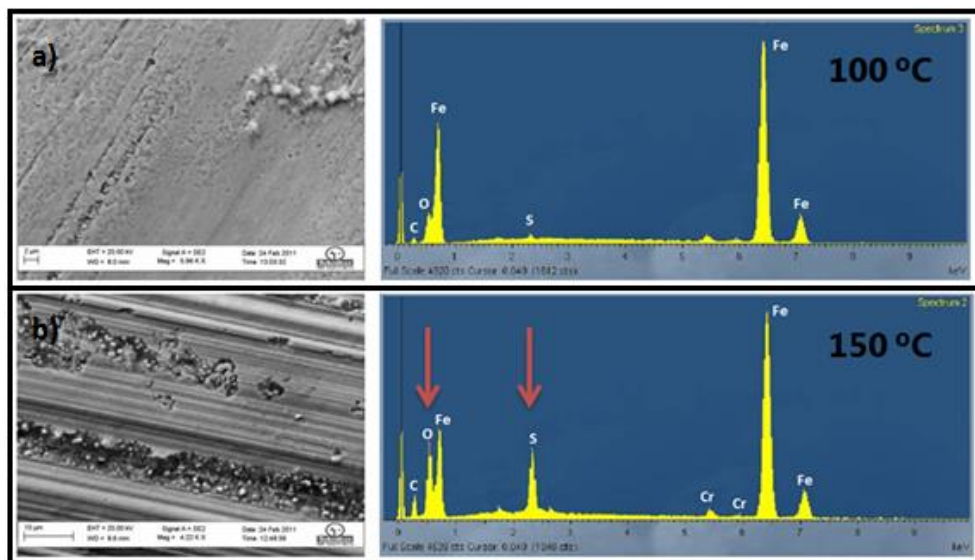


Figure 4.6 – SEM-EDS analysis comparing the ball wear scars from tribotests at 100 °C (a) and at 150 °C (b) using **MIX**. SEM image of (a) has a width of 50 μm , that of b) has a total width of 70 μm . Arrows indicate increased amounts of oxygen and sulfur in the tribofilm

Taking into consideration the ionic structures investigated, it is pointed out that **MIX** as one of the best performing IL has been prepared from **IL7** - $[\text{C}_1\text{ImCH}_2(\text{CH}_2\text{OCH}_2)_3\text{CH}_2\text{ImC}_1]^+ [\text{NTf}_2]^-_2$ and **IL9** - $[\text{C}_1\text{ImCH}_2(\text{CH}_2\text{OCH}_2)_3\text{CH}_2\text{ImC}_1]^+ [\text{C}_1\text{SO}_3]^-_2$ and provided better anti-wear properties than those exerted by the individual IL in all experiments while friction remained constant under the tribometrical conditions. Besides, it can be also stated – based on the findings – that IL with longer oligoethylene glycol chains tend to reveal better friction and wear properties, especially when **IL14** - $[\text{C}_1\text{PyrrTrCH}_2(\text{CH}_2\text{OCH}_2)_{22}\text{CH}_2\text{TrPyrrC}_1]^+ [\text{C}_1\text{SO}_3]^-_2$ and **IL15** - $[\text{C}_1\text{ImTrCH}_2(\text{CH}_2\text{OCH}_2)_{20}\text{CH}_2\text{TrImC}_1]^+ [\text{C}_1\text{SO}_3]^-_2$ with oligoethylene glycol chains are compared with **IL11** - $[\text{C}_1\text{PyrrTrCH}_2(\text{CH}_2\text{OCH}_2)_5\text{CH}_2\text{TrPyrrC}_1]^+ [\text{C}_1\text{SO}_3]^-_2$ and **IL13** - $[\text{C}_1\text{ImTrCH}_2(\text{CH}_2\text{OCH}_2)_5\text{CH}_2\text{TrImC}_1]^+ [\text{C}_1\text{SO}_3]^-_2$ with hexaethylene glycol chains. In particular at higher temperatures, superiority of **IL14** - $[\text{C}_1\text{PyrrTrCH}_2(\text{CH}_2\text{OCH}_2)_{22}\text{CH}_2\text{TrPyrrC}_1]^+ [\text{C}_1\text{SO}_3]^-_2$ and **IL15** -

$[C_1ImTrCH_2(CH_2OCH_2)_{20}CH_2TrImC_1]^+ [C_1SO_3]^-_2$, having longer linking chains, could be maintained.

4.3.2.2 Performance of binary mixtures of IL and base oil

For this part of the experiments, it has been decided to analyze only those IL that were considered more promising from a tribological point of view, in detail **IL7** - $[C_1ImCH_2(CH_2OCH_2)_3CH_2ImC_1]^+ [NTf_2]^-_2$, **MIX**, **IL14** - $[C_1PyrrTrCH_2(CH_2OCH_2)_{22}CH_2TrPyrrC_1]^+ [C_1SO_3]^-_2$ and **IL15** - $[C_1ImTrCH_2(CH_2OCH_2)_{20}CH_2TrImC_1]^+ [C_1SO_3]^-_2$. Despite the bad results shown in the neat form, **IL7** - $[C_1ImCH_2(CH_2OCH_2)_3CH_2ImC_1]^+ [NTf_2]^-_2$ was chosen because it is the main component in the formulation of **MIX**. The mixtures were provided with a concentration of 1 % w/w of IL in Synalox™ to cope with typical concentrations of anti-wear additives. In addition to the mixtures, the base oil Synalox™ was used as reference.

The SRV tribometer used for running the tribotests with the mixture was not the same that was used for the examination of the neat dicationic IL, although they are similar models. The neat ionic liquids were studied at IK4-TEKNIKER while the mixtures were studied at AC2T research GmbH. This means that the results are not recommended for direct comparison.

Figure 4. 7 shows the coefficient of friction recorded during the tribotests performed with the base oil Synalox™ and the mixtures with selected dicationic IL. The interpretation of the curve “coefficient of friction versus time” for each tribotest reveals that mixtures of base oil with **IL14** - $[C_1PyrrTrCH_2(CH_2OCH_2)_{22}CH_2TrPyrrC_1]^+ [C_1SO_3]^-_2$ and **IL15** - $[C_1ImTrCH_2(CH_2OCH_2)_{20}CH_2TrImC_1]^+ [C_1SO_3]^-_2$ had approximately the same behavior of the base oil: running-in period of 15 to 20 minutes followed by a period of degressive increase of coefficient of friction till values larger than 0.2 were observed being rather high for lubricated tribo-contact. Running-in was characterized by a very unstable COF due to frequent microwelding events.

However, the mixtures of base oil with **MIX** and **IL7** - $[C_1ImCH_2(CH_2OCH_2)_3CH_2ImC_1]^+ [NTf_2]^-_2$ exerted a completely different trend: here, the running-in period is significantly shorter with less than 5 minutes, and in the following period of time COF was constant resulting in a smooth curve. Although the general trend of **IL7** - $[C_1ImCH_2(CH_2OCH_2)_3CH_2ImC_1]^+ [NTf_2]^-_2$ and **MIX** can be considered good, the presence of a peak in the friction curve in all the repetitions done was observed. The phenomenon can be mainly ascribed to the severe tests conditions chosen, where rather high loads were applied.

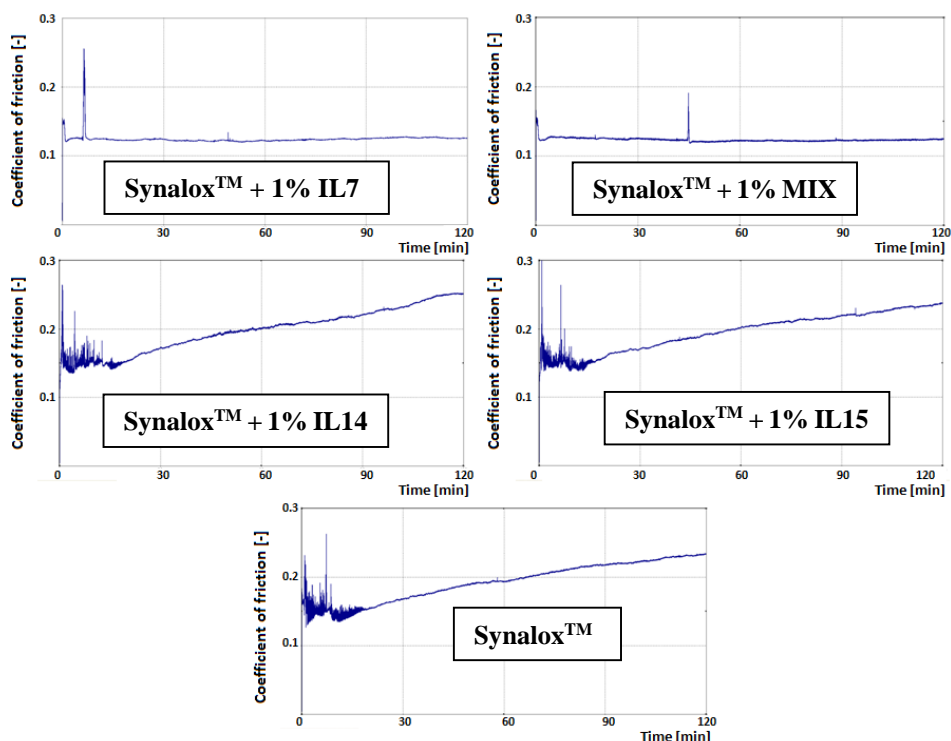


Figure 4. 7 – Progress of coefficient of friction at 100 °C over time with mixtures of 1 % w/w dicationic IL in Synalox™. Neat Synalox™ as reference.

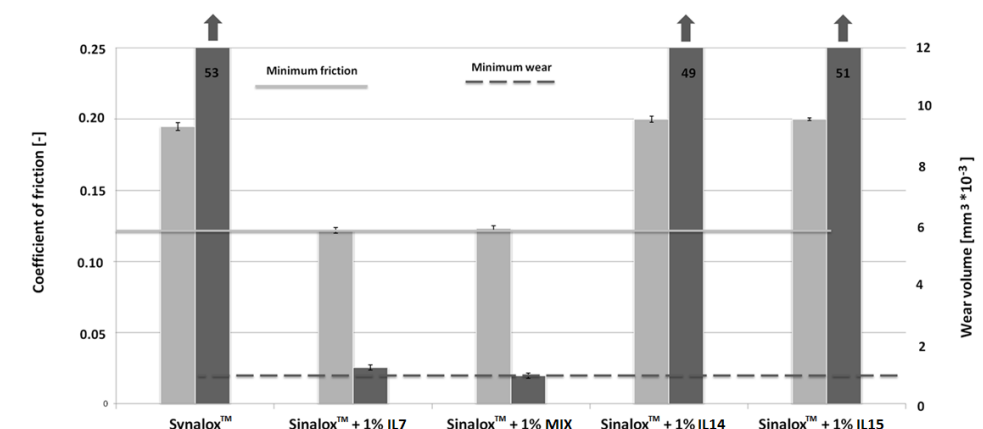


Figure 4. 8 – Ball wear volume and friction of the mixtures of IL and base oil at 100 °C, light (left) columns indicate COF, dark (right) columns indicate ball wear volume. Neat Synalox™ is used as reference. Values shown for mixtures with wear volumes exceeding scale. COF is coefficient of friction.

The comparison of the average ball wear volumes obtained with the base oil and the mixtures is shown in Figure 4. 8. The examination of the wear track by optical microscope has confirmed that the base oil and the mixtures of **IL14** - $[\text{C}_1\text{PyrrTrCH}_2(\text{CH}_2\text{OCH}_2)_{22}\text{CH}_2\text{TrPyrrC}_1]^+ [\text{C}_1\text{SO}_3]_2^-$ and **IL15** - $[\text{C}_1\text{ImTrCH}_2(\text{CH}_2\text{OCH}_2)_{20}\text{CH}_2\text{TrImC}_1]^+ [\text{C}_1\text{SO}_3]_2^-$ were not possible to provide proper protection to the rubbing surfaces. The ball wear volumes were extremely high, almost 80 times higher than the ball wear volumes determined for **IL7** - $[\text{C}_1\text{ImCH}_2(\text{CH}_2\text{OCH}_2)_3\text{CH}_2\text{ImC}_1]^+ [\text{NTf}_2]_2^-$ and **MIX** as additives.

The latter dicationic IL proved to confer significant friction and wear reduction when added to the base oil.

4.3.3 Surface analysis

XPS analysis was performed on the specimens used for the mixtures of **IL7** - $[\text{C}_1\text{ImCH}_2(\text{CH}_2\text{OCH}_2)_3\text{CH}_2\text{ImC}_1]^+ [\text{NTf}_2]_2^-$ and **IL9** - $[\text{C}_1\text{ImCH}_2(\text{CH}_2\text{OCH}_2)_3\text{CH}_2\text{ImC}_1]^+ [\text{C}_1\text{SO}_3]_2^-$ in base oil in order to understand

the lubrication mechanism. For this purpose, imaging was performed to gain knowledge about the distribution of selected elements and their binding states inside and outside the wear track of the discs.

The survey scans of a disc lubricated with the mixture of **MIX** revealed that the fluorine content is significantly higher in the worn area than outside. The further investigation of fluorine by a detail scan clearly showed, that no organic fluorine could be observed in this tribologically stressed region. Instead, inorganic fluorine with a binding energy of 684.6 ± 0.2 eV was detected, which suggests that the bis(trifluoromethanesulfonyl)imide anion is completely decomposed under these tribological conditions by the formation of an inorganic fluorine layer (Figure 4. 9). Further, sulfidic sulphur was detected in the wear track at a binding energy of 161.7 ± 0.1 eV which gives additionally evidence for breaking up of the anionic structure. This behavior of the bis(trifluoromethanesulfonyl)imide anion was already reported in previous studies [149-152].

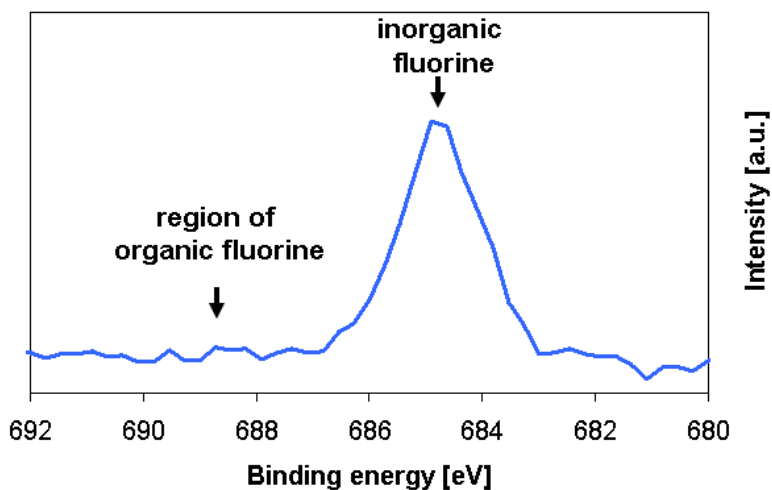


Figure 4. 9 – XPS detail spectrum of fluorine F 1s in the middle of the disc wear track from a tribotest with a mixture of 1 % w/w **MIX** in SynaloxTM showing a pronounced peak at 684.6 eV.

The distribution of the binding energies 684.6 ± 0.2 eV, inorganic fluorine, and 161.7 ± 0.1 eV, sulfidic sulfur, were investigated by an imaging XPS experiment, which clearly showed that the binding energies found are mainly located in the wear track (Figure 4. 10 A and Figure 4. 10 B). The binding energy found for iron at 711 eV suggests the formation of a FeF_2 layer besides iron oxide and iron sulfide providing the good tribological performance (Figure 4. 10 C).

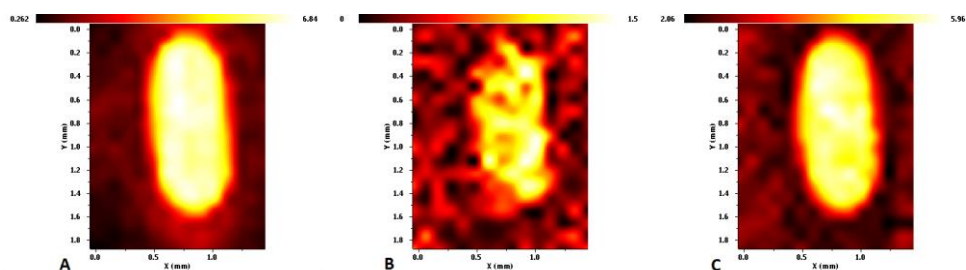


Figure 4. 10 – Distribution of (A) fluorine $F 1s$ at a binding energy of 684.6 eV, (B) sulfur $S 2p3$ 161.7 eV and (C) iron $Fe 2p3$ at a binding energy of 711 eV from a tribotest with a mixture of 1 % w/w **MIX** in Synalox™ in and outside the disc wear track visualized by the XPS imaging experiment.

Summarizing the results obtained with the mixtures of dicationic IL in Synalox™ base oil, a surprisingly good result has been obtained with **IL7** - $[\text{C}_1\text{ImCH}_2(\text{CH}_2\text{OCH}_2)_3\text{CH}_2\text{ImC}_1]^+ [\text{NTf}_2]^-_2$. This IL behaved much better in the mixture than in the neat state. Friction reduction and wear protection are in the range of the best performing neat IL (**MIX**, **IL14** - $[\text{C}_1\text{PyrrTrCH}_2(\text{CH}_2\text{OCH}_2)_{22}\text{CH}_2\text{TrPyrrC}_1]^+ [\text{C}_1\text{SO}_3]^-_2$ and **IL15** - $[\text{C}_1\text{ImTrCH}_2(\text{CH}_2\text{OCH}_2)_{20}\text{CH}_2\text{TrImC}_1]^+ [\text{C}_1\text{SO}_3]^-_2$).

MIX, being a mixture of two different dicationic IL (**IL7** - $[\text{C}_1\text{ImCH}_2(\text{CH}_2\text{OCH}_2)_3\text{CH}_2\text{ImC}_1]^+ [\text{NTf}_2]^-_2$ and **IL9** - $[\text{C}_1\text{ImCH}_2(\text{CH}_2\text{OCH}_2)_3\text{CH}_2\text{ImC}_1]^+ [\text{C}_1\text{SO}_3]^-_2$) has shown the best tribological properties both as neat lubricant and as additive, demonstrating that IL can work synergistically when appropriately mixed.

It is evident that **IL14** - $[C_1PyrrTrCH_2(CH_2OCH_2)_{22}CH_2TrPyrrC_1]^+ [C_1SO_3]^-_2$ and **IL15** - $[C_1ImTrCH_2(CH_2OCH_2)_{20}CH_2TrImC_1]^+ [C_1SO_3]^-_2$, which showed good performance in the neat state, seem not to be suitable as additives. It is likely that the concentration of 1 % w/w dicationic IL is not sufficient to develop an efficient tribofilm. Considering that **IL14** - $[C_1PyrrTrCH_2(CH_2OCH_2)_{22}CH_2TrPyrrC_1]^+ [C_1SO_3]^-_2$ and **IL15** - $[C_1ImTrCH_2(CH_2OCH_2)_{20}CH_2TrImC_1]^+ [C_1SO_3]^-_2$ have higher molecular weights due to the oligoethylene glycol linking chain, the number of available and tribologically active molecules or moieties, respectively, present in the mixture is much lower.

4.3.4 Corrosiveness

Usually, the ionic liquids present active/passive corrosion behaviour with the exception of the ILs with chloride anion that do not allow the formation of a stable passive layer [147].

Figure 4. 11 shows the surfaces of steel discs after exposure to neat dicationic IL at 100 °C for one week. Table 3 summarizes the observations of the different corrosion levels caused by the selected IL. This screening confirms the importance of including corrosion studies when working with IL, their intrinsic corrosivenesses of which can range from no visible to severe corrosion. Making a comparison between the tetraethylene glycol based IL, it can be observed that imidazolium based IL cause less corrosion than pyrrolidinium based IL: **IL7** - $[C_1ImCH_2(CH_2OCH_2)_3CH_2ImC_1]^+ [NTf_2]^-_2$ behaves better than **IL8** - $[C_1PyrrCH_2(CH_2OCH_2)_3CH_2PyrrC_1]^+ [NTf_2]^-_2$, **IL9** - $[C_1ImCH_2(CH_2OCH_2)_3CH_2ImC_1]^+ [C_1SO_3]^-_2$ better than **IL10** - $[C_1PyrrCH_2(CH_2OCH_2)_3CH_2PyrrC_1]^+ [C_1SO_3]^-_2$. Analogously, lower corrosion has been observed with bis(trifluoromethanesulfonyl)imide anion in comparison with methanesulfonate: **IL7** - $[C_1ImCH_2(CH_2OCH_2)_3CH_2ImC_1]^+ [NTf_2]^-_2$ causes less corrosion than **IL9** - $[C_1ImCH_2(CH_2OCH_2)_3CH_2ImC_1]^+ [C_1SO_3]^-_2$, **IL8** -

$[\text{C}_1\text{Pyrr} - \text{CH}_2(\text{CH}_2\text{OCH}_2)_3\text{CH}_2\text{PyrrC}_1]^+ [\text{NTf}_2]^-_2$ less than **IL10** - $[\text{C}_1\text{PyrrCH}_2(\text{CH}_2\text{OCH}_2)_3\text{CH}_2\text{PyrrC}_1]^+ [\text{C}_1\text{SO}_3]^-_2$. **MIX** shows no visible corrosion although it contains 10 % of methylsulfonate.

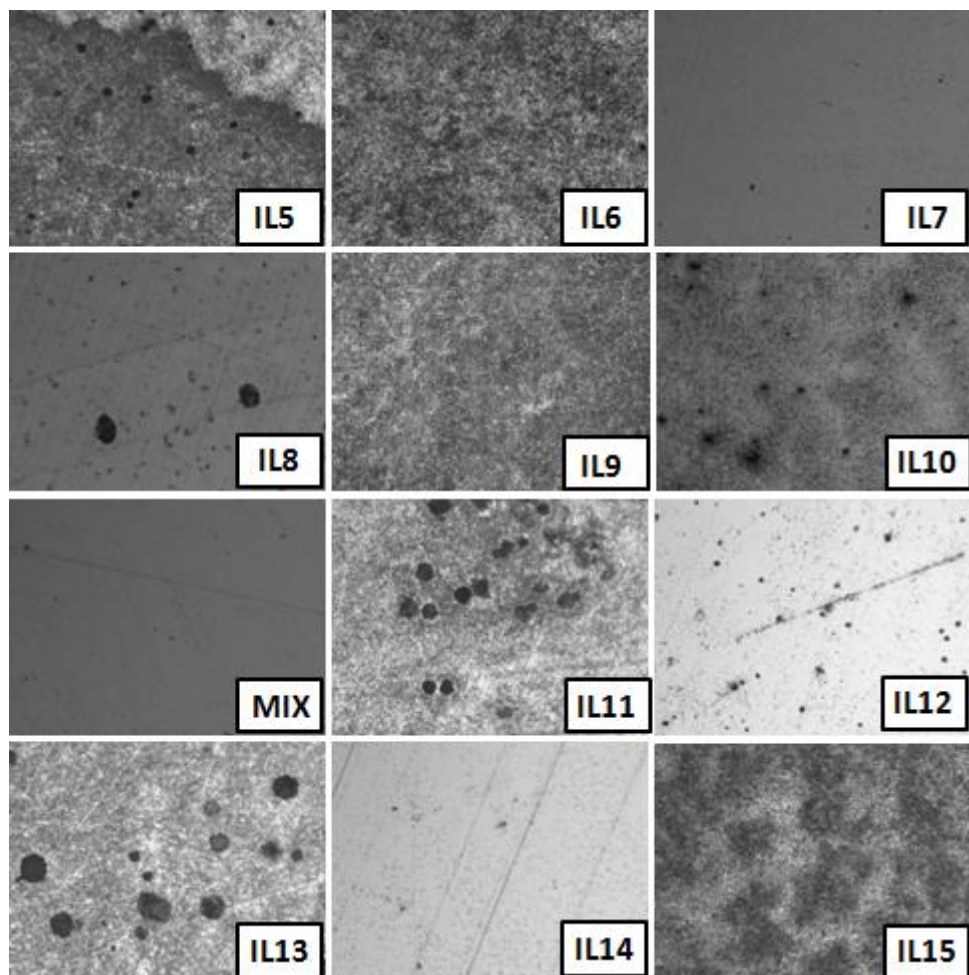


Figure 4. 11 – Surfaces of SRV discs obtained after exposure to the neat dicationic IL at 100 °C for 1 week. All images obtained with an optical microscope have a width of 400 μm .

Considering **IL11** - $[\text{C}_1\text{PyrrTrCH}_2(\text{CH}_2\text{OCH}_2)_5\text{CH}_2\text{TrPyrrC}_1]^+ [\text{C}_1\text{SO}_3]^-_2$ and **IL12** - $[\text{C}_1\text{PyrrTrCH}_2(\text{CH}_2\text{OCH}_2)_5\text{CH}_2\text{TrPyrrC}_1]^+ [\text{C}_4\text{SO}_3]^-_2$, the only difference in structure is the different length of the alkyl chain of the sulfonate type anion,

methyl and butyl, respectively. **IL12** - $[C_1\text{PyrrTrCH}_2(\text{CH}_2\text{OCH}_2)_5\text{CH}_2\text{TrPyrrC}_1]^+ [C_4\text{SO}_3]^-_2$ having the longest alkyl chain causes considerably less corrosion, supporting the anticipated mechanism that a longer chain length of the anion enhances the capability to corrosion protection.

Similarly, the comparison of **IL11** - $[C_1\text{PyrrTrCH}_2(\text{CH}_2\text{OCH}_2)_5\text{CH}_2\text{TrPyrrC}_1]^+ [C_1\text{SO}_3]^-_2$ with **IL14** - $[C_1\text{PyrrTrCH}_2(\text{CH}_2\text{OCH}_2)_{22}\text{CH}_2\text{TrPyrrC}_1]^+ [C_1\text{SO}_3]^-_2$ as well as **IL13** - $[C_1\text{ImTrCH}_2(\text{CH}_2\text{OCH}_2)_5\text{CH}_2\text{TrImC}_1]^+ [C_1\text{SO}_3]^-_2$ with **IL15** - $[C_1\text{ImTrCH}_2(\text{CH}_2\text{OCH}_2)_{20}\text{CH}_2\text{TrImC}_1]^+ [C_1\text{SO}_3]^-_2$ based on different oligoethylene glycol chain lengths reveals severe corrosion for shorter chains as in **IL11** - $[C_1\text{PyrrTrCH}_2(\text{CH}_2\text{OCH}_2)_5\text{CH}_2\text{TrPyrrC}_1]^+ [C_1\text{SO}_3]^-_2$ and **IL13** - $[C_1\text{ImTrCH}_2(\text{CH}_2\text{OCH}_2)_5\text{CH}_2\text{TrImC}_1]^+ [C_1\text{SO}_3]^-_2$. Although traces of corrosion are present on the metallic surfaces that were in contact with **IL15** - $[C_1\text{ImTrCH}_2(\text{CH}_2\text{OCH}_2)_{20}\text{CH}_2\text{TrImC}_1]^+ [C_1\text{SO}_3]^-_2$, they are not as relevant as in the case of **IL13** - $[C_1\text{ImTrCH}_2(\text{CH}_2\text{OCH}_2)_5\text{CH}_2\text{TrImC}_1]^+ [C_1\text{SO}_3]^-_2$.

It is well known that pitting corrosion can be initiated by surface defects, e.g. scratches, grain boundaries. Although polished surfaces exhibit higher resistance against this kind of corrosion, it can be observed for polished 100Cr6 as its surface is characterised by pores. The rather regular distribution of the pits observed support this assumption. Besides material imperfections, pitting corrosion is also significantly increased by the compounds involved in the corrosion process, either by impurities in the ionic liquids or, more likely, by the anion, as severe corrosion was observed for dicationic IL with methanesulfonate anion and chloride in **IL5** - $[C_1\text{ImCH}_2(\text{CH}_2\text{OCH}_2)_3\text{CH}_2\text{ImC}_1]^+ [\text{Cl}]^-_2$. It is not completely clear which is the dominating process that generates pitting corrosion with the methanesulfonate anions. It is known that methanesulfonic acid in presence of impurities can lead to corrosion even with stainless steel [154]. In this research work, it is likely that methanesulfonic acid was produced from the anion and that the presence of

impurities (as for example water content due to the presence of humidity in the working environment) has enhanced the corrosiveness of the dicationic IL.

Table 4. 4 – Summary of the results obtained from the corrosion experiments with AISI 52100 steel discs in contact with neat dicationic IL at 100 °C for one week.

Ionic liquid	Observations
IL11 - [C ₁ PyrrTrCH ₂ (CH ₂ OCH ₂) ₅ CH ₂ TrPyrrC ₁] ⁺ [C ₁ SO ₃] ⁻ ₂	Severe corrosion – both homogenous corrosion and large pitting spots
IL13 - [C ₁ ImTrCH ₂ (CH ₂ OCH ₂) ₅ CH ₂ TrImC ₁] ⁺ [C ₁ SO ₃] ⁻ ₂	
IL5 - [C ₁ ImCH ₂ (CH ₂ OCH ₂) ₃ CH ₂ ImC ₁] ⁺ [Cl] ⁻ ₂	Considerable corrosion – homogenous corrosion and small pitting spots
IL10 - [C ₁ PyrrCH ₂ (CH ₂ OCH ₂) ₃ CH ₂ PyrrC ₁] ⁺ [C ₁ SO ₃] ⁻ ₂	
IL6 - [C ₁ Pyrr CH ₂ (CH ₂ OCH ₂) ₃ CH ₂ PyrrC ₁] ⁺ [Cl] ⁻ ₂	Slight corrosion – slight homogenous corrosion on the area of interest
IL9 - [C ₁ ImCH ₂ (CH ₂ OCH ₂) ₃ CH ₂ ImC ₁] ⁺ [C ₁ SO ₃] ⁻ ₂	
IL15 - [C ₁ ImTrCH ₂ (CH ₂ OCH ₂) ₂₀ CH ₂ TrImC ₁] ⁺ [C ₁ SO ₃] ⁻ ₂	
IL8 - [C ₁ Pyrr CH ₂ (CH ₂ OCH ₂) ₃ CH ₂ PyrrC ₁] ⁺ [NTf ₂] ⁻ ₂	Localized corrosion – few spots of corrosion
IL12 - [C ₁ PyrrTrCH ₂ (CH ₂ OCH ₂) ₅ CH ₂ TrPyrrC ₁] ⁺ [C ₄ SO ₃] ⁻ ₂	
IL7 - [C ₁ ImCH ₂ (CH ₂ OCH ₂) ₃ CH ₂ ImC ₁] ⁺ [NTf ₂] ⁻ ₂	No corrosion – no indication of etched surface
MIX	
IL14 - [C ₁ PyrrTrCH ₂ (CH ₂ OCH ₂) ₂₂ CH ₂ TrPyrrC ₁] ⁺ [C ₁ SO ₃] ⁻ ₂	

4.4 CONCLUSIONS

Twelve dicationic IL have been investigated for their tribological performance in steel-steel contacts and corrosiveness to steel.

For friction and wear reduction with neat IL, both anionic moiety and chain length of the oligoethylene glycol moiety are important. The findings suggest that longer chains yielded better tribological behavior as shown for **IL14** - $[C_1\text{PyrrTrCH}_2(\text{CH}_2\text{OCH}_2)_{22}\text{CH}_2\text{TrPyrrC}_1]^+ [C_1\text{SO}_3]^-_2$ and **IL15** - $[C_1\text{ImTrCH}_2(\text{CH}_2\text{OCH}_2)_{20}\text{CH}_2\text{TrImC}_1]^+ [C_1\text{SO}_3]^-_2$.

With respect to corrosion properties, a longer chain, both in the anion and in the cation, positively influenced the IL corrosion inhibiting properties. In detail, IL with bis(trifluoromethanesulfonyl)imide anion or long oligoethylene glycol chains revealed lower corrosion as shown for **IL7** - $[C_1\text{ImCH}_2(\text{CH}_2\text{OCH}_2)_3\text{CH}_2\text{ImC}_1]^+ [\text{NTf}_2]^-_2$, **MIX** and **IL14** - $[C_1\text{PyrrTrCH}_2(\text{CH}_2\text{OCH}_2)_{22}\text{CH}_2\text{TrPyrrC}_1]^+ [C_1\text{SO}_3]^-_2$.

Merging all findings with neat IL, **MIX** – a mixture of **IL7** - $[C_1\text{ImCH}_2(\text{CH}_2\text{OCH}_2)_3\text{CH}_2\text{ImC}_1]^+ [\text{NTf}_2]^-_2$ and **IL9** - $[C_1\text{ImCH}_2(\text{CH}_2\text{OCH}_2)_3\text{CH}_2\text{ImC}_1]^+ [C_1\text{SO}_3]^-_2$ – turned out as best performing dicationic IL and hence shows some potential as lubricant, even without additives. **IL14** - $[C_1\text{PyrrTrCH}_2(\text{CH}_2\text{OCH}_2)_{22}\text{CH}_2\text{TrPyrrC}_1]^+ [C_1\text{SO}_3]^-_2$ and **IL15** - $[C_1\text{ImTrCH}_2(\text{CH}_2\text{OCH}_2)_{20}\text{CH}_2\text{TrImC}_1]^+ [C_1\text{SO}_3]^-_2$ are of particular interest, since a significant reduction of friction was observed at higher temperatures and wear formation was among the lowest measured.

Mixtures from SynaloxTM with 1 % w/w IL selected from those dicationic IL which performed well in the neat state showed that **IL7** - $[C_1\text{ImCH}_2(\text{CH}_2\text{OCH}_2)_3\text{CH}_2\text{ImC}_1]^+ [\text{NTf}_2]^-_2$ or **MIX** as additives improve the performance of the base oil. It has been established by XPS examination that **IL7** - $[C_1\text{ImCH}_2(\text{CH}_2\text{OCH}_2)_3\text{CH}_2\text{ImC}_1]^+ [\text{NTf}_2]^-_2$ and **IL9** - $[C_1\text{ImCH}_2(\text{CH}_2\text{OCH}_2)_3\text{CH}_2\text{ImC}_1]^+ [C_1\text{SO}_3]^-_2$ create a tribolayer of inorganic fluoride (FeF_2), iron sulphide and iron oxide through decomposition and reaction of bis(trifluoromethanesulfonyl)imide anion with the steel surface.

The presence of long organic chains, as in the case of **IL14** - $[\text{C}_1\text{PyrrTrCH}_2(\text{CH}_2\text{OCH}_2)_{22}\text{CH}_2\text{TrPyrrC}_1]^+ [\text{C}_1\text{SO}_3]_2^-$ and **IL15** - $[\text{C}_1\text{ImTrCH}_2(\text{CH}_2\text{OCH}_2)_{20}\text{CH}_2\text{TrImC}_1]^+ [\text{C}_1\text{SO}_3]_2^-$, can be deleterious for the performance of IL as additives, since it is anticipated that an increase of molecular weight corresponding to an inferior number of IL molecules in the mixture results in inferior effectiveness.

Corrosion caused by IL is still one of the major problems to be solved by more appropriate IL structures or by addition of corrosion inhibitors.

The example of the dicationic IL **MIX** has shown the future opportunities to significantly improve the tribological performance in terms of friction reduction and wear protection by mixing of appropriate IL.

Chapter 5

5 Phosphonium based ionic liquids as anti-wear additives in synthetic base oil

5.1 INTRODUCTION

The industrial need to continuously develop more efficient manufacturing systems has an important influence on the field of lubricant development. Until now, the consumption of synthetic oils is still limited to a low percentage of the total value of the global lubricant market [155], but this tendency seems to be destined to change. Due to their superior technical properties, synthetic lubricants are substituting mineral oils in many fields, such as in high temperature and high load applications where synthetic oils, show higher wear protection and in aerospace applications because of their negligible volatility and lower dependency of viscosity with the temperature (higher viscosity index) [156]. Therefore, it is clear that in order to promote the market of synthetic oils it is necessary to continuously improve their lubrication performances and to find new additives that work in synergy with other components (base oils, additives, and materials). One class of promising additives that have been studied in the last 15 years is ionic liquids (ILs). ILs are salts, hence composed of cations and anions, which exhibit wide liquid range with melting points

even below zero Celsius degrees and interesting characteristics, such as low vapour pressure, high thermal stability, wide liquid range, low friction and wear in metal-metal contact [83,85,144]. ILs have already demonstrated good tribological properties in many working conditions and in solution with a great variety of base lubricants [157-161], nonetheless due to the incredible variety of molecules that could be synthesized and to the complexity of their interaction with the metallic surfaces, there is still a lot of work that should be done.

Because of the difficult miscibility of ILs with common non-polar oils, many studies have been focused on the compatibility of the ionic structures with common base oils such as esters [162,163], polyalkylen glycols [130,164] or glycerol [134,165].

Yu et al. showed that phosphonium based ILs can be fully miscible both in mineral oils and synthetic lubricants [89]. In addition to the miscibility in non-polar hydrocarbon oil, they had good thermal properties with higher stability than conventional lubricants, many of them are not corrosive to ferrous or aluminium alloys and they had a good behaviour as additives for lubricants.

Also Zhu et al. focused their study on three oil-soluble phosphonium-based ILs that were blended in pentaerythritol oleate and trimethylolpropane trioleate. They compared the performance at 200 °C of the ILs with the performance of a commercially available tricresyl phosphate and found out that the ILs had better lubrication properties. Particularly promising was the behaviour of the tetradecyltriethylphosphonium *o,o'*-diethyldithiophosphate blended with the base oils in a percentage of 4%, since it was able to generate an iron phosphate protective layer on the sliding surfaces. [166]

Totolin *et al.* realized two studies on the tribological performance of methyltributylphosphonium dimethylphosphate. In one case, he compared this IL with 1 butyl-3-methylimidazolium bis(trifluoromethanesulfonyl)amide and a

conventional space lubricant, perfluoropolyether (PFPE) in vacuum conditions [167]. The results obtained in this research showed that there was no evaporation loss at a pressure of 10^{-8} Pa, and that methyltributylphosphonium dimethylphosphate was the most suitable choice for vacuum lubricant, as it had superior tribological performance when compared to the other two fluids investigated. In the second article Totolin used the IL as an additive with a molar concentration of 100 mM in a blend of two imidazolium borane ionic liquids [107]. In this case, the performance of the additive was compared with another mixture containing the same base and 1-butyl-3-methylimidazolium bis(trifluoromethanesulfonyl)amide as additive in the same molar concentration. The use of the phosphonium ionic liquid improved the tribological performance creating a phosphate layer inside of the wear scar. In the case of the halogen containing IL instead, the performance of the base was improved but there was slightly higher wear due to corrosion.

In this article, two alkylphosphonium ILs were studied as additives for a synthetic base oil. In Table 5. 1 the structures, names and codification of the ILs are represented.

We had already analyzed these two ionic liquids as neat lubricants. It was noticed that the tribochemical reactions of the phosphate anion and thiophosphate anion yield a phosphate boundary film that exhibits better tribological properties than the metal fluoride boundary film formed using bis(trifluoromethylsulfonyl)amide and trifluorotris(pentafluoroethyl)phosphate based ILs. In particular, it was highlighted how the tribolayer formation process observed with these alkylphosphonium ILs could be closely related to those of the conventional antiwear additives, as for example zinc dialkyldithiophosphate [152].

The objective of this study is to check the behaviour of these two potential anti-wear additives when they are blended in synthetic oils and to explain the tribochemical mechanism that they activate during the tribological contact of two steel surfaces.

5.2 EXPERIMENTAL

5.2.1 Materials

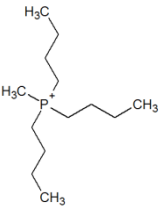
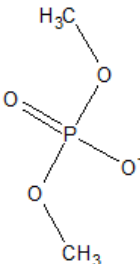
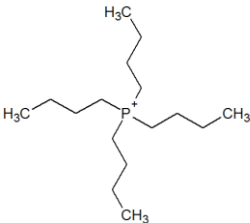
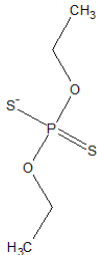
The ILs used in this study were provided by Nippon Chemical Industrial (Tokyo, Japon). Their chemical structures are shown in Table 5. 1. Both ILs are composed of phosphonium cations with alkyl side chains up to C₄ length, which according to Yu *et al.* could satisfactorily improve the miscibility of the compound in the oil [89]. The anions are dimethylphosphate in case of **IL16** - $[(H_9C_4)_3P(CH_3)]^+ [(C_1)_2PO_4]^-$ and diethylphosphorodithionate for **IL17** - $[P(C_4H_9)_4]^+ [(C_2)_2PO_2S_2]^-$.

A Synalox™ 100-30B polypropylene glycol monobutyl ether (CAS 9003-13-8), provided by The Dow Chemical Company (Midland, U.S.A.), was used as base oil to obtain binary mixtures of 0.25%, 0.50%, 1.00 %, 2.00%, 5.00% selected ILs concentrations. All the concentrations of mixtures considered have been calculated as weight/weight % (w/w). The corresponding phosphorus content is 450 ppm in the mixture with 0.25% w/w of **IL16** - $[(H_9C_4)_3P(CH_3)]^+ [(C_1)_2PO_4]^-$ and 350 ppm in the mixture with 0.25% w/w of **IL17** - $[P(C_4H_9)_4]^+ [(C_2)_2PO_2S_2]^-$.

5.2.2 Thermal analysis

Thermogravimetric analyses (TGA) were carried out using a TGA/SDTA 851E (Mettler Toledo, Greifensee, Zurich, Switzerland). The investigated temperature range spanned from ambient temperature up to 500 °C with linearly increasing heating rate of 10 °C/min. The experiments were performed under inert atmosphere, applying a constant flow of nitrogen. The crucibles used for these experiments were made of alumina and they were filled with up to 10 mg of IL.

Table 5. 1 - Structure and codification of the phosphonium ILs.

Cation	Anion
	
<p>Methyltributylphosphonium Dimethylphosphate</p> <p>IL16 - $[(\text{H}_3\text{C}_4)_3\text{P}(\text{CH}_3)]^+ [(\text{C}_1)_2\text{PO}_4]^-$</p>	
	
<p>Tetra n-butylphosphonium o,o-diethylphosphorodithionate</p> <p>IL17 - $[\text{P}(\text{C}_4\text{H}_9)_4]^+ [(\text{C}_2)_2\text{PO}_2\text{S}_2]^-$</p>	

Differential scanning calorimetry (DSC) was performed from -120 °C to 25 °C at 10 °C/min heating rate under dry nitrogen atmosphere using a Mettler-Toledo 822-E (Mettler-Toledo, Greifensee, Zurich, Switzerland). Stainless steel medium pressure crucibles (ME-29990, Mettler-Toledo) were filled with 7 mg of IL and hermetically sealed.

5.2.3 Viscosity and density

Viscosity and density of the ILs studied have been calculated as function of the temperature using a Stabinger viscometer SVM3000 (Anton Paar, Graz, Austria). The range of temperatures studied spans from 20 °C up to 100 °C with 20 °C interval. The viscosity index was also determined using this device according to the ASTM D2270-04 standard.

Concentrations with 5.00 %, 2.00 %, 1.00 %, 0.50 % and 0.25 % w/w of IL in base oil were prepared and dispersed using an ultra-sonicator Vibra Cell Model VCX500 (Sonics & Materials Inc., Newtown, CT, USA). Sonication was performed for 30 s applying 21 % of the maximum vibration amplitude with a maximum output power of 500 W and with pulses of 2 second duration in 2 second intervals. The blends of base oil and ILs were visually checked for 2 months.

5.2.4 Tribological experiments

The tribological experiments were carried out in reciprocating ball-on-disc configuration with the Schwing-Reib-Verschleiss (SRV) tribometer of Optimol Instruments Prüftechnik, (Munich, Germany). The conditions used for the experiments were chosen according to the guidelines recommended in the ASTM 6425-05 standard [118]. The duration of the tests was 2 hours, with applied load of 300 N, stroke of 1 mm, frequency of 50 Hz and with temperature fixed at 100 °C. Balls and discs were purchased from Optimol Instruments Prüftechnik. The balls were made of AISI 52100 steel with a 10 mm diameter of 0.012 µm roughness and HRC 63 ± 2 hardness. Discs were also made of AISI 52100 steel with a 24 mm diameter, 7.9 mm thickness and 0.56 µm roughness. Before the tribological experiments, the tribo pairs (balls and discs) were cleaned for five minutes in petroleum ether and five minutes in acetone, respectively using an ultrasonic bath.

As demonstrated by Bermudez *et al.* [168], the good dispersion of the ionic additive in the mixture is extremely important for achieving a valid result. Accordingly, the mixtures were prepared directly prior to tribological experiments.

The maximum contact pressure, calculated according to the Hertzian theory for contacts between a sphere and a flat surface, was 3.14 GPa [120]. Each experiment was performed twice and average COF were calculated from the data recorded during the tribotests after a running-in period of 500 s.

5.2.5 Surface analysis

After the tribological experiments, balls and discs were analyzed by an optical microscope and a white light confocal microscope (NanoFocus AG, Oberhausen, Germany). The wear volume was calculated using Matlab based software by processing the 3D topographical data obtained from the confocal microscope, as described elsewhere [169].

XPS was performed on the worn surface of the disc to study the formed tribolayer on the rubbed metal surface

and for the determination of the elemental composition and chemical environment of the elements identified inside and outside the wear scar. The equipment used was a Thermo Fisher Scientific Theta Probe (East Grinstead, United Kingdom) with a monochromatic Al K α X-ray source ($h\nu = 1486.6$ eV). The base pressure during the measurements was consistent at 3×10^{-7} Pa. The discs for XPS analysis were thoroughly cleaned directly after the tribological experiments by immersion in petroleum ether and toluene, 2-propanol, respectively, applying an ultrasonic bath for 15 minutes at room temperature for each step. Spots in and outside of the discs wear scar were defined and analyzed with a spot diameter of 100 μm at 200 eV pass energy for the survey spectra. Detail spectra were recorded at pass energy of 50 eV. For the imaging XPS experiments, in order to get a deep insight of the reaction that had taken place, the whole area around the wear scar was scanned with a spot and step size of 100 μm , for the disc lubricated with 5 % w/w of **IL16** - $[(\text{H}_9\text{C}_4)_3\text{P}(\text{CH}_3)]^+ [(\text{C}_1)_2\text{PO}_4]^-$ (as shown in Figure 5. 1) and for the disc lubricated with 5 % w/w of **IL17** - $[\text{P}(\text{C}_4\text{H}_9)_4]^+ [(\text{C}_2)_2\text{PO}_2\text{S}_2]^-$. This technique, quite advanced in comparison with

normal XPS techniques that analyze the surface just in a single point, was already used in a published article [130,170].

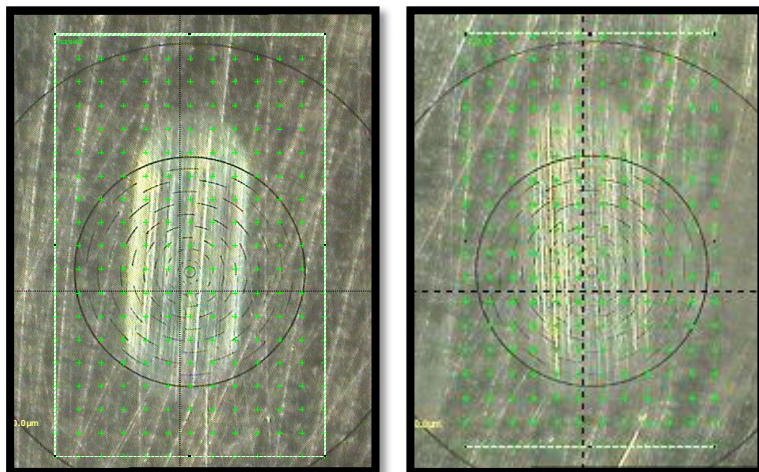


Figure 5. 1 – Grid over the disc wear track defining the spots for individual measurements (green crosses). Wear scar with **IL16** - $[(H_9C_4)_3P(CH_3)]^+ [(C_1)_2PO_4]^-$ on the left and **IL17** - $[P(C_4H_9)_4]^+ [(C_2)_2PO_2S_2]^-$ on the right.

All elements detected by the survey analyses, were recorded in the imaging XPS experiments as snap shots with a 15 eV wide binding energy window and resulting pass energy of 150.5 eV. The collected analytical data were processed with the Avantage Data System software from Thermo Fisher Scientific (East Grinstead, United Kingdom), using Gaussian-Lorentzian peak fitting.

5.2.6 Thermal degradation and corrosion

TGA in a dynamic mode is a valid instrument for the evaluation of the thermal stability of the fluids but it does not give a real idea of what is happening inside of the lubricant. In order to get a more defined idea of the decomposition of the ionic liquids because of thermal degradation, the ionic liquids were kept at high temperature for a certain period of time. The total testing period was of 3 weeks. The first week the ionic liquids were kept at the temperature of 100 °C. Instead, for the second and the third weeks the temperature was raised at 150 °C. In the vial

containing the ionic liquids was also introduced a small ball made of steel AISI 52100 with 3 mm diameter. After the tests, the samples were analyzed by ATR-FTIR in order to have a partial qualitative idea of the degradation of the ionic liquids. In this case, the use of the IR technique does not allow us to determine the nature of the by-product but at least helps to understand when some changes take place. The steel ball was also analyzed by SEM-EDS.

5.2.7 Tribocorrosion test

Tribocorrosion tests were carried out with a unidirectional MicroTest MT/10/SCM tribometer with a ball on disc configuration. The disc holder of the tribometer was placed in an electrochemical cell in order to control both mechanical and electrochemical parameters simultaneously. The electrochemical response of the system was monitored by using an Autolab-Metrohm PGSTAT30 potentiostat. As in the previous tribological experiments, the discs used were made of steel AISI 52100 but in this case an alumina ball was used as counterbody in order to electrically isolate the disc that is the working electrode. An Ag/AgCl (KCl 3M), connected through a salty bridge, was used as reference electrode. The load applied during the tribotests was 10 N with a rotation speed of 120 rpm. The track diameter was set to 5 mm. The test procedure can be divided in 2 phases.

1. The open circuit potential (OCP) was measured during 3600 seconds in order to know the evolution of the potential in a stable condition.
2. The tribotest was carried out for 30 minutes monitoring at the same time friction coefficient and OCP.

Tribocorrosion tests were realized only with the **IL16** - $[(\text{H}_9\text{C}_4)_3\text{P}(\text{CH}_3)]^+ [(\text{C}_1)_2\text{PO}_4]^-$ and a mixture of base oil and 5% of **IL16** - $[(\text{H}_9\text{C}_4)_3\text{P}(\text{CH}_3)]^+ [(\text{C}_1)_2\text{PO}_4]^-$. Initially it was thought to realize the same test also with **IL17** - $[\text{P}(\text{C}_4\text{H}_9)_4]^+ [(\text{C}_2)_2\text{PO}_2\text{S}_2]^-$ but from a first attempt it was noticed that the conductivity of the mixture of base oil

and IL was too low for the measurement. For this reason it was decided to focus only on the ionic liquid that had shown the best behavior.

5.3 RESULTS AND DISCUSSION

5.3.1 Thermal properties

Figure 5. 2 shows the results obtained by TGA. T_{start} denotes the temperature at which the first sign of continuous weight loss occurs; T_{onset} indicates the extrapolated temperature of degradation determined by the point of intersection of the tangents to two consecutive branches of the thermogravimetric curve. The ILs and base oil have similar temperature of degradation; T_{onset} was produced at 295 °C for **IL17** - $[\text{P}(\text{C}_4\text{H}_9)_4]^+ [(\text{C}_2)_2\text{PO}_2\text{S}_2]^-$ and around 320 °C for **IL16** - $[(\text{H}_9\text{C}_4)_3\text{P}(\text{CH}_3)]^+ [(\text{C}_1)_2\text{PO}_4]^-$ and base oil. Also T_{start} is rather similar; **IL16** - $[(\text{H}_9\text{C}_4)_3\text{P}(\text{CH}_3)]^+ [(\text{C}_1)_2\text{PO}_4]^-$ and base oil start to have weight loss around 240 °C while for **IL17** - $[\text{P}(\text{C}_4\text{H}_9)_4]^+ [(\text{C}_2)_2\text{PO}_2\text{S}_2]^-$ the weight loss occurs at 262 °C. It is interesting to notice that, increasing the temperature, the base oil has a continuous weight loss while with the ionic liquids the weight loss rate is more instable.

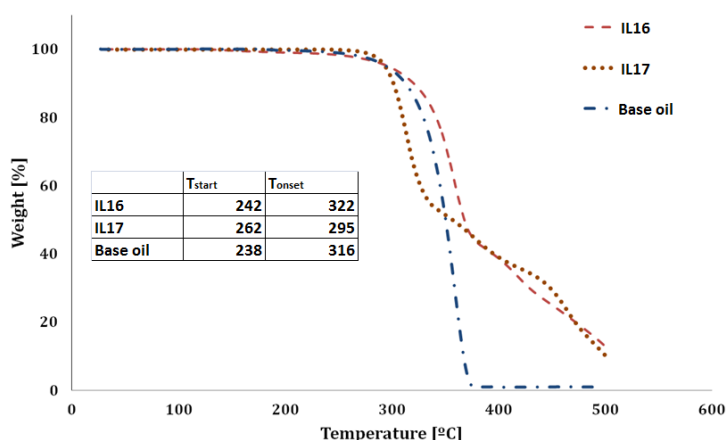


Figure 5. 2 — Thermogravimetric analysis of the ILs tested and the base oil in the range 25 °C – 500 °C.

This could mean that the degradation process of Synalox™ 100-30B is based on the rupture of the organic chains forming molecules with higher volatility. In the case of the ILs instead the decomposition of the ions creates more stable by-products.

The main objective of this experiment was to check if the ILs could withstand high temperature or if they would be degraded before the base oil. In this case it was demonstrated that it is possible to use these ILs as additive since they could be used in the same range of temperature as the selected base oil.

By DSC analyses, it was not possible to notice any melting point for the two ionic liquids tested in the range of temperature between -120 °C and ambient temperature. Instead it was possible to detect sign of glass transitions. **IL16** - $[(H_9C_4)_3P(CH_3)]^+ [(C_1)_2PO_4]^-$ has a first strong glass transition around -75 °C and a second weak one around -10 °C. **IL17** - $[P(C_4H_9)_4]^+ [(C_2)_2PO_2S_2]^-$ instead showed a very weak glass transition at the temperature of -61 °C but it was impossible to notice further status changes (Figure 5. 3).

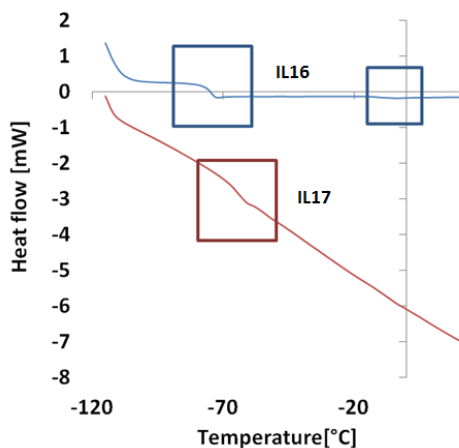


Figure 5. 3 – Differential scanning calorimetry with the **IL16** - $[(H_9C_4)_3P(CH_3)]^+ [(C_1)_2PO_4]^-$ and **IL17** - $[P(C_4H_9)_4]^+ [(C_2)_2PO_2S_2]^-$ in the range of temperature between -120 °C and 25 °C.

5.3.2 Viscosity and density

Viscosity and density as function of temperature are reported in Table 5. 2. The viscosity indexes (VI) calculated for both ILs are low in comparison with the values obtained for modern oils having VI around 200. This could be inconvenient for their use as neat lubricants, since low viscosity variation with temperature is appreciated, but it should not hinder their use as base oil additives. It is expected that the addition of a small additive percentage has a negligible effect on the final viscosity of the lubricant.

Table 5. 2 - Physicochemical properties as function of the temperature: dynamic viscosity η , kinematic viscosity ν , density ρ and viscosity index VI of phosphonium ionic liquids.

	Temperature [°C]	η [mPa·s]	ν [mm ² /s]	ρ [g/mL]	VI (viscosity index)
IL16 - [(H ₉ C ₄) ₃ P(CH ₃) ⁺] [(C ₁) ₂ PO ₄ ⁻]	20	743.32	718.21	1.0350	77.23
	40	189.49	185.41	1.0220	
	60	66.35	65.74	1.0093	
	80	29.04	29.13	0.9970	
	100	14.88	15.12	0.9842	
IL17 - [P(C ₄ H ₉) ₄] ⁺ [(C ₂) ₂ PO ₂ S ₂] ⁻	20	1831.30	1806.90	1.0135	90.73
	40	428.57	428.00	1.0013	
	60	137.61	139.05	0.9897	
	80	55.86	57.12	0.9779	
	100	27.00	27.95	0.9661	

An important parameter for the additives is their solubility in the base oil. The miscibility could be improved with the use of surfactants, but this could reduce the adsorption activity of the ILs on the metallic surface, affecting their performance as additives. In addition, it would mean a further addition of chemical compounds, therefore complication in the oil formulation. The mutual solubility of the base oil and the two selected ILs significantly differed. **IL16** - $[(\text{H}_9\text{C}_4)_3\text{P}(\text{CH}_3)]^+ [(\text{C}_1)_2\text{PO}_4]^-$ was perfectly soluble in the base at all the concentrations tested, up to 5 % w/w. On the other hand, really poor miscibility was observed for **IL17** - $[\text{P}(\text{C}_4\text{H}_9)_4]^+ [(\text{C}_2)_2\text{PO}_2\text{S}_2]^-$, where only the mixture of 0.25% w/w was stable during the whole period of the test duration (30 days). In the case of higher concentrations, rapid phase separation was observed within few days.

This result demonstrates straightforward use of **IL16** - $[(\text{H}_9\text{C}_4)_3\text{P}(\text{CH}_3)]^+ [(\text{C}_1)_2\text{PO}_4]^-$ as highly miscible lubricant additive for selected base oil type, avoiding a need of surfactant addition for solubility improvement.

5.3.3 Tribological performance

Tribological experiments were carried out using blends of polypropylene glycol base oil with different ILs content. The considered IL concentrations were 0 %, 0.25 %, 0.5 %, 1 %, 2 % and 5 % w/w. As exposed in the description of the experiments, the tribotests were performed under extreme pressure conditions at 100 °C. Figure 5. 4, Figure 5. 5 and Figure 5. 6 present the trend of the friction curves, showing the evolution of the friction coefficient with time for the experiments performed with concentrations of 0.25 %, 0.50 % and 5 % w/w of ILs. As said before, the blends of base oil and **IL17** - $[\text{P}(\text{C}_4\text{H}_9)_4]^+ [(\text{C}_2)_2\text{PO}_2\text{S}_2]^-$ were not stable during long period of time but in this case the tests were lasting just 2 hours and the solutions were prepared and sonicated just before the tribological experiments at 100 °C, hence it can be assumed that the blended lubricants were homogeneous.

The base oil without additives exhibited an unstable COF during the whole experiment; a long running-in period of approximately 15 minutes and then

continuous increase of COF until 0.23 value. In addition, the running-in period was characterized by the presence of numerous peaks in the COF, due to partial seizures. From the Figure 5. 4, it is possible to see that the influence of the additives is rather important on the tribological performance, even for such a low concentration as 0.25 % w/w. For the mixture of 0.25 % w/w **IL16** - $[(H_9C_4)_3P(CH_3)]^+ [(C_1)_2PO_4]^-$ in the selected base oil, the duration of the running-in period lasted only for a few seconds; after this period, the COF can be considered as stable. Slightly different behaviour was found with concentration of 0.25% w/w of **IL17** - $[P(C_4H_9)_4]^+ [(C_2)_2PO_2S_2]^-$ in the base oil; during the running-in period lasting just a bit more than 300 seconds, the tribometer recorded a peak in COF because of a microwelding.

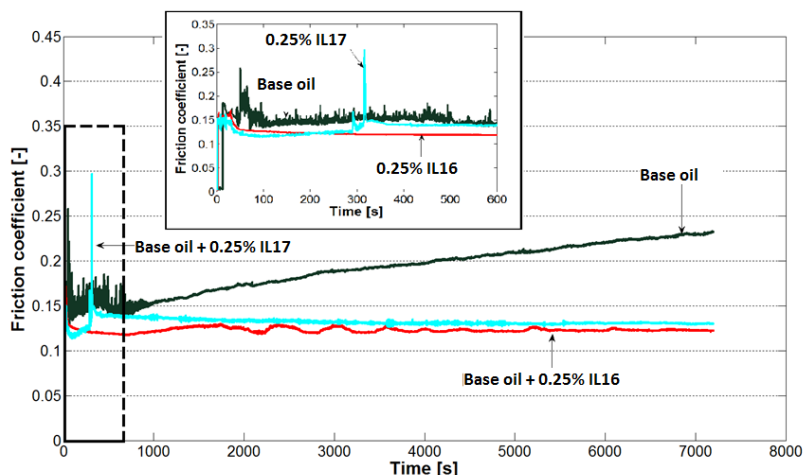


Figure 5. 4 - Progress of coefficient of friction at 100 °C over time with mixtures of 0.25 % w/w of IL in base oil. Neat base oil as reference.

The following part of the experiment is characterized by a stable and low COF. Figure 5. 5 shows the trend of the COF with 0.5 % w/w concentration of ILs; the running-in period is short and the curve shows a stable signal during the whole experiment in case of both ILs. For concentration of 1 % and 2 % w/w of IL, the behaviour is similar to that shown in Figure 5. 5 and for this reason the corresponding charts were not included. It is additionally interesting to notice that with 5 % w/w of

IL17 - $[\text{P}(\text{C}_4\text{H}_9)_4]^+ [(\text{C}_2)_2\text{PO}_2\text{S}_2]^-$ the running-in period increases again and it takes around 500 seconds for the COF to stabilize, as can be seen in Figure 5. 6. In the following section it will be shown that this unexpected behaviour had consequences also on the generated wear volume.

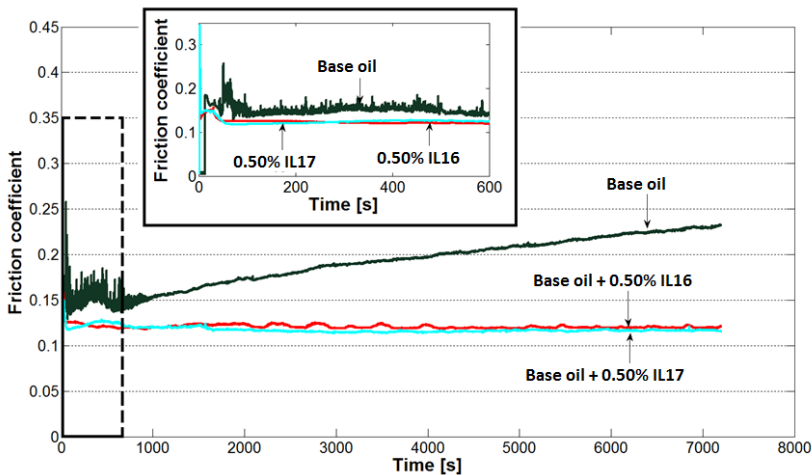


Figure 5. 5 - Progress of coefficient of friction at 100 °C over time with mixtures of 0.50 % w/w of IL in base oil. Neat base oil as reference.

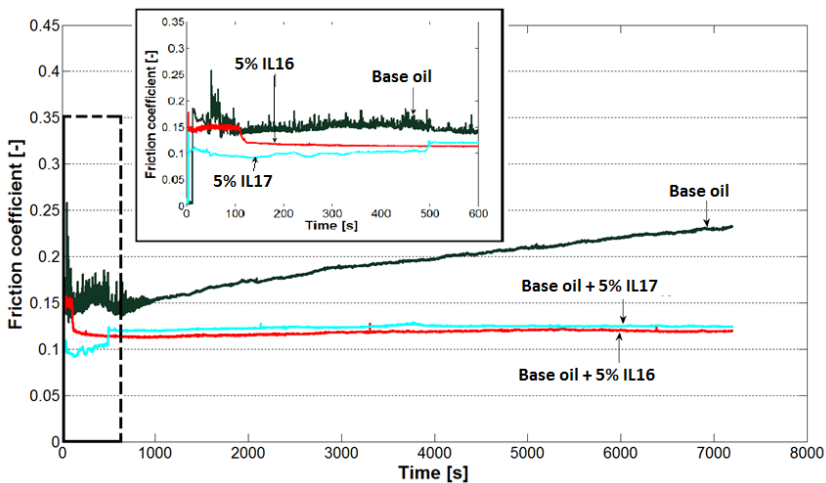


Figure 5. 6 - Progress of coefficient of friction at 100 °C over time with mixtures of 5.00 % w/w of IL in base oil. Neat base oil as reference.

Figure 5. 7 shows the average values of wear volume for balls and discs lubricated with blends of base oil and IL. The wear volume generated during the tribotests with the neat base oil was not calculated because it was easily recognized by visual evaluation as much higher and it was necessary to use microscope lens with different magnification, hence it would have been impossible to measure it with the same analytical method. Analyzing the performance in terms of friction and wear reduction obtained with blends of **IL16** - $[(\text{H}_9\text{C}_4)_3\text{P}(\text{CH}_3)]^+ [(\text{C}_1)_2\text{PO}_4]^-$, it is possible to state that, even though the variation as function of the concentration is quite low, the best results were obtained for a low amount of IL.

The blends with base oil and **IL17** - $[\text{P}(\text{C}_4\text{H}_9)_4]^+ [(\text{C}_2)_2\text{PO}_2\text{S}_2]^-$ revealed instead an important increase of wear for high (5% w/w) and low (0.25% w/w) concentration of this IL. These observations fit really well with the results that were obtained in terms of friction, where the running-in period determined was longer for 0.25% and 5 % w/w concentration levels of **IL17** - $[\text{P}(\text{C}_4\text{H}_9)_4]^+ [(\text{C}_2)_2\text{PO}_2\text{S}_2]^-$.

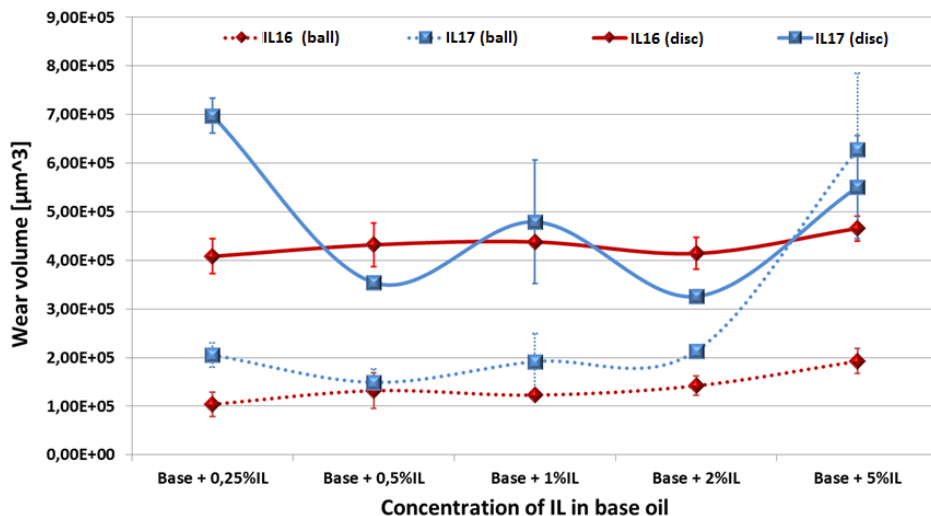


Figure 5. 7 – Ball and disc wear volume with different concentrations of ILs in base oil.

It is very likely that the reason of the failure of the additive at 0.25% and 5% w/w is different. For the low concentration the assumption is that the amount of IL

necessary for generating the formation a good tribolayer was not enough, in the other case, for a concentration of 5% w/w, the failure could be due to corrosive wear.

The analysis of the worn surfaces by confocal microscopy (Figure 5. 8) gives an insight of the different lubrication mechanisms. All the surfaces examined were abraded but it was easy to recognize a difference between scars lubricated with blends of base oil and **IL16** - $[(\text{H}_9\text{C}_4)_3\text{P}(\text{CH}_3)]^+ [(\text{C}_1)_2\text{PO}_4]^-$ and blends of base oil and **IL17** - $[\text{P}(\text{C}_4\text{H}_9)_4]^+ [(\text{C}_2)_2\text{PO}_2\text{S}_2]^-$. The surfaces lubricated just with base oil are not considered here because, as stated previously, the wear scars were too large, deep and irregular for being analysed. The mean wear scar diameter (WSD) obtained with Synalox™ 100-30B was over 1500 μm while for the other cases studied the WSD was always less than 700 μm , how can be noticed in Figure 5. 8.

From the topographies of Figure 5. 8 a, 5. 8c and 5. 8e it is possible to see that the antiwear properties of **IL16** - $[(\text{H}_9\text{C}_4)_3\text{P}(\text{CH}_3)]^+ [(\text{C}_1)_2\text{PO}_4]^-$ gave an efficient protection to the surfaces in contact. The wear scars on the discs have light abrasion marks but the grooves are shallow and smooth. No signs of corrosion were found, even after analyzing the scars with an optical microscope.

The images showing the topography of the worn surfaces lubricated with blends of **IL17** - $[\text{P}(\text{C}_4\text{H}_9)_4]^+ [(\text{C}_2)_2\text{PO}_2\text{S}_2]^-$ demonstrate the importance of the concentration of IL in the mixture. With 0.25% w/w of **IL17** - $[\text{P}(\text{C}_4\text{H}_9)_4]^+ [(\text{C}_2)_2\text{PO}_2\text{S}_2]^-$ (Figure 5. 8 b) the scars on the disc and on the ball present wide and deep grooves, probably caused by the micro welding detected during the running-in period. Increasing the concentration of ionic additive to 0.5 % w/w (Figure 5. 8 d) the protective ability of the lubricant improves, thus only a few scratches are visible. Similar behavior was observed with concentrations of 1% and 2% w/w of **IL17** - $[\text{P}(\text{C}_4\text{H}_9)_4]^+ [(\text{C}_2)_2\text{PO}_2\text{S}_2]^-$. However, after increasing the additive percentage to 5% w/w (Figure 5. 8 f) it is evident that the lubricant lost its antiwear properties. The grooves on the wear scar are deeper and larger and the wear scar diameter is bigger. In this case the ionic liquid has probably reacted with the steel surface but the mechanical resistance of the layer

generated is too low for protecting the surface, so it is easily removed during the tribocontact. In this way, fresh surface is exposed again and can react again with the ionic liquid resulting in continuous tribocorrosion process [171].

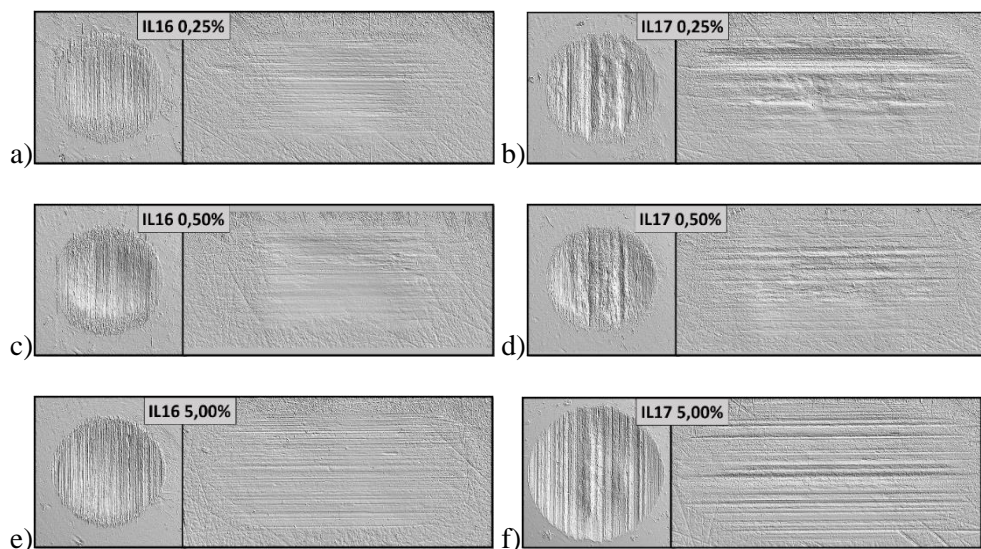


Figure 5. 8 – Micrographies of the wear scar of the ball (left) and disc (right) for different IL dilutions of ILs in base oil (0,25-5% w/w). The height of the images is 700 μm .

5.3.4 Surface analysis

XPS analyses were performed on the specimens used for the blends with 5% w/w **IL16** - $[(\text{H}_9\text{C}_4)_3\text{P}(\text{CH}_3)]^+ [(\text{C}_1)_2\text{PO}_4]^-$ and with 5% w/w of **IL17** - $[\text{P}(\text{C}_4\text{H}_9)_4]^+ [(\text{C}_2)_2\text{PO}_2\text{S}_2]^-$ in base oil in order to investigate the presence of a protective tribolayer. For this purpose, imaging was performed to gain knowledge about the distribution of selected elements and their binding states in and outside the wear track.

The elements selected for the analysis of the surface worn with **IL16** - $[(\text{H}_9\text{C}_4)_3\text{P}(\text{CH}_3)]^+ [(\text{C}_1)_2\text{PO}_4]^-$ and base oil were phosphorus, oxygen and iron. The first important result from this analysis was that for phosphorus a binding energy of 133.5 eV [172] was detected mainly inside the worn track of the disc. This binding energy can be related to the presence of phosphorus in the binding state of a phosphate. It is visible from Figure 5. 9 that the concentration of phosphorus was

particularly high on the worn track. It is also interesting to observe how the oxygen is present in a different chemical binding state inside and outside the wear track.

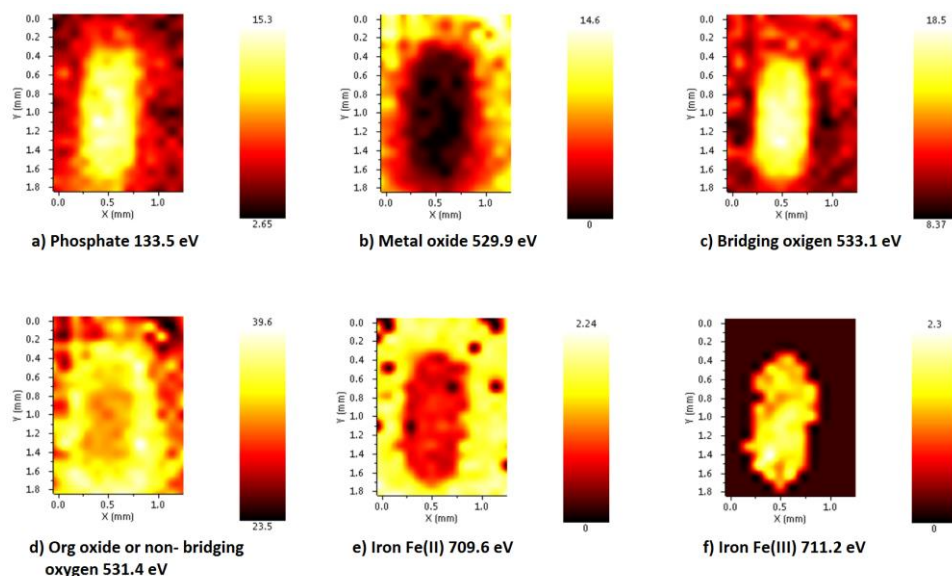


Figure 5. 9 - XPS analysis on the disc surface rubbed during the experiment with 5% w/w of **IL16** - $[(H_9C_4)_3P(CH_3)]^+ [(C_1)_2PO_4]^-$. a) Phosphate 133.5 eV, b) Oxygen in metal oxide 529.9 eV, c) bridging oxygen 533.1 eV, d) Organic oxide or non-bridging oxygen 531.4 eV, e) iron Fe(II) 709.6 eV, f) iron Fe(III) 711.2 eV.

The binding energy of 529.9 eV for oxygen which can be related to the binding state of metal oxide is high outside the wear track, while it is low or zero inside. On the contrary, the concentration of bridging oxygen, as for example P-O-P (533.1 eV) [172] is much higher inside the wear track than outside. There is a high content of organic oxide or non bridging oxygen on the whole surface of the disc but the concentration is slightly higher on the border of the wear track. The presence of iron(III) phosphate ($FePO_4$) in the wear track can also be confirmed by Figure 5. 9 f. It seems that part of the iron present was oxidized and transformed from Fe(II) to Fe(III) due to the prevailing contact pressure and temperature in the worn area during the tribotest.

XPS analysis on the surface worn during the experiments with **IL17** - $[\text{P}(\text{C}_4\text{H}_9)_4]^+ [(\text{C}_2)_2\text{PO}_2\text{S}_2]^-$ showed slightly different results (Figure 5. 10). The presence of higher concentration of phosphorus in the wear track was confirmed but in this case the organic oxide was in majority in the wear track and not on the border. Even the abundance and binding states of iron have changed slightly. The presence of sulfide and sulfoxides was not in a significant amount, however they were detected.

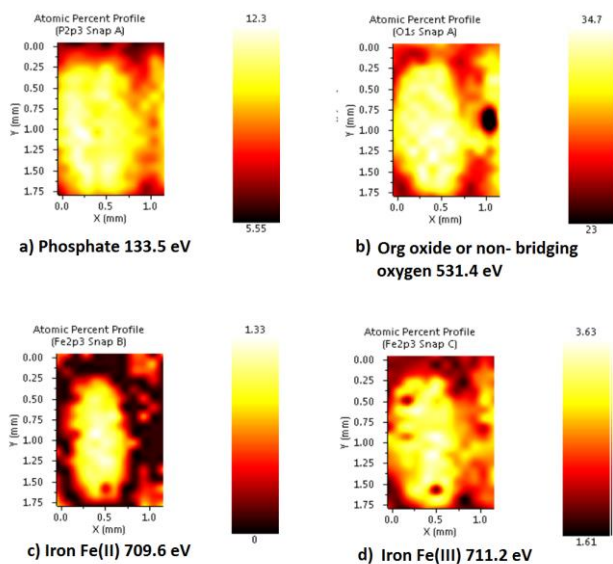


Figure 5. 10 - XPS analysis on the disc surface rubbed during the experiment with 5% w/w of **IL17** - $[\text{P}(\text{C}_4\text{H}_9)_4]^+ [(\text{C}_2)_2\text{PO}_2\text{S}_2]^-$. a) Phosphate 133.5 eV, b) Organic oxide or non-bridging oxygen 531.4 eV, c) iron Fe(II) 709.6 eV, d) iron Fe(III) 711.2 eV.

5.3.5 Thermal degradation and corrosion analysis

In Figure 5. 11 and Figure 5. 12 it is possible to see the results obtained by infrared (IR) spectroscopy after the degradation tests realized on the ionic liquids **IL16** - $[(\text{H}_9\text{C}_4)_3\text{P}(\text{CH}_3)]^+ [(\text{C}_1)_2\text{PO}_4]^-$ and **IL17** - $[\text{P}(\text{C}_4\text{H}_9)_4]^+ [(\text{C}_2)_2\text{PO}_2\text{S}_2]^-$.

The structures analyzed have similarities that can be appreciated also in the IR spectra. In the range between 2820 and 3000 cm^{-1} there are the C-H stretching vibrations of the alkyl groups. Close to 2960 cm^{-1} there is the asymmetric CH_3

stretching, around 2930 cm^{-1} there is the CH and CH_2 asymmetric stretching and at 2872 cm^{-1} there should be the symmetric CH and CH_3 stretching. The asymmetric and symmetric H-C-H bending modes were found respectively close to 1466 cm^{-1} and 1382 cm^{-1} . At 1422 cm^{-1} there could be the P-C bond linked with a scissoring of the CH_2 . At 1313 it was observed a peak just for the **IL16** - $[(\text{H}_9\text{C}_4)_3\text{P}(\text{CH}_3)]^+ [(\text{C}_1)_2\text{PO}_4]^-$ that correspond to the vibrations of CH_3 -P. The P-O-C bond for aliphatic compound appeared at 1260 , 1160 and 1100 cm^{-1} . **IL17** - $[\text{P}(\text{C}_4\text{H}_9)_4]^+ [(\text{C}_2)_2\text{PO}_2\text{S}_2]^-$ has P-S and P=S vibration at 806 , 758 and 674 cm^{-1} .

The thermal degradation test started with the samples kept in the oven at $100\text{ }^\circ\text{C}$ during one week. In Figure 5. 11 it is possible to see that the **IL16** - $[(\text{H}_9\text{C}_4)_3\text{P}(\text{CH}_3)]^+ [(\text{C}_1)_2\text{PO}_4]^-$ did not suffer great changes during the first week since there is no change in the spectrum. This means that the ionic liquid was stable at this temperature. Looking at Figure 5. 12, instead, some changes were observed in the lower range of the spectrum, corresponding to the bonds of sulfur and phosphorus. A peak had appeared also in the area close to 1170 cm^{-1} . These changes give confirm that a degradation process has already began in the **IL17** - $[\text{P}(\text{C}_4\text{H}_9)_4]^+ [(\text{C}_2)_2\text{PO}_2\text{S}_2]^-$.

For the second week of test, it was decided to increase the temperature at $150\text{ }^\circ\text{C}$. Also in this case, the **IL16** - $[(\text{H}_9\text{C}_4)_3\text{P}(\text{CH}_3)]^+ [(\text{C}_1)_2\text{PO}_4]^-$ it is possible to see some small changes in the absorbance level but the structure seems to be still quite unchanged. The degradation of **IL17** - $[\text{P}(\text{C}_4\text{H}_9)_4]^+ [(\text{C}_2)_2\text{PO}_2\text{S}_2]^-$ instead becomes even more evident and the whole spectra between 600 nm and 1300 nm has changed. Considering the wide range of peaks, it can be assumed that the by-products generated can have different nature.

The test continued for a third week and the temperature was set again at $150\text{ }^\circ\text{C}$. In this case, more signs of degradation were found also on the **IL16** - $[(\text{H}_9\text{C}_4)_3\text{P}(\text{CH}_3)]^+ [(\text{C}_1)_2\text{PO}_4]^-$. Also in this case, the degradation can be seen in the lowest part of the spectrum, between 800 and 700 cm^{-1} and a new peak with low intensity appeared around 1700 cm^{-1} .

The spectra obtained with the **IL17** - $[P(C_4H_9)_4]^+ [(C_2)_2PO_2S_2]^-$ did not change during this third week. This seems evidence that the ionic liquid was already completely degraded after the second week and that no further transformation occurred.

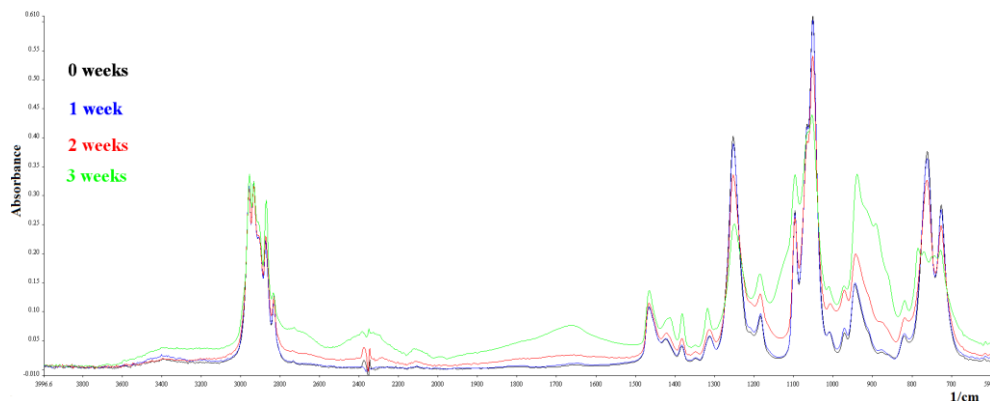


Figure 5. 11 – ATR-FTIR analysis of the ionic liquid **IL16** - $[(H_9C_4)_3P(CH_3)]^+ [(C_1)_2PO_4]^-$ after the thermal degradation test in the oven.

The analysis of the balls exposed to the action of the neat ionic liquids gave interesting information about corrosiveness of these fluids. As explained before, a steel ball was sunk in the ionic liquids samples used for the thermal degradation test. Photos and the SEM-EDS analysis of Figure 5. 13 represent the balls that were kept in the oven for three weeks.

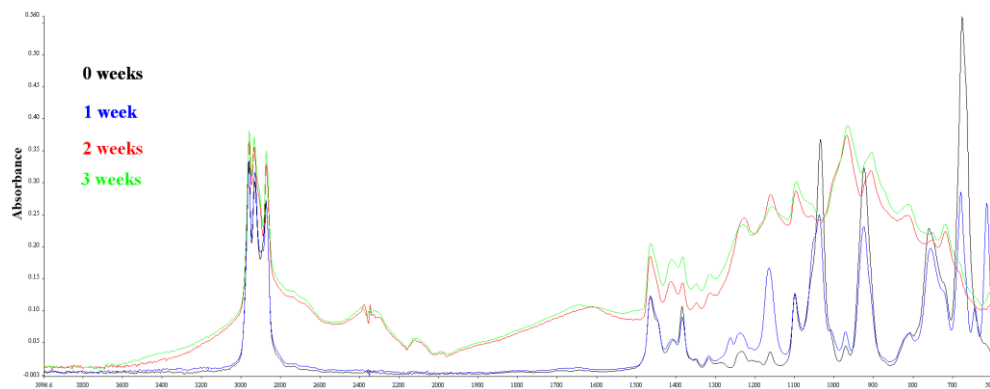


Figure 5. 12 – ATR-FTIR analysis of the ionic liquid **IL17** - $[P(C_4H_9)_4]^+ [(C_2)_2PO_2S_2]^-$ after the thermal degradation test in the oven.

From the photos taken, it is possible to see that the ball that was exposed to the **IL16** - $[(\text{H}_9\text{C}_4)_3\text{P}(\text{CH}_3)]^+ [(\text{C}_1)_2\text{PO}_4]^-$ seems unaffected and does not have signs of corrosion. The ball that was in the vial with the **IL17** - $[\text{P}(\text{C}_4\text{H}_9)_4]^+ [(\text{C}_2)_2\text{PO}_2\text{S}_2]^-$ instead, was completely black.

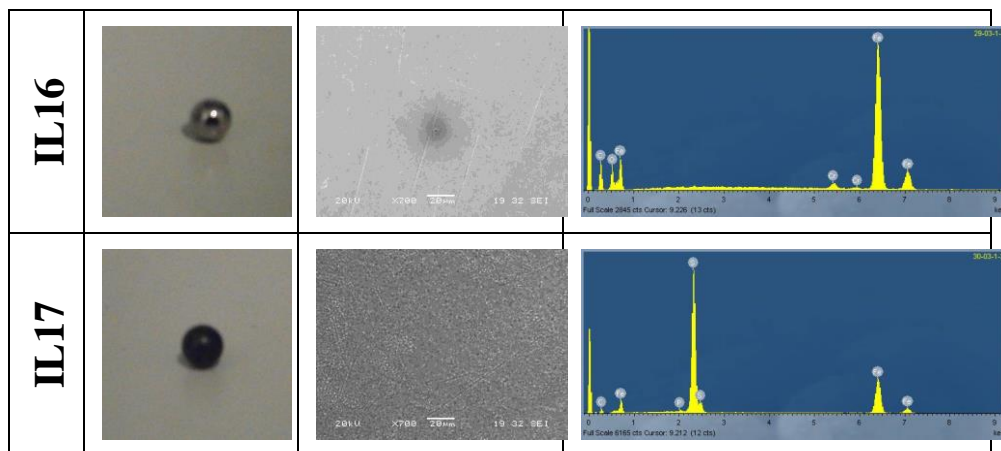


Figure 5. 13 - Photos and SEM-EDS analysis on the balls exposed to the ionic liquids in a oven for three weeks. On the left there is the photo taken with digital camera, at the center there is the SEM image of the surface and at the right there is the result of the EDS analysis.

The photo taken by SEM confirms what had been visually observed, the dimethylphosphate ionic liquid did not leave any mark of corrosion on the steel surface even after three weeks at high temperature while the diethylphosphorodithionate ionic liquid generated corrosion all over the surface. By EDS analysis it was possible to see that on the surface exposed to **IL17** - $[\text{P}(\text{C}_4\text{H}_9)_4]^+ [(\text{C}_2)_2\text{PO}_2\text{S}_2]^-$ there is a quite high concentration of sulphur and just a small percentage of phosphorus. This could give the idea that the decomposition of the anion was responsible for the corrosion generated.

5.3.6 Tribocorrosion analysis

The tribocorrosion tests were realized on the neat **IL16** - $[(\text{H}_9\text{C}_4)_3\text{P}(\text{CH}_3)]^+ [(\text{C}_1)_2\text{PO}_4]^-$ and on a mixture of IL and base oil. As reference, an equivalent tribotest was realized on the base oil. It was impossible to realize electrochemical

measurements on the base oil during tribocorrosion test because the conductivity was too low and the noise of the signal was too high.

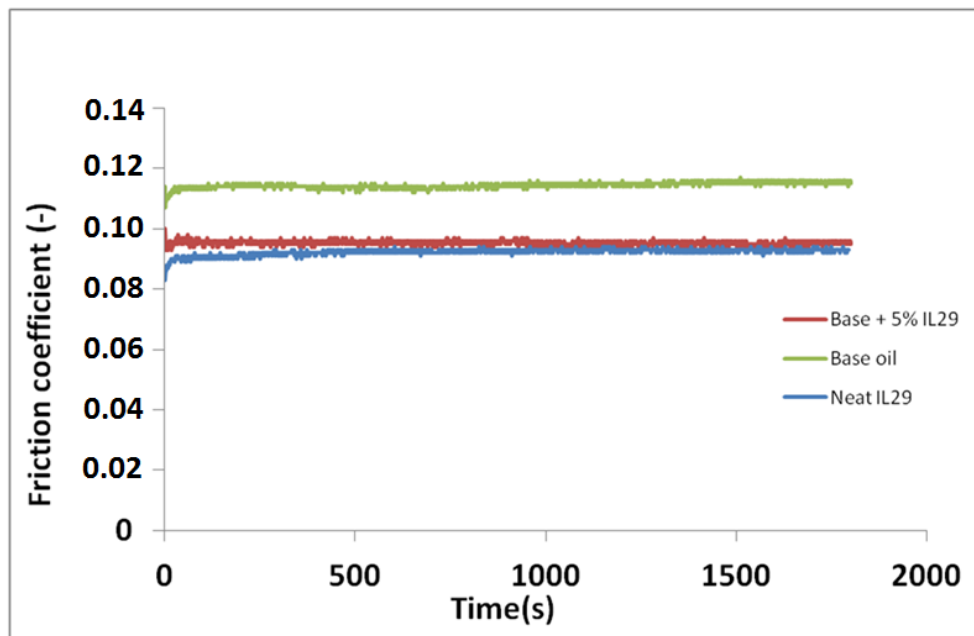


Figure 5. 14 – Friction coefficient measured during the tribocorrosion tests.

The results of the friction coefficient measured during the tests are shown in Figure 5. 14. The friction is very stable during the whole test with all the lubricants examined. The highest friction value was found with the base oil, around 0.115. For the neat IL and for the mixture of base oil and IL instead the friction was always lower than 0.1, with the neat IL performing slightly better. I should be pointed out the fact in the previous tribotests the friction registered was higher (especially in the case of the base oil) but this could depend on the fact that the counter materials used were different and that the conditions and configuration used for the tribotests were more severe.

After 3600 of exposure to the IL and to the mixture, the values of the OCP of the steel were -0.062 V and 0.141 V respectively. After this period of potential stabilization, the potential is again monitored during the tribological process in order

to see the effect of the applied load on the electrochemical response of the steel surface. The evolution of the OCP before, during and after the sliding process for both, IL and mixture is shown in Figure 5. 15.

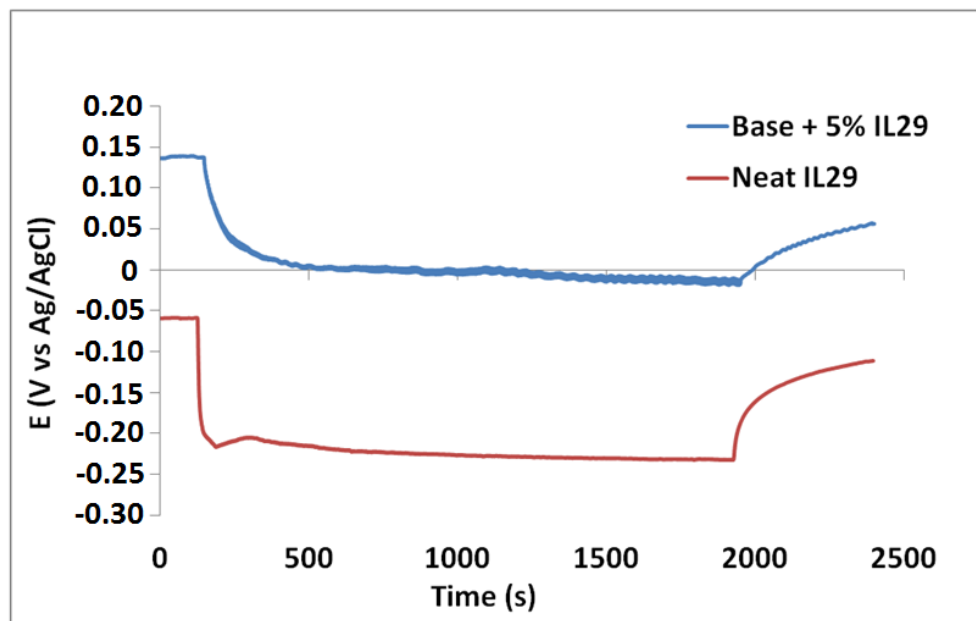


Figure 5. 15 - Open circuit potential of the tribotests during the sliding phase.

In both cases, it was observed a shift of the potential toward more negative values. This is a behavior typical when a surface has reached a passive state and by applying a mechanical stress on the surface, the external passive layer is removed allowing the contact between the underlayer steel and the corrosive media. In this case, the worn area is exposed again to the action of the fluids and can react to create a new passive layer. This kind of behavior is observed when the systems are working under tribocorrosion conditions. From the analysis of the curves, it was noticed that when the steel is in contact with the neat ionic liquid, the potential has a more negative value and the potential drop is faster when the tribotest starts. After the end of the sliding process, it was seen also that with neat ionic liquid, the potential increase toward the initial values is faster. These observations can allow to conclude that the

ionic liquid is more reactive with the surface when it is in its neat state than when it is mixed with the base oil.

5.4 CONCLUSIONS

Two phosphonium based ionic liquids were investigated as additives for polypropylene glycol base oil. The results demonstrated that both ionic liquids have physical and chemical properties that do not limit their use in mixture with the base oil. They had good thermal properties with thermal degradation in the order of 300 °C. Although the VI was not as high as in the case of modern lubricants, the addition of a smaller amounts will not negatively affect the viscometric properties of the base oil. **IL16** - $[(\text{H}_9\text{C}_4)_3\text{P}(\text{CH}_3)]^+ [(\text{C}_1)_2\text{PO}_4]^-$ had a very good miscibility with the base oil while **IL17** - $[\text{P}(\text{C}_4\text{H}_9)_4]^+ [(\text{C}_2)_2\text{PO}_2\text{S}_2]^-$ would need the use of surfactants to form a stable blend of base and additive.

The antiwear properties of the ionic compounds substantially improved the tribological properties of the base oil, both in terms of friction and wear reduction.

IL16 - $[(\text{H}_9\text{C}_4)_3\text{P}(\text{CH}_3)]^+ [(\text{C}_1)_2\text{PO}_4]^-$ demonstrated good performance at all of the concentration levels tested, from 0.25% till 5% w/w. On the other hand, **IL17** - $[\text{P}(\text{C}_4\text{H}_9)_4]^+ [(\text{C}_2)_2\text{PO}_2\text{S}_2]^-$ had the optimum performance in the range between 0.50% and 2% w/w of ionic liquid in base oil, while it is observed an insufficient protection at 0.25% w/w of additive and a possible tribocorrosion effect at a concentration as high as 5%.

The surface analysis by XPS provided an insight of the tribolayer formation. The phosphates present on the wear scar of the disc lubricated with **IL16** - $[(\text{H}_9\text{C}_4)_3\text{P}(\text{CH}_3)]^+ [(\text{C}_1)_2\text{PO}_4]^-$ and **IL17** - $[\text{P}(\text{C}_4\text{H}_9)_4]^+ [(\text{C}_2)_2\text{PO}_2\text{S}_2]^-$ confirmed the formation of a tribolayer with both ionic liquids. Moreover, the XPS results with **IL16** - $[(\text{H}_9\text{C}_4)_3\text{P}(\text{CH}_3)]^+ [(\text{C}_1)_2\text{PO}_4]^-$ demonstrated that in the wear scar there is a prevalence of iron Fe(III) while outside there is mainly Fe(II).

The thermal degradation tests showed that the **IL17** - $[\text{P}(\text{C}_4\text{H}_9)_4]^+ [(\text{C}_2)_2\text{PO}_2\text{S}_2]^-$ undergo a chemical decomposition if it is exposed for a prolonged time at high temperature. The decomposition leads to the formation of corrosive by-products. The corrosion was attributed to the presence of sulphur. The **IL16** - $[(\text{H}_9\text{C}_4)_3\text{P}(\text{CH}_3)]^+ [(\text{C}_1)_2\text{PO}_4]^-$ instead, appears to be much more stable and the first consistent sign of degradation was detected after three weeks at high temperature. After three weeks at high temperature, the ionic liquid did not promote corrosion on the steel ball.

The tribocorrosion tests realized with **IL16** - $[(\text{H}_9\text{C}_4)_3\text{P}(\text{CH}_3)]^+ [(\text{C}_1)_2\text{PO}_4]^-$ showed that under sliding conditions, the potential decreases due to the effect of the fresh exposed area. This shows that probably the wear mechanism analysed with the ionic liquid is due to tribocorrosion.

It was confirmed that using ionic liquids mixed with synthetic base oil can help in reducing the corrosion problems.

In conclusion, both ionic liquids investigated were suitable as additives for polypropylene glycol with **IL16** - $[(\text{H}_9\text{C}_4)_3\text{P}(\text{CH}_3)]^+ [(\text{C}_1)_2\text{PO}_4]^-$ being the best performer, since it is characterised by better miscibility and similar tribological performance regardless of the concentration used.

Chapter 6

6 Triboreactivity in vacuum of halogen-free ionic liquids

6.1 INTRODUCTION

Solid lubricants and coatings are normally preferred to liquid lubricants in vacuum and space applications because of volatility and risk of contamination. Nonetheless, in many situations it is recognized that the use of a liquid lubricant could improve significantly the performance of the system and extend its lifetime. Solid lubricants and coatings, as for example molybdenum disulfide and Diamond-Like Carbon (DLC) coatings, can have good performance for a limited time because they can wear out and are difficult to replace. In spite of their quite high thermal resistance, they are not suggested for using under severe conditions, when high friction forces are expected, since they do not provide thermal dissipation. Finally, their performance depends very much on the working environment; often they are not able to operate properly both in vacuum and atmospheric conditions [173-177].

In order to respond to the requirements of different systems, many kind of lubricant formulations have been developed. Perfluoropolyethers (PFPE), multiple alkylated cyclopentanes (MAC), polyalphaolephins (PAO), silicones and silicic hydrocarbons are the most common classes of liquid lubricants in vacuum applications [178]. All

of them have a common characteristic that is essential for working in this environment, an extremely low vapour pressure.

PFPEs are probably the most used liquid lubricants for vacuum. They show high thermal and chemical stability, low pour point and high viscosity index. They are very suitable for working under hydrodynamic and elastohydrodynamic lubrication regimes but their tribological properties are poor in boundary conditions since they degrade easily under high contact pressures [179,180]. In addition, they have low compatibility with other compounds, which make it difficult to find valid additives [181-183].

MACs are composed of a cyclopentane ring with two to five alkyl groups substituted on the ring. Together with PFPE, they are the oils that exhibit the lowest vapour pressure. By using different kind of MACs or using proper alkyl groups, it is possible to obtain higher viscosity index. It is also possible to get lower freezing points by using longer alkyl groups [184]. PAOs are synthetic hydrocarbons with low freezing point. The vapour pressure of these fluids is slightly higher than in the case of PFPEs and MACs. Both PAOs and MACs, need to use proper additives for enhancing their tribological performance in boundary conditions [185]. Fortunately, being based on a hydrocarbon structure, they have the advantage of being miscible with many common lubricant additives [186,187].

Silicones are polymers with the main chain composed of alternated silicon and oxygen atoms combined with carbon and other elements. Due to their low volatility and low freezing point, they were used as lubricants during the first space missions but later they were rejected because it was demonstrated that they were giving problems of creep. The lubricant was spreading out of the contact surface [186].

Silohydrocarbons contain silicon, hydrogen and carbon atoms, which have shown low volatility and the possibility of easily synthesize structures with different viscosities by changing the length of the alkyl chains. In addition to this, it is also possible to use conventional additives for their full formulation [183,188].

Additionally to the oils mentioned, also the ionic liquids have shown promising characteristic for working under vacuum. Thanks to the ionic nature of the interaction between cations and anions, they have pretty low vapour pressure. Furthermore, they are considered easily tunable since it is possible to obtain an incredible number of combinations by arranging together different cations and anions, by changing functional groups or by using longer or shorter alkyl chains.

The potentiality of ionic liquids as vacuum lubricants were shown by Zhang et al., who realized vacuum tests on steel against steel and studied the performance of four phosphonium phosphate ionic liquids as lubricants and additives taking a MAC lubricant as reference and base oil [189]. The study provided principally information about the tribological behavior. It was possible to see that, in comparison with MAC, the ionic liquids don't need the addition of antiwear additives in order to work in boundary regime. They are able to generate an efficient protective layer that reduces friction and wear. In addition to this, it was demonstrated that the structure with longer alkyl chains, tri(2-ethylhexyl)tetradecylphosphonium bis(2-ethylhexyl) phosphate, was fully miscible in MAC and was able to activate its antiwear properties even in a concentration of 1% (w/w).

In a previous study realized in IK4-TEKNIKER within the frame work of the MINILUBES project, vacuum experiments were carried out on 1-butyl-3-methylimidazolium bis(trifluoromethanesulfonyl)imide and tributylmethylphosphonium dimethylphosphate [167]. They were compared with PFPE lubricant for a steel/steel contact. The results showed that the ionic liquids had lower friction and wear in comparison with PFPE. It was demonstrated that the bis(trifluoromethanesulfonyl)imide anion was able to form an iron fluoride tribolayer while the phosphonium phosphate ionic liquid generated iron phosphate on the worn surface.

In this chapter, the tribological properties of a new class of ionic liquids are analyzed in vacuum and atmospheric conditions. These ionic liquids were selected considering

their characteristics. They have an alkylphosphonium cation, which should provide oleophilic properties to the cation, thanks to a long alkyl chain. In addition, the long alkyl chain can be able to lower the friction forces during the sliding motion of the surfaces and the phosphonium group should be able to act as antiwear reagent, since it could generate metal phosphate boundary film. The anion of the ionic liquids instead was composed of a trialkylsilyl group that should have oleophilic properties and also should have favourable rheological properties. It had also an alkylsulphonate group that should improve the tribological properties of the lubricant by functioning as an anchor to the metal surface. This molecular design was proposed by professor Minami and these ionic liquids were already studied in atmospheric conditions [112].

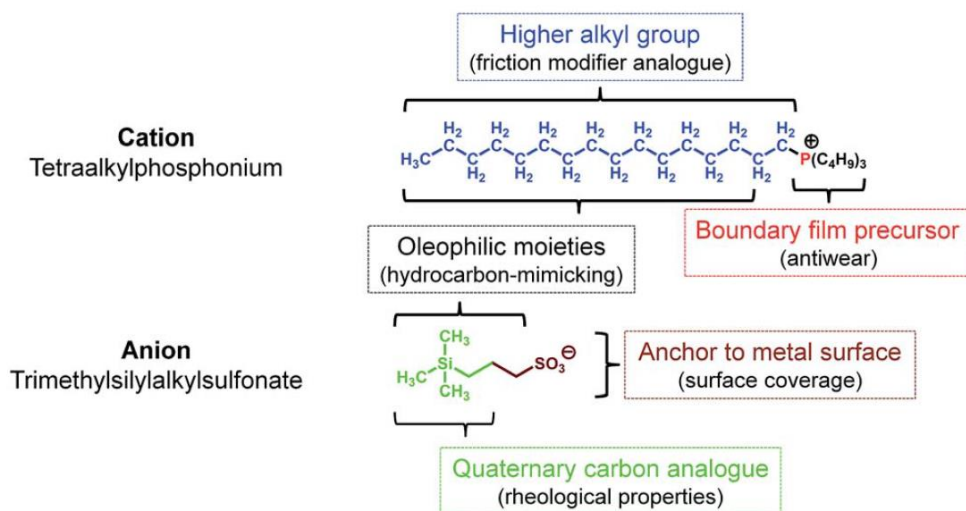


Figure 6. 1 - Expected function of the ionic structure of the ionic liquids [112].

In this chapter, the tribological performance of these five ionic liquids was studied in boundary conditions. For this study, the lubricants were tested with a SiN₃ ball rubbing against steel and titanium surfaces. The tests were realized in the CATRI © UHV, realizing a gas analysis with a mass spectrometer during the tests in vacuum. The results of these tests show that, during the lubrication with ionic liquids on

titanium surface, a degradation process of the lubricants takes place and the rupture of the anionic and cationic molecules lead to a slight decrease of friction coefficient. X-ray photoelectron spectroscopy was realized on the worn surface in order to describe the triboreactions that are triggered on the rubbed surfaces [117].

6.2 EXPERIMENTAL

6.2.1 Materials

Ionic liquids: In this work, five alkylphosphonium ionic liquids were analyzed under vacuum conditions in order to evaluate their tribological behavior and to understand the process occurring during the tribocontact. The codification of the different ionic liquids is based on their structure and it is explained in Table 6. 1. In the upper part of the figure, there is the representation of the structure and in the lower part the corresponding codification.

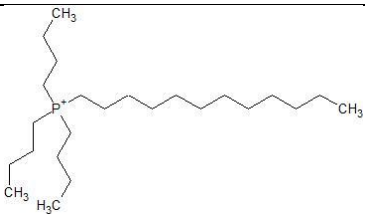
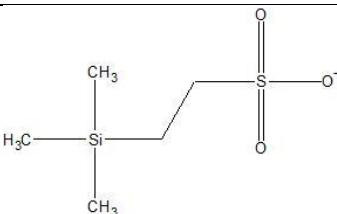
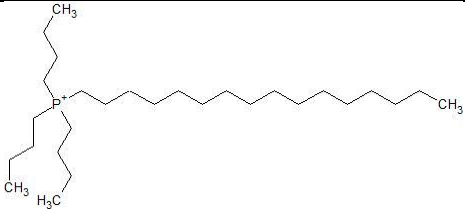
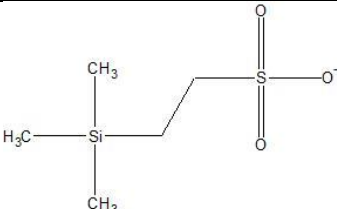
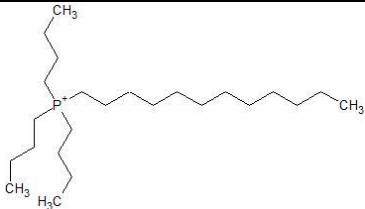
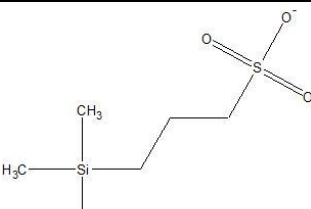
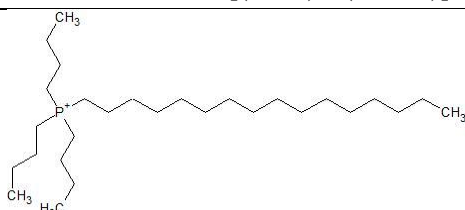
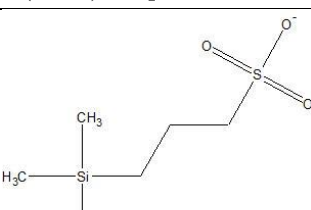
Physico-chemical characteristics of the ionic liquids (density, viscosity, melting point, thermal resistance and water content) were already measured by the supplier

Reference oil: The performance of the ILs was compared with the performance of PFPE, a lubricant commonly used for space and vacuum applications. PFPEs are considered an outstanding lubricant for space applications because of the good thermal and oxidative stability at temperature higher than 260 °C, they are fire resistant and have good low-temperature flow characteristics. In addition to these properties, PFPEs have extremely low vapour pressure, which is essential for working in vacuum condition.

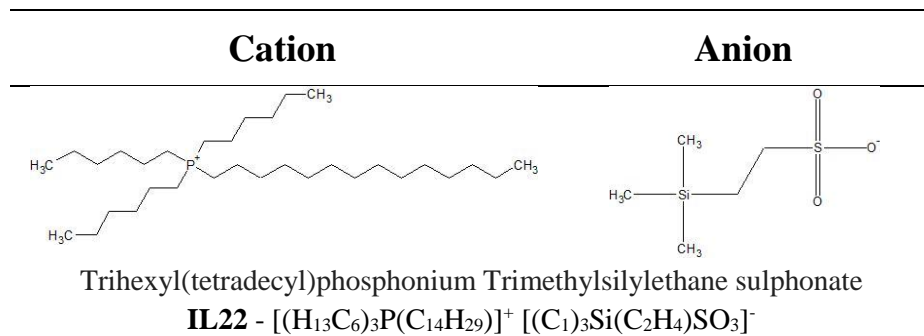
Table 6. 2 is partially reported in an article published by Nyberg et al. [112].

It seems that the ionic liquids with longest cationic alkyl chain have slightly lower viscosity at room temperature while at higher temperature the anionic chain plays a more relevant effect. The shortest anionic alkyl chain gives higher viscosity.

Table 6. 1 - Structure and codification of siliconsulphonate ILs.

Cation	Anion
	
<p>Tributyl(dodecyl)phosphonium Trimethylsilylethane sulphonate IL18 - $[(H_9C_4)_3P(C_{12}H_{25})]^+ [(C_1)_3Si(C_2H_4)SO_3]^-$</p>	
	
<p>Tributyl(hexadecyl)phosphonium Trimethylsilylethane sulphonate IL19 - $[(H_9C_4)_3P(C_{16}H_{33})]^+ [(C_1)_3Si(C_2H_4)SO_3]^-$</p>	
	
<p>Tributyl(dodecyl)phosphonium Trimethylsilylpropane sulphonate IL20 - $[(H_9C_4)_3P(C_{12}H_{25})]^+ [(C_1)_3Si(C_3H_6)SO_3]^-$</p>	
	
<p>Tributyl(hexadecyl)phosphonium Trimethylsilylpropane sulphonate IL21 - $[(H_9C_4)_3P(C_{16}H_{33})]^+ [(C_1)_3Si(C_3H_6)SO_3]^-$</p>	

Continue from Table 6. 1



It is well known from literature that the temperature of degradation of the ionic liquids is highly influenced by the anion. In this case, it seems that the anions with short chain behave slightly better than the anion with long chain and should provide higher viscosity index.

6.2.2 Tribological experiments

The tribological test configuration used for the experiments was “Ball on flat”. The balls used had diameter of 3 mm and were made of Si₃N₄. Two different kind of materials, employed in vacuum environments, were used as counterpart: titanium Grade 5 (also called Ti-6Al-4V) and stainless steel 440C. The specimens were subsequently cleaned in three different solvents (toluene, isopropanol and petroleum ether) for 10 min each, using an ultrasound bath, before and after the experiments. The composition of titanium grade 5 and stainless steel 400C is listed in Table 6. 3. The testing conditions used are summarized in The molecular and fragments ions coming from the tribosystem during the tribological test were monitored by a Fast Response Quadrupole Mass Spectrometer (Q-MS) from Hidden (UK) in Bar Mode for molecular masses between 1 and 300.

Table 6. 4. The experiments were performed twice in order to confirm repeatability.

The experimental system CATRI © UHV with reciprocating ball-on-flat configuration was used for characterization of the ionic liquids in the Chapter 3.4. This is a tribometer designed in IK4-TEKNIKER for studying solid or liquid lubricating systems simulating atmospheric, vacuum, high vacuum or ultra-high vacuum conditions [115,190]. It is possible to realize experiments in the range of temperature between -55 °C and 350 °C with loads in the range between 0.1 N and 20 N, speeds in the range of 0.02 mm/s and 10 mm/s and maximal displacement of the pin of 20 mm. The tribometer uses a force sensor that was developed and patented in IK4-TEKNIKER [116].

Table 6. 2 Physical-chemical characteristics of the ionic liquids.

Code	Density [g/cm ³]	Viscosity [mPa s]		Melting point [°C]	10% weight loss at [°C]	Stated water content [ppm]
	@ 25 °C	@ 25 °C	@ 60 °C			
IL18	0,9	2570	208	-6	311	68
IL19	0,91	1932	269	5	316	137
IL20	0,93	2429	104	2	291	93
IL21	0,9	1735	142	-5	299	68
IL22	0,92	1879	200	-19	310	83

Table 6. 3 – Composition of the discs that were used for the tribological tests: stainless steel 440C and titanium grade 5.

Steel		C	Mn	Si	P	S	Cr	Mo
440C	min. [%]	0.95	-	-	-	-	16	-
	max. [%]	1.20	1	1	0.04	0.03	18	0.75
Titanium		C	Fe	N ₂	O ₂	Al	V	H ₂
Grade 5	min. [%]	-	-	-	-	5,5	3.5	-
	max. [%]	0.08	0.25	0.05	0.2	6.76	4.5	0.0125

The molecular and fragments ions coming from the tribosystem during the tribological test were monitored by a Fast Response Quadrupole Mass Spectrometer (Q-MS) from Hidden (UK) in Bar Mode for molecular masses between 1 and 300.

Table 6. 4 - Testing conditions used during the tribotests.

Test parameters	Chapter 6
Tribometer used	CATRI © UHV
Normal load [N]	10
Velocity [mm/s]	3
Stroke [mm]	3
Frequency [Hz]	0.5
Temperature [°C]	Room temperature
Duration [s]	1200
Ball Material	Si ₃ N ₄
Ball diameter [mm]	3
Disc material	AISI 440C – Ti6Al4V
Base lubricant/Reference	PFPE
Concentrations [%]	0; 100

The quadrupole mass spectrometer detector is closed to the friction zone of the specimens. Even so, during the tribodesorption measurements, the main pumping valve of the main chamber remains closed so that the gas fragments cannot escape, and only a small orifice is open in order to avoid excessive variations in the pressure. Air was pumped out from the main chamber until reaching ultra-high vacuum regime

(around 1×10^{-7} Pa), and then the tribodesorption experiments were carried out in high vacuum regime (around 10^{-6} Pa) by closing the pumping valves.

The wear scars were examined using a DM 2500 MH Optical Microscope from Leica (Germany) and images were obtained with a magnification of x25. Moreover, the topographies of the worn surfaces were analyzed using an Eclipse ME600 Confocal Microscope from Nikon Instruments Inc. (Japan), and disc wear volumes were calculated from these topographies using a Matlab script developed in IK4-TEKNIKER.

6.2.3 Surface analysis

An additional surface analysis was performed on the specimen surface after sliding tests using a Thermo Fisher Scientific Theta Probe (East Grinstead, UK) equipped with a monochromatic Al K α X-ray source ($h\nu=1486.6$ eV) and a hemispherical analyzer in order to characterize the chemical composition of it. The elemental and chemical composition of the wear track surfaces on the discs was obtained by spot analysis with an X-ray beam. Three different points of the specimen's surface were examined:

- REF: the surface outside of the wear track
- MI: the surface in the middle of the wear track
- TP: the turning point at the extremity of the wear track.

The spectra were analyzed with the Avantage Data System software (East Grinstead, UK), using Gaussian-Lorentzian peak fitting.

6.3 RESULTS AND DISCUSSION

6.3.1 Tribological performance

The friction coefficients recorded during the tribological tests, are reported in Figure 6. 2 and Figure 6. 3. Figure 6. 2 shows the data collected from the tests performed

on steel specimens while Figure 6. 3 shows the results from the tests with titanium specimens.

The ionic liquids work excellently when they are lubricating steel against Si_3N_4 . The coefficient of friction is quite stable during the whole test and the average values obtained are quite low in relation to PFPE lubricant. Except for the **IL22** - $[(\text{H}_{13}\text{C}_6)_3\text{P}(\text{C}_{14}\text{H}_{29})]^+ [(\text{C}_1)_3\text{Si}(\text{C}_2\text{H}_4)\text{SO}_3]^-$ which has slightly higher coefficient (0.068), the others have average values between 0.052 and 0.059. The lubricant selected as reference has instead quite higher coefficient of friction, around 0.120.

Completely different behavior was found when the tests were performed with titanium specimens. The coefficient of friction was quite unstable during the tests and even though it was decreasing with time, it was still fairly high. It could be said that none of the lubricants selected was able to form a stable protective tribo-layer capable of reducing effectively the friction.

Figure 6. 4 shows a summary the average coefficient of friction recorded during the tests and put in comparison the performances obtained with the different lubricants and materials.

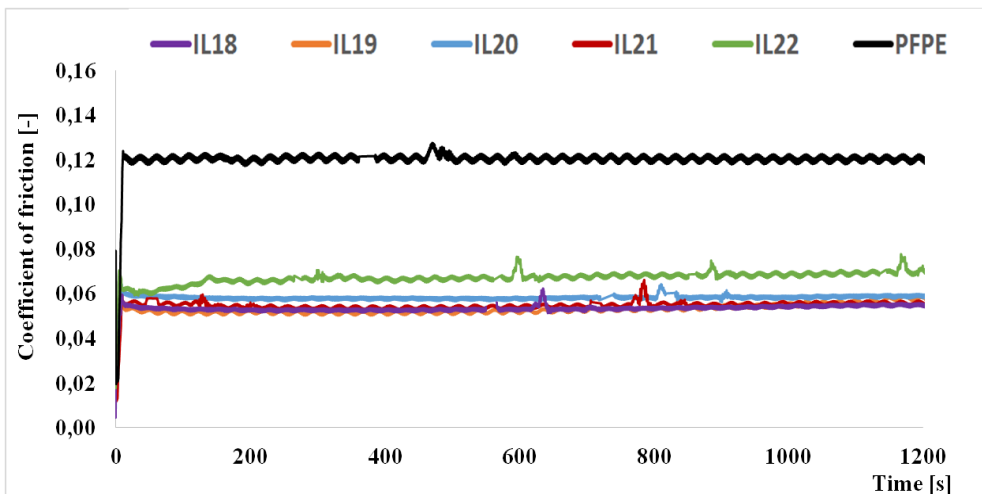


Figure 6. 2 - Friction coefficient for the tests performed on steel surface in vacuum conditions.

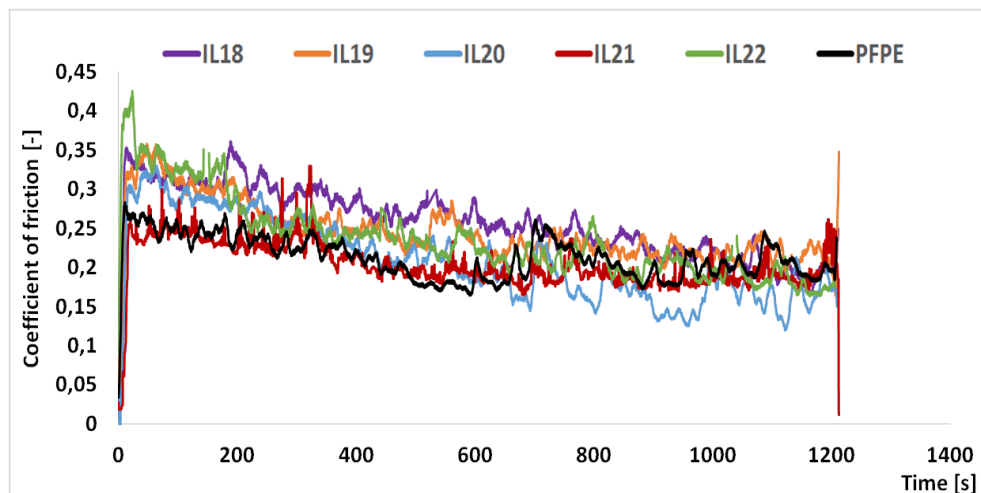


Figure 6. 3 - Friction coefficient for the tests performed on titanium surface in vacuum conditions.

With this graph it is possible to appreciate that the ILs are rather good lubricants for steel but that they are not good enough when the lubricated surface is titanium. The lowest friction value on titanium discs was obtained by **IL20** - $[(H_9C_4)_3P(C_{12}H_{25})]^+ [(C_1)_3Si(C_3H_6)SO_3]^-$ but it was almost the same friction that was registered with **PFPE**.

The high friction values and the irregular friction coefficient could have been foreseen since titanium has the tendency to cause adhesion during the tribocontact and, up to now, there are no lubricants that shows outstanding performance with this metal [184-187].

Figure 6. 5 shows the micrographies captured with the optical microscope for the surfaces lubricated with **IL22** - $[(H_{13}C_6)_3P(C_{14}H_{29})]^+ [(C_1)_3Si(C_2H_4)SO_3]^-$ and with **PFPE**. The images with the other ionic liquids were not included because they were all showing similar behaviour. There is a huge difference between the marks left on the steel samples and the marks left on titanium. On steel, the lubricants provided an efficient tribolayer and the surface of the scar seems very smooth. On the contrary,

the titanium surfaces presented a deep and wide wear scar, with presence evident signs of abrasion and adhesions.

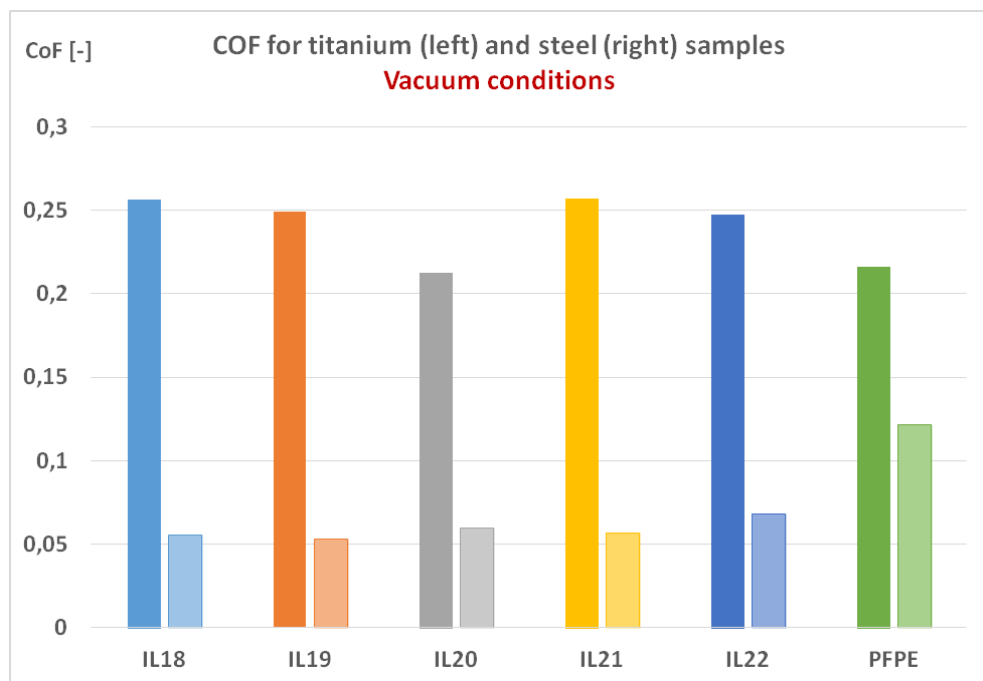


Figure 6. 4 - Average friction coefficient. In blue the values obtained with titanium specimens and in orange the results obtained with steel specimens. The tests were realized in vacuum.

It was not easy to notice differences between the wear scar produced with the different lubricants. Measuring the width of the wear scar it was possible to see that they were approximately the same.

In order to obtain a more reliable data of the wear volume, the wear scars were analyzed by confocal microscopy. Figure 6. 6 gives the values of wear volume measured on the wear scar. The wear on the samples lubricated with steel was one order of magnitude lower than the wear on the titanium sample. With titanium, **IL20** - $[(H_9C_4)_3P(C_{12}H_{25})]^+ [(C_1)_3Si(C_3H_6)SO_3]^-$ was the IL that showed the lowest coefficient of friction but in terms of wear it is amongst the worst. The same can be said about the PFPE; the (relatively) good friction result is not followed by a

(relatively) low wear volume. The lowest wear volume was measured on the wear scar of the discs lubricated with **IL18** - $[(H_9C_4)_3P(C_{12}H_{25})]^+ [(C_1)_3Si(C_2H_4)SO_3]^-$ and **IL22** - $[(H_{13}C_6)_3P(C_{14}H_{29})]^+ [(C_1)_3Si(C_2H_4)SO_3]^-$.

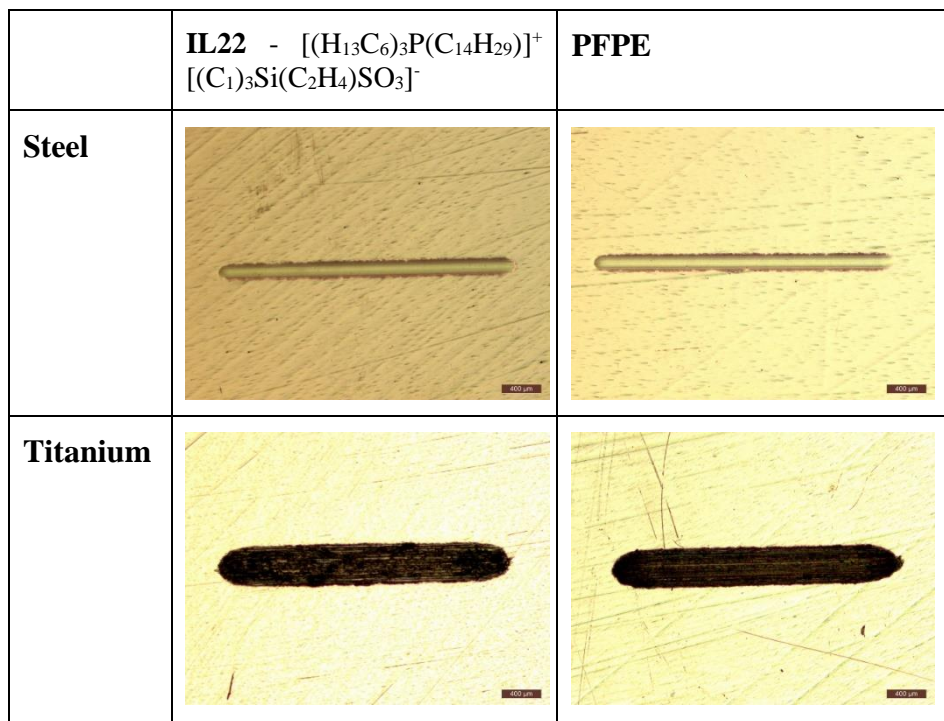


Figure 6. 5 - Wear tracks of the samples tested in vacuum conditions

For the wear scar on the steel samples, the Wv on the discs lubricated with the ILs **IL18-IL21** was quite similar. The higher wear was measured on the samples lubricated with PFPE, but the worst performance was obtained with **IL22** - $[(H_{13}C_6)_3P(C_{14}H_{29})]^+ [(C_1)_3Si(C_2H_4)SO_3]^-$.

Most of the times, systems that should operate in vacuum need to be tested also in atmospheric conditions since they could spend part of their lifetime in presence of air or other gasses. For this reason, the same set of tests was realized at atmospheric pressure.

Figure 6. 8 put together the friction coefficients that were obtained from the tests realized on steel samples in atmospheric and vacuum conditions. The trend that was registered in vacuum conditions is more or less the same also in atmospheric conditions. The most important fact that can be highlighted is that the coefficient of friction in vacuum is always lower than at atmospheric pressure. The only lubricant that has almost the same behavior in air and in vacuum is **IL22** - $[(\text{H}_{13}\text{C}_6)_3\text{P}(\text{C}_{14}\text{H}_{29})]^+ [(\text{C}_1)_3\text{Si}(\text{C}_2\text{H}_4)\text{SO}_3]^-$. Also in atmospheric conditions, PFPE has the highest coefficient of friction, almost the double of the coefficient of friction registered in contact with the ionic liquids. The analysis of the wear scars shows that the performance of the lubricants is worst in atmospheric conditions (Figure 6. 8). For the ionic liquids **IL18-IL20** the wear increase is around the 25% going from vacuum conditions to atmospheric conditions. For the **IL21** - $[(\text{H}_9\text{C}_4)_3\text{P}(\text{C}_{16}\text{H}_{33})]^+ [(\text{C}_1)_3\text{Si}(\text{C}_3\text{H}_6)\text{SO}_3]^-$ the increase is quite higher, around the 65%. **IL22** - $[(\text{H}_{13}\text{C}_6)_3\text{P}(\text{C}_{14}\text{H}_{29})]^+ [(\text{C}_1)_3\text{Si}(\text{C}_2\text{H}_4)\text{SO}_3]^-$ has almost the same wear volume, the difference is of 1%. The biggest difference was found with **PFPE** that, in atmospheric conditions, has doubled the wear volume that was measure in vacuum.

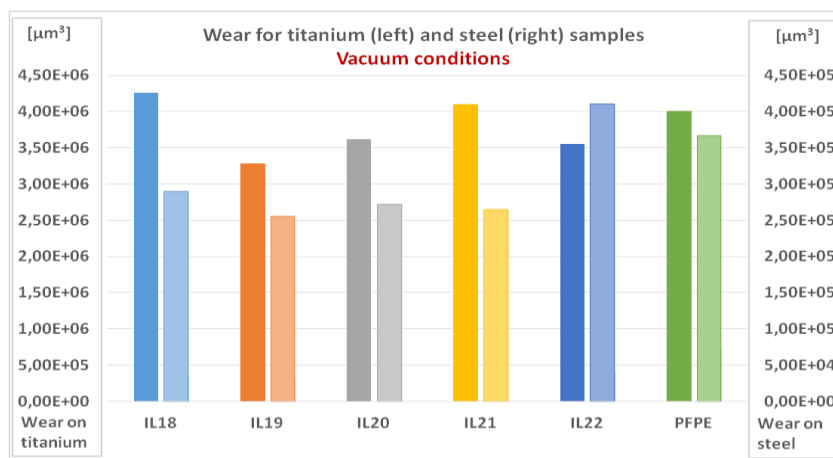


Figure 6. 6 - Measure of the wear volume on the scar of the flat samples in vacuum conditions. Two different scale were considered for titanium and steel samples, because of the large difference in wear volume.

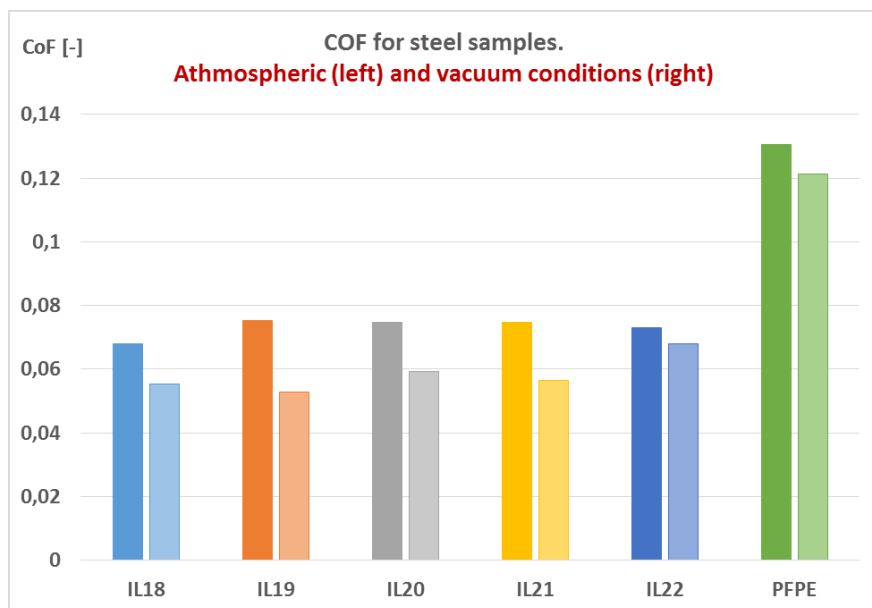


Figure 6. 7 - Comparison of the friction coefficient obtained on steel samples in atmospheric pressure (left column) and in vacuum (right column).

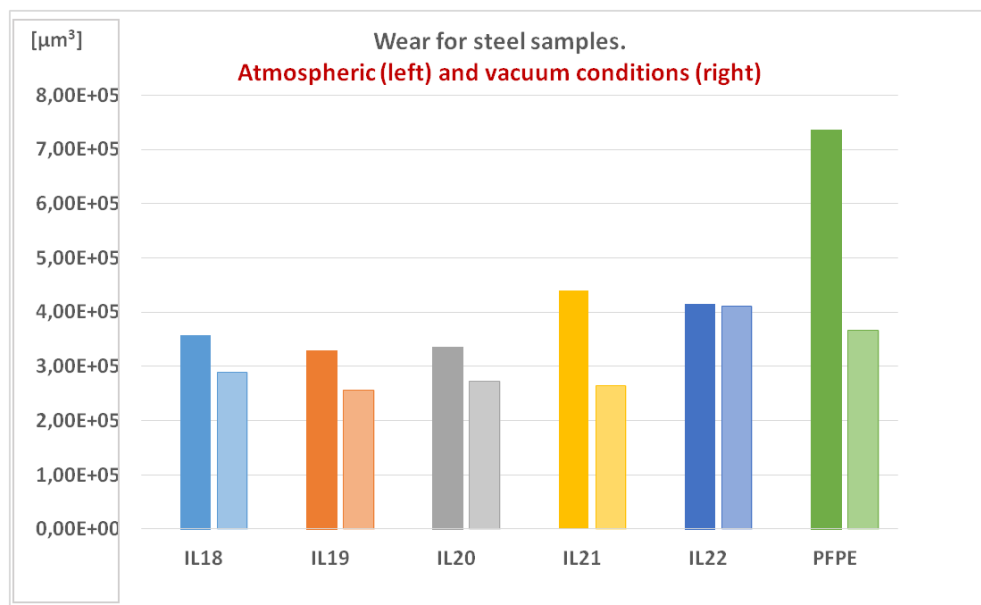


Figure 6. 8 - Comparison of the wear volume obtained on steel samples in atmospheric pressure (left column) and in vacuum (right column).

The comparison of the friction coefficient obtained on titanium samples at atmospheric pressure and in vacuum is reported in Figure 6. 9. In this case, the coefficient of friction measured with the ionic liquids in atmospheric conditions was slightly higher than in vacuum. Anyway, in the case of **IL19** - $[(\text{H}_9\text{C}_4)_3\text{P}(\text{C}_{16}\text{H}_{33})]^+ [(\text{C}_1)_3\text{Si}(\text{C}_2\text{H}_4)\text{SO}_3]^-$ and **IL21** - $[(\text{H}_9\text{C}_4)_3\text{P}(\text{C}_{16}\text{H}_{33})]^+ [(\text{C}_1)_3\text{Si}(\text{C}_3\text{H}_6)\text{SO}_3]^-$ the friction could be considered approximately the same. Also in the case of PFPE, the friction coefficient is approximately the same in the two conditions, but in this case, the value measured is a little bit higher in vacuum.

The differences between vacuum and atmospheric conditions are more evident analyzing the wear scars (Figure 6. 10). In the case of the ILs, the wear in atmospheric conditions is in the range between 40% and 80% higher than in vacuum conditions. The highest difference, approximately 80%, is obtained with **IL19** - $[(\text{H}_9\text{C}_4)_3\text{P}(\text{C}_{16}\text{H}_{33})]^+ [(\text{C}_1)_3\text{Si}(\text{C}_2\text{H}_4)\text{SO}_3]^-$, but this is due also to the fact that this IL has the lowest wear lubricating properties. The highest wear in atmospheric conditions was found with **IL21** - $[(\text{H}_9\text{C}_4)_3\text{P}(\text{C}_{16}\text{H}_{33})]^+ [(\text{C}_1)_3\text{Si}(\text{C}_3\text{H}_6)\text{SO}_3]^-$.

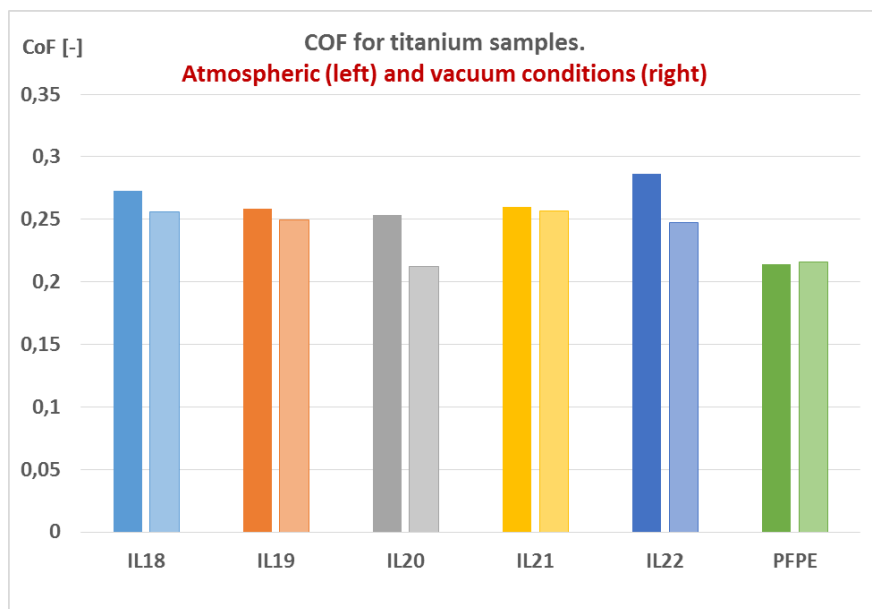


Figure 6. 9 - Comparison of the friction coefficient obtained on titanium samples at atmospheric pressure (left column) and in vacuum (right column).

The behavior of **PFPE** in atmospheric conditions was not so dissimilar from what was observed in vacuum. The difference in this case is of 23% and the wear in air was the lowest for the lubrication of titanium.

The wear volume on the titanium samples was calculated and the results are shown in Figure 6. 10.

During the tribotests, the emission of gasses in the chamber was checked by mass spectrometry. In Figure 6. 11 there is the trend of the normalized total counts of ions per second for the tests realized on titanium and steel with **IL18** - $[(H_9C_4)_3P(C_{12}H_{25})]^+ [(C_1)_3Si(C_2H_4)SO_3]^-$ and with PFPE. The counts include the sum of the counts recorded for all the mass/charge between 1 and 300. The number of counts/second that appears close to the curves represents the normalization factor. Since the variation of number of counts/seconds was big between the different curves it has been necessary to normalize the results. During the tribotests with the other ILs, the MS detected variation of the same masses.

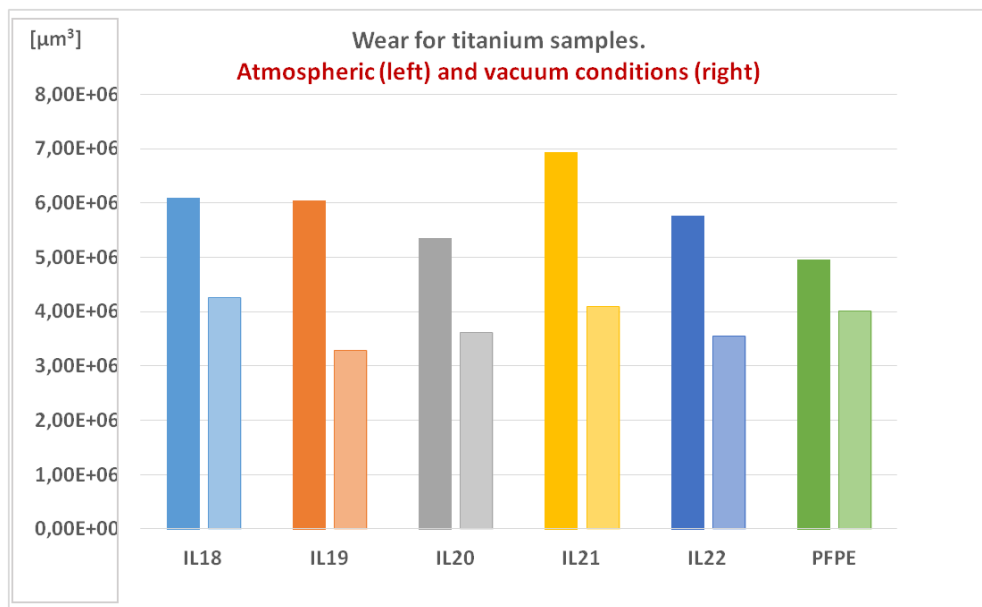


Figure 6. 10 - Comparison of the wear volume obtained on titanium samples at atmospheric pressure (left column) and in vacuum (right column).

Considering that the tribotests started 7 cycles after the beginning of the mass spectroscopy (each MS cycle has a duration of 30 seconds), it is evident that, with the ionic liquid, the sliding contact on the titanium surface has an influence on the tribodesorption of gasses. In the other cases, the behavior is almost unchanged. Only with PFPE and titanium, there is a light change in the emission of gasses at the beginning of the sliding.

For the **IL18** - $[(H_9C_4)_3P(C_{12}H_{25})]^+ [(C_1)_3Si(C_2H_4)SO_3]^-$, all the masses with mass to charge ratio (m/z) between 1 and 300 were analyzed and it was observed that that the variation of concentration was not the same for all the m/z but it was centered in specific intervals that have been listed in Table 6. 5.

*Table 6. 5 - Intervals and peaks of m/z in the MS analysis of the gasses desorbed during the tribotests with **IL18** - $[(H_9C_4)_3P(C_{12}H_{25})]^+ [(C_1)_3Si(C_2H_4)SO_3]^-$.*

Variation interval	Max peak
1-2	2
14-18	16
25-30	28
39-44	43
55-59	58
67-75	68 & 73
82-87	85
110-111	111
204	204

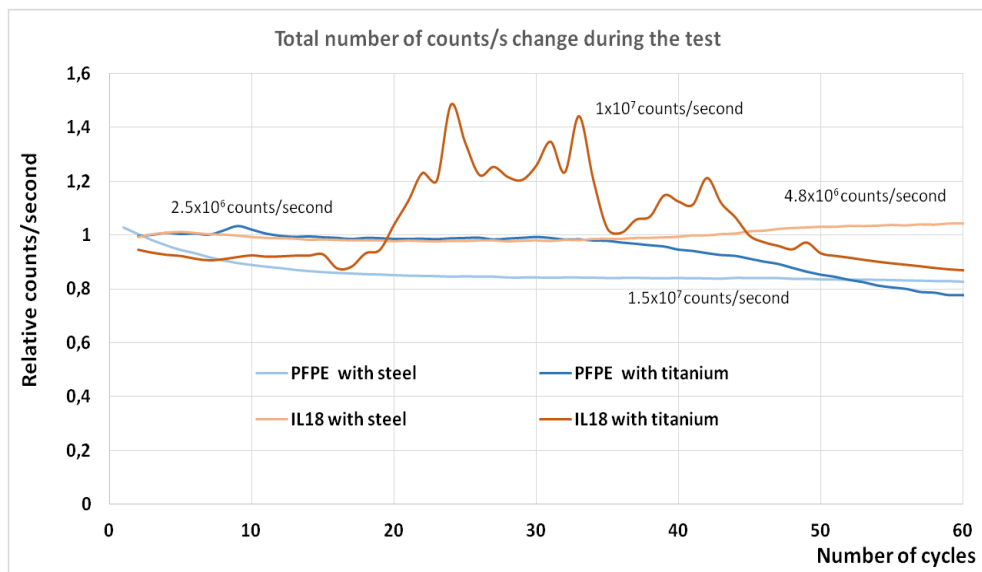


Figure 6. 11 - Relative desorbed gas counts/second recorded by mass spectra.

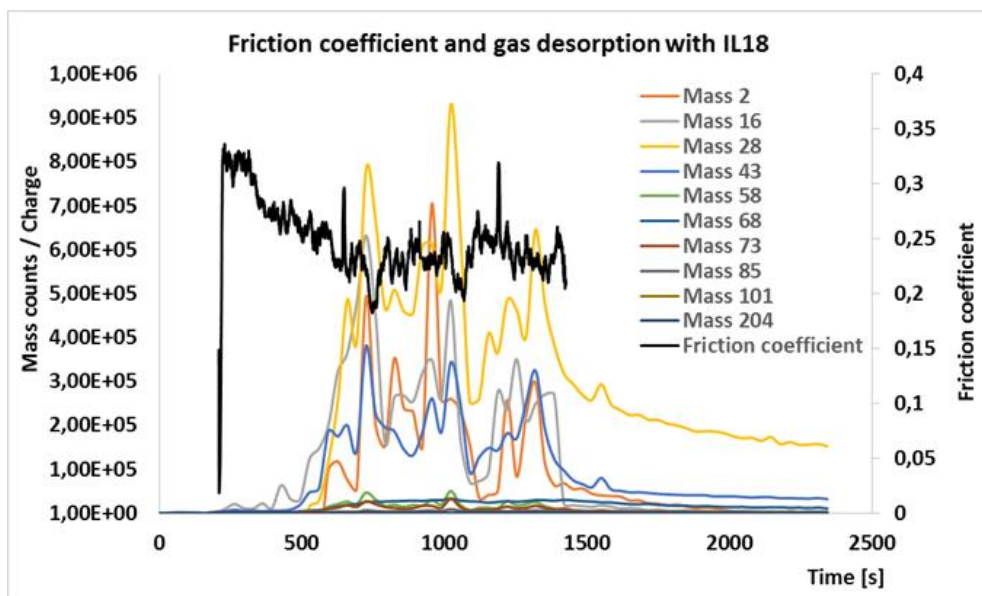


Figure 6. 12 Friction coefficient and analysis of the gasses desorbed during one of the tribotests realized with **IL18** - $[(H_9C_4)_3P(C_{12}H_{25})]^+ [(C_1)_3Si(C_2H_4)SO_3]^-$. The masses were normalized and the normalization factors are listed in the graph below each mass.

In Figure 6. 12 there are the curves representing the variation of gas concentration in the vacuum chamber during one of the tests with **IL18** - $[(H_9C_4)_3P(C_{12}H_{25})]^+ [(C_1)_3Si(C_2H_4)SO_3]^-$ lubricating the titanium surface. In the picture, were selected only the masses which concentration was changing during the test. The concentration of gasses with lower mass was much higher than the concentration of gasses with higher mass. For this reason, in order to give an insight to all the masses, normalization factors were included in the image just below the corresponding masses. In the same picture, it is also possible to see the friction coefficient during the test.

It seems that there is a time lag of almost 300 seconds between the beginning of the test and the significant release of gasses. In a similar period of time, it seems that there is a sort of running-in for the friction to decrease from 0.32 to 0.25. It seems that these two phenomena are correlated calling the induction period, to time slap until the gas desorption starts catalyzing the tribofilm generation that reduce the friction coefficient. Similar phenomena were already observed studying other lubricants and the results were presented during two international conferences [195,196].

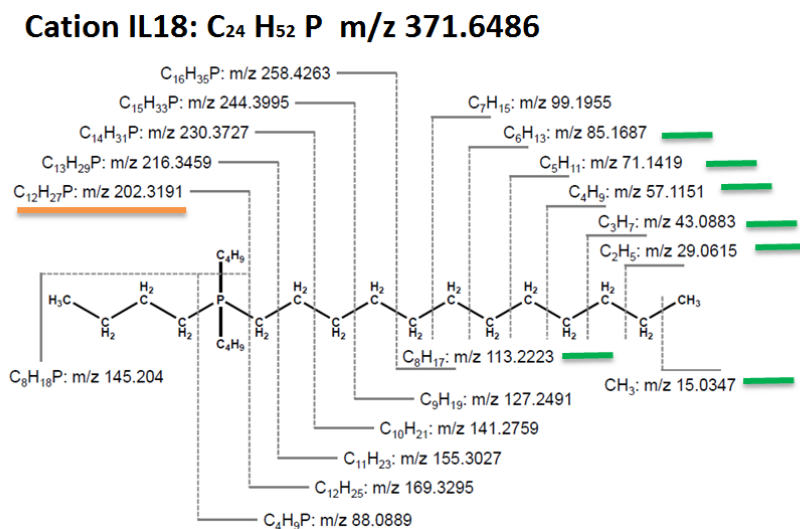


Figure 6. 13 - Analysis of the cationic fragments that could have been found by MS.

An analysis of the cation and of the anion can give the opportunity to identify the molecules were captured by MS. Figure 6. 13 shows the structure of the cation of the **IL18** - $[(H_9C_4)_3P(C_{12}H_{25})]^+ [(C_1)_3Si(C_2H_4)SO_3]^-$ and the fragments that could be separated from it. In the same way, Figure 6. 14 shows the anion and the possible fragments.

The signal obtained for m/z around 16 is very similar to the signal expected for the methane and could be due to the rupture of a methyl group CH_3 . Also many other groups of m/z can come from the rupture of the alkyl chain, but some of the variation intervals can also be caused by the degradation of the anion.

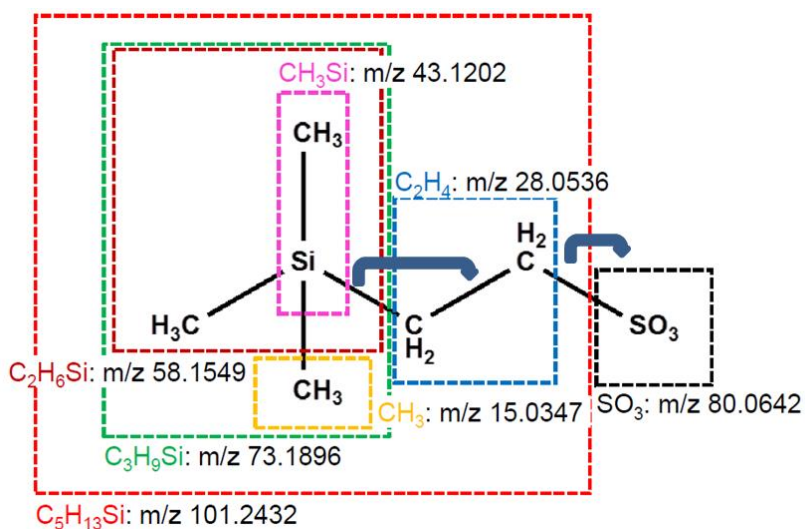


Figure 6. 14 - Analysis of the fragments of the anion that could have been found by MS

The m/z between 39 and 44 could be either CH_3Si or C_3H_7 . For m/z 58 there is the possibility that it is either C_2H_6Si or C_4H_9 . The interval between 67 and 75 has 2 peaks and the possible groups are C_3H_9Si and C_5H_{11} . Finally the mass of 204 there is the possibility that it is due to the phosphonium group $C_{12}H_{27}P$.

Considering the correlation between the friction reduction and the emission of molecules that comes from the degradation of the ions, it is possible to think that the

tribocontact catalyzed the reaction of the ionic liquid with the titanium surface, reducing the friction coefficient.

6.3.2 Surface analysis

After the tests, the surfaces were examined by SEM and the composition close to the surface was analyzed by EDS. Since the composition of the ionic liquids was quite similar and the main elements were the same, the analysis was realized only on the disc lubricated with **IL18** - $[(H_9C_4)_3P(C_{12}H_{25})]^+ [(C_1)_3Si(C_2H_4)SO_3]^-$ and **PFPE**. The results for the analysis on the steel samples are shown in Figure 6. 15.

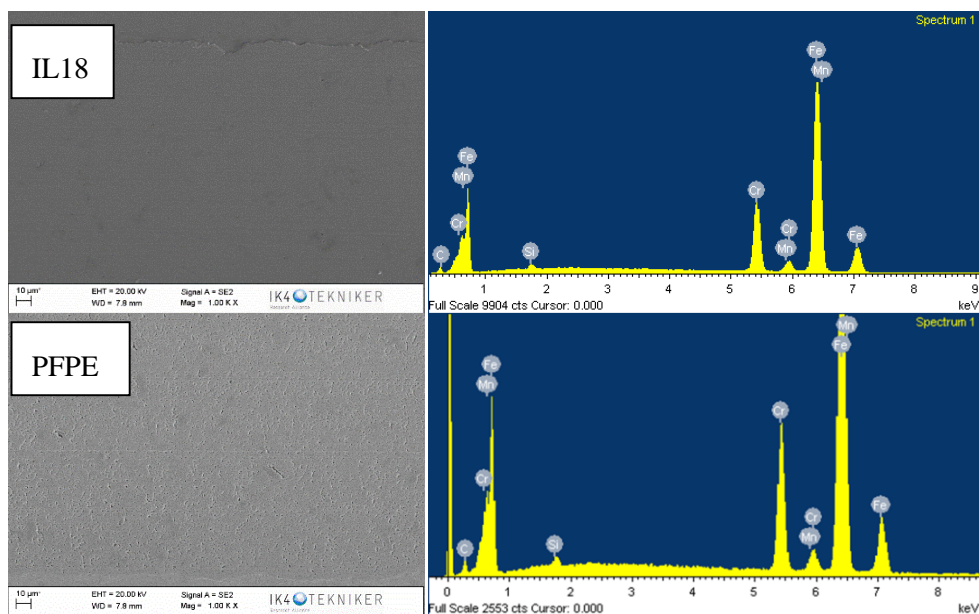


Figure 6. 15 - SEM/EDS analysis on the steel surface lubricated with **IL18** - $[(H_9C_4)_3P(C_{12}H_{25})]^+ [(C_1)_3Si(C_2H_4)SO_3]^-$ (on the top) and with PFPE (on the bottom).

The surface lubricated with ionic liquid is very smooth. There are no significant signs of abrasion or crack, which shows that the lubrication mechanism was quite effective and successful. The examination of the surface lubricated with PFPE instead shows many micro-pittings distributed all over the wear scar. Even though the dimension of the pits is quite small, it represents a sign of inadequate lubrication and of stress on the surface. Moreover, the presence of micropitting can be the first sign of fatigue

wear, which could lead to serious failures [12]. EDS did not show any significant trace of sulfur or phosphorous on the surface lubricated with **IL18** - $[(H_9C_4)_3P(C_{12}H_{25})]^+ [(C_1)_3Si(C_2H_4)SO_3]^-$ and no traces of fluorine on the disc lubricated with **PFPE**. The anion of the ILs contained also Si, which was found on the surface but, since it is present already in the composition of the stainless steel 440C, it cannot be said that it was due to the decomposition of the ionic liquid.

Table 6. 6 -Elements found by XPS on the steel specimen.

SS 440C		Steel – REF		Steel - MI		Steel - TP	
Element	Structure	BE (eV)	at%	BE (eV)	at%	BE (eV)	at%
Si	Sum						6.2
						97.8	2.5
	SiOX					101.8	3.8
S	Sum						1.9
	Sulfide					161.6	1.9
C	Sum		7.0		6.8		7.2
	Carbide	282.9	3.2	283.0	2.4	282.9	2.8
	C-C	284.9	3.8	284.7	4.4	284.9	4.4
	C-O/C-N	286.9	2.1	286.7	2.3		
O	Sum		55.3		56.7		52.6
	Metal oxide	530.1	36.2	530.2	37.2	530.2	32.9
	Org. Oxygen	531.3	19.1	531.4	19.5	531.4	19.7
Cr	Sum		10.8		9.6		9.4
	Cr met./carbide	574.1	2.3	574.1	2.1	574.1	1.7
	CrOX	576.3	8.5	576.4	7.5	576.4	7.7
Fe	Sum		24.8		24.6		22.8
	Fe met.	706.7	4.2	706.7	4.3	706.8	3.9
		707.7	4.0				
				708.7	9.5	708.8	9.4
	FeO	709.5	12.1				
				710.6	10.9	710.7	9.4
	FeOOH	711.6	4.6				

Like in the case of the SEM-EDS analysis, since the structure of the ionic liquids was quite similar, the XPS analysis was carried out only on the samples lubricated with **IL18** - $[(\text{H}_9\text{C}_4)_3\text{P}(\text{C}_{12}\text{H}_{25})]^+ [(\text{C}_1)_3\text{Si}(\text{C}_2\text{H}_4)\text{SO}_3]^-$.

As explained in the section 6.2.3 Surface analysis, 3 different points were considered: the part outside of the wear scar (REF), the center of the wear scar (MI) and the turning point (TP) at the extremity of the wear scar (where the sample start to move in opposite direction).

Table 6. 6 shows the results of the XPS analysis on the steel surface lubricated with **IL18** - $[(\text{H}_9\text{C}_4)_3\text{P}(\text{C}_{12}\text{H}_{25})]^+ [(\text{C}_1)_3\text{Si}(\text{C}_2\text{H}_4)\text{SO}_3]^-$. In the middle of the wear scar there was no presence of sulfur or silicon, but it was possible to find them on the turning point. Both silicon and sulfur are present in the composition of the steel but, since they did not appear in the middle of the scar or on the metallic surface outside of the wear scar, it is possible that what was detected was due to the triboreaction of the ionic liquid. The presence of this elements only on the turning point could be explained by the fact that in this area the working conditions are harsher than in the middle of the scar.

During reciprocating tests, the speed is maximum in the middle of the scar and decreases till zero in the turning point. The sulfur found was in its sulfidic binding state, which could mean that it was forming FeS_x or CrS_x . It was impossible to detect P, present in the cation, and this gives the idea that the tribolayer formation was due to the interaction of the surface with the anion more than with the cation.

Table 6. 7 shows the results of the XPS analysis realized on the titanium sample. There was no sign of elements as Si, S or P, which could have been an evidence of tribolayer formation. The only interesting sign was the increase in the concentration of carbon inside the wear scar, especially in the TP area.

Table 6. 7 - Elements found by XPS on the titanium specimen.

Ti grade 5		Ti – REF		Ti – MI		Ti – TP	
Element	Structure	BE (eV)	at%	BE (eV)	at%	BE (eV)	at%
Al	sum		9.2		7.1		7.2
	AlTi ₃	71.6	1.5	71.7	1.9	71.8	1.8
	Al ₂ O ₃	74.5	7.7	74.5	5.2	74.4	5.4
C	sum		2.0		8.7		14.5
	Carbide (TiC)	282.4	0.5	282.0	3.2	282.0	6.0
	C-C	285.2	1.5	285.2	5.4	285.2	8.5
Ti	sum		28.4		32.1		31.1
	Ti met			454.2	7.1	454.4	7.9
	TiC/TiO	455.3	10.1	455.3	9.2	455.4	8.7
	TiO ₂	458.4	18.3	458.0	15.8	458.0	14.6
O	sum		60.4		52.2		47.2
	Metal oxyde	530.9	39.9	531.0	38.8	530.9	31.8
		532.2	20.5	532.4	13.4	532.1	15.4
AlTi ₃	Aluminium titanium intermetallic alloy						

6.4 CONCLUSIONS

Five ionic liquids and PFPE as reference oil were studied as possible lubricants for vacuum applications in the CATRI © UHV Tribometer. The results obtained show that:

- The ionic liquids studied had lower friction coefficient than PFPE when they are used for lubricating steel surfaces. The friction coefficient observed is approximately half of the friction coefficient measured with the reference oil.
- None of the lubricants used in this study could form an effective tribo-layer with titanium samples.
- Due to the high reactivity of the titanium it was possible to see a considerable number of gas desorption picks in the mass spectra.

- XPS analysis showed that the ionic liquids lubricating steel surface forms an effective tribo-layer thanks to the interaction of the anion with the steel surface. The product of this reaction is probably FeS_x or CrS_x .
- Halogen free ionic liquids can lubricate in an efficient way steel under vacuum conditions but to lubricate titanium, it seems that it still necessary to use halogen-containing lubricants to reduce the friction in these lubricants.

With the titanium samples, the wear tracks of halogen free ionic liquids were on the same order of magnitude of halogen containing reference lubricant, but still too high to achieve enough surface protection.

Conclusions

7 Conclusions

In order to understand their potential in tribological applications, different classes of ionic liquids were studied, both as neat lubricants and as additives in base oil. The findings of this research are summarized below:

- The thermal analysis of the ILs synthesized in laboratory showed that dicationic ILs incorporating polyethylene glycol chains, present higher thermal stability than simple monocationic ILs. Among the anionic structures analyzed, bis(trifluoromethanesulfonyl)imide had better thermal stability.
- The dicationic ionic liquids showed better properties than the monocationic ones from a tribological point of view and they presented also higher thermal stability. Nonetheless, the more complex synthetic path could be an obstacle to the diffusion of these structures for tribological applications.
- The use of a mixture of two ionic liquids gave a better result than what was obtained with each one of them. This demonstrates the possibility to design combinations of ionic liquids for obtaining a synergistic effect.

- With the exception of a few structures, the ionic liquids have shown low coefficient of friction and low wear as neat lubricants for steel surfaces but some of them have shown problems related with corrosion, which is still one of the main problems related with the use of the ionic liquids.
- As additives, the ionic liquids showed promising properties. Structure containing bis(trifluoromethanesulfonyl)imide anions were able to generate an efficient tribolayer containing inorganic fluoride while with phosphate anions it was possible to observe the presence of phosphorous bond with Fe(III) inside the wear scar and bonded with Fe(II) outside of the wear scar. Very low concentrations of ionic liquid (0.25% for **IL16** - $[(\text{H}_9\text{C}_4)_3\text{P}(\text{CH}_3)]^+ [(\text{C}_1)_2\text{PO}_4]^-$) were enough to guarantee a very good performance in extreme pressure conditions.
- In addition to TGA tests, the thermal degradation of the ionic liquids should be studied for long-term period and it is also very important to analyze the reaction of the by-products with the surfaces in contact, since corrosion can be caused in some cases (as for example in the case of **IL17** - $[\text{P}(\text{C}_4\text{H}_9)_4]^+ [(\text{C}_2)_2\text{PO}_2\text{S}_2]^-$).
- Vacuum tests demonstrated a good performance of some halogen free ionic liquids for steel lubrication, but quite poor performance when they were lubricating titanium. The decomposition and tribolayer formation of the ionic liquid during the tribotests was discussed thanks to mass spectrometry during the tests and XPS analysis.
- It is likely that the rather high price in comparison with common base lubricants, excludes the possibility to use them in the neat state for normal applications. However their use could still be appreciated in vacuum since they showed better performance than PFPE, and they could be used as additives since can reduce friction and wear of the base oils.

Bibliography

Bibliography

- [1] Global energy consumption due to friction in passenger cars. K. Holmberg, P. Andersson, A. Erdemir. 2012, *Tribology International*, 47, pp 221-234.
- [2] Global energy consumption due to friction in trucks and buses. K. Holmberg, P. Andersson, N. O. Nylund, K. Mäkelä, A. Erdemir. 2014, *Tribology International*, 78, pp 94-114.
- [3] Global energy consumption due to friction in paper machines. K. Holmberg, R. Siilasto, T. Laitinen, P. Andersson, A. Jäsberg. 2013, *Tribology International*, 62, pp 58-77.
- [4] Interview with Luminary Professor H. Peter Jost - The Man who Gave Birth to the Word "Tribology". Fitch, J. 2006, *Machinery Lubrication*.
- [5] Tribology - Origin and future. Jost, P. H. 1990, *Wear*, 136 (1), pp 1-17.
- [6] De la resistance causée dans les Machines, tant par les frottemens des parties qui les composent, que par roideur des cordes qu'on y employe, & la maniere de calculer l'un & l'autre. Amontons, G. 1699, *Histoire de l'Académie royale des sciences*, pp 206-222.
- [7] D. Dowson, B. J. Hamrock. *History of Ball Bearings*. s.l.: NASA, 1981.
- [8] Kugellager für beliebige Belastungen. R. Stribeck, s.l.: *Zeitschrift des Vereines deutscher Ingenieure*, 1901, *Zeitschrift des Vereines deutscher Ingenieure*, 45 (3), pp 73-79.
- [9] Die wesentlichen Eigenschaften der Gleit- und Rollenlager (pt I, pt II, pt III). R. Stribeck, 1902, *Zeitschrift des Vereines deutscher Ingenieure*, 46, pp 1341-1348, 1432-1438, 1463-1470.
- [10] M.Theo. *Lubricants in the Tribological System*. Wilfried Dresel Theo Mang. *Lubricants and Lubrication*. Weinheim: WILEY-VCH Verlag GmbH & Co. KGaA, 2007, pp 7-22.
- [11] A Study of Oxidation Phenomena in Corrosive Wear. F. F. Tao, 1969, *ASLE Transactions*, 12, pp 97-105.
- [12] G. W. Stachowiak, A. W. Batchelor. *Engineering Tribology*. s.l.: Butterworth-Heinemann, 2001.

- [13] Abrasive, erosive and cavitation wear. Andrew W. Batchelor Gwidon W. Stachowiak. Engineering tribology. s.l.: Butterworth-Heinemann, 2001, pp 483-532.
- [14] H. Czichos, K. H. Habig. Tribologie Handbuch. Wiesbaden: Vieweg, 1992.
- [15] On the Theory of Lubrication and its Application to Mr Beauchamp Tower's Experiments Including an Experimental Determination of the Viscosity of Olive Oil. Reynolds, O. 1886, Phil. Trans., Roy. Soc. London, 177, pp 157-234.
- [16] EFSA, European Food Safety Authority. Scientific Opinion on Mineral Oil Hydrocarbons in Food. Parma: EFSA Journal 2012, 2012, 10.
- [17] Vegetable oil-based lubricants—A review of oxidation. N.J. Fox, G.W. Stachowiak. 2007, Tribology International, 40, pp 1035–1046.
- [18] G. Spengler, F. Wunsch. Schmierung und Lagerung in der Feinwerktechnik. Dusseldorf: VDI, 1970.
- [19] Lansdown, A. R. Lubrication and Lubricant Selection. London: Mechanical Engineering Publications, 1996.
- [20] Miyoshi, Kazuhisa. Solid Lubricants and Coatings for Extreme Environments: State-of-the-Art Survey. Cleveland: NASA, 2007.
- [21] Solid lubricant materials for high temperatures—a review. Sliney, H.E. 1982, Tribology International, 15, pp 303-315.
- [22] A. Erdemir, Solid Lubricants and Self-Lubricating Films. Ali Erdemir. Modern Tribology Handbook. s.l.: CRC Press, 2000.
- [23] P. J. John, J. S. Zabinski, Sulfate based coatings for use as high temperature lubricants. 1999, Tribology Letters, 7, pp 31-37.
- [24] H. E. Sliney, Rare Earth Fluorides and Oxides – An Exploratory Study of Their Use as Solid Lubricant at Temperatures to 1800 °F (1000 °C). Cleveland: NASA TN D-5301, 1969
- [25] A. Erdemir, Lubrication from mixture of boric acid with oils and greases. 5431830 US Patent, 1992.
- [26] Boron nitride as a lubricant additive. Yoshitsugu Kimura, Toshiaki Wakabayashi, Kazumi Okada, Tetsuya Wada, Hiroshi Nishikawa. 1999, Wear, pp 199-206.
- [27] A. Wells, D. J. De Wet, The use of platinum in thin tribological coatings. 1988, Wear, 127, 269-281.
- [28] M. A. Sherbiny, J. Halling, Friction and wear of ion-plated soft metallic films. 1977, Wear, 45, pp 211-220.
- [29] H. Hesmat, The Effect of Slider Geometry on the Performance of a Powder Lubricated Bearing — Theoretical Considerations. 2000, Tribology Transactions, 43, pp 213-220.

- [30] C. F. Higgs, C. A. Hesmat, H. Hesmat, Comparative Evaluation of MoS₂ and WS₂ as Powder Lubricants in High Speed, Multi-Pad Journal Bearings. 1999, *Journal of Tribology*, 121, pp 625-630.
- [31] R. M. Gresham, Bonded solid lubricants. E. R. Booser, *CRC Handbook of lubrication: theory and practice of tribology*, Vol. III. 1997, CRC Press, Boca Raton
- [32] P. A. Asseff, Lubricant. 2261047 US Patent, 1941.
- [33] E.W. Cook, W.D. Thomas, Jr., Crankcase lubricant and chemical compound therefor. 2344392 US Patent, 1944.
- [34] H. C. Freuler, Modified lubricating oil. 2364284 US Patent, 1944.
- [35] H. C. Freuler, Modified lubricating oil. 2364283 US Patent, 1944.
- [36] E.W. Cook, W.D. Thomas, Jr. Lubricating oils. 2369632 US Patent, 1945.
- [37] I. M. Hutchings, *Tribology: friction and wear of engineering materials*. London: CRC Press, 1992.
- [38] Review of the lubrication of metallic surfaces by zinc dialkyl-dithiophosphates. M. A. Nicholls, T. Do, P. R. Norton, M. Kasrai , G.M. Bancroft. 2005, *Tribology International* Volume 38, Issue 1, pp. 15-39.
- [39] Mechanism of tribochemical film formation: stability of tribo- and thermally-generated ZDDP films. G.M. Bancroft, M. Kasrai, M. Fuller, Z. Yin, K. Fyfe, K.H. Tan. 1997, *Tribology Letters*, 3, pp 47-51.
- [40] Application of soft X-ray absorption spectroscopy in chemical characterization of antiwear films generated by ZDDP Part I: the effects of physical parameters. Z. Yin, M. Kasrai, M. Fuller, G.M. Bancroft, K. Fyfe, K.H. Tan. 1997, *Wear*, 202, pp 172-191.
- [41] Friction-induced amorphization with ZDDP—an EXAFS study. J.M. Martin, M. Belin, J.L. Mansot, H. Dexpert, P. Lagarde. 1986, *ASLE Transactions*, 29 (4), pp 523-531.
- [42] Morphology and nanomechanical properties of ZDDP antiwear films as a function of tribological contact time. M. Aktary, M.T. McDermott, G.A. McAlpine. 2002, *Tribol Lett*, 12 (3), pp 155-162.
- [43] Formation mechanism of a low friction ZDDP tribofilm on iron oxide. K. Ito, J.M. Martin, C. Minfray, K. Kato. 2007, *Tribol Trans*, 50 (2), pp 211-216.
- [44] The correlation between ZDDP tribofilm morphology and the microstructure of steel. J. Jelita Rydela, K. Pagkalisb, A. Kadiricb, P.E.J. Rivera-Díaz-del-Castillo. 2016, *Tribology International*, pág. In press.
- [45] H. M. Ghose, J. Ferrate, F. C. Honey. *The Effect of Tricresyl-Phosphate (TCP) as an Additive on Wear of Iron (Fe)*. Cleveland, Ohio: NASA, 1987.
- [46] Crystal structures of imidazolium bis(trifluoromethanesulfonyl)imide ‘ionic liquid’ salts: the first organic salt with a cis-TFSI anion conformation. J. D. Holbrey, W. M. Reichert, R. D. Rogers. 2004, *Dalton Transactions*, pp 2267-2271.

- [47] Direct fluorination of bis(trifluoromethanesulfonyl)imide and its lithium salt and related studies. R. E. Banks, V. Murtagh, H. M. Marsden, R. G. Syvret. 2001, *Journal of fluorine chemistry*, 112, pp 271-275.
- [48] Carboranes: A New Class of Weakly Coordinating Anions for Strong Electrophiles, Oxidants, and Superacids. Reed, C. A. 1998, *Accounts of Chemical Research*, 31, pp 133-139.
- [49] Weakly Coordinating Anions, and the Exceptional Conductivity of Their Nonaqueous Solutions. W. Xu, C. A. Angell. 2001, *Electrochemical and Solid-State Letters*, 4.
- [50] P. Wasserscheid, T. Welton. *Ionic Liquids in Synthesis*. Weinheim, Germany: Wiley-VCH, 2003.
- [51] Ionic liquid crystals: hexafluorophosphate salts. C. M. Gordon, J. D. Holbrey, A. R. Kennedy, K. R. Seddon: "Ionic liquid crystals: hexafluorophosphate salts". (1998) *J. Mater. Chem.*, 8, 2627-2636. 1998, *J. Mater. Chem.*, 8, pp 2627-2636.
- [52] The phase behaviour of 1-alkyl-3-methylimidazolium tetrafluoroborates: ionic liquids and ionic liquid crystals. J.D. Holbrey, K. R. Seddon. 1999, *J. Chem. Soc.*, pp 2133-2139.
- [53] Influence of chloride, water, and organic solvents on the physical properties of ionic liquids. Seddon, K.R., Stark, A. and Torres, M.-J. 2000, *Pure Appl. Chem.*, pp 2275-2287.
- [54] *Ionic Liquids*. J.D. Holbrey, K.R. Seddon. New York: Springer-Verlag, 1999, *Clean Products and Processes*, 1, pp 223-236.
- [55] C. Friedel, J.M. Crafts). 1877, *Compt. Rend.*, 84, pp 1392, 1450.
- [56] Room temperature ionic liquids: Solvents for synthesis and catalysis. H. J. Wilkins, S. Sugden. 1929, *Chem. Soc.*, pp 1291-1298.
- [57] N. Nambu, N. Hiraoka, K. Shigemura, S. Hamanaka, M. Ogawa. 1976, *Bull. Chem Soc. Jpn.*, 49, pág. 3637.
- [58] Ueber einige Abkömmlinge des Propylamins. S. Gabriel, J. Weiner. 1888, *J. Chem. Ber.*, 21, pp 2669-2679.
- [59] Walden, P. 1914, *Bull. Acad. Imper. Sci.*, pág. 1800.
- [60] Graenacher, C. *Manufacture and Application of New Cellulose Solutions and Cellulose Derivatives Produced therefrom*. 19433176 US, 1934.
- [61] Hurley, F.H. *Electrodeposition of aluminium*. 4446331 US, 1948.
- [62] *The Electrodeposition of Aluminum from Nonaqueous solution at Room Temperature*. F. H. Hurley, T. P. Wier. 1951, *J. Electrochem. Soc*, 98, pág. 207.
- [63] Thermodynamic activity of reciprocal molten salt systems. H. Bloom, B.J. Welch. 1961, *Discuss. Faraday Soc*, 32, pp 115-121.
- [64] Reactions of Triethylamine with Copper(I) and Copper(II) Halides. J. T. Yoke, J. F. Weiss, G. Tollin. 1963, 2, *Inorg. Chem.*, pp 1210-1212.
- [65] B. E. Conway, J. O'M. Bockris. *Modern Aspects of Electrochemistry*. London: Butterworths, 1973.

- [66] Electrochemical scrutiny of organometallic iron complexes and hexamethylbenzene in a room temperature molten salt. H. L. Chum, V. R. Koch, L. L. Miller, R. A. Osteryoung. s.l. : J. Am. Chem. Soc., 97, 1975, J. Am. Chem. Soc., 97, pp 3264-3265.
- [67] The activity and stability of alkaline phosphatase in solutions of water and the fused salt ethylammonium nitrate. D. K. Magnuson, J. W. Bodley, D. F. Evans. 1984, Journal of Solution Chemistry, 13, pp 583-587.
- [68] Air and water stable 1-ethyl-3-methylimidazolium based ionic liquids. J. S. Wilkes, M. J. Zaworotko. 1992, J. Chem. Soc., Chem. Commun., pp 965-967.
- [69] Applications of ionic liquids in the chemical industry. N. V. Plechkova, K. R. Seddon. 2008, Chem. Soc. Rev., 37, pp 123-150.
- [70] The distillation and volatility of ionic liquids. M. J. Earle, J. M. S. S. Esperanca, M. A. Gilea, J. N. C. Lopes, L. P. N. Rebelo, J. W. Magee, K. R. Seddon, J. A. Widegren. 2006, Nature, 439, pp 831-834.
- [71] Chemistry: Volatile times for ionic liquids. Wasserscheid, P. 2006, Nature, 439, pág. 797.
- [72] Structural analysis of low melting organic salts: perspectives on ionic liquids. P. M. Dean, J. M. Pringle, D. R. MacFarlane. 2010, Physical Chemistry Chemical Physics, 12, pp 9144-9153.
- [73] Thermal properties of imidazolium ionic liquids. H. L. Ngo, K. LeCompte, L. Hargens, A. B. McEwen. (2000), 97-102. 2000, Thermochemica Acta, 357-358, pp 97-102.
- [74] Thermal stability of low temperature ionic liquids revisited. M. Kosmulski, J. Gustafsson, J. B. Rosenholm. 2004, Thermochemica Acta, 412, pp 47-53.
- [75] Ionic liquids: Physico-chemical, solvent properties and their applications in chemical processes. G. Singh, A. Kumar. 2008, Indian J. of Chem., 47A, pp 495-503.
- [76] Density and viscosity of several pure and water-saturated ionic liquids. J. Jacquemin, P. Husson, A. A. H. Padua, V. Majer. 2006, Green Chem., 8, pp 172-180.
- [77] Temperature dependence of viscosity for room temperature ionic liquids. O. O. Okoturo, T. J. Vander Noot. 2004, Journal of Electro analytical Chemistry, 568, pp 167-181.
- [78] Ionic liquids as lubricants or lubrication additives: An ecotoxicity and biodegradability assessment. S. Stolte, S. Steudte, O. Areitioaurtena, F. Pagano, J. Thöming, P. Stepnowski, A. Igartua. 2012, Chemosphere, 89, pp 1135-1141.
- [79] Assessing the factors responsible for ionic liquid toxicity to aquatic organisms via quantitative structure-property relationship modelling. D. J. Couling, R. J. Bernot, K. M. Docherty, J. K. Dixon, E. J. Maginn. 2006, Green Chem., 8, pp 82-90.

- [80] Preparation and characterization of some ionic liquids and their use in dimerization reaction of 2-methylpropene. Karkkainen, J. 2007, Oulu University Press.
- [81] Room-temperature ionic liquids: a novel versatile lubricant. C. Ye, W. Liu, Y. Chen. 2001, *Chemical Communications*, pp 2244-2245. DOI:10.1039/B106935G.
- [82] Ionic Liquids as Alternative Lubricants for Special Applications. T. Predel, B. Pohrer, E. Schlücker. 2010, *Chemical Engineering & Technology*, 33, pp 132–136.
- [83] A Review of Ionic Liquid Lubricants. A. E. Somers, P. C. Howlett, D. R. MacFarlane, M. Forsyth. 3-21, s.l.: *Lubricants*, 2013, Vol. 1. DOI:10.3390/lubricants1010003.
- [84] Film Thickness of Ionic Liquids Under High Contact Pressures as a Function of Alkyl Chain Length. H. Xiao, D. Guo, S. Liu, G. Pan, X. Lu. 2011, *Tribology Letters*, 41, pp 471-477.
- [85] Ionic liquids in tribology. Minami, I. 2286-2305, s.l.: *Molecules* 2009, 2009.
- [86] Effects of Carboxylic Acids on Wear and Friction Reducing Properties for Alkylimidazolium-derived Ionic Liquids. H. Kamimura, T. Chiba, N. Watanabe, T. Kubo, H. Nanao, I. Minami, S. Mori. 2006, *Tribology Online*, 1, pp 40-43.
- [87] Effect and mechanism of additives for ionic liquids as new lubricants. H. Kamimura, T. Kubo, I. Minami, S. Mori. 2007, *Tribology International*, 40, pp 620–625.
- [88] F. P. Bowden, D. Tabor. *The Friction and Lubrication of Solids*. Oxford: Oxford University Press, 2001. pp 200-227.
- [89] Oil-miscible and non-corrosive phosphonium-based ionic liquids as candidate lubricant additives. B. Yu, D. G. Bansal, J. Q. X. Sun, H. Luo, S. Dai, P. J. Blau, B. G. Bunting, G. Mordukhovich, D. J. Smolenski. 58-64, s.l.: *Wear*, 2012, Vol. 289.
- [90] Tribo-Chemistry of Phosphonium-Derived Ionic Liquids. I. Minami, T. Inada, R. Sasaki, H. Nanao. 2010, *Tribol Lettters*, 40, pp 225-235.
- [91] Ionic Liquids Composed of Phosphonium Cations and Organophosphate, Carboxylate, and Sulfonate Anions as Lubricant Antiwear Additives. Y. Zhou, J. Dyck, T. Graham, H. Luo, D. Leonard, J. Qu. 2014, *Langmuir*, 30, pp 13301–13311.
- [92] Phosphonium-Organophosphate Ionic Liquids as Lubricant Additives: Effects of Cation Structure on Physicochemical and Tribological Characteristics. W. C. Barnhill, J. Qu, H. Luo, H. Meyer, C. Ma, M. Chi, B. L. Papke. 2014, *ACS Applied Materials & Interfaces*, 6, pp 22585–22593.
- [93] 1-N-alkyl -3-methylimidazolium ionic liquids as neat lubricants and lubricant additives in steel–aluminium contacts. A. E. Jimenez, M. D.

- Bermudez, P. Iglesias, F. J. Carrion, G. Martinez-Nicolas. 2006, *Wear* 260, pp 766–782.
- [94] Fluidos Iónicos en Lubricación de Contactos Aluminio-Acero. Interacciones Superficiales y Triboquímicas. Jimenez, A. E. [ed.] Universidad de Cartagena. 2007.
- [95] Room temperature ionic liquids as lubricant additives in steel–aluminium contacts: Influence of sliding velocity, normal load and temperature. A. E. Jiménez, M. D. Bermúdez, F. J. Carrión, G. Martínez-Nicolás. 2006, *Wear*, 261, pp 347-359.
- [96] Ionic liquids as lubricants for steel–aluminum contacts at low and elevated temperatures. A. E. Jiménez, M. D. Bermúdez. 2007, *Tribology Letters*, 26, pp 53-60.
- [97] Ionic liquid lubrication effects on ceramics in a water environment. B. S. Phillips, J. S. Zabinski. 2004, *Tribology Letters*, 17, pp 533–541.
- [98] The Effect of the Electric Double Layer on a Very Thin Water Lubricating Film. P. Wong, P. Huang, Y. Meng. 2003, *Tribology Letters*, 14, pp 197-203.
- [99] Formation of tribochemical layer of ceramics sliding in water and its role for low friction. J. Xu, K. Kato. 2000, *Wear*, 245, pp 61-75.
- [100] Lubricant film formation properties of alkylimidazolium tetrafluoroborate and hexafluorophosphate ionic. H. Arora, P. M. Cann. 2010, *Tribology International*, 43, pp 1908–1916.
- [101] Hydrolysis of tetrafluoroborate and hexafluorophosphate counter ions in imidazolium-based ionic liquids. M. G. Freire, C. M. S. S. Neves, I. M. Marrucho, J. A. P. Coutinho, A. M. Fernandes. 2009, *Journal of Phys Chem A*, 114, pp 3744–3749.
- [102] Friction, wear and tribofilm formation with a [NTf₂] anion-based ionic liquid as neat lubricant. A. Hernández Battez, D. Blanco, A. Fernández-González, M. T. Mallada, R. González, J. L. Viesca. 2016, *Tribology International*, 103, pp 73–86.
- [103] FAP₂ Anion Ionic Liquids Used in the Lubrication of a Steel–Steel Contact. J. L. Viesca, A. García, A. Hernández Battez, R. González, R. Monge, A. Fernández-González, M. Hadfield. 2013, *Tribol Lett*, 52, pp 431-437.
- [104] The Tribological Properties of Ionic Liquids Composed of Trifluorotris(pentafluoroethyl) Phosphate as a Hydrophobic Anion. I. Minami, M. Kita, T. Kubo, H. Nanao, S. Mori. 2008, *Tribology Letters*, 30, pp 215-223.
- [105] Thermo-oxidative stability of ionic liquids as lubricating fluids. I. Minami, H. Kamimura, S. Mori. 2007, *Journal of Synthetic Lubrication*, 24, pp 135–147.

- [106] Tribological Characteristics of Alkylimidazolium Diethyl Phosphates Ionic Liquids as Lubricants for Steel–Steel Contact. L. Zhang, D. Feng, B. Xu. 2009, *Tribology Letters*, 34, pp 95–101.
- [107] Halogen-free borate ionic liquids as novel lubricants for tribological applications. V. Totolin, I. Minami, C. Gabler, N. Dörr.
- [108] Tribological properties of halogen-free ionic liquids. I. Minami, T. Inada, Y. Okada. 2012, *Proceedings of the Institution of Mechanical Engineers, Part J: Journal of Engineering Tribology*, 226, pp 891 - 902.
- [109] Liquid imidazole–borane complex. N. Matsumi, A. Mori, K. Sakamoto, H. Ohno. 2005, *Chemical Communications*, 36, pp 4557–4559.
- [110] Pyridinium based dicationic ionic liquids as base lubricants or lubricant additives. M. Mahrova, F. Pagano, V. Pejakovic, Emilia Tojo, Angel Valea, Mitjan Kalin, Amaya Igartua. 2015, *Tribology International*, 82, pp 245-254.
- [111] Mahrova, M. PhD Thesis: Diseño y síntesis de nuevos Líquidos Iónicos como potenciales lubricantes. Vigo: Universidad de Vigo, 2013.
- [112] Molecular design of advanced lubricant base fluids: hydrocarbon-mimicking ionic liquids. E. Nyberg, C. Y. Respatiningsih, Ichiro Minami. s.l.: RSC Advances, 7, 2017, pp 6364-6373.
- [113] CETR-UMT-3 Multi-specimen Test System - Software operating manual.
- [114] Pejakovic, V. Doctoral thesis: Effect of Ionic Liquids on the Boundary Lubrication of Steel Surfaces. s.l.: University of Ljubljana, 2016.
- [115] Ultrahigh vacuum system for advanced tribology studies: Design principles and applications. R.A. Nevshupa, M. Conte, A. Igartua, E. Roman, J.L. de Segovia. 28-35, s.l.: *Tribology International* 2015, 2015, Vol. 86.
- [116] R. Nevshupa, M. Conte, A. Delgado, A. Igartua, F. Egaña, A. Aranzabe. Force measuring device. 8789430 US, 29 de December de 2009.
- [117] Ultrahigh Vacuum System for advanced Tribology studies: “Design principles and applications”. A. Nevshupa, M. Conte, A. Igartua, E. Roman, J. L. Segovia. 2015, *Tribology International*, 86, pp 28-36.
- [118] Standard ASTM D6425-11. Standard Test Method for Measuring Friction and Wear Properties of Extreme Pressure (EP) Lubricating Oils Using SRV Test Machine. 2011.
- [119] Standard DIN 51834-2. Prüfung von Schmierstoffen - Tribologische Prüfung im translatorischen Oszillations-Prüfgerät - Teil 2: Bestimmung von Reibungs- und Verschleißmessgrößen für Schmieröle. 2010-11.
- [120] G. W. Stachowiak, A. W. Batchelor. *Engineering tribology*. Boston: Butterworth-Heinemann, 2005.
- [121] Improved technique for measuring the ball volume removed in a ball-on-disk test. S. J. Harris, G. G. Krauss. 3, s.l.: *Tribology Letters*, 2001, Vol. 10.

- [122] Tribological characterisation and surface analysis of diesel lubricated sliding contacts. von H. Hunger, U. Litzow, S. Genze, N. Dörr, D. Karner, C. Eisenmenger-Sittner. Ostfildern, Germany: Proceedings of TAE, 2008. ISBN: 3-924813-73-6.
- [123] A Review of Ionic Liquids for Green Molecular Lubrication in Nanotechnology. M. Palacio and B. Bhushan, 2010, 40, 247. 2010, Tribology Letters, 40, pp 247–268.
- [124] Research on liquid lubricants for space mechanisms. W. R. Jones Jr, B. Shogrin, M. Jansen. 2000, Journal of Synthetic Lubrication, 17, pp 109-122.
- [125] Polyethylene glycol functionalized dicationic ionic liquids with alkyl or polyfluoroalkyl substituents as high temperature lubricants. C. Jin, C. Ye, B. Phillips, J. Zabinski, X. Liu, W. Liu, J. M. Shreeve. 2006, Journal of Materials Chemistry, 16, pág. 1529.
- [126] Structure and properties of high stability geminal dicationic ionic liquids. J. Anderson, R. Ding, A. Ellern, D. Armstrong. 2005, Journal of the American Chemical Society, 127, pp 593-604.
- [127] Toxicity and biodegradability of dicationic ionic liquids. S. Steudte, S. Bemowsky, M. Mahrova, U. Bottin-Weber, E. Tojo-Suarez, P. Stepnowski, S. Stolte. 2014, RSC Advances, 4, pp 5198-5205.
- [128] High-Temperature Tribological Properties of 2-Substituted Imidazolium Ionic Liquids for Si 3 N 4-Steel Contacts. M. Yao, Y. Liang, Y. Xia, F. Zhou, X. Liu. 2008, Tribology Letters, 32, pp 73-79.
- [129] Polyfluoroalkyl, Polyethylene Glycol, 1,4-Bismethylenebenzene, or 1,4-Bismethylene-2,3,5,6-Tetrafluorobenzene Bridged Functionalized Dicationic Ionic Liquids: Synthesis and Properties as High Temperature Lubricants. Z. Zeng, B. S. Phillips, J.Chang Xiao, J. M. Shreeve. 2008, Chemistry of Materials, 20, pp 2719-2726.
- [130] Dicationic ionic liquids as lubricants. F. Pagano, C. Gabler, P. Zare, M. Mahrova, N. Dörr, R. Bayon, X. Fernandez, W. H. Binder, M. Hernaiz, E. Tojo, A. Igartua. s.l.: Proceedings of the Institution of Mechanical Engineers, Part J: Journal of Engineering Tribology, 2012, Vol. 226.
- [131] The design and synthesis of biodegradable pyridinium ionic liquids. J. R. Harjani, R. D. Singer, M. T. Garcia, P. J. Scammells. 2008, Green Chemistry, 10, pp 436-438.
- [132] Biodegradable pyridinium ionic liquids: design, synthesis and evaluation. J. R. Harjani, R. D. Singer, M. T. Garcia, P. J. Scammells. 2009, Green Chemistry, 11, pp 83-90.
- [133] Pyrrolidinium sulfate and ammonium sulfate ionic liquids as lubricant additives for steel/steel contact lubrication. V. Pejaković, M. Kronberger, M. Mahrova, M. Vilas, E. Tojo, M. Kalin. 2012, Proceedings of the Institution of Mechanical Engineers, Part J: Journal of Engineering Tribology, 226, pp 923-932.

- [134] How anion and cation species influence the tribology of a green lubricant based on ionic liquids. M. Kronberger, V. Pejakovic, C. Gabler, M. Kalin. 933-951, s.l.: Proceedings of the Institution of Mechanical Engineers, Part J: Journal of Engineering Tribology, 2012, Vol. 226.
- [135] Synthesis and characterization of new polysubstituted pyridinium-based ionic liquids: application as solvents on desulfurization of fuel oils. P. Verdía, E. González, B. Rodríguez-Cabo, E. Tojo. 2011, *Green Chemistry*, 113, pp 2768-2776.
- [136] C. Kajdas, S.S.K. Harvey, E. Wilusz. *Encyclopedia of tribology*, 15. Amsterdam: Elsevier Science Publishers, 1990.
- [137] Environmentally benign catalyst: Synthesis, characterization, and properties of pyridinium dicationic molten salts (ionic liquids) and use of application in esterification. A. Chinnappan, H. Kim. 2012, *Chemical Engineering Journal*, 187, pp 283–288.
- [138] Electrochemical studies and self diffusion coefficients in cyclic ammonium based ionic liquids with allyl substituents. T. Wu, S. G. Su, Y. C. Lin, M. W. Lin, I. W. Sun. 2011, *Electrochimica Acta*, 56, pp 3209-3218.
- [139] Phase equilibria of mixtures of mutually immiscible ionic liquids. A. Arce, M. J. Earle, S. P. Katdare, H. Rodríguez, K. R. Seddon. 2007, *Fluid Phase Equilibria*, 261, pp 427-433.
- [140] Investigation of the lubricity and antiwear behavior of guanidinium ionic liquids at high temperature. G. Huang, Q. Yu, M. Cai, F. Zhou, W. Liu. 2017, *Tribology International*, 114, pp 65–76.
- [141] The distillation and volatility of ionic liquids. M. J. Earle, J. M. S. S. Esperanca, M. A. Gilea, J. N. C. Lopes, L. P. N. Rebelo, J. W. Magee, K. R. Seddon, J. A. Widegren. 2006, *Nature*, 439, pp 831-834.
- [142] (Eco)toxicity and biodegradability of selected protic and aprotic ionic liquids. B. Peric, J. Sierra, E. Martí, R. Cruañas, M. A. Garau, J. Arning, Ulrike Bottin-Weber, S. Stolte. 2013, *Journal of Hazardous Materials*, 261, pp 99–105.
- [143] Modelling for antimicrobial activities of ionic liquids towards *Escherichia coli*, *Staphylococcus aureus* and *Candida albicans* using linear free energy relationship descriptors. C. W. Cho, J. S. Park, Stefan Stolte, Y. S. Yun. 2016, *Journal of Hazardous Materials*, 311, pp 168-175.
- [144] Ionic liquids as advanced lubricant fluids. M. D. Bermúdez, A. E. Jiménez, J. Sanes, F. J. Carrión. 2888-2908, s.l.: *Molecules*, 2009, Vol. 14.
- [145] A review on ionic liquids as sustainable lubricants in manufacturing and engineering: Recent research, performance, and applications. S.A.S. Amiril, E.A. Rahim, S. Syahrullail. 2017, *Journal of Cleaner Production* (In press).

- [146] Structure and Properties of High Stability Geminal Dicationic Ionic Liquids. J. L. Anderson, R. Ding, A. Ellern, and D.W. Armstrong. 2005, *Journal of the American Chemical Society*, pp 593-604.
- [147] Nanotribological properties of novel lubricants for magnetic tapes. M. Palacio, B. Bhushan. 2009, *Ultramicroscopy*, 109, pp 980-990.
- [148] Polyethylene glycol functionalized dicationic ionic liquids with alkyl or polyfluoroalkyl substituents as high temperature lubricants. C. M. Jin, C. Ye, B. S. Phillips, J. S. Zabinski, X. Liu, W. Liu and J. M. Shreeve. 2006, *Journal of Materials Chemistry*, 16.
- [149] Study of tribochemical decomposition of ionic liquids on a nascent steel surface. R. Lu, S. Mori, K. Kobayashi, H. Nanao. 2009, *Applied Surface Science*, 255, pp 8965–8971.
- [150] Room temperature ionic liquid 1-ethyl-3-hexylimidazolium bis(trifluoromethylsulfonyl)-imide as lubricant for steel-steel contact. Q. Lu, H. Wang, C. Ye, W. Liu, Q. Xue. 2004, *Tribology International*, 37, pp 547–552.
- [151] Effect and mechanism of additives for ionic liquids as new lubricants. [18] H. Kamimura, T. Kubo, I. Minami, S. Mori: “. 2007, *Tribology International*, 40, pp 620–625.
- [152] Tribo-Chemistry of Phosphonium-Derived Ionic Liquids. I. Minami, T. Inada, R. Sasaki, H. Nanao. 225-235, s.l.: *Tribology Letters*, 2010, Vol. 40. DOI 10.1007/s11249-010-9626-0.
- [153] Thermal Stability and Corrosivity Evaluations of Ionic Liquids as Thermal Energy Storage Media. R. G. Reddy, Z. J. Zhang, M. F. Arenas, D. M. Blake Thermal Stability and Corrosivity. 2003, *High Temperature Materials and Processes*, 22, pp 87-94.
- [154] Corrosion behaviour of stainless steels in aqueous solutions of methanesulfonic acid. M. Finšgar, I. Milošev: “. 2010, *Corrosion Science*, 52, pp 2430–2438.
- [155] *Synthetic Lubricants*. s.l.: IHS MARKIT, 2015.
- [156] Dresel, W. *Synthetic Base Oils*. [aut. libro] Wilfried Dresel Theo Mang. *Lubricants and lubrication* 2nd edition. Weinheim, Germany: Wiley-VCH Verlag GmbH & Co. KGaA, 2007.
- [157] Influence of concentration and anion alkyl chain length on tribological properties of imidazolium sulfate ionic liquids as additives to glycerol in steel–steel contact lubrication. V. Pejaković, C. Tomastik, N. Dörr, M. Kalin. 234-243, s.l.: *Tribology International*, 2016, Vol. 97.
- [158] Tribological performance of functionalized ionic liquid and Cu microparticles as lubricating additives in sunflower seed oil. Mengnan Qu, Yali Yao, Jinmei He, Xuerui Ma, Shanshan Liu, Juan Feng, Lingang Hou. 166-174, s.l.: *Tribology International*, 2016, Vol. 104.

- [159] Probing the lubricating mechanism of oil-soluble ionic liquids additives. G. Huang, Q. Yu, Z. Ma, M. Cai, W. Liu. 152-162, s.l.: Tribology International, 2017, Vol. 107.
- [160] Two phosphonium cation-based ionic liquids used as lubricant additive. Part II: Tribofilm analysis and friction torque loss in cylindrical roller thrust bearings at constant temperature. A. Hernández Battez, Carlos M.C.G. Fernandes, Ramiro C. Martins, Beatriz M. Graça, M. Anand, D. Blanco, Jorge H.O. Seabra. 496-504, s.l.: Tribology International, 2017, Vol. 109. <http://dx.doi.org/10.1016/j.triboint.2017.01.020>.
- [161] Effectiveness of phosphonium cation-based ionic liquids as lubricant additive. R. González, M. Bartolomé, D. Blanco, J.L. Viesca, A. Fernández-González, A. Hernández Battez. 82-93, s.l.: Tribology International, 2016, Vol. 98.
- [162] Miscibility and tribological investigations of ionic liquids in biodegradable esters. M. Kronberger, F. Pagano, V. Pejakovic, A. Igartua, E. Urbistondo, M. Kalin. 463–487, s.l.: Lubrication Science, 2014, Vol. 26. DOI: 10.1002/lis.1274.
- [163] Imidazolium ionic liquids as additives of the synthetic ester propylene glycol dioleate in aluminium–steel lubrication. A. E. Jiménez, M. D. Bermúdez. 787–798, s.l.: Wear, 2008, Vol. 265. <http://dx.doi.org/10.1016/j.wear.2008.01.009>.
- [164] Bisimidazolium ionic liquids as the high-performance anti-wear additives in poly(ethylene glycol) for steel–steel contacts. Yao M., Liang Y., Xia Y., Zhou F. 467-471, s.l.: ACS Appl Mater Interfaces, 2009, Vol. 1. <http://dx.doi.org/10.1021/am800132z>.
- [165] Influence of temperature on tribological behaviour of ionic liquids as lubricants and lubricant additives. V. Pejaković, M. Kronberger, M. Kalin. 107-115, s.l.: Lubrication Science, 2014, Vol. 26.
- [166] Investigation on three oil-miscible ionic liquids as antiwear additives for polyol esters at elevated temperature. L. Zhu, G. Zhao, X. Wang. 336-345, s.l.: Tribology International 109 (2017) 336–345, 2017, Vol. 109. <http://dx.doi.org/10.1016/j.triboint.2016.10.032>.
- [167] Tribological investigations of ionic liquids in ultra-high vacuum environment. V. Totolin, Conte, E. Berriozábal, F. Pagano, I. Minami, N. Dörr, J. Brenner, A. Igartua. 514-524, s.l.: Lubrication Science, 2013, Vol. 26. DOI: 10.1002/lis.1224.
- [168] Imidazolium ionic liquids as additives of the synthetic ester propylene glycol dioleate in aluminium–steel lubrication. A. Jimenez, M. D. Bermudez. 787–798, s.l.: Wear, 2008, Vol. 265.
- [169] Tribological characterisation and surface analysis of diesel lubricated sliding contacts. H. Hunger, U. Litzow, S. Genze, N. Dörr, D. Karner, C. Eisenmenger-Sittner. Ostfildern (D): Proceedings of TAE, TAE, 2008. ISBN: 3-924813-73-6..

- [170] Influence of cationic moieties on the tribolayer constitution shown for bis(trifluoromethylsulfonyl)imide based ionic liquids studied by X-ray photoelectron spectroscopy. C. Gabler, N. Dörr, G. Allmaier. 90-97, s.l.: Tribology International, 2014, Vol. 80.
- [171] The corrosion and lubrication properties of 2-Mercaptobenzothiazole functionalized ionic liquids for bronze. Y. Li, S. Zhang, Q. Ding, D. Feng, B. Qin, L. Hu. 2017, Tribology International, 114, pp 121–131.
- [172] R. Heuberger, A. Rossi, N. Spencer. 185, s.l.: Tribol Lett, 2007, Vol. 25.
- [173] Miyoshi, K. Friction and wear properties of selected solid lubricating films: a case study. Solid lubrication fundamentals and applications . Cleveland - Ohio: NASA, 2000.
- [174] The Tribological Properties of Low-friction Hydrogenated Diamond-like Carbon Measured in Ultrahigh Vacuum. F. Gao, A. Erdemir, W. T. Tysoc. 2005, Tribology Letters, 20 (2005) 20: 221.
- [175] Ronkainen, H. Tribological properties of hydrogenated and hydrogen-free diamond-like carbon coatings. [PhD Thesis]. s.l.: Helsinki University of Technology, 2001.
- [176] Toward Low Friction in High Vacuum for Hydrogenated Diamondlike Carbon by Tailoring Sliding Interface. L. Cui, Z. Lu, L. Wang. 2013, ACS Applied Materials & Interfaces, 5, pp 5889–5893.
- [177] Tribological Performance of MoS₂ Coatings in Various Environments. Thomas Gradt, Thomas Schneider. 2016, Lubricants, 4, pág. 32.
- [178] M. J. Jansen, W. R. Jones Jr., R. E. Predmore, S. L. Loewenthal. Relative lifetime of several space liquid lubricants using a vacuum spirla orbit tribometer (SOT). s.l.: NASA/TM-2001-210966, 2001.
- [179] Lubrication performance of perfluoropolyalkylethers under high vacuum. M. Masuko, I. Fujinami, H. Okabe. 1992, Wear, 159, pp 249-256.
- [180] Tribological characteristics of perfluoropolyether liquid lubricants under sliding conditions in high vacuum. M. Masuko, W. R. Jones Jr., L. S. Helmick. 1994, Journal of Synthetic Lubrication, 11, pp 111-119.
- [181] A study of the tribological behaviour of perfluoro-polyethers Wear, vol. 108, no. 3, pp. E. Cosmacini, V. Veronesi. 1986, Wear, 108, pp 269-283.
- [182] Lubrication performance of perfluoropolyalkylethers under high vacuum. M. Masuko, I. Fujinami, and H. Okabe. 1992, Wear, 159, pp 249-256.
- [183] W. R. Jones Jr., A. K. Polowski, B. A. Shogrin, P. Herrera-Fierro, M. J. Jansen. Evaluation of several space lubricants using a vacuum four-ball tribometer. 1998. NASA/TM-1998-208654.
- [184] Characterizing a lubricant additive for 1,3,4-tri-(2-octylododecyl) cyclopentane: Computational study and experimental verification. J. Nian, Y. Si, Z. Guo, P. Gao, W. Liu. 2016, Friction, 4, pp 257–265.
- [185] Lubrication performance of multialkylatedcyclopentane oils for sliding friction of steel under vacuum condition. M. Masuko, H. Mizuno, A.

- Suzuki, S. Obara, A. Sasaki. 2007, *Journal of Synthetic Lubrication*, 24, pp 217–226.
- [186] Liquid lubricants for space engineering and methods for their testing. T. Kaldonski, P. P. Wojdyna. 2011, *Journal of KONES Powertrain and Transport*, 18, pp 163-184.
- [187] The anti-seizure effect of Ag nanoparticles additive in multialkylated cyclopentanes oil under vacuum condition. S. Zhang, L. Hu, H. Wang, D. Feng. 2012, *Tribology International*, 55, pp 1–6.
- [188] Tribological Performance of Silahydrocarbons Used as Steel-Steel Lubricants under Vacuum and Atmospheric Pressure. H. Z. Wang, S. W. Zhang, D. Qiao, D. P. Feng, W. M. Liu. 2014, *Journal of Nanomaterials*.
- [189] Vacuum tribological performance of phosphonium-based ionic liquids as lubricants and lubricant additives of multialkylated cyclopentanes. S. Zhang, L. Hu, D. Qiao, D. Feng, H. Wang. 2013, *Tribology International*, 66, pp 289-295.
- [190] “New test rig Catri for tribological and numerical characterization of materials, coatings and lubricant in UHV. R. Nevshupa, M. Conte, E. Berriozaba, E. Roman, A. Igartua. Vienna, Austria: s.n., 2011. 3rd European Conference on Tribology.
- [191] Ionic Liquids as Lubricants of Titanium–Steel Contact. A. E. Jimenez, M. D. Bermudez. 2009, *Tribology Letters*, 33, pp 111–126.
- [192] Surface interactions in lubrication of titanium, aluminium, and titanium–aluminium alloys with the ionic liquid [C₂mim]Tf₂N under increasing temperature. M. D. Bermudez, A. E. Jimenez. 2012, *Proceedings of the Institution of Mechanical Engineers, Part J: Journal of Engineering Tribology*, 226, pp 977–990.
- [193] Fluorides and Silicofluorides as Extreme Pressure Additives in Lubricating Fluids for Titanium. Shapiro, A. M. 1969, *Tribology Transactions*, 12, pp 80-85.
- [194] Friction and wear performance of titanium alloy against tungsten carbide lubricated with phosphate ester. Y. Yang, C. Zhang, Y. Wang, Y. Dai, J. Luo. 2016, *Tribology International*, 95, pp 27–34.
- [195] Lubricants for vacuum and space applications. A. Igartua, E. Berriozabal, F. Pagano, L. Muntada, E. Ortega. Barcelona: ELGI Annual General Meeting, 2015.
- [196] Mechanism of tribo-chemical reactions of ionic liquids on titanium alloys. E. Berriozabal, A. Igartua, F. Pagano, J. F. Cambra, I. Minami, N. Doerr, C. Gabler. s.l.: Ibertrib, 2015.

List of Figures

Figure 1. 1 -Reproduction of the painting found in the tomb of Djehutihotep. It belongs to the Egiptian period and depicts a man who is facilitating the transport of a statue by pouring a lubricant.

Figure 1. 2 – A plan made by Leonardo Da Vinci that illustrate some friction experiments realized. This sketch is included in the Codex Arundel.

Figure 1. 3 Model of corrosive wear by repeated removal of passivating films [11,12].

Figure 1. 4 - Stribeck graph according to H. Czichos and K.-H. Habig [14,15].

Figure 1. 5 – Effect of EHL on the sliding surfaces. Even though there is not a direct contact of the surfaces, the pressure exercised by the fluid is enough to generate elastic deformation on the rollers [10].

Figure 1. 6 - Formation of a hydrodynamic liquid lubricant film and development of pressure in the hydrodynamic film in a rolling element [10].

Figure 1. 7 - Antiwear additive's activation mechanism: tribochemical reaction and surface adsorption.

Figure 1. 8 - Cations normally used for ionic liquids synthesis: a) imidazolium, b) ammonium, c) pyrrolidinium, d)phosphonium.

Figure 1. 9 – Anions normally used in the synthesis of ionic liquids: a)hexafluorophosphate, b)tetrafluoroborate, c)bis(trifluoromethylsulfonyl)imide and d)dialkylphosphate.

Figure 1. 10 – Two partial phase diagrams for $[C_4Py]Cl-AlCl_3$ [66].

Figure 1. 11 – Schematic representation of the BASIL process [69].

Figure 1. 12 – Number of publications found on Scopus with the terms “ionic liquids” and “ionic liquid” + tribology. The results correspond to the global number in the year indicated.

Figure 1. 13 – Difference between the melting point and the freezing point of isopropylmethyl imidazolium PF6 ionic liquid [73].

Figure 1. 14 - Effect of the scan rate on the same ionic liquid. [74].

Figure 1. 15 - Toxicity tests: *Daphnia magna*, *Selenastrum capricornutum*, *Vibrio fischeri*, Cytotoxicity and Acetylcholinesterase

Figure 1. 16 - Interaction of the ionic liquid with the metallic surface [84].

Figure 1. 17 - Structure–friction relationship for NTf_2 salts. Influence of the cationic alkyl chain on the tribological performance [87].

Figure 1. 18 - Proposed model of boundary film derived from phosphonium [90]. In the graph BMIM is butylmethylimidazolium, Bu_3MeP is tributylmethylphosphonium, BU_4P is tetrabutylphosphonium, TFSA is bis(trifluoromethylsulfonyl)amide, MePhos is dimethylphosphate and EtTPhos is diethylphosphorodithioate.

Figure 1. 19 - A proposed model of boundary film for lubrication with ionic liquids containing FAP anion [104].

Figure 2. 1 - Schematic representation of the UMT CETR tribometer [113].

Figure 2. 2 - Optimol SRV on the left and schematic representation on the right: 1) ball; 2) disc; 3) disc holder; 4) ball holder; 5) loading mechanism; 6) piezo sensor; 7) testing cell; 8) heating system; 9) reciprocating sliding mechanism [114].

Figure 2. 3 – Tribometer CATRI © UHV at IK4-TEKNIKER.

Figure 2. 4 MicroTest MT/10/SCM tribometer with the electrodes installed for the tribocorrosion test.

Figure 2. 5 – Determination of the wear scar diameter (WSD)

Figure 2. 6 - Contact between a sphere and a flat surface

Figure 2. 7 - Schematic drawing of a ball with a missing “cap”, corresponding to a wear scar. [121]

Figure 2. 8 - Wear scar analysis: a) Confocal white light microscope, b) Wear scar region on ball [122].

Figure 2. 9 – FE-SEM Gemini ULTRA plus

Figure 2. 10 - XPS Thermo Fisher Scientific Theta Probe (East Grinstead, United Kingdom) at AC2T research GmbH.

Figure 3. 1 - Comparison of COF and WSD of the balls for neat ILs and glycerol.

Figure 3. 2 - Wear scar on the steel AISI 52100 ball after lubrication with: (a) neat glycerol (magnification 100X); (b) **IL1** - $[C_1PyC_2H_4(CH_2OCH_2)_3C_2H_4PyC_1]^+ [C_1SO_4]^-_2$ (magnification 50X); (c) **IL2** - $[C_1PyC_2H_4(CH_2OCH_2)_3C_2H_4PyC_1]^+ [NTf_2]^-_2$ (magnification 100X); (d) **IL3** - $[C_1Py]^+ [C_1SO_4]^-$ (magnification 50X); (e) **IL4** - $[C_1Py]^+ [NTf_2]^-$ (magnification 100X).

Figure 3. 3 - Wear scar on the test specimens. Discs lubricated with: a) glycerol, b) **IL2** - $[C_1PyC_2H_4(CH_2OCH_2)_3C_2H_4PyC_1]^+ [NTf_2]^-_2$, c) **IL4** - $[C_1Py]^+ [NTf_2]^-$.

Figure 3. 4 - SEM micrographics with two different magnification of the discs rubbed in the tribotests lubricated with glycerol (a and c) and neat IL **IL4** - $[C_1Py]^+ [NTf_2]^-$ (b and d).

Figure 3. 5 - Representation of the registered average coefficient of friction (COF) with the mixtures of tested lubricants. The friction measured with neat **IL3** - $[C_1Py]^+ [C_1SO_4]^-$ was out of scale and the average COF is indicated in the graph.

Figure 3. 6 - Wear scar on the 100Cr6 balls after lubrication with mixture of 0.25 wt % of IL in glycerol: (a) 0.25 wt % of **IL1** - $[C_1PyC_2H_4(CH_2OCH_2)_3C_2H_4PyC_1]^+ [C_1SO_4]^-_2$; (b) 0.25 wt% of **IL2** - $[C_1PyC_2H_4(CH_2OCH_2)_3C_2H_4PyC_1]^+ [NTf_2]^-_2$; (c) 0.25 wt % of **IL3** - $[C_1Py]^+ [C_1SO_4]^-$; (d) 0.25 wt % of **IL4** - $[C_1Py]^+ [NTf_2]^-$.

Figure 3. 7 - Representation of the wear scars obtained by confocal microscope on the discs lubricated with: a) glycerol, b) **IL4** - $[C_1Py]^+ [NTf_2]^-$, c) mixture of glycerol and 1% of **IL2** - $[C_1PyC_2H_4(CH_2OCH_2)_3C_2H_4PyC_1]^+ [NTf_2]^-_2$, d) mixture of glycerol and 1% of **IL4** - $[C_1Py]^+ [NTf_2]^-$.

Figure 4. 1 – Grid over the disc wear track defining the spots for individual measurements (green crosses).

Figure 4. 2 – DSC curves with **IL14** - $[C_1PyrrTrCH_2(CH_2OCH_2)_{22}CH_2TrPyrrC_1]^+ [C_1SO_3]^-_2$ and **IL15** - $[C_1ImTrCH_2(CH_2OCH_2)_{20}CH_2TrImC_1]^+ [C_1SO_3]^-_2$ in the temperature range

from 22 °C to 300 °C. Curve at temperatures higher than 300 °C was excluded due to strongly irregular progress caused by ionic liquid degradation.

Figure 4. 3 – Ball wear volume and friction of the ionic liquids at 50 °C, light (left) columns indicate COF, dark (right) columns indicate ball wear volume.

Figure 4. 4 – Ball wear volume and friction of the ionic liquids at 100 °C, light (left) columns indicate COF, dark (right) columns indicate ball wear volume.

Figure 4. 5 – Ball wear volume and friction of the ionic liquids at 150 °C, light (left) columns indicate COF, dark (right) columns indicate ball wear volume.

Figure 4. 6 – SEM-EDS analysis comparing the ball wear scars from tribotests at 100 °C (a) and at 150 °C (b) using **MIX**. SEM image of (a) has a width of 50 μm, that of b) has a total width of 70 μm. Arrows indicate increased amounts of oxygen and sulfur in the tribofilm

Figure 4. 7 – Progress of coefficient of friction at 100 °C over time with mixtures of 1 % w/w dicationic IL in Synalox™. Neat Synalox™ as reference.

Figure 4. 8 – Ball wear volume and friction of the mixtures of IL and base oil at 100 °C, light (left) columns indicate COF, dark (right) columns indicate ball wear volume. Neat Synalox™ is used as reference. Values shown for mixtures with wear volumes exceeding scale. COF is coefficient of friction.

Figure 4. 9 – XPS detail spectrum of fluorine F 1s in the middle of the disc wear track from a tribotest with a mixture of 1 % w/w **MIX** in Synalox™ showing a pronounced peak at 684.6 eV.

Figure 4. 10 – Distribution of (A) fluorine F 1s at a binding energy of 684.6 eV, (B) sulfur S 2p₃ 161.7 eV and (C) iron Fe 2p₃ at a binding energy of 711 eV from a tribotest with a mixture of 1 % w/w **MIX** in Synalox™ in and outside the disc wear track visualized by the XPS imaging experiment.

Figure 4. 11 – Surfaces of SRV discs obtained after exposure to the neat dicationic IL at 100 °C for 1 week. All images obtained with an optical microscope have a width of 400 μm.

Figure 5. 1 – Grid over the disc wear track defining the spots for individual measurements (green crosses). Wear scar with **IL16** - $[(\text{H}_9\text{C}_4)_3\text{P}(\text{CH}_3)]^+ [(\text{C}_1)_2\text{PO}_4]^-$ on the left and **IL17** - $[\text{P}(\text{C}_4\text{H}_9)_4]^+ [(\text{C}_2)_2\text{PO}_2\text{S}_2]^-$ on the right.

Figure 5. 2 — Thermogravimetical analysis of the ILs tested and the base oil in the range 25 °C – 500 °C.

Figure 5. 3 – Differential scanning calorimetry with the **IL16** - $[(\text{H}_9\text{C}_4)_3\text{P}(\text{CH}_3)]^+ [(\text{C}_1)_2\text{PO}_4]^-$ and **IL17** - $[\text{P}(\text{C}_4\text{H}_9)_4]^+ [(\text{C}_2)_2\text{PO}_2\text{S}_2]^-$ in the range of temperature between -120 °C and 25 °C.

Figure 5. 4 - Progress of coefficient of friction at 100 °C over time with mixtures of 0.25 % w/w of IL in base oil. Neat base oil as reference.

Figure 5. 5 - Progress of coefficient of friction at 100 °C over time with mixtures of 0.50 % w/w of IL in base oil. Neat base oil as reference.

Figure 5. 6 - Progress of coefficient of friction at 100 °C over time with mixtures of 5.00 % w/w of IL in base oil. Neat base oil as reference.

Figure 5. 7 – Ball and disc wear volume with different concentrations of ILs in base oil.

Figure 5. 8 – Micrographies of the wear scar of the ball (left) and disc (right) for different IL dilutions of ILs in base oil (0,25-5% w/w). The height of the images is 700 μm .

Figure 5. 9 - XPS analysis on the disc surface rubbed during the experiment with 5% w/w of **IL16** - $[(\text{H}_9\text{C}_4)_3\text{P}(\text{CH}_3)]^+ [(\text{C}_1)_2\text{PO}_4]^-$. a) Phosphate 133.5 eV, b) Oxygen in metal oxide 529.9 eV, c) bridging oxygen 533.1 eV, d) Organic oxide or non-bridging oxygen 531.4 eV, e) iron Fe(II) 709.6 eV, f) iron Fe(III) 711.2 eV.

Figure 5. 10 - XPS analysis on the disc surface rubbed during the experiment with 5% w/w of **IL17** - $[\text{P}(\text{C}_4\text{H}_9)_4]^+ [(\text{C}_2)_2\text{PO}_2\text{S}_2]^-$. a) Phosphate 133.5 eV, b) Organic oxide or non-bridging oxygen 531.4 eV, c) iron Fe(II) 709.6 eV, d) iron Fe(III) 711.2 eV.

Figure 5. 11 – ATR-FTIR analysis of the ionic liquid **IL16** - $[(\text{H}_9\text{C}_4)_3\text{P}(\text{CH}_3)]^+ [(\text{C}_1)_2\text{PO}_4]^-$ after the thermal degradation test in the oven.

Figure 5. 12 – ATR-FTIR analysis of the ionic liquid **IL17** - $[\text{P}(\text{C}_4\text{H}_9)_4]^+ [(\text{C}_2)_2\text{PO}_2\text{S}_2]^-$ after the thermal degradation test in the oven.

Figure 5. 13 - Photos and SEM-EDS analysis on the balls exposed to the ionic liquids in a oven for three weeks. On the left there is the photo taken with digital

camera, at the center there is the SEM image of the surface and at the left there is the result of the EDS analysis.

Figure 5. 14 – Friction coefficient measured during the tribocorrosion tests.

Figure 5. 15 - Open circuit potential of the tribotests during the sliding phase.

Figure 6. 1 - Expected function of the ionic structure of the ionic liquids [112].

Figure 6. 2 - Friction coefficient for the tests performed on steel surface in vacuum conditions.

Figure 6. 3 - Friction coefficient for the tests performed on titanium surface in vacuum conditions.

Figure 6. 4 - Average friction coefficient. In blue the values obtained with titanium specimens and in orange the results obtained with steel specimens. The tests were realized in vacuum.

Figure 6. 5 - Wear tracks of the samples tested in vacuum conditions

Figure 6. 6 - Measure of the wear volume on the scar of the flat samples in vacuum conditions. Two different scale were considered for titanium and steel samples, because of the large difference in wear volume.

Figure 6. 7 - Comparison of the friction coefficient obtained on steel samples in atmospheric pressure (left column) and in vacuum (right column).

Figure 6. 8 - Comparison of the wear volume obtained on steel samples in atmospheric pressure (left column) and in vacuum (right column).

Figure 6. 9 - Comparison of the friction coefficient obtained on titanium samples at atmospheric pressure (left column) and in vacuum (right column).

Figure 6. 10 - Comparison of the wear volume obtained on titanium samples at atmospheric pressure (left column) and in vacuum (right column).

Figure 6. 11 - Relative desorbed gas counts/second recorded by mass spectra.

Figure 6. 12 Friction coefficient and analysis of the gasses desorbed during one of the tribotests realized with **IL18** - $[(H_9C_4)_3P(C_{12}H_{25})]^+ [(C_1)_3Si(C_2H_4)SO_3]^-$. The

masses were normalized and the normalization factors are listed in the graph below each mass.

Figure 6. 13 - Analysis of the cationic fragments that could have been found by MS.

Figure 6. 14 - Analysis of the fragments of the anion that could have been found by MS

Figure 6. 15 - SEM/EDS analysis on the steel surface lubricated with **IL18** - $[(H_9C_4)_3P(C_{12}H_{25})]^+$ $[(C_1)_3Si(C_2H_4)SO_3]^-$ (on the top) and with PFPF (on the bottom).

List of Tables

Table 2. 1 - Structure and codification of the ionic liquids used. In the codification Py=Pyridinium, Im=Imidazolium, Pyrr=Pyrrolidinium, Tr=Triazole

Table 2. 2 - Properties of the base lubricant SYNALOX™ 100-30B

Table 2. 3 – Properties of PFPE 107/500 according to the data provided by the supplier.

Table 2. 4 - Testing parameters used for the tribological tests in the different case study presented

Table 3. 1 – Structure and codification of the Pyridinium ionic liquids used

Table 3. 2 - Tribological test parameters and materials tested

Table 3. 3 Thermal properties of synthesized pyridinium ILs, where T_m , melting temperature (°C); T_f , freezing temperature (°C); T_{start} , the start of decomposition temperature (100), $T_{d,onset}$ (°C), the onset of decomposition temperature (100).

Table 4. 1 - Structure and codification of the ionic liquids synthesized in the Martin Luther University Halle-Wittenberg

Table 4. 2 - Structure and codification of the ionic liquids synthesized in the University of Vigo

Table 4. 3 Thermal stability measured by TGA

Table 4. 4 – Summary of the results obtained from the corrosion experiments with AISI 52100 steel discs in contact with neat dicationic IL at 100 °C for one week.

Table 5. 1 - Structure and codification of the phosphonium ILs.

Table 5. 2 - Physicochemical properties as function of the temperature: dynamic viscosity η , kinematic viscosity ν , density ρ and viscosity index VI of phosphonium ionic liquids.

Table 6. 1 - Structure and codification of siliconsulphonate ILs.

Table 6. 2 Physical-chemical characteristics of the ionic liquids.

Table 6. 3 – Composition of the discs that were used for the tribological tests: stainless steel 440C and titanium grade 5.

Table 6. 4 - Testing conditions used during the tribotests.

Table 6. 5 - Intervals and peaks of m/z in the MS analysis of the gasses desorbed during the tribotests with **IL18** - $[(H_9C_4)_3P(C_{12}H_{25})]^+ [(C_1)_3Si(C_2H_4)SO_3]^-$.

Table 6. 6 -Elements found by XPS on the steel specimen.

Table 6. 7 - Elements found by XPS on the titanium specimen.

Articles published

Dicationic ionic liquids as lubricants

F Pagano¹, C Gabler², P Zare³, M Mahrova⁴, N Dörr², R Bayon¹,
X Fernandez¹, WH Binder³, M Hernaiz¹, E Tojo⁴ and A Igartua¹

Proc IMechE Part J
J Engineering Tribology
226(11) 952–964
© IMechE 2012
Reprints and permissions:
sagepub.co.uk/journalsPermissions.nav
DOI: 10.1177/1350650112458873
pjj.sagepub.com
SAGE

Abstract

Twelve dicationic ionic liquids have been investigated for their potential inlubricants. The dications selected were synthesized from oligoethylene glycols linking two cationic moieties based on either N-methylimidazolium or N-methylpyrrolidinium at the extremities. As anions, chloride, bis(trifluoromethanesulfonyl)imide (Tf₂N), methanesulfonate and butansulfonate were chosen. Thermal stability of the IL has been evaluated by thermogravimetric analysis and differential scanning calorimetry showing good properties up to 150 °C for all IL. SRV tribotests of neat IL using steel–steel contacts with ball-on-disc geometry were performed at 50 °C, 100 °C and 150 °C. Friction and wear were significantly influenced by both anion structure and chain length of the oligoethylene glycol moiety where longer chains yielded better tribological behavior. The tribological behavior improved with a mixture of different types of IL containing F, O, S in their anions. A large variation of ionic liquids corrosiveness and corrosion inhibition, respectively, was found attributed to structure variation. A general tendency of improving the corrosion resistance when increasing the chain length of the neat IL has been found. In addition to the neat dicationic ionic liquids, mixtures of 1% of the most interesting IL in polypropylene glycol base oil have been studied at 100 °C resulting in more favorable tribological properties for ionic liquids with Tf₂N anion. X-ray photoelectron spectroscopy analysis showed that the structures with Tf₂N anion create a tribofilm of inorganic fluorine that greatly improves the performance of the base oil.

Keywords

Dicationic ionic liquids, tribology, X-ray photoelectron spectroscopy, corrosion, friction, wear

Date received: 22 December 2011; accepted: 26 July 2012

Introduction

Ionic liquids (IL) are most commonly defined as organic salts with melting points below 100 °C. Although this description gives a clear idea of their ionic nature and their liquid state at a relatively low temperature, it is worth to stress the importance of IL in comparison to molten salts. Usually, fusion temperature of a salt is considerably high, for example 801 °C in the case of sodium chloride, which excludes its use in many applications. However, by the consideration of IL, it is possible to benefit from properties emerging from ionic bonds between the moieties, as low volatility and excellent electrochemical characteristics, but at a relatively low temperature, often significantly below room temperature.

In order to decrease the melting point, IL are generally constituted from an organic cation with low symmetry and a weakly coordinated anion. This way, lattice energy is lower and the anion–cation interaction is minimized due to the asymmetric and delocalized charge.¹

The reason for the growing interest in IL can be explained by their excellent physical–chemical properties: large electrochemical window,² controlled miscibility,³ high thermal stability,¹ negligible vapor pressure^{4,5} and in some cases, environmental harmlessness.⁶ In addition to these qualities, it is pointed out that it is possible to obtain compounds with tailor-designed properties by tuning the structure through substitution and structural modification of the anion or of the cation.

In 2001, Liu et al. started the first tribological investigation with IL. This research group studied imidazolium

¹Fundación TEKNIKER, Eibar, Spain

²Austrian Centre of Competence for Tribology – AC²T research GmbH, Wiener Neustadt, Austria

³Institute of Chemistry, Macromolecular Chemistry, Martin-Luther University Halle-Wittenberg, Germany

⁴Department of Organic Chemistry, University of Vigo, Spain

Corresponding author:

F Pagano, Fundación TEKNIKER, Avda. Otaola, 20, 20600 Eibar, Spain.
Email: fpagano@tekniker.es



Contents lists available at ScienceDirect

Tribology International

journal homepage: www.elsevier.com/locate/triboint



Pyridinium based dicationic ionic liquids as base lubricants or lubricant additives



M. Mahrova^a, F. Pagano^b, V. Pejakovic^c, A. Valea^d, M. Kalin^e, A. Igartua^b, E. Tojo^{a,*}

^a Department of Organic Chemistry, University of Vigo, 36310 Vigo, Spain

^b Tribology Unit, IK4-TEKNIKER, C/ Itagi Goenaga 5, 20600 Eibar, Spain

^c AC2T research GmbH, Viktor Kaplan Straße 2, 2700 Wiener Neustadt, Austria

^d University of the Basque Country (UPV/EHU), 48012 Bilbao, Spain

^e Laboratory for Tribology and Interface Nanotechnology, University of Ljubljana, 1000 Ljubljana, Slovenia

ARTICLE INFO

Article history:

Received 4 June 2014

Received in revised form

20 October 2014

Accepted 21 October 2014

Available online 30 October 2014

Keywords:

Ionic liquids

Dicationic

Lubricants

Friction

ABSTRACT

A series of eight new dicationic ionic liquids incorporating polyethylene glycol chains linking two *N*-alkylpyridinium moieties through rings position 2, were synthesized and investigated for their potential use as lubricants or lubricant additives. Alkylsulfate and bis(trifluoromethanesulfonyl)imide [NTf₂] were selected as anions. Dicationic ionic liquids containing [NTf₂] anion demonstrated good properties as neat lubricants showing low coefficient of friction and wear comparable with the reference lubricant (glycerol). Even more interesting could be their use as friction modifier additives since an important decrease in the coefficient of friction was achieved with a really low concentration of ionic liquid. The thermal analysis of all ionic liquids by thermal gravimetric analysis (TGA) and differential scanning calorimetry (DSC) is also described.

© 2014 Elsevier Ltd. All rights reserved.

1. Introduction

Ionic liquids (ILs) have gained increasing importance both in the scientific and industrial engineering community during last decade. Due to their remarkable and interesting properties, such as negligible vapor pressure, non-flammability, high polarity, and high thermal stability [1], ILs are finding widespread use as engineering fluids or as novel lubricating systems [2,3]. Moreover, the polar nature of ILs is directly connected with good tribological behavior, since their strong interactions with surfaces lead to the formation of adsorbed films, reducing friction and wear.

The first experiment of ILs in tribology was reported in 2001 with the work of Liu et al. [4]. In that research, imidazolium tetrafluoroborate was tested as IL-based lubricant for various tribo-pairs and, in all experiments, the use of the IL showed significant friction reduction. Since that time, the interest of scientists in tribological properties of ILs has considerably increased [5,6]. Jones et al. have shown that the presence of polyether chains can significantly improve tribological behavior of liquid lubricants or lubricant additives [7]. Jin et al. have examined some polyethylene glycol functionalized ILs as high temperature lubricants, showing how the presence of fluorine in the IL

favorably boosts its anti-wear performance [8]. On the other side, dicationic ILs based on imidazolium and pyrrolidinium cation and traditional anions as BF₄⁻ or PF₆⁻, have shown good thermal stability comparing with their monocationic analogues [9]. It has also been shown that the acute toxicity of DILs is in many cases below the levels observed for those monocationic and that the use of head groups connected via polyethylene glycol could be identified as structural elements reducing the toxicity [10]. Hence, the combination of the tribologically favorable properties of polyethylene glycol and DILs may lead to a series of novel and advanced lubricating systems.

Previous works on the use of DILs derived from imidazolium [11,12] and pyrrolidinium [13] for lubrication have shown very promising results. Nevertheless, to our knowledge, no papers were published about using pyridinium DILs as lubricants or lubricant additives. It is known that pyridinium cation can show exceptionally high levels of biodegradation under aerobic conditions and can be classified as “ready biodegradable” [14]. In addition, studies on the acute toxicity of DILs have shown levels below those observed for monocationic ILs [15]. Several recent studies dealing with tribological properties of ionic liquids exposed to extreme conditions [16,17], as well as with the stability of lubricant mixtures of ionic liquids with conventional base oils [18], has been published. Generated knowledge of ionic liquids in tribology can also be found in several review articles [2,19].

* Corresponding author. Tel.: +34 986 812 290; fax: +34 986 812 262.

E-mail address: etojo@uvigo.es (E. Tojo).

Patent related with the results of this thesis

P. Aswath, X. Chen, V. Sharma, A. Igartua, F. Pagano, W. Binder, P. Zare, N. Doerr, “Synergistic mixtures of ionic liquids with other ionic liquids and/or with ashless thiophosphates for antiwear and/or friction reduction applications”. US 20130331305 A1 (2013)

Other publications of the author related with the ionic liquids

S. Stolte, S. Steudte, O. Areitioaurtena, F. Pagano, J. Thöming, P. Stepnowski, A. Igartua. “Ionic liquids as lubricants or lubrication additives: An ecotoxicity and biodegradability assessment”. *Chemosphere*, 89, pp. 1135–1141 (2012).

M. Kronberger, F. Pagano, V. Pejakovic, A. Igartua, E. Urbistondo, M. Kalin. “Miscibility and tribological investigations of ionic liquids in biodegradable esters”. *Lubrication Science*, 26 pp. 463–487 (2014) DOI: 10.1002/lis.1274.

V. Totolin, Conte, E. Berriozábal, F. Pagano, I. Minami, N. Dörr, J. Brenner, A. Igartua. “Tribological investigations of ionic liquids in ultra-high vacuum environment”. *Lubrication Science*, 26 pp.514-524 (2013) DOI: 10.1002/lis.1224.

Article under accepted and under revision

F. Pagano, I. Minami, L. Pizarova, C. Gabler, V. Totolin, N. Doerr, R. Bayon, A. Igartua, A. Valea. “Phosphonium based ionic liquids as anti-wear additives in synthetic base oil”. *Applied Sciences MDPI*

Congresses of the author related with the subject of the thesis

F. Pagano, A. Igartua, I. Minami, N. Doerr, C. Gabler, A. Valea. “Analysis of the tribochemical behaviour of ionic liquids in contact with steel and titanium substrates in high vacuum environment”. STLE 2016 Las Vegas, USA. 15-19/5/2016

F. Pagano, A. Igartua, I. Minami, N. Doerr, A. Valea. “Ionic Liquids Working under high vacuum conditions” 20th International Colloquium Tribology – Esslingen. Stuttgart, Germany. 12 14/1/2016

A. Igartua, E. Berriozabal, B. Zabala, F. Pagano, I. Minami, N. Doerr, C. Gabler, R. Nevshupa, E. Roman, L. PlethNielsen, S. Lourcing, L. Muntada. “Lubricity and tribochemical reactivity of advanced materials under high vacuum”. ESMATS 2015 Bilbao, Spain 23-25-/9/2015

A. Igartua, E. Berriozabal, F. Pagano, L. Muntada, E. Ortega “Lubricants for vacuum and space applications”. ELGI AGM 2015 Barcelona, Spain 18-21/4/2015

E. Berriozabal, A. Igartua, F. Pagano, J. F. Cambra, I. Minami, N. Doerr, C. Gabler. “Mechanism of tribo-chemical reactions of ionic liquids on titanium alloys”. Ibertrib 2015 Cartagena, Spain 18-19/6/2015

F. Pagano, M. Hernaiz, A. Villar, N. Uranga, A. Igartua. “Tribological characterization of an hybrid ionic liquid” Lubmat 2014 Manchester, UK 25-27/6/2014

F. Pagano, M. Mahrova, R. Bayon, A. Valea Pérez, A. Igartua. “Tribological comparison of monocationic and dicationic pyridinium ionic liquids”. WTC 2013 Turin, Italy 8-13/09/2013

F. Pagano, R. Bayon, M. Kronberger, N. Doerr, A. Igartua. “Phosphonium ionic liquids used in Tribology. A tribocorrosion study”. Eurocorr 2012 Istanbul, Turquia 9-13/9/2012

F. Pagano, P. Zare, A. Valea, R. Bayon, M. Kronberger, V. Pejakovic, W. H. Binder, A. Igartua. “Tribological comparison of a group of bis(trifluoromethylsulfonyl)imide) Ionic Liquids as additives in poly(propylene glycol) monobutyl ether base oil”. Lubmat 2012 Bilbao, España 6 8/6/2012

V. Pejaković, F. Pagano, A. Igartua, M. Kalin. “Ionic liquids as lubricant additives in steel/steel contact lubrication”. Lubmat 2012 Bilbao, España 6-8/6/2013

M. Kronberger, F. Pagano, M. Kalin, A. Igartua, E. Urbistondo. “Finely dispersed ionic liquids as additives in biodegradable base oils”. Lubmat 2012 Bilbao, España 6-8/6/2013

V. Totolin, M. Conte, E. Berriozabal, F. Pagano, I. Minami, N. Doerr, J. Brenner, A. Igartua. “Tribological Investigations of Ionic Liquids in Ultra-high Vacuum Environment”. Lubmat 2012 Bilbao, España 6-8/6/2013

F. Pagano, A. Valea, R. Bayon, X. Fernandez, A. Igartua. “Utilizzo dei liquidi ionici per migliorare le prestazioni dei lubrificanti”. 3° Workshop AIT “Tribologia e Industria” Milano, Italia 22 23/2/2013

F. Pagano, V. Pejaković, M. Kronberger. “Tribological investigation of ionic liquids as lubricant fluid”. Minilubes Scientific Fellow’s Congress Vigo, España 1-3/6/2013

F. Pagano, P. Zare, R. Bayon, W. Binder, X. Fernandez, A. Igartua. “Tribological evaluation of tetraethylen glycol functionalized ionic liquids”. Ecotrib 2011 Viena, Austria 07-09/06/2011